



WP 5 – Action 5.3 – Final report

Thermal and geomorphic permafrost response to present and future climate change in the European Alps

Citation reference

Kellerer-Pirklbauer A., Lieb G.K., Schoeneich P., Deline P., Pogliotti P. eds (2011). *Thermal and geomorphic permafrost response to present and future climate change in the European Alps*. PermaNET project, final report of Action 5.3. On-line publication ISBN 978-2-903095-58-1, 177 pp.

Downloadable on: www.permanet-alpinespace.eu

Editors

Andreas Kellerer-Pirklbauer and Gerhard Karl Lieb, Institute of Geography and Regional Science, University of Graz, Austria (IGRS)

Philippe Schoeneich, Institut de Géographie Alpine, Université de Grenoble, France (IGA-PACTE)

Philip Deline, EDYTEM, Université de Savoie, France (EDYTEM)

Paolo Pogliotti, Regional Agency for the Environmental Protection of the Aosta Valley, Italy (ARPA VdA)

Project reference

The *PermaNET – Permafrost long term monitoring network (2008-2011)* project is part of the European Territorial Cooperation and co-funded by the European Regional Development Fund (ERDF) in the scope of the Alpine Space Programme www.alpine-space.eu

Authors

Baroni, Carlo	University of Pisa (Italy)
Bodin, Xavier	University Joseph Fourier, Grenoble (France)
Cagnati, Anselmo	Regional Agency for the Environmental Protection of Veneto (Italy)
Carollo, Federico	E.P.C. European Project Consulting S.r.l. (Italy)
Coviello, Velio	National Center for Scientific Research EDYTEM, Grenoble (France)
Cremonese, Edoardo	Regional Agency for the Environmental Protection of the Aosta Valley (Italy)
Crepaz, Andrea	Regional Agency for the Environmental Protection of Veneto (Italy)
Dall'Amico, Matteo	Mountain-eering srl (Italy)
Defendi, Valentina	Regione Veneto, Direzione Geologia e Georisorse, Servizio Geologico (Italy)
Deline, Philip	National Center for Scientific Research EDYTEM, Grenoble (France)
Drenkelfluss, Anja	University of Bonn (Germany)
Galuppo, Anna	Regione Veneto, Direzione Geologia e Georisorse, Servizio Geologico (Italy)
Gruber, Stephan	University of Zurich (Switzerland)
Kellerer-Pirklbauer, Andreas	University of Graz (Austria)
Kemna, Andreas	University of Bonn (Germany)
Klee, Alexander	Central Institute for Meteorology and Geodynamics (Austria)
Krainer, Karl	University of Innsbruck (Austria)
Krautblatter, Michael	University of Bonn (Germany)
Kroisleinter, Christine	Central Institute for Meteorology and Geodynamics (Austria)
Krysiecki, Jean-Michel	University Joseph Fourier, Grenoble (France)
Le Roux, Olivier	Association pour le développement de la recherche sur les glissements de terrain (France)
Lieb, Gerhard Karl	University of Graz (Austria)
Lorier, Lionel	Association pour le développement de la recherche sur les glissements de terrain (France)
Magnabosco, Laura	Regione Veneto, Direzione Geologia e Georisorse, Servizio Geologico (Italy)
Magnin, Florence	National Center for Scientific Research EDYTEM, Grenoble (France)
Mair, Volkmar	Autonomous Province of Bolzano (Italy)
Malet, Emmanuel	National Center for Scientific Research EDYTEM, Grenoble (France)
Marinoni, Francesco	Freelancer (Italy)
Morra di Cella, Umberto	Regional Agency for the Environmental Protection of the Aosta Valley (Italy)
Noetzli, Jeanette	University of Zurich (Switzerland)
Pogliotti, Paolo	Regional Agency for the Environmental Protection of the Aosta Valley (Italy)
Ravanel, Ludovic	National Center for Scientific Research EDYTEM, Grenoble (France)
Reisenhofer, Stefan	Central Institute for Meteorology and Geodynamics (Austria)
Riedl, Claudia	Central Institute for Meteorology and Geodynamics (Austria)
Rigon, Riccardo	University of Trento (Italy)
Schoeneich, Philippe	University Joseph Fourier, Grenoble (France)
Schöner, Wolfgang	Central Institute for Meteorology and Geodynamics (Austria)
Seppi, Roberto	University of Pavia (Italy)
Vallon, Michel	University Joseph Fourier, Grenoble (France)
Zampedri, Giorgio	Geological Survey, Autonomous Province of Trento (Italy)
Zischg, Andreas	Abenis Alpinexpert GmbH/srl (Italy)
Zumiani, Matteo	Geologist (Italy)

ADRA - Association pour la diffusion de la recherche alpine

14 bis av. Marie-Reynoard,

F-38100 Grenoble

ISBN 978-2-903095-58-1



Contents and list for chapter publications

1. Permafrost Response to Climate Change

Schoeneich P., Lieb G.K., Kellerer-Pirklbauer A., Deline P., Pogliotti P. (2011). Chapter 1: Permafrost Response to Climate Change. In Kellerer-Pirklbauer A. et al. (eds): *Thermal and geomorphic permafrost response to present and future climate change in the European Alps*. PermaNET project, final report of Action 5.3. On-line publication ISBN 978-2-903095-58-1, p. 4-15.

2. Climate Change in the European Alps

Kroisleitner Ch., Reisenhofer S., Schöner W. (2011). Chapter 2: Climate Change in the European Alps. In Kellerer-Pirklbauer A. et al. (eds): *Thermal and geomorphic permafrost response to present and future climate change in the European Alps*. PermaNET project, final report of Action 5.3. On-line publication ISBN 978-2-903095-58-1, p. 16-27.

3. Case studies in the European Alps

3.1 Overview on case studies

Kellerer-Pirklbauer A, Lieb G.K. (2011). Chapter 3.1: Case studies in the European Alps – Overview on case studies. In Kellerer-Pirklbauer A. et al. (eds): *Thermal and geomorphic permafrost response to present and future climate change in the European Alps*. PermaNET project, final report of Action 5.3. On-line publication ISBN 978-2-903095-58-1, p. 28-34.

3.2 Hochreichart, Eastern Austrian Alps

Kellerer-Pirklbauer A (2011). Chapter 3.2: Case studies in the European Alps – Hochreichart, Eastern Austrian Alps. In Kellerer-Pirklbauer A. et al. (eds): *Thermal and geomorphic permafrost response to present and future climate change in the European Alps*. PermaNET project, final report of Action 5.3. On-line publication ISBN 978-2-903095-58-1, p. 35-44.

3.3 Dösen Valley, Central Austrian Alps

Kellerer-Pirklbauer A (2011). Chapter 3.3: Case studies in the European Alps – Dösen Valley, Central Austrian Alps. In Kellerer-Pirklbauer A. et al. (eds): *Thermal and geomorphic permafrost response to present and future climate change in the European Alps*. PermaNET project, final report of Action 5.3. On-line publication ISBN 978-2-903095-58-1, p. 45-58.

3.4 Hoher Sonnblick, Central Austrian Alps

Klee A, Riedl C. (2011). Chapter 3.4: Case studies in the European Alps – Hoher Sonnblick, Central Austrian Alps. In Kellerer-Pirklbauer A. et al. (eds): *Thermal and geomorphic permafrost response to present and future climate change in the European Alps*. PermaNET project, final report of Action 5.3. On-line publication ISBN 978-2-903095-58-1, p. 59-65.

3.5 Rock Glacier Hohebenkar, Western Austrian Alps

Krainer K. (2011). Chapter 3.5: Case studies in the European Alps – Rock Glacier Hohebenkar, Western Austrian Alps. In Kellerer-Pirklbauer A. et al. (eds): *Thermal and geomorphic permafrost response to present and future climate change in the European Alps*. PermaNET project, final report of Action 5.3. On-line publication ISBN 978-2-903095-58-1, p. 66-76.

3.6 Rock Glacier Laurichard, Northern French Alps

Schoeneich P., Bodin X., Krysiecki J.-M. (2011). Chapter 3.6: Case studies in the European Alps – Rock Glacier Laurichard, Northern French Alps. In Kellerer-Pirklbauer A. et al. (eds): *Thermal and geomorphic permafrost response to present and future climate change in the European Alps*. PermaNET project, final report of Action 5.3. On-line publication ISBN 978-2-903095-58-1, p. 77-86.

3.7 Rock Glacier Bellecombes, Northern French Alps

Schoeneich P., Krysiecki J.-M., Le Roux O., Lorier L., Vallon M. (2011). Chapter 3.7: Case studies in the European Alps – Rock Glacier Bellecombes, Northern French Alps. In Kellerer-Pirklbauer A. et al. (eds): *Thermal and geomorphic permafrost response to present and future climate change in the European Alps*. PermaNET project, final report of Action 5.3. On-line publication ISBN 978-2-903095-58-1, p. 87-96.

3.8 Aiguille du Midi, Mont Blanc massif, French Alps

Deline P., Cremonese E., Drenkelfluss A., Gruber S., Kemna A., Krautblatter M., Magnin F., Malet E., Morra di Cella U., Noetzli J., Pogliotti P., Ravanel L. (2011). Chapter 3.8: Case studies in the European Alps – Aiguille du Midi, Mont Blanc massif, French Alps. In Kellerer-Pirklbauer A. et al. (eds): *Thermal and geomorphic permafrost response to present and future climate change in the European Alps*. PermaNET project, final report of Action 5.3. On-line publication ISBN 978-2-903095-58-1, p. 97-108.

3.9 Rockfalls in the Mont Blanc massif,

Deline P., Ravanel L. (2011). Chapter 3.9: Case studies in the European Alps – Rockfalls in the Mont Blanc massif, French-Italian Alps. In Kellerer-Pirklbauer A. et al. (eds): *Thermal and geomorphic permafrost response to present and future climate change in the European Alps*. PermaNET project, final report of Action 5.3. On-line publication ISBN 978-2-903095-58-1, p. 109-118.

3.10 Cime Bianche Pass, Italian Alps

Pogliotti P, Cremonese E., Morra di Cella U. (2011). Chapter 3.10: Case studies in the European Alps – Cime Bianche Pass, Italian Alps. In Kellerer-Pirklbauer A. et al. (eds): *Thermal and geomorphic permafrost response to present and future climate change in the European Alps*. PermaNET project, final report of Action 5.3. On-line publication ISBN 978-2-903095-58-1, p. 119-128.

3.11 Maroccaro rock glacier, Val di Genova, Italian Alps

Seppi R., Baroni C. Carton A., Dall'Amico M., Rigon R., Zampedri G., Zumiani M. (2011). Chapter 3.11: Case studies in the European Alps – Maroccaro rock glacier, Val di Genova, Italian Alps. In Kellerer-Pirklbauer A. et al. (eds): *Thermal and geomorphic permafrost response to present and future climate change in the European Alps*. PermaNET project, final report of Action 5.3. On-line publication ISBN 978-2-903095-58-1, p. 129-139.

3.12 Amola rock glacier, Val d'Amola, Italian Alps

Seppi R., Baroni C. Carton A., Dall'Amico M., Rigon R., Zampedri G., Zumiani M. (2011). Chapter 3.12: Case studies in the European Alps – Amola rock glacier, Val d'Amola, Italian Alps. In Kellerer-Pirklbauer A. et al. (eds): *Thermal and geomorphic permafrost response to present and future climate change in the European Alps*. PermaNET project, final report of Action 5.3. ISBN 978-2-903095-58-1, p. 140-150.

3.13 Piz Boè rock glacier, Dolomites, Eastern Italian Alps

A. Crepaz A., Cagnati A., Galuppo A., Carollo F., Marinoni F., Magnabosco L., Defendi V. (2011). Chapter 3.13: Case studies in the European Alps – Piz Boè rock glacier, Dolomites, Eastern Italian Alps. In Kellerer-Pirklbauer A. et al. (eds): *Thermal and geomorphic permafrost response to present and future climate change in the European Alps*. PermaNET project, final report of Action 5.3. On-line publication ISBN 978-2-903095-58-1, p. 151-158.

3.14 Upper Sulden Valley, Ortler Mountains, Italian Alps

Zischg A., Mair V. (2011). Chapter 3.14: Case studies in the European Alps – Upper Sulden Valley, Ortler Mountains, Italian Alps. In Kellerer-Pirklbauer A. et al. (eds): *Thermal and geomorphic permafrost response to present and future climate change in the European Alps*. PermaNET project, final report of Action 5.3. On-line publication ISBN 978-2-903095-58-1, p. 159-169.

4. Synthesis of Case Studies

Lieb G.K., Kellerer-Pirklbauer A. (2011). Chapter 4: Synthesis of case studies. In Kellerer-Pirklbauer A. et al. (eds): *Thermal and geomorphic permafrost response to present and future climate change in the European Alps*. PermaNET project, final report of Action 5.3. On-line publication ISBN 978-2-903095-58-1, p. 170-177.

1.

Permafrost Response to Climate Change

Citation reference

Schoeneich P., Lieb G.K., Kellerer-Pirklbauer A., Deline P., Pogliotti P. (2011). Chapter 1: Permafrost Response to Climate Change. In Kellerer-Pirklbauer A. et al. (eds): *Thermal and geomorphic permafrost response to present and future climate change in the European Alps*. PermaNET project, final report of Action 5.3. On-line publication ISBN 978-2-903095-58-1, p. 4-15.

Authors

Coordination: Philippe Schoeneich

Involved project partners and contributors:

- Institut de Géographie Alpine, Université de Grenoble, France (IGA-PACTE) – Philippe Schoeneich
- Institute of Geography and Regional Science, University of Graz, Austria (IGRS) – Andreas Kellerer-Pirklbauer, Gerhard Karl Lieb
- EDYTEM, Université de Savoie, France (EDYTEM) – Philip Deline
- Regional Agency for the Environmental Protection of the Aosta Valley, Italy (ARPA VdA) – Paolo Pogliotti

Content

Summary

1. Introduction
2. Thermal permafrost response
3. Geomorphic permafrost response
4. Final remarks

References

Summary

Permafrost is defined as subsurface material that remains below 0°C also during the summer. Thus permafrost is a thermal phenomenon whose characteristics largely depend on the climatic conditions. This means that a changing climate also affects the thermal regime of the underground. The interactions between the atmosphere and the surface as well as the subsurface temperatures yet are highly complex depending on several environmental factors like e.g. the substrate itself (coarse-grained blocky material, fine-grained material, bedrock), the character of the relief (e.g. depression vs. ridge), the exposure relative to the sun or the snow cover characteristics (onset and disappearance date, length of snow cover period, thickness, dynamics).

In this chapter the occurrence types of frost and their altitudinal distribution is described first. Then permafrost reactions to climate change are discussed under two aspects – the thermal and the geomorphic one according to the already existing knowledge.

Main thermal reactions are: (a) increasing ground temperature and hence permafrost warming, (b) thawing of permafrost leading to reduction in its spatial extent, active layer thickening and changing ground-water circulation, (c) changes in the number of freeze-thaw cycles and magnitude of freezing and thawing periods.

Main geomorphic reactions are: (a) changes in the rate of rock glacier displacement, (b) changes in the displacement mode of rock glaciers, (c) changes in solifluction rates, (d) changes in cryogenic weathering, (e) changes in the volume and extent of unstable materials, (f) changes in frequency and magnitude of mass movement events, and (g) surface instabilities caused by thermokarst processes/melting of permafrost ice. Some of these geomorphic reactions are also true for non-permafrost periglacial areas, meaning alpine and subalpine environments at lower elevations.

Summing up it is shown here quite well that ongoing climate change has a number of complex influences on the ground temperature but also ground stability on the mountain permafrost of the European Alps.

1. Introduction

Permafrost is an effect of frost and negative temperatures and results from a negative energy balance at the ground surface. The energy balance mainly depends on the direct incoming solar radiation and on the sensible heat flux. Thus it is encountered in the Alps at high elevations, where air temperature (controlling the sensible heat flux) is low. Permafrost is more extensive and occurs at lower altitudes on north facing than on south facing slopes, because of a reduced incoming solar radiation due to slope angle and shadowing effects.

1.1 The occurrence types of frost

Permafrost is not the only effect of frost. Frost occurs at all altitudinal levels in the Alps, with various intensity and duration. One usually distinguishes the following occurrences of frost:

- *Diurnal freeze-thaw cycles* consist of the freezing and subsequent thawing of material during a night-day cycle or several consecutive days or weeks. They are driven by air temperature cycles. Climatologists define *frost days* (FD) as days where the minimum temperature is negative, and *ice days* (ID) as days where the maximum temperature remains below zero, hence inducing freeze conditions over at least one day. *Freeze-thaw days* (FTD) are defined as days with negative minimum and positive maximum temperature. In soil and rock, freeze-thaw cycles have to be distinguished according to their duration, intensity and penetration depth. Diurnal frost is usually of moderate intensity and has a limited penetration depth, whereas periods of consecutive very cold ice days have the highest penetration depth and intensity. Freeze-thaw cycles induce frost shattering of rocks and are the main controlling factor of debris production. To be efficient, the frost must have a minimal intensity and duration. Diurnal frost cycles have only a limited impact. Cycles of several days reaching temperatures of -5°C and less are considered to be most efficient.
- *Seasonal frost* defines material that experiences one annual freeze-thaw cycle, of a duration of at least several weeks up to several months, but with a total thawing during the warm season. Frost duration and depth depend more on the mean temperature than on individual cycles. Seasonal frost induces geomorphic processes like solifluction and similar shallow soil creeping phenomena.
- *Permafrost* is defined formally as a subsurface material (rock, debris or soil) that remains at a temperature below zero during the whole year. It consists of two parts: the surface layer, called *active layer* that thaws seasonally and refreezes during the cold season, and the *permafrost sensu strictu* that remains constantly below zero. From the climatic point of view, permafrost occurs where the annual heat balance is negative. Due to some characteristics of the surface layers (known as the thermal offset), this does not occur at the 0°C isotherm, but at a mean annual air temperature of -1 to -2°C. Permafrost is usually subdivided into continuous, discontinuous, sporadic and isolated permafrost, according to the percentage of the area covered by permafrost. The usual thresholds are the following ones but partly vary between authors (cf. French 2007):
 - *isolated*: less than 10% of the surface affected by permafrost
 - *sporadic*: between 10 and 50 % of the surface affected by permafrost
 - *discontinuous*: between 50 and 90 % of the surface affected by permafrost
 - *continuous*: more than 90 % of the surface affected by permafrost.

Furthermore, some authors distinguish:

- *cold permafrost*, with a mean ground temperature below -1°C
- *temperate* or *warm permafrost*, with a ground temperature close to 0 °C (typically -0.1 to -0.2 °C).

This point raises the question of the melting point temperature in permafrost, especially in an ice-debris mixture.

1.2 Altitudinal distribution

The various occurrences of frost show an altitudinal distribution, controlled by the altitudinal gradients of the controlling climate factors.

- *Diurnal freeze-thaw cycles* occur in winter at low altitudes, in spring and autumn at middle altitudes and in summer at high altitudes. Their maximal frequency is observed at middle altitudes. Intensity and duration of the freeze-thaw cycles increase with altitude.
- *Seasonal frost* occurs at middle altitudes and its duration and penetration depth increase with altitude. It passes to permafrost at high altitudes.
- *Permafrost* occurs sporadically at middle altitudes. At high altitudes discontinuous permafrost occurs, with a progressive transition to more continuous coverage with increasing altitude.

This altitudinal distribution of frost occurrences is associated with an altitudinal distribution of frost related processes and landforms:

- Frost shattering and talus production are related to freeze-thaw cycles.
- Shallow solifluction processes are related to seasonal frost.
- Deep creep processes (rock glaciers) are related to permafrost.

This altitudinal morpho-climatic distribution has been described by several authors, especially Chardon (1984, 1989) who distinguishes the following belts:

- The *infra-periglacial* belt is concerned by freeze-thaw cycles and seasonal frost, and processes are dominated by talus production and solifluction.
- The *periglacial belt* sensu stricto is concerned by discontinuous permafrost, and processes are dominated by solifluction and rock glaciers.
- The *supra-periglacial* belt is concerned by continuous permafrost. In the Alps it covers mainly rock faces and processes are dominated by episodic rockfalls and glaciers.

2. Thermal permafrost response

Climate warming induces an increase of air temperature, hence an increase of the sensible heat flux. Thus the energy balance should become less negative. A general warming of ground temperatures can therefore be expected.

However, climate warming will most probably neither change solar radiation nor altitudinal gradients, so that the overall altitudinal distribution of frost types and effects will remain, but is expected to shift towards higher altitudes.

Heat transfers from both solar radiation and heat flux to the ground are influenced by the snow cover. Thus the evolution of the ground temperature will not only depend on the evolution of the temperature, but also on the amount and type of winter precipitation and subsequently of the distribution, duration and thickness of the winter snow cover.

2.1 Migration of permafrost belts

Temperature changes will affect all phenomena related to frost: diurnal freeze-thaw cycles, seasonal frost as well as permafrost. In general, a climate warming should induce a migration of all climate related limits and belts towards higher altitudes. The following main changes can be expected:

- Concerning freeze-thaw cycles:
 - Lower frequency and intensity at middle altitudes
 - Migration of maximal frequency and intensity towards higher altitudes
 - Seasonal shift of cycle frequency towards earlier/later season
 - Increase of frequency at high altitudes
- Concerning seasonal frost:
 - Decrease of frequency and depth at middle altitudes
 - Decrease of depth and duration at higher altitudes
 - Replacement of permafrost by seasonal frost at the lower permafrost limit
- Concerning permafrost:
 - Disappearance of sporadic permafrost at middle altitudes
 - Migration of the lower permafrost limit towards higher altitudes
 - Replacement of continuous by discontinuous permafrost

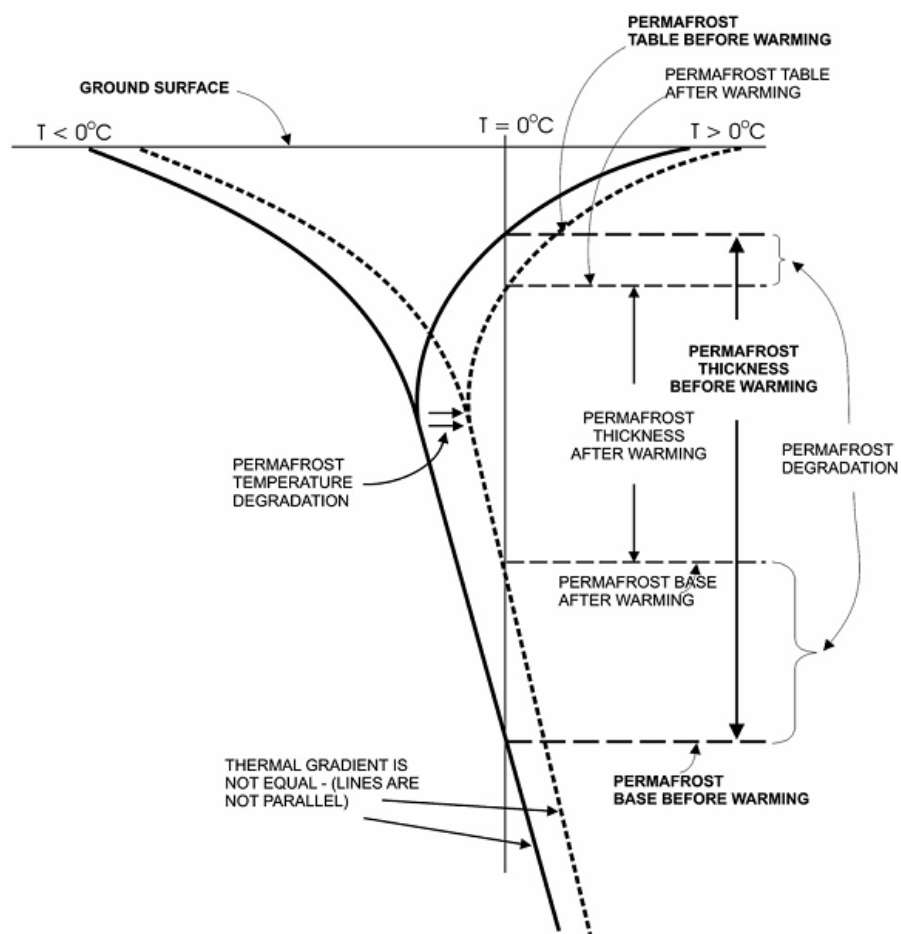


Fig. 1 - Processes which may occur within permafrost shown as a process of degradation (from Dobinski 2011).

2.2 Changes in thermal profiles of the ground

Temperature changes will affect permafrost mainly by the following processes visualised also in Fig. 1: (a) thickening of the active layer, (b) warming of the permafrost temperature, (c) reduction of the permafrost thickness, and (d) decrease of the ice content.

Increase of active layer thickness

The first effect of climate warming will be the increase of the active layer thickness. This responds directly to interannual variations. It depends both on the thermal state acquired during the preceding winter and on the summer temperature.

On rock glaciers there is often a strong contrast between the coarse blocky active layer and the underlying ice-rich and finer grained permafrost. In such cases, an increase of the active layer will induce a loss of ice at the permafrost table and a general lowering of the surface.

If the thawing of permafrost gets deeper than the seasonal frost depth, this seasonal freezing will not be able to refreeze the entire thawed layer, and a *talik* (=unfrozen layer) will remain during winter between the seasonally frozen surface layer and the residual deeper permafrost. This situation occurs when the permafrost warms up, and stops to be cooled from the surface. It can be transitional (after a particularly warm year) or permanent (inactivation of permafrost). Such situations are likely to occur in the future at the lower limits of discontinuous permafrost.

Warming of the permafrost

Due to a low thermal conductivity of the ground, the heat transfer towards depth is very slow, especially in ice-rich permafrost. It therefore can take years to propagate through the profile. The permafrost temperature is therefore expected to react rather to decadal trends than to interannual variations.

The downprofile propagation of *heat waves* can already be interpreted from some borehole profiles, where the minimal temperature is registered at a greater depth than the ZAA (zero annual amplitude). With time, a reduction of the cooling from the surface will also allow a warming from the bottom upwards, due to the geothermal heat flux.

The role of the snow cover

All above mentioned evolutions postulate a linear response of ground temperature to air temperature. However, ground surface temperature monitoring series show that the link is not straightforward. The snow cover plays an important role through its insulation capacity, and can induce significant deviations from the air temperature trends.

The onset and thickness of the snow cover in early winter plays the major role: in November to January, the days are the shortest and the direct radiation at a minimum, whereas air temperatures reach already very low values. If there is no snow cover, the soil will drastically cool down. A shallow snow cover may even increase the heat loss. On the contrary, an early and thick snow cover will prevent the soil from cooling and “keep” the accumulated heat of the previous summer and autumn. The snow cover history in early winter will thus largely determine the winter ground surface temperature, and the *winter equilibrium temperature* (WEqT), i.e. the mean ground surface temperature in February and March. On areas of seasonal frost, it will determine the freezing or no freezing of the soil, as well as the frost depth.

The thickness of the snow cover during the winter has of course also a great importance. A thick cover (at least ca. 0.8-1 m) insulates the ground from air temperature variations, and keeps the thermal state acquired during autumn and early winter. A shallow or discontinuous (through wind deflation) snow cover allows a continued cooling of the ground during the whole winter.

The duration of the snow cover in spring has an inverse effect than in early winter. A late snow melt prevents the soil from the direct solar radiation, in a period where it is at a maximum, and protects it from the sensible heat flux. On the contrary, an early snow melt will allow an earlier warming of the soil. Thus, the winter cooling effect of a shallow snow cover can be compensated by an earlier snow melt.

The effect of the snow cover is well visible on the interannual temperature variability. It can induce significant departures from the atmospheric temperature variations, e.g. cooling during rather moderate winters, or warming despite of cool winters. Its real influence on middle to long term temperature trends remains an open question. Temperature records in boreholes at ca 10 m depth show a distinct warming trend from 1987 to 1994, and then a stabilisation (PERMOS 2009), but no real cooling, unlike the surface temperatures.

The thermal evolution of permafrost, and more generally of ground temperatures, will thus depend on both air temperature and snow cover. Most climate models predict an increase of winter precipitations. If this occurs as snowfall, it can have various effects, depending on its seasonality:

- Early snow falls would increase warming
- A thick high winter snow cover will rather increase warming
- A late snow melt would prevent ground from warming.

The snow cover only impacts areas of moderate slopes where a thick snow cover can develop and stay during winter. On steep rock faces the snow cover has no influence.

2.3 Rates of change

As mentioned above, the heat transfer towards depth is very slow, especially in ice-rich permafrost. It therefore can take years to propagate through the profile. The permafrost temperature is therefore rather expected to react to decadal trends than to interannual variations. Model calculations show that it takes decades to reach a new equilibrium at depths of 20 to 30 m. In bedrock, the heat propagation can be much faster.

The role of ice content

The propagation of temperature changes into the soil is strongly dependent from the ice content. Due to the high amount of latent heat needed to melt ice, high ice content strongly reduces the thermal conductivity of the ground. One dimensional heat transfer models show that an ice content of 60% almost totally blocks the propagation of seasonal temperature variations, and that the melting of the ice body may need several decades.

From the thermal point of view, ice-rich permafrost is therefore less sensitive to climate change than “dry” permafrost. On the other hand, the high ice content can lead to subsidence and thermokarst phenomena, due to volume loss. In flat terrain the thawing of ice-rich permafrost therefore leads to greater disturbance and damage than the thawing of “dry” permafrost.

3. Geomorphic permafrost response

Climate change will affect both spatial distribution and intensity of frost related processes. As mentioned above, thermal effects of frost show a clear altitudinal distribution. Thus, the frost related geomorphic processes and landforms should migrate to higher altitudes, together with their driving climate parameters. This however will mainly happen through changes in magnitude (intensity, duration, frequency) of these processes. In addition to the altitudinal shift, some particular or even so far unknown phenomena may occur, due to transient states of ground conditions that are not usually observed under climatically stable conditions.

3.1 Frost shattering and debris production

Frost shattering and debris production are controlled by freeze-thaw cycles, and it is usually admitted that the maximal debris production occurs at altitudes of maximal cycle frequency, corresponding to spring and autumn cycles. This altitudinal range has been defined as the *talus window* (Hales & Roering 2005).

The *talus window* is thus expected to move towards higher altitudes. Some studies already show a decrease of talus production in the upper subalpine belt (Arquès 2005, Corona 2007), as well as a decrease of the torrential activity on talus supplied torrents (Garitte 2006). This evolution could lead to an overall decrease of geomorphic activity in middle altitudes, and favour the re-vegetation of scree slopes.

On the upper end, the normal state of high altitudinal rock walls in the continuous permafrost belt is a high stability of rock faces, with only limited sporadic debris supply from occasional rockfalls. These slopes where freeze-thaw cycles were yet limited to the summer season could experience an increase of talus production. Departure zones of rockfalls are frequently concentrated in the lower parts of the continuous permafrost belt. Both rockfalls and debris production are clearly related to warm periods during summer months, inducing a deepening of the heat penetration in rock faces (Deline & Ravanel 2011).

Regarding debris production from cliffs and rock faces, climate warming will induce significant effects on two different altitudinal levels:

- The *talus window* can be expected to shift towards higher altitudes. As a consequence, talus production should decrease in the lower parts, and increase in the upper parts of the belt. This belt is characterized by a regular production of small debris.
- A new belt of increased debris production is developing at the lower limit of the continuous permafrost belt. This belt is characterized by a sporadic production of coarse debris, up to large or even very large rockfalls. Due to often high and steep slopes, these processes can impact zones situated far lower downslope.

Indirect effects on other processes can be expected:

- Rock glaciers are usually situated in the upper part of the *talus window*. An increase of the talus production at this level could therefore induce an increase of the debris supply to rock glaciers. On a much longer time scale, the increase in volume of some talus bodies could induce the formation of new rock glaciers. However, fast climate warming and hence permafrost degradation will make the formation of new rock glaciers more difficult.
- Accumulation zones of glaciers are often situated at the foot of high altitude rock walls. An increase of sporadic debris supply from these rock walls will induce an increase of debris cover and debris content of the glaciers, and consequently an increase of the extent of debris cover on glaciers. This impact the dynamic of these glaciers as for instance the Miage Glacier

in Italy (Deline & Orombelli 2005) or the Pasterze Glacier in Austria (Kellerer-Pirklbauer *et al.* 2008).

3.2 Solifluction and seasonal frost

Solifluction phenomena are related to seasonal frost and need a sufficient frost depth in order to allow a water-saturated thawed layer to form in spring over a still frozen impermeable soil. After complete thawing, the soil drains and solifluction processes stop. A decrease of the seasonal frost depth will therefore induce a shortening of the activity period and hence a decrease of movement rates. For a more detailed classification of solifluction types refer to Matsuoka (2001).

In addition, some processes like bounded solifluction are connected with fine grained soils and with the presence of a vegetation cover. The upwards migration of such phenomena will depend on the presence of fine grained material and on the development of alpine meadows. Solifluction processes are very difficult to study and only few long-term monitoring sites are known in the Alps (e.g. Stingl *et al.* 2010). In general, there is a lack of data on seasonal frost and on related processes.

3.3 Rock glaciers

The most prominent features of Alpine permafrost are rock glaciers. They are also the most mobile ones. The possible evolution scenarios of rock glacier dynamics are therefore a central concern for Alpine mountain regions. Displacement time series and reconstructions of a dozen of rock glaciers throughout the Alps, indicate different types of behaviour at various time scales.

At the interannual timescale (Delaloye *et al.* 2008, Bodin *et al.* 2009, Kellerer-Pirklbauer & Lieb 2011):

- Most rock glaciers show interannual velocity variations, and thus react to climate variability.
- These velocity variations are best correlated with a 12 month running mean of the ground surface temperature.
- The velocity variations show a time lag of ca 1 year towards air and ground temperature.
- These variations are reversible with warming leading to a velocity increase and cooling to a velocity decrease. The velocity rates remain in the range of 0.1 to a few m/y^{-1} .

Some rock glaciers have shown a distinct change in dynamic behaviour during the last decades or years, with a strong increase of velocities on parts or the whole of the rock glacier (e.g. Avian *et al.* 2005). Several types of behaviours can be distinguished (see PermaNET report 6.2 for study cases and more detail):

- Strong acceleration with opening of crevasses. The velocities increase by an order of magnitude, up to several m/y^{-1} . Crevasses show that the deformation rates exceed the flow capacity of the ice.
- Rupture and dislocation of the lower part of the rock glacier. In these cases, a distinct rupture with a scarp appears in the rock glacier and separates the lower, fast part, from the upper, “normal” moving part.
- Total collapse of the lower part. Only one case is known yet, where the lower part totally collapsed into a mudflow (Krysiecki *et al.* 2008).
- Extreme acceleration of the rock glacier. One case is known, with velocities of several tens of m/y^{-1} (Delaloye *et al.* 2010).

All these evolutions are apparently not reversible, but observation times are not yet sufficient to know the end of the story. The accelerated lower parts tend to dislocate, whereas the upper parts possibly form a new rock glacier front. Several questions arise:

- Interannual variations are hard to explain. One possible explanation could be a higher plasticity of ice with higher temperature. However, the main deformation rates occur in the basal layer of rock glaciers, as shown by the few existing inclinometer profiles. The thermal conductivity of ice-rock mixtures is very low, and it is unlikely that interannual temperature variations reach the bottom of the ice-rich body. Another explanation could be an increased presence of interstitial water, facilitating internal movements between ice grains.
- The very high velocity increase observed on accelerating rock glaciers (some authors even talk about “surging” rock glaciers) implies a change of displacement mode. Rock glaciers are usually considered to move at the same way as cold based glaciers, by deformation of ice and shear of the basal ice layer. Velocities of several m/y^{-1} and even more seem to indicate the onset of a basal sliding. This would mean that these rock glaciers have changed from a “cold glacier” to a “temperate glacier” displacement mode. The latter point is crucial for future development, and has to be related to the question of the melting point temperature.
- The conditions that lead a rock glacier to accelerate or not are unknown yet. The presence of a convex slope seems to be necessary for the onset of strong accelerations of the lower part (e.g. Avian *et al.* 2005). The total collapse occurred on a rock glacier made of fine material, and is possibly unlikely to happen on a coarse blocky rock glacier.

From these considerations, the following most probable evolution scenarios can be proposed:

- Interannual variations will continue. Velocity increases are expected to happen mainly after very hot summers associated with snow rich winters. Such episodes may occur more frequently and on an increasing number of rock glaciers.
- Strong accelerations are likely to occur on an increasing number of rock glaciers.
- Acceleration episodes are a transient state, and will last only as long as the ice content is sufficient to allow creeping. After ice loss is sufficient and the permafrost is no longer supersaturated with ice, movements should slow down and stop.
- Total collapse or extreme accelerations will possibly remain exceptional cases, but a better knowledge is requested in order to be able to evaluate their probability.

3.4 Thermokarst phenomena

If permafrost is supersaturated in ice, the melting of ice due to permafrost degradation induced a volume loss of the substrate affected which leads to instabilities at the surface and finally to settlement of the surface. These processes can especially be observed in areas with low inclinations where they create a more rugged topography than it has existed before. If there is an impermeable layer beneath (e.g. the permafrost table itself) thermokarst lakes may get formed.

Settlement processes do not only lower the surface and change its topography but are also of special significance for buildings and other infrastructures because they create the need to adapt the constructions in order to avoid damage.

4. Final remarks

Table 1 gives an overview of the thermal and geomorphic reactions of permafrost to climate change as they can be expected according to considerations given in the previous paragraphs. The changes listed in the table served as guidelines for carrying out the case studies in Chapter 3 and interpreting the results which are summarized in Chapter 4.

Table 1 - Possible thermal and geomorphic permafrost reactions relevant for PermaNET.

Possible thermal permafrost reactions
Increasing ground temperature (in bedrock, fine and coarse sediments) and hence permafrost warming
Thawing of permafrost with three effects: (1) reduction in the spatial extent of permafrost, (2) active layer thickening, and (3) increasing ground-water circulation and pressure
Changes in the number of freeze-thaw cycles and magnitude (duration and intensity) of freezing and thawing periods
Possible geomorphic permafrost reactions
Changes in the rate of rock glacier displacement (vertically and horizontally)
Changes in displacement mode of rock glaciers (initiation of basal sliding, collapse)
Changes in solifluction rates*
Changes in cryogenic weathering (freeze-thaw cycles, ice segregation)*
Changes in the volume and extent of unstable/unconsolidated materials
Changes in frequency and magnitude of mass movement events (e.g. rock fall, rock slide, debris flow)*
Surface instabilities caused by thermokarst processes/ melting of permafrost ice*

*not strictly related to only permafrost but to periglacial environments in general

Monitoring of permafrost temperature is performed on three different kinds of permafrost sites primarily using miniature temperature dataloggers (MTD) or thermistor-chains located in boreholes (from very shallow to deep):

- Permafrost and active layer in bedrock (from near-vertical rock walls to flat morphologies)
- Permafrost and active layer in fine grained material (rather flat morphology)
- Permafrost and active layer in coarse grained and blocky material (scree slopes, rock glaciers; from steep slopes to rather flat morphologies)

Climate conditions at permafrost sites are monitored by meteorological stations. Monitoring of dynamic conditions in permafrost environments is carried out by geodetic, photogrammetric, terrestrial laserscanning (LiDAR or TLS), differential SAR interferometry (DINSAR) and DGPS techniques as well as visual observations and calculations. This monitoring focuses on:

- Mass movement (e.g. rock fall) frequency and magnitude
- Rate of rock glacier displacement (vertically and horizontally)
- Physical weathering (freeze-thaw cycles)

To sum up Action 5.3 uses a wide range of methods in the assessment of the thermal and dynamic reaction scenarios of different permafrost typologies. Research in this action is carried out in two steps: (i) Establishment of the relationship between measured climate data and observed thermal and geomorphic permafrost reactions (Table 1) using available datasets collected during the last years and decades (*cf.* Chapter 3). (ii) Combining the established relationships with data from the climate scenario for the year 2050 presented in Chapter 2 forms the basis for estimations of future changes in permafrost distribution (vertically and horizontally), in the active layer thickness or in the rates of rock glacier displacement.

References:

- Arquès S., 2005: *Géodynamique et biodiversité des versants asylvatiques du massif de la Grande Chartreuse. Evolution liée au réchauffement climatique et problème de gestion*. Thèse Université Joseph Fourier, Grenoble.
- Avian M., Kaufmann V. & Lieb G.K., 2005: Recent and Holocene dynamics of a rock glacier system: The example of Hinteres Langtalkar (Central Alps, Austria). *Norwegian Journal of Geography*, 59, 149-156.

- Bodin X., Thibert E., Fabre D., Ribolini A., Schoeneich P., Francou B., Reynaud I. & Fort M., 2009: Two decades of responses (1986–2006) to climate by the Laurichard rock glacier, French Alps. *Permafrost and Periglacial Processes*, 20, 331-344.
- Chardon M., 1984: Montagne et haute montagne alpine, critères et limites morphologiques remarquables en haute montagne. *Revue de Géographie Alpine* 72(2-4): 213-224.
- Chardon M., 1989: Essai d'approche de la spécificité des milieux de la montagne alpine. *Revue de Géographie Alpine* 77(1-3): 15-18.
- Corona C., 2007: *Evolution biostatique du paysage, géodynamique nivéo-périglacière et fluctuations climatiques récentes dans la haute vallée de la Romanche (Alpes du Nord, France)*. Thèse Université Joseph Fourier, Grenoble.
- Deline P. & Orombelli G., 2005: Glacier fluctuations in the western Alps during the Neoglacial, as indicated by the Miage morainic amphitheatre (Mont Blanc massif, Italy). *Boreas*, 34: 456–467.
- Deline P. & Ravanel L. (2011). Chapter 3.9: Case studies in the European Alps – Rockfalls in the Mont Blanc massif, French-Italian Alps. In Kellerer-Pirklbauer A. et al. (eds): *Thermal and geomorphic permafrost response to present and future climate change in the European Alps*. PermaNET project, final report of Action 5.3. On-line publication ISBN 978-2-903095-58-1.
- Delaloye R., Perruchoud E., Avian M., Kaufmann V., Bodin X., Hausmann H., Ikeda A., Käab A., Kellerer-Pirklbauer A., Krainer K., Lambiel C., Mihajlovic D., Staub B., Roer I., Thibert E., 2008: Recent interannual variations of rockglacier creep in the European Alps. *9th International Conference on Permafrost*, Fairbanks, University of Alaska: 343–348.
- Delaloye R., MORARD S., Abbet D., Hilbich C., 2010. The Slump of the Grabengufer Rock Glacier (Swiss Alps). *3rd European Conference on Permafrost (EUCOP III)*, Svalbard, Norway: 157.
- Dobinski W., 2011: Permafrost. *Earth-Science Reviews* 108: 158–169.
- French HM., 2007: *The Periglacial Environment. 3rd edition*. West Sussex: John Wiley and Sons, 458 pp.
- Garitte G., 2006: *Les torrents de la vallée de la Clarée (Htes Alpes, France). Approche géographique et contribution à la gestion du risque torrentiel dans une vallée de montagne*. Thèse Université scientifique et technique de Lille.
- Hales TC, Roering JJ., 2005: Climate-controlled variations in scree production, Southern Alps, New Zealand. *Geology* 33: 701-704.
- Kellerer-Pirklbauer A. & Lieb G.K., 2011: Recent rock glacier velocity behaviour and related natural hazards in the Hohe Tauern Range, central Austria. PermaNET Project Report - Contribution of IGRS to Action 6.2/Group 1 – Rock glacier.
- Kellerer-Pirklbauer A., Lieb G.K., Avian M. & Gspurning J. 2008: The response of partially debris-covered valley glaciers to climate change: The Example of the Pasterze Glacier (Austria) in the period 1964 to 2006. *Geografiska Annaler*, 90 A (4): 269-285.
- Krysiecki, J.M., Bodin, X., Schoeneich, P., 2008. Collapse of the Bérard Rock Glacier (Southern French Alps). *9th International Conference on Permafrost*, Fairbanks, University of Alaska: 153–154.
- Matsuoka N., 2001: Solifluction rates, processes and landforms: a global review. *Earth Science Reviews*, 55, 107-134.
- PERMOS 2009: *Permafrost in Switzerland 2004/2005 and 2005/2006*. Nötzli J., Naegeli B., Vonder Mühl D. (eds). Glaciological Report Permafrost N° 6/7, Cryospheric Commission of the Swiss Academy of Sciences.
- Stingl, H., Garleff, K., Höfner, T., Huwe, B., Jaesche, P., John, B. and Veit, H., 2010: Grundfragen des alpinen Periglazials - Ergebnisse, Probleme und Perspektiven periglazialmorphologischer Untersuchungen im Langzeitprojekt „Glorer Hütte“ in der Südlichen Glockner-/ Nördlichen Schobergruppe (Südliche Hohe Tauern, Osttirol). *Salzburger Geographische Arbeiten*, 15-42.

2.

Temperature Change in the European Alps

Citation reference

Kroisleitner Ch., Reisenhofer S., Schöner W. (2011). Chapter 2: Climate Change in the European Alps. In Kellerer-Pirklbauer A. et al. (eds): *Thermal and geomorphic permafrost response to present and future climate change in the European Alps*. PermaNET project, final report of Action 5.3. On-line publication ISBN 978-2-903095-58-1, p. 16-27.

Authors

Coordination: Christine Kroisleitner

Involved project partners and contributors:

- Central Institute for Meteorology and Geodynamics (ZAMG) – Christine Kroisleinter, Stefan Reisenhofer, Wolfgang Schöner

Content

Summary for decision makers

1. Temperature change in the recent past
2. Projected temperature change until 2050

References

Summary

The air temperature in the European Alps has increased by about 2°C since the late 19th century. The warming was particularly pronounced since the beginning of the 1980s. The temperature increase was associated with degradation of the Alpine permafrost. This paper summarizes the observed changes of air temperature and uses results from climate model simulations to derive future scenarios of air temperature in the Alps for the period 2021-2050. In order to provide more relevant information on thermal response of permafrost the paper uses an empirical model to relate air temperature data to number of frost days, number of ice days and number of freeze-thaw days for the Alps at altitudes above 1800m a.s.l. for both the present climate (reference period 1961-90) and for a future climate 2021-2050. The model results show that highest numbers of freeze-thaw days are simulated for altitudes of 1800m a.s.l. (even higher values are modeled for lower elevations) with about 100 days per year and decreasing number of freeze-thaw days with increasing elevation. Moreover, the model shows that the number of freeze-thaw days will generally increase for altitudes above 1800m a.s.l. by values up to 4 days a year until 2021-2050, thus increasing the weathering at all elevations above 1800m a.s.l.

1. Temperature change in the recent past

The Alps as one of the major topographic forms in Europe influences the atmospheric circulation over a wide range of scales. The consequences of this fact are a variety of different climates, from maritime to continental and from lowland to mountainous. In a climate analysis of the Greater Alpine Region (GAR) Brunetti *et al.* (2009) highlighted an average GAR warming trend of about 1.3°C over the common period covered by all the climate variables (1886-2005), 1.4°C for the reference IPCC-period (1906-2005) which is a warming about twice as large as the global trend referred to by IPCC (2007). Furthermore, Brunetti *et al.* (2009) found out, that for the GAR region the majority of the warmest years in the period 1774-2005 were measured in the past 15 to 20 years. The most extreme summer was found for 2003, whereas the most extreme summer cold event happened in 1816 after the volcanic eruptions of Tambora. It is worth noticing that the 2003 summer temperature was 4.2 standard deviations above the corresponding 2003 summer normal value, but the 1816 cold extreme was only 2.6 standard deviations lower than the summer normal value corresponding to summer 1816.

The 20th century climate in Europe varied not only in time, but also from location to location. 1900 to 1940, the mean annual air temperature (MAAT) increased in western and northern Europe, while most of the remaining part of the continent experienced only small changes. From 1940 to 1975 was a period of cooling in the arctic, but in continental Europe just the northern part was affected by this trend. The eastern part of Europe experienced a slight warming during that time and the southern part kept nearly constant. In the period 1975-2000 widespread climate warming in Europe was recorded. Generally the South-West of Europe and Scandinavia were most affected, but seasonally there were large regional deviations from this annual trend. In winter the temperature in northern and western Europe was increasing, whereas in spring the temperature rose especially in the central and south-western parts. Summer temperatures were characterized by an increase all over Europe, most pronounced in the southern part. Autumn's temperature was mainly characterized by its spatial variability (Harris *et al.*, 2009).

Climate change in the past 250 years in the Alps has been extensively studied in the project HISTALP (Auer *et al.*, 2007). The HISTALP database covers the Greater Alpine Region (GAR) with monthly homogenised records of temperature, pressure, precipitation, sunshine and cloudiness for times dating back to 1760 for temperature and 1800 for precipitation. The long-term warming trend visible in the seasonal and annual mean temperature time series of GAR could not be confirmed for other climate parameters, like precipitation, for which Auer *et al.* (2005) detected two antagonistic trends, a wetting trend in the North-west of the Alps (since the 1860s) and a drying trend in the South-east (since 1800). Remarkably, even the highest mountain observatories within the Alps such as Sonnblick, Jungfrauoch and Zugspitze show the same temperature trends as Munich, Vienna, Milano or Sarajevo. The global mean temperature series show only half of the long-term warming of the Alps since the mid-19th century.

2. Projected temperature changes until 2050

2.1 Introduction

As in the past, the Alps will also in future be exposed to a stronger warming than the earth in general. According to the IPCC (2007) scenarios, the temperature for whole Europe will rise for 3.3°, whereas the Alps will have to face a temperature rise of 3.9°C until the end of the 21st century (Figure 1). In the high-mountain areas above 1500m a.s.l. the warming from climate model projections could be even higher (4.2°C ; EEA Report No. 8, 2009).

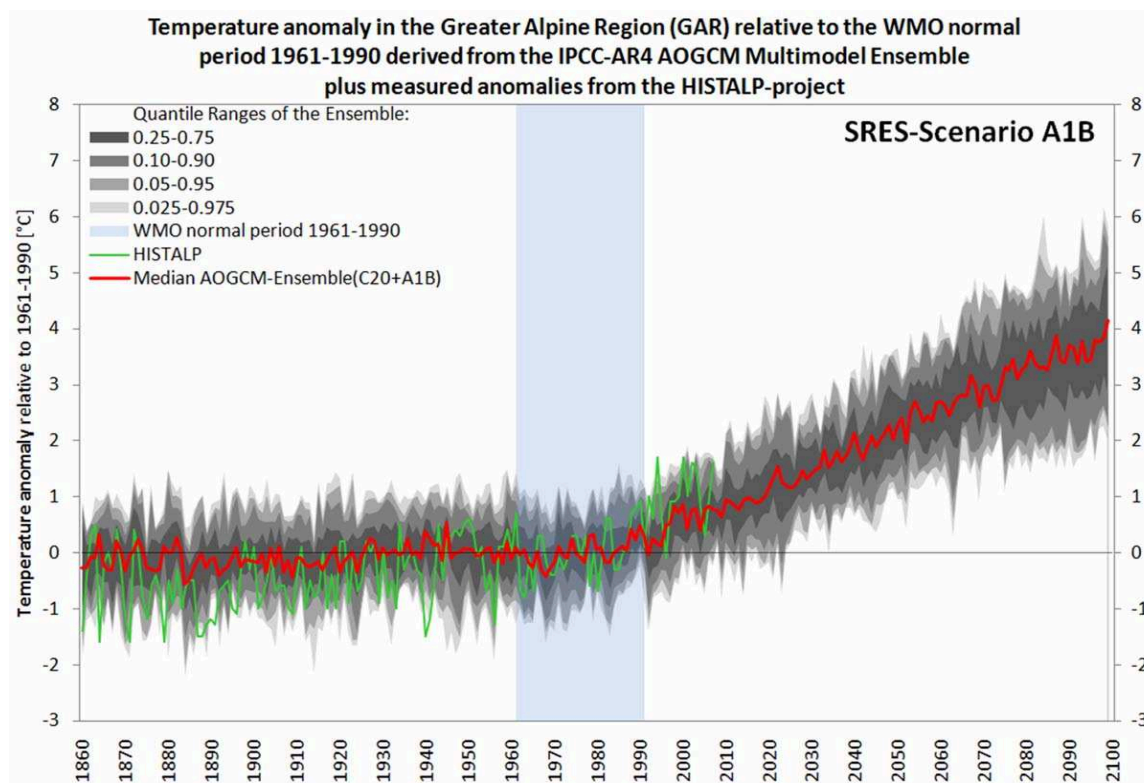


Fig. 1 – Temperature anomaly 1860 to 2100 for the Greater Alpine Region (GAR) relative to the WMO normal period 1961-1990 derived from the IPCC-AR4 AOGCM Multimodel Ensemble (anthropogenic and natural forcing prior to 2001, anthropogenic forcing only from 2001-2100). The green line shows measured temperature anomalies from the HISTALP-project. (Source: Schöner *et al.*, 2011).

2.2 Experimental design

Although permafrost in the high mountain areas is not very well known yet, it is obvious that there is a relationship to climatic elements. However, if this relationship would be easy to describe, it would have been done decades ago. The relationship of near-surface permafrost temperatures and air temperature is strongly affected by snow thickness and duration, which are themselves driven by atmospheric conditions (Harris *et al.*, 2009). This investigation does not focus on change in the permafrost-distribution, but on the change in atmospheric frost-behaviour. The presence of frost above the earth's surface is crucial for the existence of permafrost, but furthermore for the development and conservation of a snowcover.

The core of this investigation is the comparison of frost-, ice-, and freeze-thaw days between the climate periods 1961-90 and 2021-2050. A day becomes classified as frost day (FD), when the daily minimum temperature is below zero. If also the daily maximum temperature is below the freezing point, the day is classified as ice day (ID). The difference between ice days and frost days, which means all days with a daily minimum temperature below 0°C and a daily maximum above this limit, get classified as freeze-thaw days (FTD). It is obvious from future climate scenarios, that frost frequency will get less.

According to the climatic trend, several Alpine regions experienced a decrease in frost frequency (FF) and an extension of the frost-free season (Auer *et al.* 2005). In Austria observations indicate, that during the 20th century a reduction of the frost season by 17 days in the flat eastern region (Vienna) and by 22 days in the high Alpine region around the mountain peak station of Sonnblick (3100m a.s.l.) has happened.

It can be assumed, that in a warmer climate the intensity of frost weathering changes, caused by the spreading of the freeze-thaw-cycles-zone to higher altitudes. How this change could happen in an A1B climate scenario was investigated for the high mountainous zone of the entire Alps above 1800m a.s.l.

2.3 Empirical approach to estimate frost days, ice days and freeze-thaw days

Auer *et al.* (2005) found an empirical relationship of a tangens hyperbolicus function to estimate frost frequency (FF) from monthly mean air temperature. FF is defined by the number of frost days divided by the number of days within the considered month. The tanh-function was calculated using temperature data from 363 climate stations in Austria including the high alpine station Sonnblick (3105 m a.s.l.). Auer *et al.* (2005) calculated at least 66% FF (20.5 FD) for January in Austria for all stations. In April the FF covered a wide spectrum, from 100% (30 FD) at the mountain peak station Sonnblick to nearly no frost in the lowlands. In July only at the mountain station Sonnblick frost days were registered. Hence, without taking into account high-elevation mountain stations it would be impossible to receive robust coefficients for the model. Overall, the tanh-model was able to explain about 55% of the the variance of FF data from air temperature data. Validation of the model with data from the entire GAR showed that there is almost no difference in the performance if the models are calibrated on Austrian data or on data for the entire GAR (see Auer *et al.*, 2005, for details).

In contrary to Auer *et al.* (2005) in our study we used 30-years climate normals (1961-90) to relate annual frost days to annual air temperature means, which significantly increased the performance of statistical relationships. This approach is motivated from the aim of this study to compare present mean climate with a future climate mean scenario for both frost days and ice days. Consequently, the frequency of ice days (as the number of ice days divided by the number of days within the considered month) were related in a same manner to mean annual air temperature using a tanh-fit for the reference period 1961-90. The statistics of the derived tanh-models are shown in Tables 1 and 2. In a final step the freeze-thaw days were calculated from the difference between ice days and frost days.

Table 1 –Statistical model (general model, coefficients and goodness of fit) in order to compute annual frost day frequency (f(x)) from annual air temperature (x)for the reference period 1961-90

General model	Coefficients (with 95% confidence bounds)	Goodness of fit
$f(x) = 50+(50*\tanh(a*x+b))$	a=-0.09316 (-0.0947, -0.09163) b=0.3437 (0.3328, 0.3546)	SSE: 3530 R-square: 0.9847 Adjusted R-square: 0.9847 RMSE: 2.77

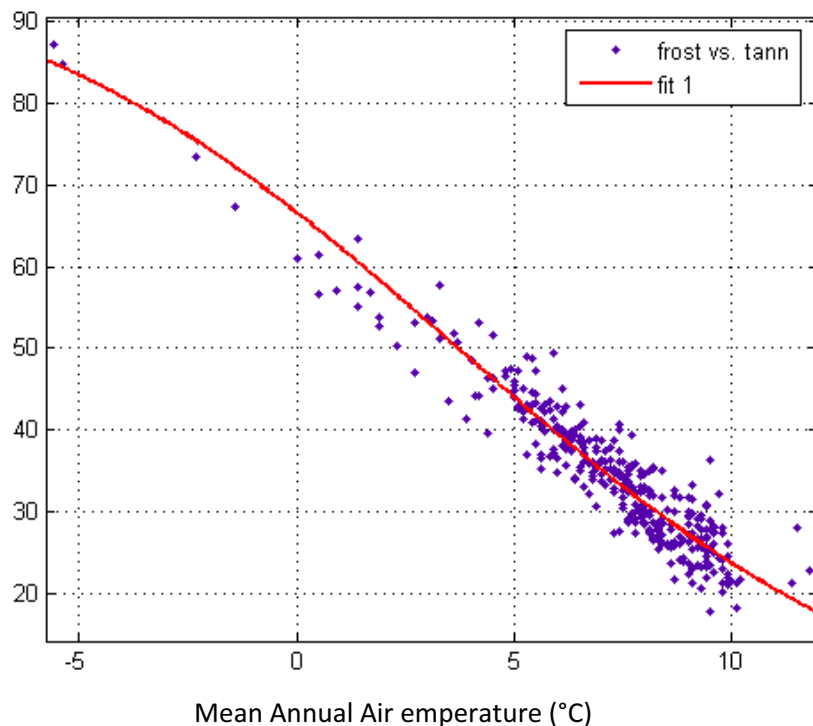


Fig. 2 – Ratio frost days to total days versus mean annual air temperature in Austria using data from 363 climate stations in Austria for the period 1961-90. The red line is a tanh-fit. Statistical measures of the fit are shown in Table 1.

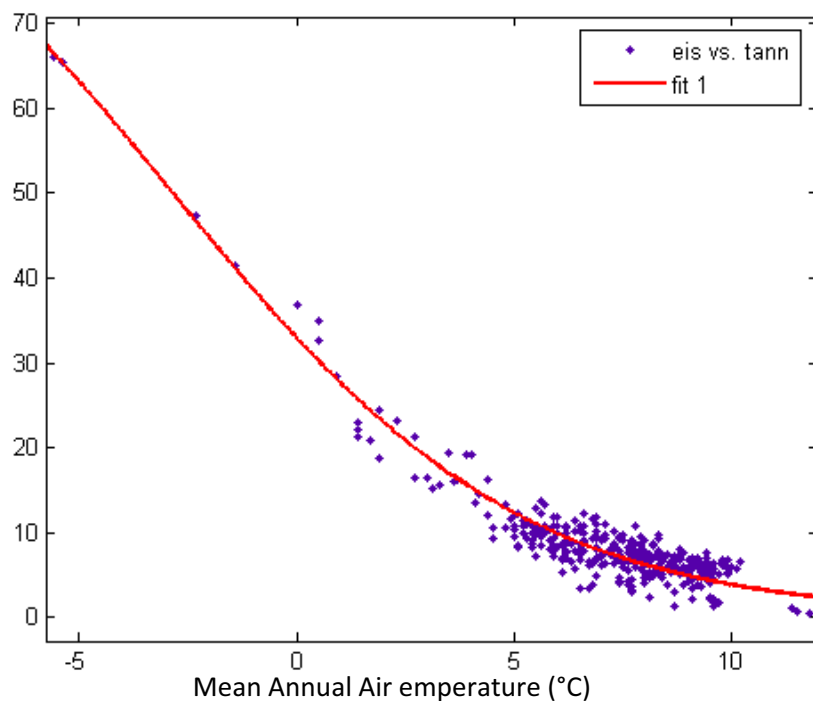


Fig. 3 – Ratio ice days to total days versus mean annual air temperature in Austria using data from 363 climate stations in Austria for the period 1961-90. The red line is a tanh-fit. Statistical measures of the fit are shown in Table 2.

Table 2 – Statistical model (general model, coefficients and goodness of fit) in order to compute annual ice day frequency $f(x)$ from annual air temperature (x) for the reference period 1961-90

General model	Coefficients (with 95% confidence bounds)	Goodness of fit
$f(x) = 50 + (50 * \tanh(a * x + b))$	a=-0.1248 (-0.1259, -0.1236) b=-0.3573 (-0.3638, -0.3507)	SSE: 1323 R-square: 0.9951 Adjusted R-square: 0.995 RMSE: 1.696

2.4 Empirical approach to estimate frost days, ice days and freeze-thaw days for the entire Alps

We used the spatially high-resolution temperature climatology of Hiebl *et al.* (2009) to compute the number of frost days, the number of ice days and the number of freeze-thaw days for the Alpine region for both the present climate and the future climate 2021-2050. However, our study was restricted to the Alpine area above 1800m a.s.l. as the zone most relevant for permafrost. In a first step the ~1km resolution GAR monthly temperature climatology (1961-90) was downscaled using the ~30m-resolution ASTER GDEM for the high mountain area of the Alps. The temperature-grid was recalculated according to the approach of Hiebl *et al.* (2009), which he used for the development of the ~1km spatial resolution GAR-climatology based on 1961-1990 climate normals. The work of Hiebl *et al.* (2009) is based on a station network of 1,726 climate stations for the Greater Alpine Region, which were carefully quality checked and homogenized.

According to Hiebl *et al.* (2009) we used several geographical variables to compute air temperature by means of a multilinear regression approach:

- The longitudinal gradients take into account the underlying oceanic to continental transition, which occurs from the western to the eastern edge of the GAR. However, the variance of temperature explained from longitude is limited to 1% of the annual variance.
- On the contrary to this small amount, latitude explained 19% of the variance of annual air temperature by mainly capturing the effect of the South-North solar radiation gradient on temperature.
- As expected, the largest part of temperature variance could be explained by elevation. The vertical regression model explains as much as 69% of the temperature variance for the yearly averages, although during winter due to stable atmospheric layering the value decreases to around 45%.
- For considering different temperature behaviours at low altitude areas and high altitude areas Hiebl *et al.* (2009) introduced a 3 vertical layers-model. The lowest layer ranges from 600m in the southern parts up to 800m in the western parts of the GAR. The high elevation layers vertical extent begins at 1800m a.s.l. Between the two layers the temperatures were simply interpolated. In our study we used only the highest (above 1800m a.s.l.) layer.
- Slopes got implemented in the model by using an analysis of Auer & Böhm (2003) which systematically analysed data from 85 Austrian sites with detailed site description. They found

monthly deviations from the mean for North- and South-facing slopes ranging from -0.2 to 1.0°C.

- Maritime influence was taken into account by establishing a topographically weighted field of distances from the coast. Hiebl *et al.* (2009) found a surprisingly strong dependency of temperature on distance from the coast. At a yearly average the distance to the coast variable explained 41% of the temperature variance.

The 30year high-alpine monthly mean temperatures were calculated from the following regression equation:

$$t01 = 9.412932 + -0.190362 * [\text{lon}_1] + -0.035543 * [\text{lat}_1] + -0.005002 * [\text{DEM}] + -0.003347 * [\text{coast}]$$

[lon_1] → longitude

[lat_1] → latitude

[DEM] → digital elevation model

[coast] → coast distance grid

As shown by Hiebl *et al.* (2009), considering longitude, latitude and the distance from the coasts besides elevation reduced the average monthly standard error to 0.79°C per month. Furthermore Hiebl *et al.* (2009) used the GTOPO30-DEM with a spatial resolution of 30 arc seconds, which corresponds to about 1km. GTOPO30 has a root mean square error of about 18m. Applied on monthly lapse rate models, the DEM inaccuracy leads to a temperature error of 0.09 °C on average.

In this study we used the empirical temperature model of Hiebl *et al.* (2009) but replaced the GTOPO30-DEM by the ASTER GDEM, thus refining the spatial resolution of temperature grid to 1 arc second (~30m). Compared to GTOPO, with an error of surface elevation of about 18m, the ASTER GDEM has an overall root mean square error of 10.87m. The error of surface elevation can be assumed to be approximately 20m at a confidence level of 95%.

Based on the refined climatology (climate normal 1961-90) of annual air temperature and the empirical models for frost days (Tab. 1 and Fig. 2) and for ice days (Tab. 2 and Fig. 3) 30m-raster data of climate normals (reference period 1961-90) of frost days and ice days for the Alpine region were computed.

2.5 Estimation of future frost, ice and freeze-thaw-cycles days scenarios for the period 2021-2050

For projecting the temperature of the Alps for the future period 2021-2050 we used the regional climate model experiment of Hollweg *et al.* (2008) which dynamically downscaled the ECHAM5-MPIOM-A1B scenario (Röckner *et al.*, 2003) by means of the regional climate model CLM. The performance of this CLM model run for the GAR was extensively tested in Schöner *et al.* (2011). Particularly, it was shown by Schöner *et al.* (2011) that compared to an ensembles simulation for the Alpine region (used from the PRUDENCE ensembles; see Frei *et al.*, 2006) the used CLM simulation shows a temperature change which lies close to the ensembles median. The spatial pattern of the temperature change for 2021-2050 relative to 1976-2007 derived from the CLM simulation is shown in Figure 4. The spatial resolution of the CLM grid is 18x18km.

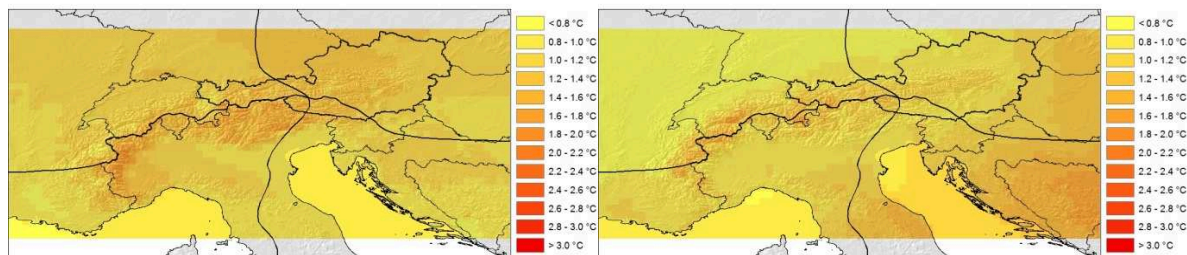


Fig. 4 - Change of seasonal mean temperature (left: winter season, right: summer season) for the Greater Alpine Region for 2021-2050 relative to 1976-2007 (from Schöner et al., 2011, source for CLM data : Hollweg et al., 2008).

The spatial distributions of the number of frost days, the number of ice days and the number of freeze-thaw days for the climate reference period 1961-90 for the region of the European Alps with elevations higher 1800m a.s.l. are shown in Figures 5, 6 and 7. The highest number of freeze-thaw days were computed for lowest elevations close to 1800m a.s.l. With higher elevations the number of freeze-thaw days decreases from about 100 days at 1800m a.s.l. to less than 15 days at highest elevations of the Alps. Changes in the number of frost days, the number of ice days and the number of freeze-thaw days are displayed in Figures 8, 9 and 10 for the period 2021-2050 relative to 1961-90 based on the temperature change from the CLM simulations. Temperature increase will generally increase the number of freeze-thaw days by numbers up to 4 days per year, thus increasing also the frost weathering.

Acknowledgements. – The digital elevation model was contributed by METI and NASA to the Global Earth Observation System of Systems (GEOSS) and was downloaded from the Earth Remote Sensing Data Analysis Center (ERDSAC) of Japan and NASA's Land Process Distributed Active Archive Center (LP DAAC) <http://asterweb.jpl.nasa.gov/gdem.asp>. Climate model results of CLM regional climate model were provided by Deutsches Klimarechenzentrum within the frame of the project *Anpassungsstrategien an den Klimawandel für Österreichs Wasserwirtschaft*.

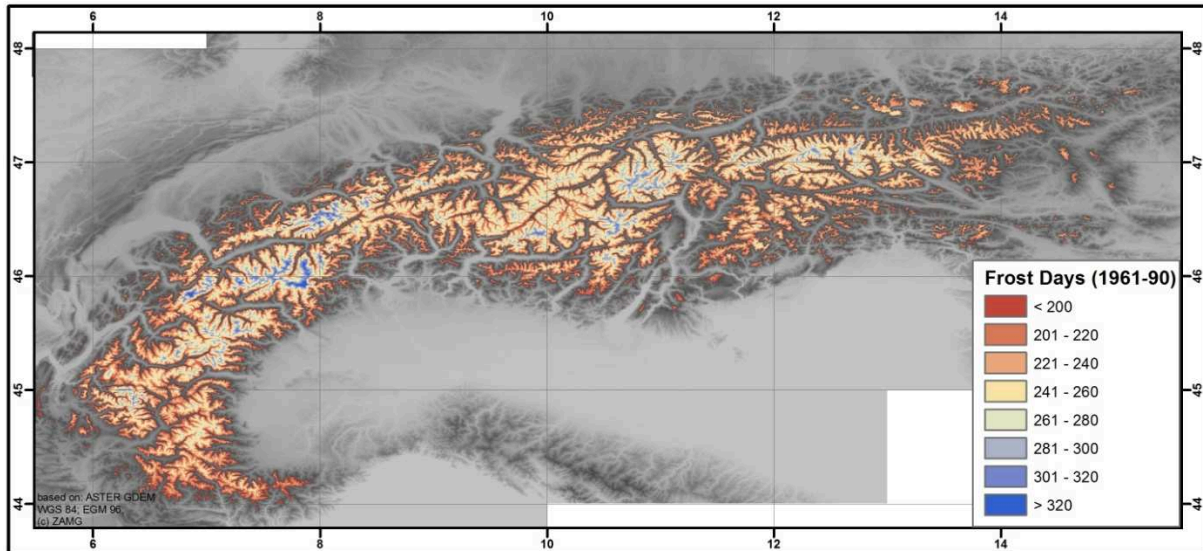


Fig. 5 – Frost days (1961-90) in the Alps for the subregion with elevation above 1800m a.s.l.

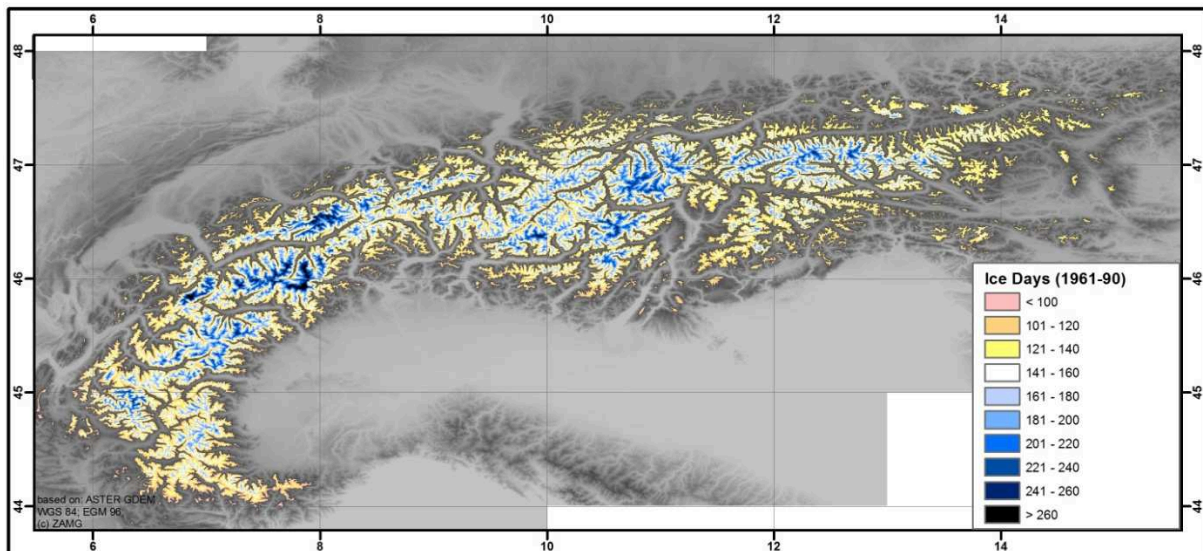


Fig. 6 – Ice days (1961-90) in the Alps for the subregion with elevation above 1800m a.s.l.

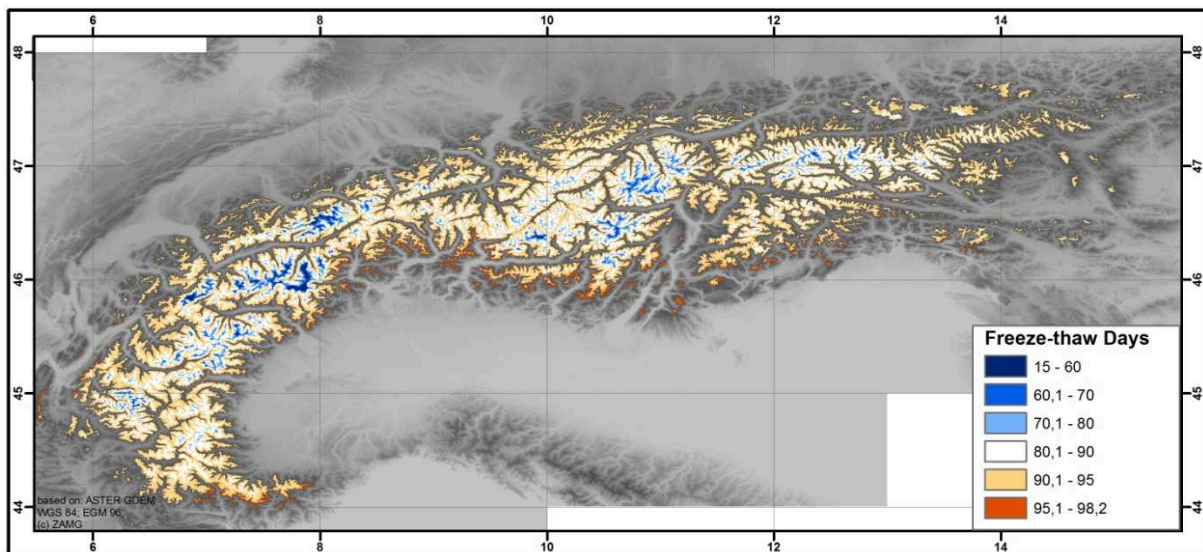


Fig. 7 – Freeze-thaw days (1961-90) in the Alps for the subregion with elevations above 1800m a.s.l.

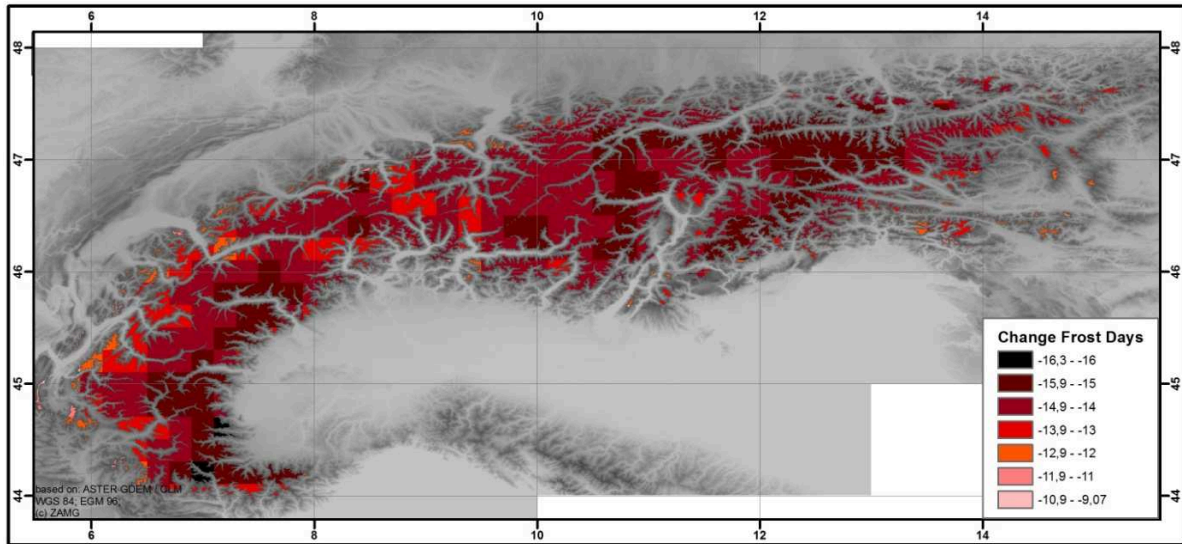


Fig. 8 – Estimated difference in frost days between 1961-90 and 2021-2050 for the subregion with elevations above 1800m a.s.l.

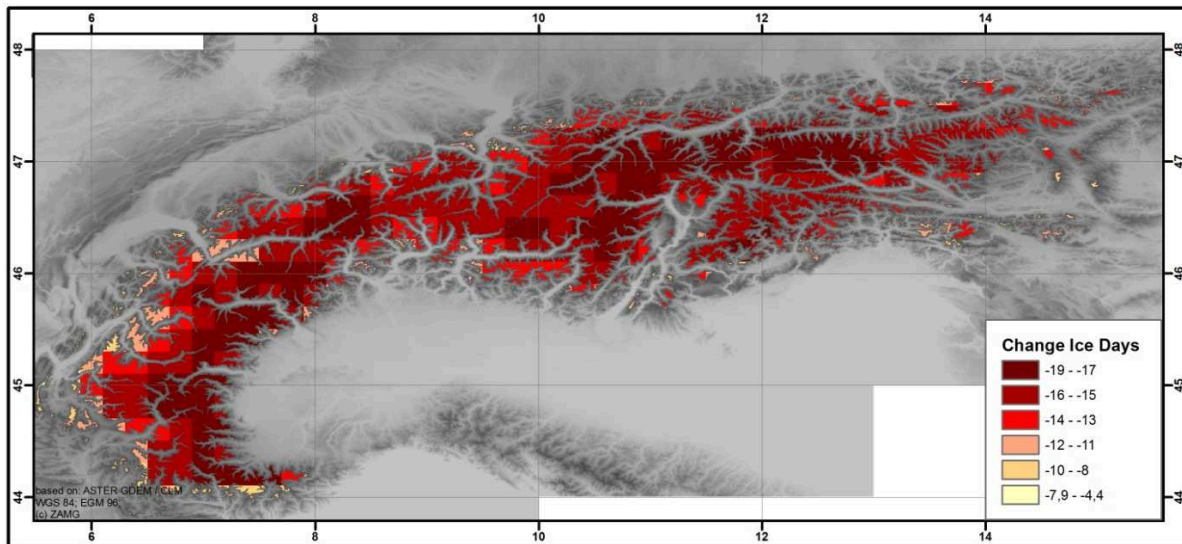


Fig. 9 – Estimated difference in ice days between 1961-90 and 2021-2050 for the subregion with elevations above 1800m a.s.l.

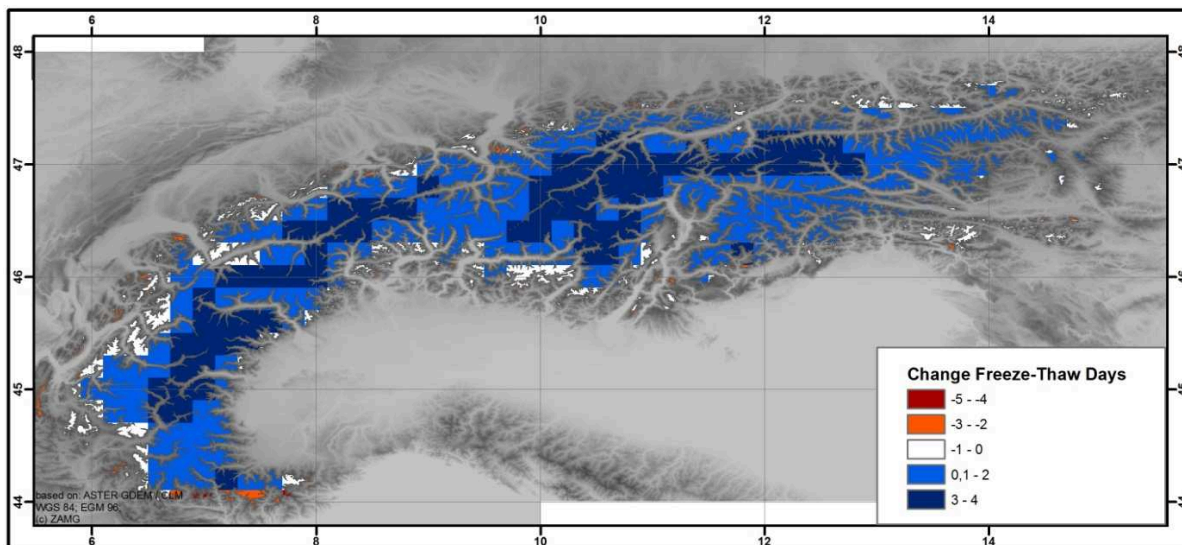


Fig. 10 – Estimated difference in freeze-thaw days between 1961-90 and 2021-2050 for the subregion with elevations above 1800m a.s.l.

References:

- ASTER GDEM Validation Team, 2009: METI/ERSDAC, NASA/LPDAAC, USGS/EROS, (2009): ASTER Global DEM Validation Summary Report, June 2009
- Auer I. & Böhm R., 2003: Jahresmittel der Lufttemperatur. *Hydrologischer Atlas Österreichs*. Österreichischer Kunst- und Kulturverlag, Vienna, Map Sheet 1.6.
- Auer I., Matulla C., Böhm R., Ungersböck M., Maugeri M., Nanni R., Pastorelli R., 2005: Sensitivity of frost occurrence to temperature variability in the European Alps. *Int. Journal of Climatology*, 25, 1749-1766.
- Auer I., Böhm R., Jurkovic A., Lipa W., Orlik A., Potzmann R., Schöner W., Ungersböck M., Matulla Ch., Briffa K., Jones P., Efthymiadis D., Brunetti M., Nanni T., Maugeri M., Mercalli L., Mestre O., Moisselin J.-M., Begert M., Müller-Westermeier G., Kveton V., Bochnicek O., Stastny P., Lapin M., Szalai S., Szentimrey T., Cegnar T., Dolinar M., Gajic-Capka M., Zaninovic K., Majstorovic Z. & Nieplova E. 2007: HISTALP – Historical instrumental climatological surface time series of the Greater Alpine Region 1760-2003. *International Journal of Climatology*, 27, 17-46.
- Brunetti M., Lentini G., Maugeri M., Nanni R., Auer I., Böhm R., Schöner W., 2009: Climate variability and change in the Greater Alpine Region over the last two centuries based on multi-variable analysis. *Int. Journal of Climatology*, Vol. 29, Issue 15, 2197-2225 DOI: 10.1002/joc.1857
- EEA Report No. 8, 2009: Regional climate change and adaptation. The Alps facing the challenge of changing water resources. *European Environment Agency*, Copenhagen, 143pp.
- Frei C., Schöll R., Fukutome S., Schmidli J., Vidale P. L., 2006 : Future change of precipitation extremes in Europe: Intercomparison of scenarios from regional climate models. *Journal of Geophysical Research*, 111: D06105
- Harris C., Arenson L. U., Christiansen H. H., Etzelmüller B., Frauenfelder R., Gruber S., Haeberli W., Hauck C., Hölzle M., Humlum O., Isaksen K., Käab A., Kern-Lütschg A.M., Lehning M., Matsouka N., Muron J.B., Mötzli J., Philips M., Ross N., Seppälä M., Springman S.M., Vonder Mühll D., 2009: Permafrost and climate in Europe: Monitoring and modelling thermal, geomorphological and geotechnical responses. *Earth-Science Reviews*, 92, 117-171.
- Hiebl J., Auer I., Böhm R., Schöner W., Maugeri M., Lentini G., Spinoni J., Brunetti M., Nanni T., Tadić Perčec M., Bihari Z., Dolinar M., Müller-Westermeier G., 2009: A high-resolution 1961-1990 monthly temperature climatology for the Greater Alpine Region. *Meteorologische Zeitschrift*, 18, 507-530.
- Hollweg H. D., Böhm U., Fast I., Hennemuth B., Keuler K., Keup-Thiel E., Lautenschlager M., Legutke S., Radtke K., Rockel B., Schubert M., Will A., Woldt M., Wunram C., 2008 : Ensemble simulations over Europe with the regional climate model CLM forced with IPCC AR4 Global Scenarios. *M & D Technical Report*, 3, 2008.
- IPCC, 2007: Climate Change 2007: The Physical Science Basis. Contribution from the Working Group I to the Fourth Assessment Report of the Intergovernmental Panel on Climate Change. Cambridge University Press: Cambridge, United Kingdom and New York, NY, USA, 996pp.
- Röckner E., Bäuml G., Bonaventura L., Brokopf R., Esch M., Giorgetta M., Hagemann S., Kirchner I., Kornblueh L., Manzini E., Rhodin A., Schlese U., Schulzweida U., Tompkins A., 2003: The atmospheric general circulation model ECHAM-5, Part I: Model description. *Max-Planck-Institut für Meteorologie, Report 349*.
- Schöner W., Böhm R., Haslinger K., 2011: Klimaänderung in Österreich – hydrologisch relevante Klimaelemente. *Österr. Wasser- und Abfallwirtschaft* 1-2/2011, 11-20

3.

Case studies in the European Alps

3.1

Overview on case studies

Citation reference

Kellerer-Pirklbauer A, Lieb G.K. (2011). Chapter 3.1: Case studies in the European Alps – Overview on case studies. In Kellerer-Pirklbauer A. et al. (eds): *Thermal and geomorphic permafrost response to present and future climate change in the European Alps*. PermaNET project, final report of Action 5.3. On-line publication ISBN 978-2-903095-58-1, p. 28-34.

Authors

Coordination: Andreas Kellerer-Pirklbauer

Involved project partners and contributors:

- Institute of Geography and Regional Science, University of Graz, Austria (IGRS) – Andreas Kellerer-Pirklbauer, Gerhard Karl Lieb

Content

Summary

1. The regional distribution of the case studies
2. Project partners and research activities
3. Structure of the case studies

References

Summary

The case studies provide information relevant of the reactions of permafrost to climate change from study sites which are distributed between 47°22' and 44°59'N and between 06°10' and 14°41' E, respectively, covering a great part of the Alpine Arc. From a spatial point of view, the results thus can be considered sufficiently representative for the entire Alps. The methodology used covers a broad spectrum of techniques making the results well reliable.

All the activities were carried out by scientific institutions which are well provided with best local field experience and in many cases with regional actor networks. All the case studies have a similar conceptual structure beginning with a short presentation of the site, then giving concise information on the methods used and the results elaborated.

Each case study finally provides some assumptions on the future development of permafrost in the respective area taking into account the climate scenario presented in Chapter 2.

1. The regional distribution of the case studies

The assessment of thermal and dynamic reaction scenarios of different permafrost sites is carried out at 13 sites within the European Alps. Figures 1 and 2 depict the location of the study sites within the Alpine Arc as well as visual impressions of the study sites. Table 1 gives an overview for each of these study sites. The study sites are distributed between 47°22' and 44°59' N and between 6°10' and 14°41' E, respectively, with Hochreichart (A) being the northernmost and easternmost and Bellecombes (F) the westernmost and southernmost site. Thus the sites cover a great part of the Alpine Arc with the exception of the Swiss Alps (which are missing due the composition of the project staff). The sites also cover the most important geological units of the Alps (e.g. metamorphic rocks of the Central Zone of the Eastern Alps and limestones of the Southern Alps as well as granites of the Central Massives of the Western Alps). Thus, in terms of the geographical distribution, the results can be considered sufficiently representative for the entire Alps.

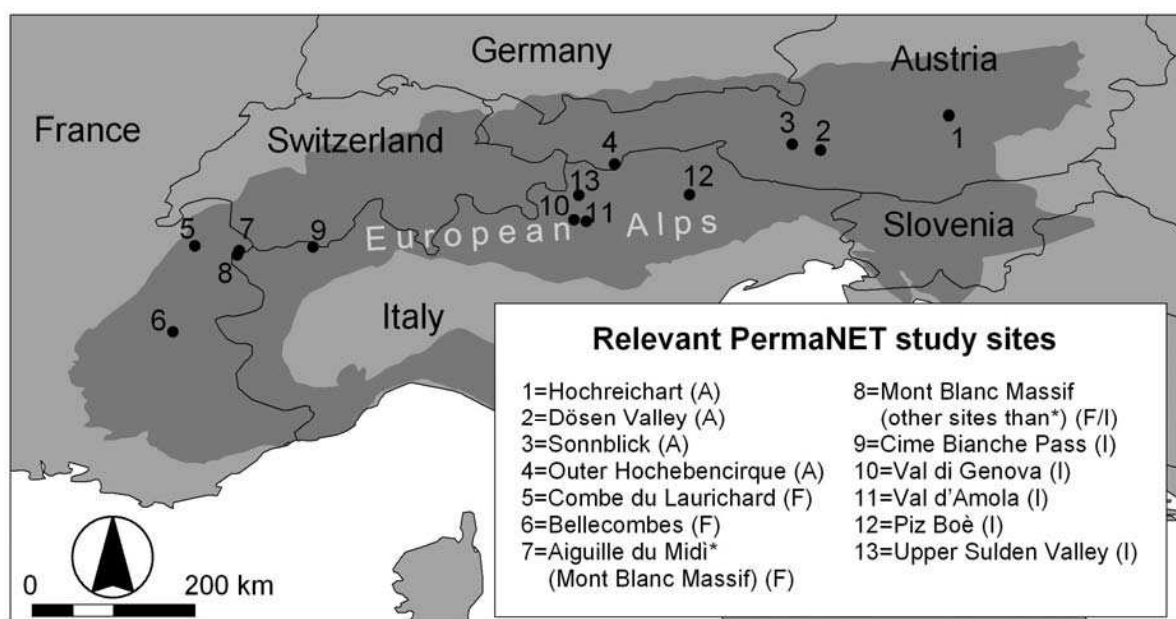


Fig. 1 – Location of the 13 PermaNET study sites relevant for the assessment of thermal and dynamic reaction scenarios of different permafrost sites in the European Alps.

2. Project partners and research activities

Table 1 gives an overview on the study sites containing for each one its name, country, location, elevation, studied landform and processes, research initiation, type of permafrost monitoring site and the institution which has responsibly coordinated the documentation of the respective case study. All persons involved in elaborating the case studies are kindly acknowledged and listed in Table 2. Information on the relevance of the character of the different permafrost monitoring sites as well as landforms and processes is given in Chapter 4.

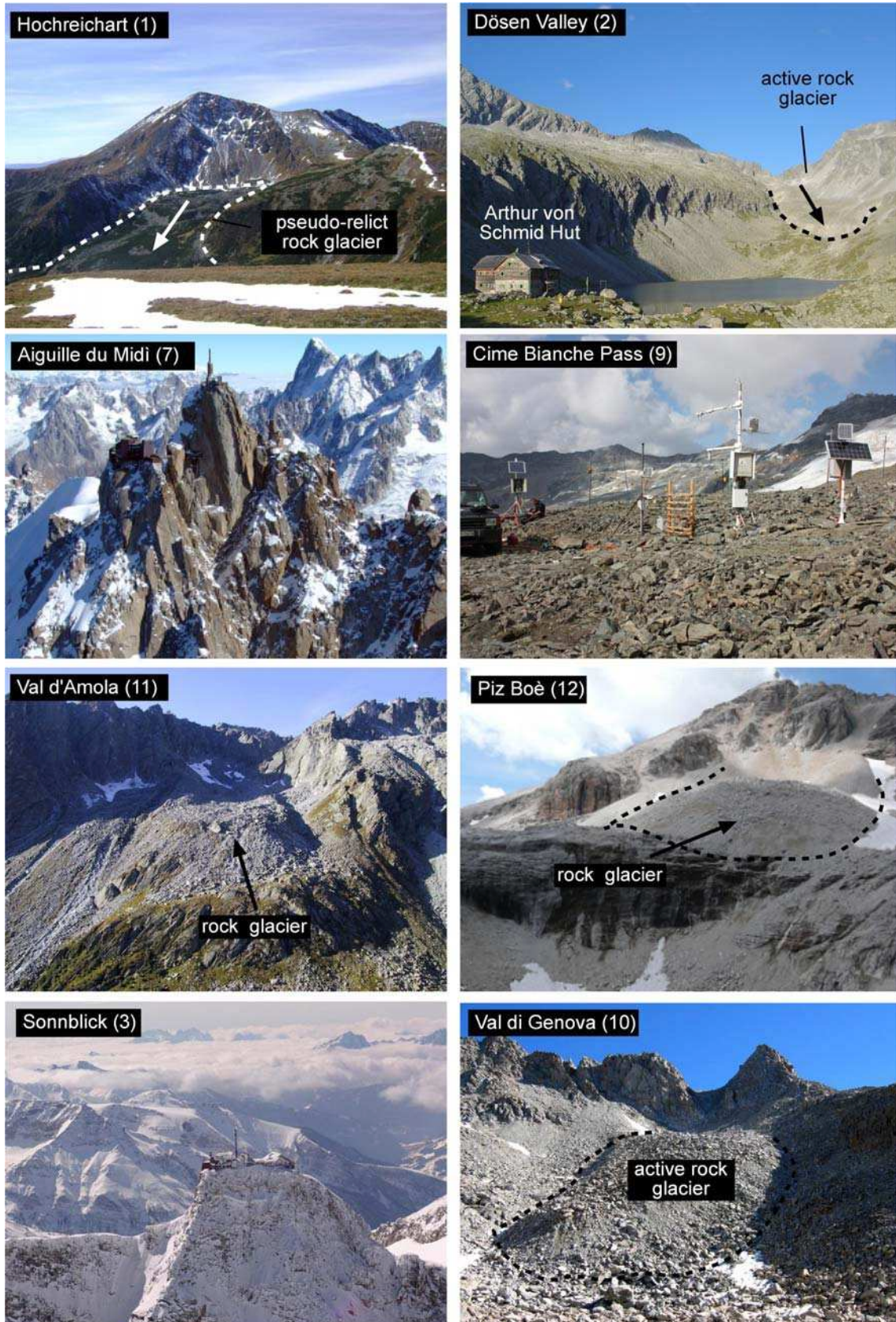


Fig. 2 – Visual impressions of 9 of the 13 PermaNET study sites relevant for the assessment of thermal and dynamic reaction scenarios. The numbers in brackets refer to the numbers in Fig. 1. The study sites range from just below 2000 m a.s.l. (study site Hochreichart) to about 4000 m a.s.l. (study sites in the Aiguille du Midi). All photographs provided by the authors.

Table 1 – Overview of the study sites investigated in order to assess the thermal and dynamic reaction of permafrost to climate change in the Alps within action 5.3 of the project PermaNET. The different types of permafrost monitoring sites are: **PF-bedrock**=Permafrost in bedrock (from near-vertical rockwalls to flat morphologies); **PF-fine**=Permafrost in fine-grained material (flat morphology); **PF-coarse**=Permafrost in coarse-grained and blocky material (scree slopes, rock glaciers; from slopes to rather flat morphologies). Project partners and collaborators: **ARPA VdA**=Regional Agency for the Environmental Protection of Valle d'Aosta, Aosta, Italy; **ARPAV**=Environment Protection Regional Agency of Veneto; **UIBK**=Institute of Geology, University of Innsbruck, Innsbruck, Austria; **IGRS**=Institute of Geography and Regional Science, University of Graz, Graz, Austria; **ZAMG**=Central Institute for Meteorology and Geodynamics, Vienna, and Regional Office for Salzburg and Upper Austria, Salzburg, Austria; **IGA-PACTE**=Institut de Géographie Alpine, University of Grenoble, France; **EDYTEM**=EDYTEM Lab, Université de Savoie; **Uni Pavia**=Earth Science Department, University of Pavia, Pavia, Italy; **Abenis**=Abenis Alpinexpert GmbH/srl, Bozen/Bolzano, Italy.

Name of study site (code see Fig. 1)	Con.	Latitude	Longitude	Elevation range/ max. (m a.s.l.)	Main studied landform or process	Re-search initiation	Permafrost monitoring site	Coordinator's institution
Hochreichart (1)	A	47°22'N	14°41'E	1920-2415	rock glacier, rock wall, detritus	2004	PF-bedrock PF-coarse	IGRS
Dösen Valley (2)	A	46°59'N	13°17'E	2400-3000	rock glacier, rock wall	1995	PF-bedrock PF-fine PF-coarse	IGRS
Hoher Sonnblick (3)	A	47°03'N	12°57'E	3105	bedrock, detritus	2007	PF-bedrock PF-coarse	ZAMG
Outer Hocheben Cirque (4)	A	46°50'	11°01'	2360-2840	rock glacier	1938	PF-coarse	UIBK
Combe du Laurichard (5)	F	45°56'N	06°24'E	2450-2630	rock glacier	1979	PF-coarse	IGA-PACTE
Bellecombes (6)	F	44°59'N	06°10'E	2600-2800	rock glacier	2007	PF-coarse	IGA-PACTE
Aiguille du Midi* (Mont Blanc Massif) (7)	F	45°53'N	06°53'E	3840	near-vertical rockwalls	2005	PF-bedrock	EDYTEM
Mont Blanc Massif (other sites as*) (8)	F	45°50'N	06°52'E	3000-4000	near-vertical rockwalls	2006	PF-bedrock	EDYTEM
Cime Bianche Pass (9)	I	45°55'N	07°41'E	3100	bedrock, detritus	2005	PF-bedrock PF-coarse	ARPA VdA
Val di Genova (10)	I	46°13'N	10°34'E	2750-2860	rock glacier	2001	PF-coarse	Uni Pavia
Val d'Amola (11)	I	46°12'N	10°42'E	2330-2480	rock glacier	2001	PF-coarse	Uni Pavia
Piz Boè (12)	I	46°30'N	11°50'E	2900-2950	rock glacier	2005	PF-coarse PF-bedrock	ARPAV
Upper Sulden Valley (13)	I	46°30'N	10°37'E	2600-3150	detritus	1992	PF-coarse PF-fine	Abenis Alpinexpert

Table 2 – Persons involved in elaborating the case studies of Action 5.3 and their affiliations.

Name	Institution	Case study (Chapter)
Baroni, Carlo	University of Pisa (Italy)	3.11., 3.12.
Bodin, Xavier	University Joseph Fourier, Grenoble (France)	3.6.
Cagnati, Anselmo	Regional Agency for the Environmental Protection of Veneto (Italy)	3.13.
Carollo, Federico	E.P.C. European Project Consulting S.r.l. (Italy)	3.13.
Coviello, Velio	National Center for Scientific Research EDYTEM, Grenoble (France)	3.8.
Cremonese, Edoardo	Regional Agency for the Environmental Protection of the Aosta Valley (Italy)	3.8., 3.10.
Crepaz, Andrea	Regional Agency for the Environmental Protection of Veneto (Italy)	3.13.
Dall'Amico, Matteo	Mountain-eering srl (Italy)	3.11., 3.12.
Defendi, Valentina	Regione Veneto, Direzione Geologia e Georisorse, Servizio Geologico (Italy)	3.13.
Deline, Philip	National Center for Scientific Research EDYTEM, Grenoble (France)	editor, 3.8., 3.9.
Drenkelfluss, Anja	University of Bonn (Germany)	3.8.
Galuppo, Anna	Regione Veneto, Direzione Geologia e Georisorse, Servizio Geologico (Italy)	3.13.
Gruber, Stephan	University of Zurich (Switzerland)	3.8.
Kellerer-Pirklbauer, Andreas	University of Graz (Austria)	editor, 3.2, 3.3
Kemna, Andreas	University of Bonn (Germany)	3.8.
Klee, Alexander	Central Institute for Meteorology and Geodynamics (Austria)	3.4.
Krainer, Karl	University of Innsbruck (Austria)	3.5.
Krautblatter, Michael	University of Bonn (Germany)	3.8.
Krysiecki, Jean-Michel	University Joseph Fourier, Grenoble (France)	3.6.
Le Roux, Olivier	Association pour le développement de la recherche sur les glissements de terrain (France)	3.7.
Lieb, Gerhard Karl	University of Graz (Austria)	editor, 3.2, 3.3
Lorier, Lionel	Association pour le développement de la recherche sur les glissements de terrain (France)	3.7.
Magnabosco, Laura	Regione Veneto, Direzione Geologia e Georisorse, Servizio Geologico (Italy)	3.13.
Magnin, Florence	National Center for Scientific Research EDYTEM, Grenoble (France)	3.8.
Mair, Volkmar	Autonomous Province of Bolzano (Italy)	3.14.
Malet, Emmanuel	National Center for Scientific Research EDYTEM, Grenoble (France)	3.8.
Marinoni, Francesco	Freelancer (Italy)	3.13.
Morra di Cella, Umberto	Regional Agency for the Environmental Protection of the Aosta Valley (Italy)	3.8., 3.10.
Noetzli, Jeanette	University of Zurich (Switzerland)	3.8.
Pogliotti, Paolo	Regional Agency for the Environmental Protection of the Aosta Valley (Italy)	editor, 3.8., 3.10.
Ravel, Ludovic	National Center for Scientific Research EDYTEM, Grenoble (France)	3.8., 3.9.
Riedl, Claudia	Central Institute for Meteorology and Geodynamics (Austria)	3.4.
Rigon, Riccardo	University of Trento (Italy)	3.11., 3.12.
Schöner, Wolfgang	Central Institute for Meteorology and Geodynamics (Austria)	editor, 3.6., 3.7.
Seppi, Roberto	University of Pavia (Italy)	3.11.
Vallon, Michel	University Joseph Fourier, Grenoble (France)	3.7.
Zampedri, Giorgio	Geological Survey, Autonomous Province of Trento (Italy)	3.11., 3.12.
Zischg, Andreas	Abenis Alpinexpert GmbH/srl (Italy)	3.14.
Zumiani, Matteo	Geologist (Italy)	3.11., 3.12.

3. Structure of the case studies

In order to facilitate the comparison between the different case studies all of them use more or less the same structure as follows:

- Summary
- Short introduction into the case study site and the relevant landform (in most cases with detailed maps and photographs)
- Methodology (in most cases a set of different methods has been used, see discussion in Chapter 4)
- Recent thermal and/or geomorphic evolution of the relevant landform(s) (in most cases with graphs, for the covered time spans see discussion in Chapter 4)
- Assumptions on possible future thermal/geomorphic response of this landform to predicted climate change (taking into account the climate scenario presented in Chapter 2)
- Reference list.

3.

Case studies in the European Alps

3.2

Hochreichart, Eastern Austrian Alps

Citation reference

Kellerer-Pirklbauer A (2011). Chapter 3.2: Case studies in the European Alps – Hochreichart, Eastern Austrian Alps. In Kellerer-Pirklbauer A. et al. (eds): *Thermal and geomorphic permafrost response to present and future climate change in the European Alps*. PermaNET project, final report of Action 5.3. On-line publication ISBN 978-2-903095-58-1, p. 35-44.

Authors

Coordination: Andreas Kellerer-Pirklbauer

Involved project partners and contributors:

- Institute of Geography and Regional Science, University of Graz, Austria (IGRS) – Andreas Kellerer-Pirklbauer

Content

Summary

1. Introduction and study area
2. Permafrost indicators and recent thermal evolution
3. Possible future thermal response to predicted climate change

References

Summary

Knowledge regarding marginal permafrost zones in the European Alps is fairly limited. A permafrost research project in the Seckauer Tauern, focusing particularly on the Mt. Hochreichart-Reichart Cirque area (47°22'N, 14°41'E), Austria, was initiated in 2004 by the author. Since 2006, the research activities were carried out within the projects *ALPCHANGE* and *PermaNET*. Based on geomorphic mapping, numerical permafrost modelling, multi-annual measurements of the bottom temperature of the snow cover (BTS), continuous measurements of ground surface, near ground surface and air temperatures by miniature temperature dataloggers (MTD), geoelectrics and optical snow-cover monitoring by a remote digital camera (RDC) the existence of permafrost was proven. Patches of permafrost are strongly related to elevation, aspect, grain size of the sediments, and characteristics of winter snow cover. Therefore, the study site is the most easterly evidence of existing permafrost found in the entire European Alps at 14°41'E in elevations as low as 1900 m asl. Predicting climate warming will substantially influence the permafrost distribution and geomorphic dynamics in the study area Hochreichart-Reichart Cirque. By 2050, permafrost will be almost completely thawed apart from few high-elevated sites where the substrate material (coarse-blocky material) and topoclimatic conditions (radiation, snow cover) still allow small patches of permafrost.

1. Introduction and study area

Mountain permafrost is a widespread phenomenon in alpine regions in the European Alps. For instance, some 2000 km² or 4% of the Austrian Alps are underlain by permafrost (Lieb 1998). Up to recent times most research on permafrost issues in Austria focused on the central and highest section of the Austrian Alps. By contrast, knowledge concerning marginal permafrost zones is fairly limited so far.

To increase knowledge about the easternmost limit of permafrost in the European Alps, a research project focusing on the Seckauer Tauern Mountains (14°30'E to 15°00'E) and particularly on the Mt. Hochreichart area (47°22'N, 14°41'E) was initiated in 2004 by the author (Fig. 1). First permafrost results were published in Kellerer-Pirklbauer (2005). The research activities were continued between 2006 and 2010 within the project *ALPCHANGE* and since 2008 within *PermaNET*.

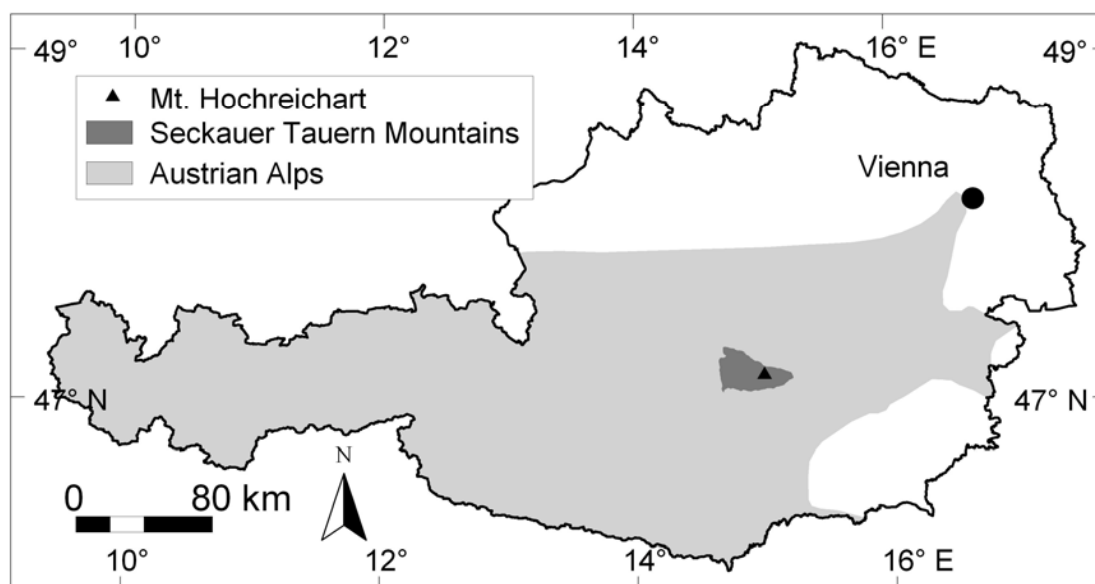


Fig. 1 – Location of the study region Seckauer Tauern Mountains and the study area Mt. Hochreichart

The Seckauer Tauern Mountains are the eastern most mountains of the Tauern Range which covers almost 9,500 km² in Austria and Italy. The Seckauer Tauern have a spatial extent of 626 km² and its highest peak is Mt. Geierhaupt reaching 2417 m asl (Kellerer-Pirklbauer 2008). Research in the Seckauer Tauern Mountains focuses spatially on the summit area of Mt. Hochreichart (2416 m asl) and the north-east facing Reichart Cirque.

The study area covers about 1 km² in total, ranging in elevation from about 1800 to 2416 m asl. Bedrock is predominantly quartzite and gneiss. The Reichart Cirque is covered by a large relict polymorphic rock glacier with a vertical extent of c.450 m ranging from about 1500 m asl to 1950 m asl at the uppermost part of the rooting zone (Fig. 2A).

The higher elevations of the study area were exposed to intensive periglacial weathering during the cold periods in the Pleistocene causing the formation of coarse-grained autochthonous blockfields (mountain-top detritus) and rectilinear slopes with solifluction landforms, partly with material sorting by frost action (Fig 2B). According to own air temperature measurements between Sept. 2008 and August 2009, the mean annual air temperature (MAAT) at the summit at 2416 m asl (AT1) is -1.4°C, in the cirque at 1920 m asl (AT2) is about +2.2°C, revealing a mean lapse rate of 0.0072°C/m.

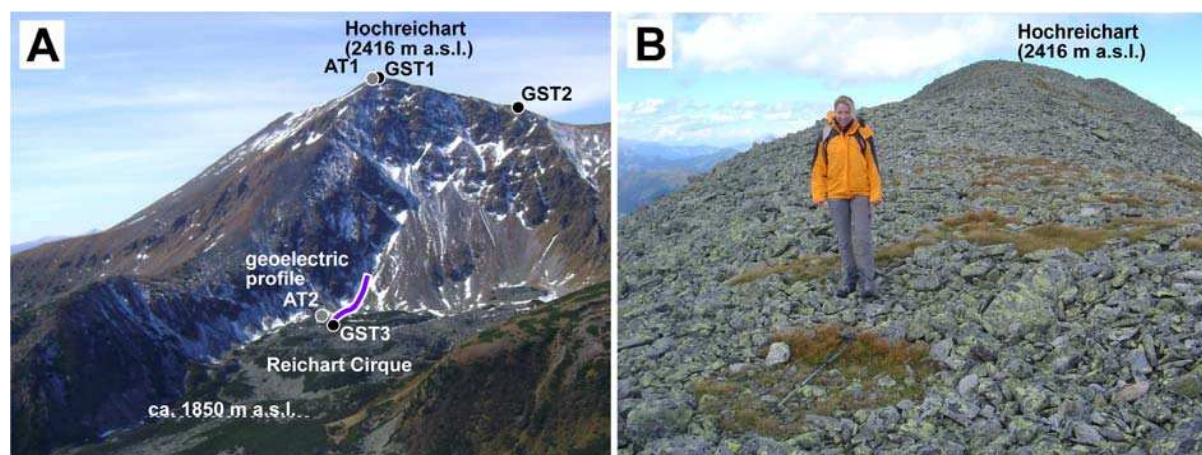


Fig. 2 – (A) Mt. Hochreichart (2416 m asl) and Reichart Cirque with the uppermost part of a polymorphic quasi-relict (i.e. contains small patches of permafrost) rock glacier. Locations of the miniature temperature dataloggers/MTD where ground surface temperature (GST, black dots) and air temperature (AT, grey dots) are measured and the profile where geoelectrical measurements were carried out in 2008 (blue and white line) are indicated. (B) Summit of Hochreichart with coarse-grained autochthonous blockfields with material sorting by frost action (note the vegetation patch in front of the person). Photographs by A. Kellerer-Pirklbauer (A) 22.09.2007 and (B) 22.08.2007.

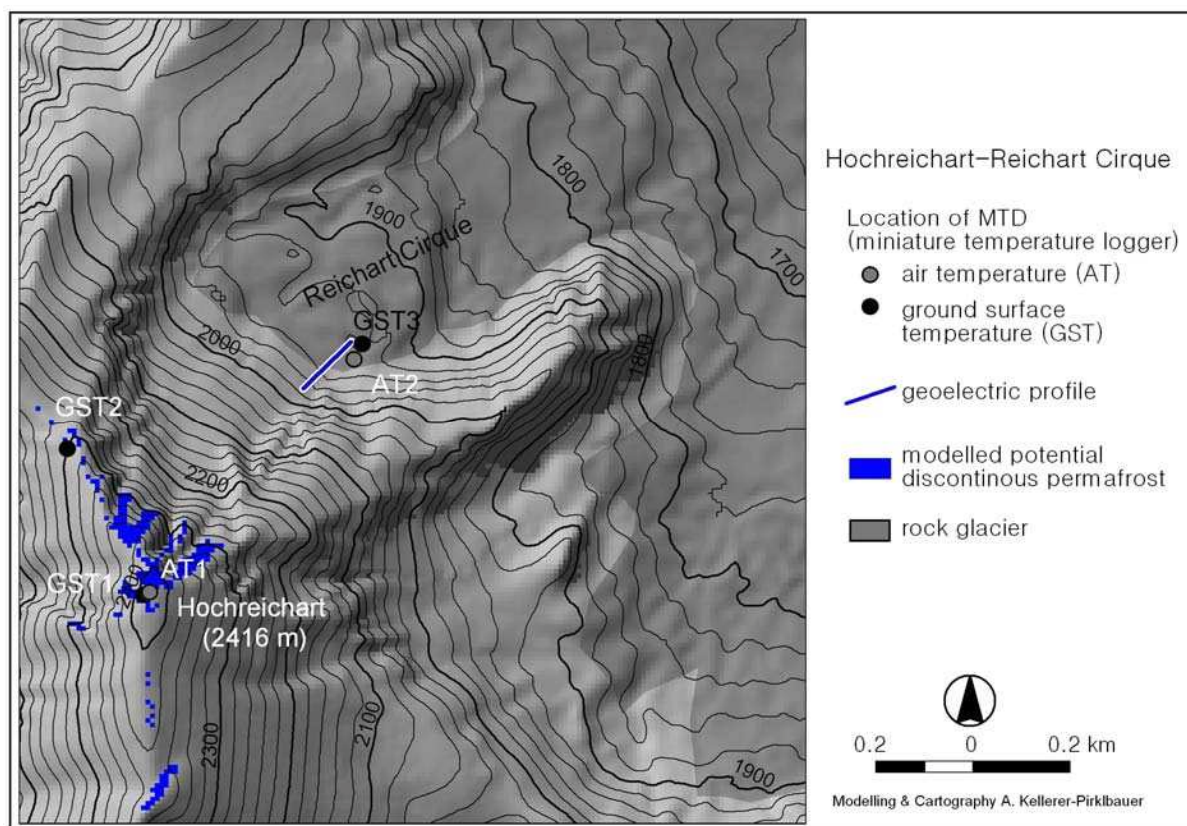


Fig. 3 – The study area Hochreichart-Reichart Cirque: The distribution of the modelled potential discontinuous permafrost, areas of rock glacier depositis, location of air (AT) and ground surface temperature (GST) measurement sites, and the location of the geoelectric profile are indicated.

2. Permafrost indicators and recent thermal evolution

2.1 Methods

Since 2004 a suite of methods has been applied such as geomorphic mapping, numerical permafrost modelling, multi-annual measurements of the bottom temperature of the snow cover (BTS), continuous measurements of ground surface, near ground surface and air temperatures by miniature temperature dataloggers (MTD), geoelectrics and optical snow-cover monitoring by a remote digital camera (RDC).

The spatial distribution of potential discontinuous permafrost in the study area was modelled by an adaptation of the program PERMAKART (Keller 1992), using GIS ArcView and ArcInfo. Details and results of this modelling approach were published in Kellerer-Pirklbauer (2005).

MTDs were used at nine locations during different periods. The results from three sites (Fig. 1) with ground surface temperature (GST) measurements logged at 1 h interval are presented here. The used loggers are produced by GeoPrecision, Model M-Log1 with PT1000 temperature sensors (accuracy $\pm 0.05^{\circ}\text{C}$, range -40 to $+100^{\circ}\text{C}$, calibration drift $<0.01^{\circ}\text{C}/\text{yr}$). Data of continuous measurements of ground surface temperature at the three sites GST1 to GST3 were available for the 47-month period 09.10.2006 to 21.09.2010. At site GST3 malfunction of the logger caused a data gap between 18.05.2007 and 12.08.2007. In order to allow comparison between the sites as well as allowing full-year data analysis, the three full-year periods 01.11.2006-31.10.2007, 01.11.2007-31.10.2008 and 01.11.2008-31.10.2009, were analysed. At GST3, only the second and third year was considered. The data analysis focused on frost day (FD), ice day (ID), freeze-thaw day (FTD) and frost-free day (FFD). A day got classified as FD, when the daily minimum temperature is below zero. If also the daily maximum temperature is among the freezing point, the day got classified as ice day ID. The difference between ice days and frost days, which means all days with a daily minimum temperature below 0°C and a daily maximum above this limit, got classified as FTD. Finally, a day with positive minimum temperature got classified as FFD.

BTS was measured at Reichart Cirque annually between winter 2004 and 2009 using a thermocouple probe PT 100 (1/3 DIN class B) fixed to the bottom of a 3 m long steel rod (System KRONEIS, Vienna). BTS is known to be a good indicator of the occurrence or absence of permafrost. The measured BTS values indicate: $\text{BTS} > -2^{\circ}\text{C}$: permafrost unlikely; $\text{BTS} -2$ to -3°C : permafrost possible; $\text{BTS} < -3^{\circ}\text{C}$: permafrost probable (Haeberli 1973). However, the interpretation of measured BTS values should be made very carefully and interannual variation at a given site might vary substantial from one year to the next.

In order to verify the temperature data and to extend the spatial knowledge about permafrost distribution beyond point information, a geoelectrical survey was carried out at the end of August 2008 by applying the electrical resistivity tomography (ERT) method along a 120 m long profile covering the upper part of the rooting zone of a (more-or-less) relict rock glacier and the talus slope above. For this survey the two-dimensional (2D) electrical surveys was performed using the Wenner-Alfa configuration with 2.5 m spacing and an LGM-Lippmann 4-Punkt light hp resistivity-meter. The ERT measurements were carried out by B. Kühnast (KNGeoelektrik) jointly with E. Niesner (University of Leoben) (Kellerer-Pirklbauer & Kühnast 2009).

Finally, a RDC system was set up at a nearby mountain (Feistererhorn 2081m asl.) to monitor the snow cover dynamics in the cirque and summit are of Mt. Hochreichart. The core parts of the RDC system are a standard hand-held digital camera (Nikon Coolpix), a remote control, a water proof casing with a transparent opening, a 12V/25Ah battery and solar panels with a charge controller.

2.2 Results on current permafrost distribution

Permafrost modelling

Permafrost distribution according to this the chosen modelling approach revealed that permafrost is very likely at north-facing aspects at highest elevations, but not occurring at altitudes below 2270 m asl. According to this model result, the entire Reichart Cirque is permafrost free (Fig. 3).

Thermal regime based on miniature temperature datalogger

Results of the continuous measurements of ground surface temperature at the three sites GST1 to GST3 are shown in Fig. 4. The mean values for the three year period at the highest site (GST1, FD 235) for FD is 15 days higher compared to the site 116 m lower in elevation (GST2, FD 220). For ID, the difference is more substantial with 19 days, whereas the number of FTD is slightly higher at the lower of the two sites. The lowest of the three sites (GST3) experiences substantially less FD but only slightly less FTD compared to GST2. Regarding interannual variations, the number of FD at all three sites is relatively stable, whereas the number of ID as well as of FTD varies a bit more.

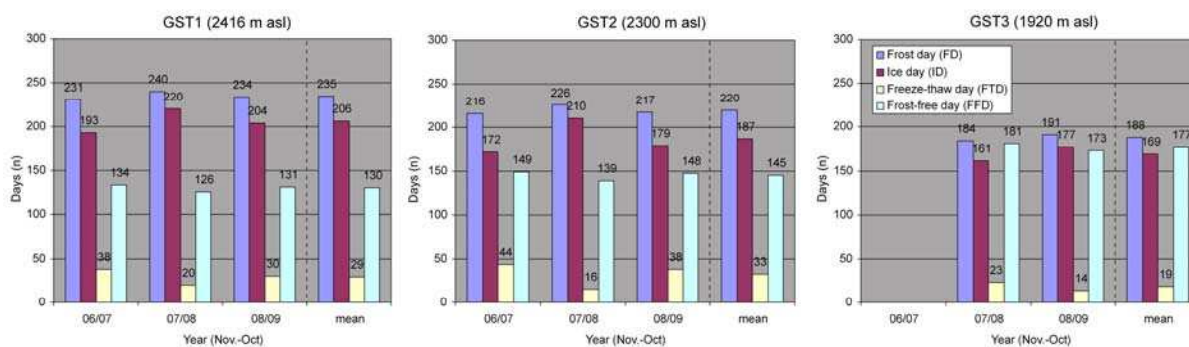


Fig. 4 – Thermal regime at the three sites GST1 to GST3 between Nov. 2006 and October 2009. Number of frost days (including ice days), ice days, freeze-thaw days and frost-free. Results of single years and the mean for the entire period are shown.

Fig. 5 shows the mean annual ground surface temperature (MAGST) as well as the elevation of the computed-zero degree isotherm based on a lapse rate of $0.0065^{\circ}\text{C}/\text{m}$. This graph clearly depicts that the MAGST values at site GST1 and GST2 are all negative indicating permafrost, whereas at the low elevation site GST3 the temperature at the ground surface is at around $+2^{\circ}\text{C}$. However, GST3 is located on coarse-grained blocky material in the rooting zone of a rock glacier. Due to the thermal behaviour of soil material (in particular coarse-grained blocky material with open voids in between), the temperature at the ground surface (i.e. MAGST) is warmer compared to the temperature at the top of permafrost (TTOP), possibly up to several degrees (“thermal offset”; Smith and Riseborough 2002). Therefore, despite the fact that positive MAGST are measured at the surface, permafrost might still exist in the ground.

The diagram showing the computed-zero degree isotherm for the three sites indicates that in general, the lowest computed zero-degree isotherm was calculated for site GST3, whereas the highest computed zero-degree isotherm was calculated for the highest site GST1. Explanation for this is the different buffering effect of the winter snow cover. At site GST1, snow cover is of substantially less importance (summit site, small local depression) compared to site GST3 (foot-slope position, rooting zone of rock glacier with more efficient snow accumulation and long lying snow cover). This clearly highlights the importance of snow influencing the thermal regime of the ground (cf. “nival offset”; Smith and Riseborough 2002)

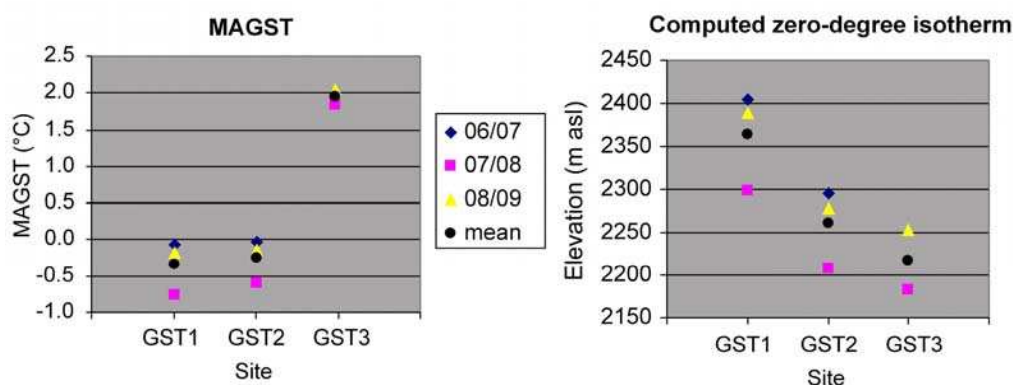


Fig. 5 – Mean annual ground surface temperature (MAGST) and computed zero-degree isotherm (using a lapse rate of $0.0065^{\circ}\text{C}/\text{m}$) at the three sites. Results of single years and the entire period are shown.

Figure 6 shows the results of two BTS-campaigns in the Reichart cirque. The maps show that the general pattern is the same, but BTS values in 2008 were cooler. In 2008 more measurement locations were within the possible (-2 to -3°C) and probable ($< -3^{\circ}\text{C}$) permafrost classes. BTS measurements indicate that patchy permafrost probably exists in the cirque at two different types of topographical positions: (i) a north to north-east facing footslope, and (ii) at the foot of a steep north to north-west facing rockface at elevations as low as 1850 m asl. According to this method, the uppermost part of the rock glacier including the root zone are presumably underlain by patches of permafrost.

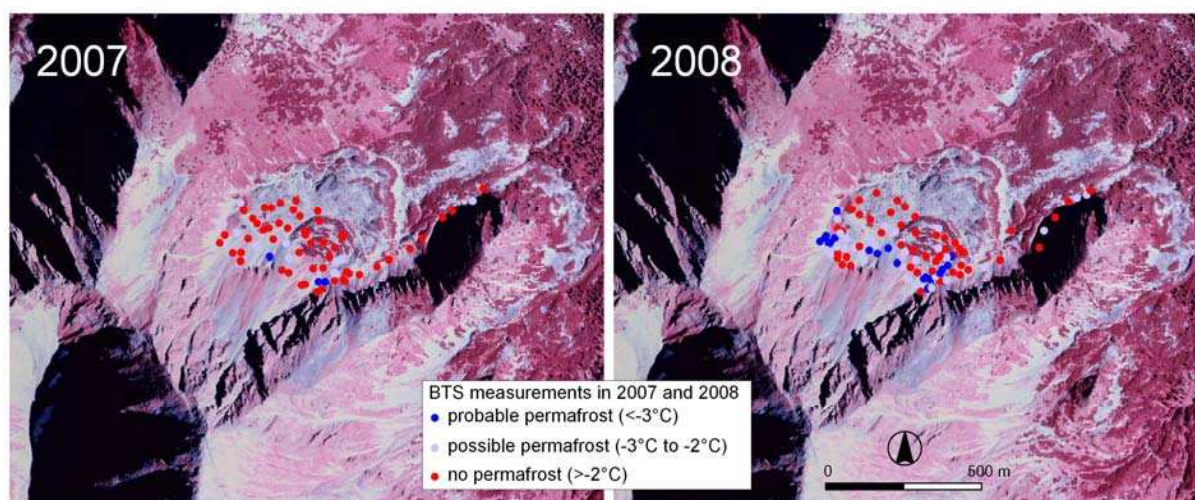


Fig. 6 – BTS measurements in late winter 2007 and 2008 in the Reichart Cirque. The measurements in 2008 indicate substantial cooler ground temperatures. Note the pronounced morphology of the relict rock glacier (Orthophotograph kindly provided by © GIS Steiermark).

Geoelectrical measurements

The ERT results (Fig. 7) indicate an active layer of 2 to 4 m underlain by a permafrost body along 3/4 of the entire profile with resistivity values between 50 to 100 $\text{k}\Omega\cdot\text{m}$ and extending to a depth of 10 to 15 m. The permafrost body is substantially thicker at the lower part of the profile (rock glacier; first 50 m of profile) compared to most of the upper part (talus slope). Focusing on the talus slope, the permafrost body is thickest on the central section of the profile ($\sim 5\text{-}6$ m thickness). In contrast, at

the lower part of the talus slope the permafrost body is most likely very thin (less than 1 m) whereas at the uppermost part permafrost is absent.

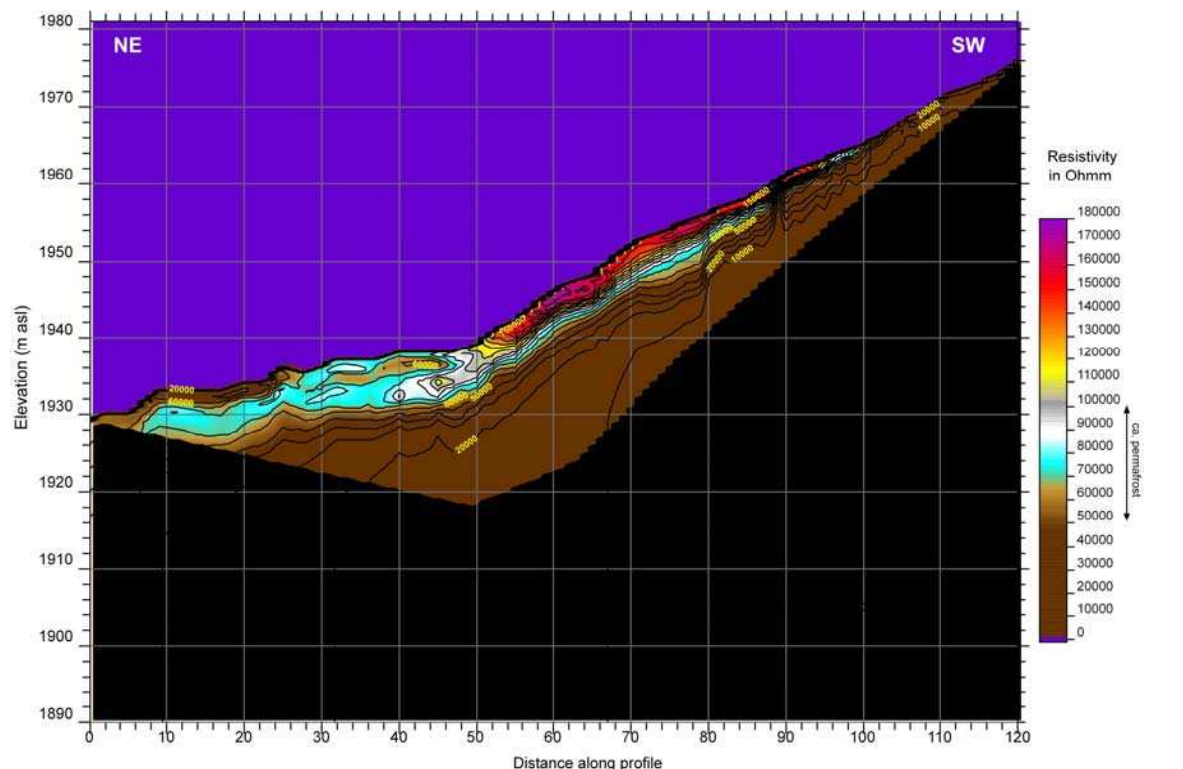


Fig. 7 – Electrical resistivity tomography (ERT) of the 120 m long profile measured in the Reichart Cirque (see Fig. 2 for location). Measurements carried out by KNGeoElektrik

2.3 Summary of current permafrost distribution

Based on the permafrost research carried out so far, one can conclude that the existence of permafrost is proven in the study area Mt. Hochreichart. The mountain permafrost occurs as patches in the lower parts as for instance in the rooting zone of the of a pseudo-relict rock glacier where the substrat consists of coarse-grained sediments. This cooling effect of coarse blocks has been recognised since decades (*cf.* Gruber & Hoelzle 2008). In higher elevations, permafrost is more widespread affecting the entire summit area. MAGST near 0°C at elevations higher ca. 2300 m asl indicate that permafrost is thin and in general warm. The redistribution of snow and characteristics of the winter snow cover as well as the type of substrat (bedrock, fine material, coarse-grained blocky material) are the dominant local factor for presence or absence of permafrost.

Fig. 8 depicts the snow cover situation in the study area Mt. Hochreichart in November 2006, 2007, 2008 and 2009 based on the own RDC system. These four images exemplarily show that snow cover varies substantially from year to year during similar periods. Early snow fall in autumn producing a protecting snow cover inhibits ground cooling. In contrast, long lying snow (e.g. foot slope position in cirque) inhibits ground warming in spring. Regarding substrat, sites with rather thick layers (several meters) of coarse-grained blocky material in the uppermost part of the Reichart Cirque (talus and rooting zone of the rock glacier) are more likely underlain by permafrost as shown by the ERT measurements. Summarising, this site is the most easterly evidence of existing permafrost found in the entire European Alps at 14°41'E at elevations as low as 1900 m asl.

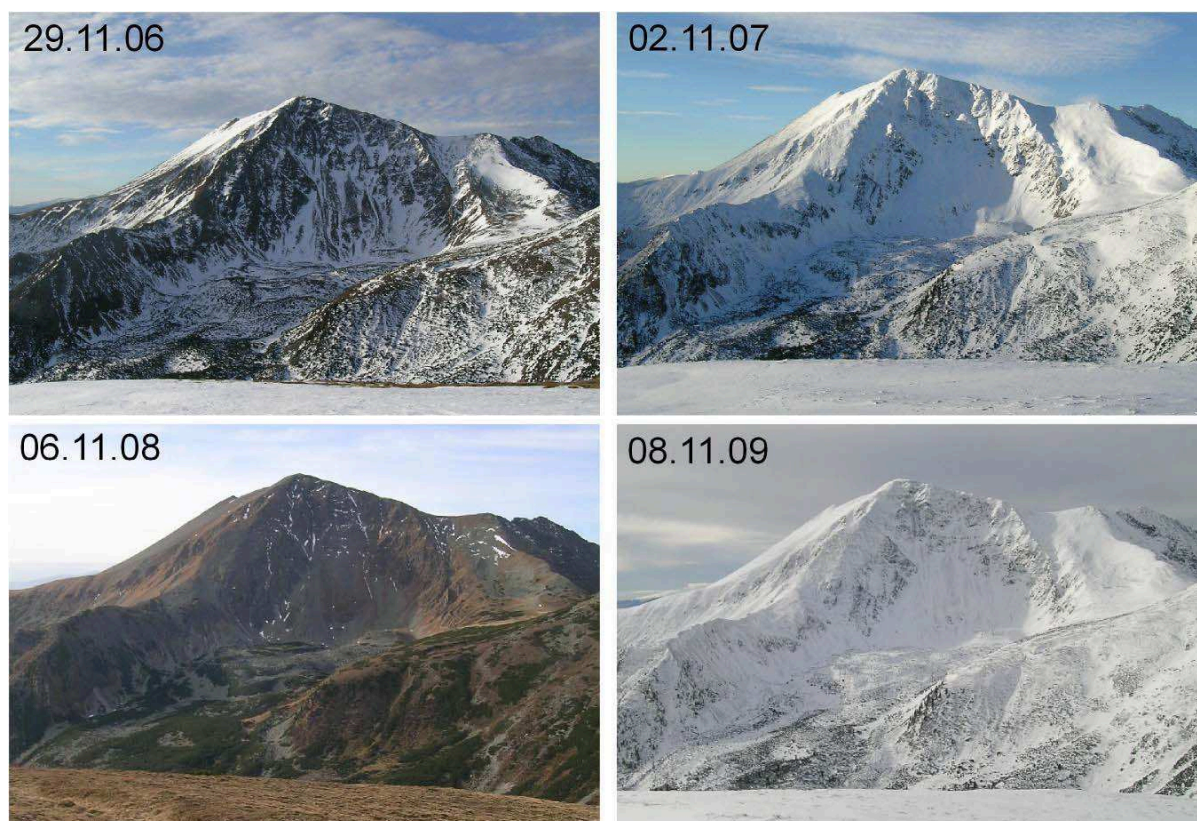


Fig. 8 – Snow cover distribution in the cirque and in the summit area of Mt. Hochreichart in November 2006, 2007, 2008 and 2009. cf. Fig. 2.

3. Possible future thermal response to predicted climate change

As presented above, permafrost in the study area Hochreichart-Reichart Cirque is restricted to the highest elevations and to locations, where the snow cover regime and/or the characteristics of the substrat material is favourable for permafrost existence. Climate change with the predicted temperature increase for the Greater Alpine Region (GAR) by using the relatively optimistic CLM A1B scenario indicates a temperature increase of around 2°C by 2050 (see Chapter 2.)

The estimates for frost day (FD), ice day (ID) and (FTD) for the periods 1961-1990 and 2021-2050 based on air temperature data reveal for the study area Hochreichart-Reichart Cirque the following results: The number of FD will decrease by 13 to 14 days per year. For the summit area, this would mean 207-227 FD instead of 221-240 FD hence a reduction of FD by up to 6.3%. The number of ID will decrease also by some 13 to 14 days per year, which means 127-147 ID instead of 141-160. In relative number, this is almost 10%. In contrast, the number of FTD will presumably remain more or less at the same level with a small increase by 0.1 to 2 days per year.

The predicted warming based on the CLM A1B scenario causing the modelled changes in FD, ID and FTD will severely influence the permafrost distribution and geomorphic dynamics in the study area Hochreichart-Reichart Cirque. By 2050, permafrost in the study area will be restricted to few high elevated locations in the summit area where the substrat and the snow cover conditions will still allow the existence of permafrost. In contrast, permafrost in the cirque will be completely thawed despite the fact of large areas of coarse-grained sediments.

Acknowledgements. – This study was partly carried out within the framework of the projects *ALPCHANGE*, financed by the Austrian Science Fund (FWF) through project no. FWF P18304-N10, and *PermaNET*. The *PermaNET* project is part of the European Territorial Cooperation and co-funded by the European Regional Development Fund (ERDF) in the scope of the Alpine Space Programme www.alpinespace.eu

References:

- Gruber S. & Hoelzle M., 2008: The cooling effect of coarse blocks revisited: a modeling study of a purely conductive mechanism. *Proceedings of the Ninth International Conference on Permafrost (NICOP)*, University of Alaska, Fairbanks, June 29 – July 3, 2008, 557-561.
- Haeberli W., 1973: Die Basis-Temperatur der winterlichen Schneedecke als möglicher Indikator für die Verbreitung von Permafrost in den Alpen. *Zeitschrift für Gletscherkunde und Glazialgeologie*, 9, 221-227.
- Keller F., 1992: Automated mapping of mountain permafrost using the program PERMAKART within the Geographical Information System ARC/INFO. *Permafrost and Periglacial Processes*, 3, 133-138.
- Kellerer-Pirklbauer A., 2005: Alpine permafrost occurrence at its spatial limits: First results from the eastern margin of the European Alps, Austria. *Norsk Geografisk Tidsskrift-Norwegian Journal of Geography*, 59, 184-193.
- Kellerer-Pirklbauer A., 2008: Aspects of glacial, paraglacial and periglacial processes and landforms of the Tauern Range, Austria. *Unpublished PhD-Thesis*, University of Graz, 200 p.
- Kellerer-Pirklbauer A. & Kühnast B., 2009: Permafrost at its limits: The most easterly evidence of existing permafrost in the European Alps as indicated by ground temperature and geoelectrical measurements. *Geophysical Research Abstracts* 11: EGU2009-2779.
- Lieb G.K., 1998: High-mountain permafrost in the Austrian Alps (Europe). *Proceedings of the 7th International Permafrost Conference* (Yellowknife, 23–27 June 1998), Collection Nordicana 57, 663–668. Centre d'études nordiques, Université Laval, Québec.
- Smith M.W. & Riseborough D.W., 2002: Climate and the limits of permafrost: a zonal analysis. *Permafrost and Periglacial Processes*, 13, 1-15.

3.

Case studies in the European Alps

3.3

Dösen Valley, Central Austrian Alps

Citation reference

Kellerer-Pirklbauer A (2011). Chapter 3.3: Case studies in the European Alps – Dösen Valley, Central Austrian Alps. In Kellerer-Pirklbauer A. et al. (eds): *Thermal and geomorphic permafrost response to present and future climate change in the European Alps*. PermaNET project, final report of Action 5.3. On-line publication ISBN 978-2-903095-58-1, p. 45-58.

Authors

Coordination: Andreas Kellerer-Pirklbauer

Involved project partners and contributors:

- Institute of Geography and Regional Science, University of Graz, Austria (IGRS) – Andreas Kellerer-Pirklbauer

Content

Summary

1. Introduction and study area
2. Permafrost indicators and recent thermal evolution
3. Possible future thermal response to predicted climate change

References

Summary

Permafrost research in the Dösen Valley (46°59'N and 13°17'E), Hohe Tauern Range, Central Austria was initiated in the 1990s. Since then, a number of different methods have been applied to understand permafrost distribution and rock glacier dynamics. Results show that at present permafrost exists at permafrost favourable sites (north-exposed, well sheltered, coarse-blocky material) at elevations down to 2200 m asl. In contrast, on south-exposed slopes covered by coarse-blocky material the lower limit is at around 2600 m asl. Local conditions such as substrate material (i.e. fine/coarse sediments, thick/thin sediments, bedrock) and topoclimatic conditions (radiation sheltered, timing and characteristics of snow cover) alter the general pattern of decreasing ground surface temperature with increasing elevation substantially and makes the permafrost distribution pattern in the study area complex. Rock glacier velocities seem to react quicker after a cool period with deceleration. In contrast, rock glaciers seem to need more time to react after warmer periods with movement acceleration indicating the inertia of the rock glacier system towards ground warming and velocity changes. By 2050, south-facing slopes not covered by coarse-blocky material will be permafrost free. Only the highest north-facing slopes will still be influenced by widespread permafrost. The role of substrate material and snow cover dynamics will be even more important for the remaining permafrost than today. Temperature increase will eventually lead to inactivation of all presently active rock glaciers in the study area.

1. Introduction and study area

Permafrost research in the Hohe Tauern Range in Central Austria was initiated in the 1990s. One of the main study areas for permafrost research is the Dösen Valley near Mallnitz (Fig. 1A). Since then, different methods have been applied in order to understand permafrost distribution and rock glacier dynamics in this valley (Table 1). Present permafrost research in this study area is carried out within the framework of the projects *ALPCHANGE* (2006-2010), *PermaNET* (2008-2011) and *permafrost* (2010-2012) by researchers from the University of Graz, the Graz University of Technology as well as the University of Leoben.

Table 1 – Applied methods and publications at the study area Dösen Valley

Method	initiated /carried out	Publications
Geodetic surveys	1995	Buck & Kaufmann 2008 Delaloye <i>et al.</i> 2008 Kaufmann & Ladstädter 2007 Kaufmann <i>et al.</i> 2007 Kellerer-Pirklbauer 2008 Kellerer-Pirklbauer <i>et al.</i> 2008a, 2008b Kenyi & Kaufmann 2003 Kienast & Kaufmann 2004 Lieb 1991, 1996, 1998 Schmölter & Fruhwirth 1996
Photogrammetric surveys	1954	
Geophysical campaigns (seismics, geomagnetics and georadar/GPR)	1994	
Geomorphological mapping and observations	1994	
Meteorological monitoring	2006	
Monitoring of snow cover dynamics in the rooting zone by automatic digital cameras	2006	
Ground temperature monitoring	1995 (continuous since 2006)	
Near-surface ground temperature monitoring	1995 (continuous since 2006)	
Relative dating of rock glacier surface	2007	

The study area is situated in the Ankogel Mountains at the inner part of the glacially shaped, E-W trending Dösen Valley at about N46°59' and E13°17'. The elevation of the study area ranges between 2270 m asl at the cirque threshold near the Arthur-von-Schmid Hut to slightly more than 3000 m asl at the nearby Säuleck peak. This part of the valley is characterised by a number of rock glaciers and distinct terminal moraines in relatively flat parts, a cirque floor with a tarn lake, slopes covered by coarse debris and steep rock faces partly acting as debris supply areas for the rock glaciers. Geologically, the study area is located within the central gneiss complex of the Hochalm/Ankogel area with predominantly west-dipping biotite gneiss (Lieb 1996). (Fig. 1B). The moraines were presumably formed during the Egesen-maximum advance and are thus of early Younger Dryas (YD) age (Lieb 1996). In Austria, the early YD is 10Be-dated to around 12.3–12.4 ka (Kerschner & Ivy-Ochs 2007). At present, only some perennial snow patches are found in the study area.

The nine rock glaciers in the Dösen Valley depicted in Fig. 1B predominantly consist of granitic gneiss (Kaufmann *et al.* 2007) and were formed after deglaciation in the Lateglacial and Holocene period. According to the “Rock Glacier Inventory of Central and Eastern Austria” (Lieb *et al.* 2010, Kellerer-Pirklbauer *et al.* 2010), three of these rock glaciers (mo236, mo239.1, mo239.2) are considered to be relict and six are regarded as intact still containing permafrost (mo237, mo237.1, mo238, mo238.1, mo238.2, mo239). Previous permafrost research – including velocity measurements – focused particularly on the rock glacier mo238 (for details see Lieb 1996 or Kaufmann *et al.* 2007). This rock glacier is characterised by an altitudinal range of 2355-2650 m asl, a length of 950 m, a width of 250 m and an area of 0.19 km². The rock glacier is an active monomorphic tongue-shaped rock glacier situated at the end of the inner Dösen valley with present mean surface velocity rates of around 15-25 cm per year (Fig. 2).

According to air temperature measurements by the own meteorological station located at the surface of rock glacier mo238 (for location see Fig. 1) in the 4-years period September 2006 to August 2010, the mean annual air temperature (MAAT) at the 2603 m asl is -1.7°C . The coldest month is January with a monthly value of up to -11.8°C whereas the warmest month is August with a monthly mean value of up to 7.8°C .

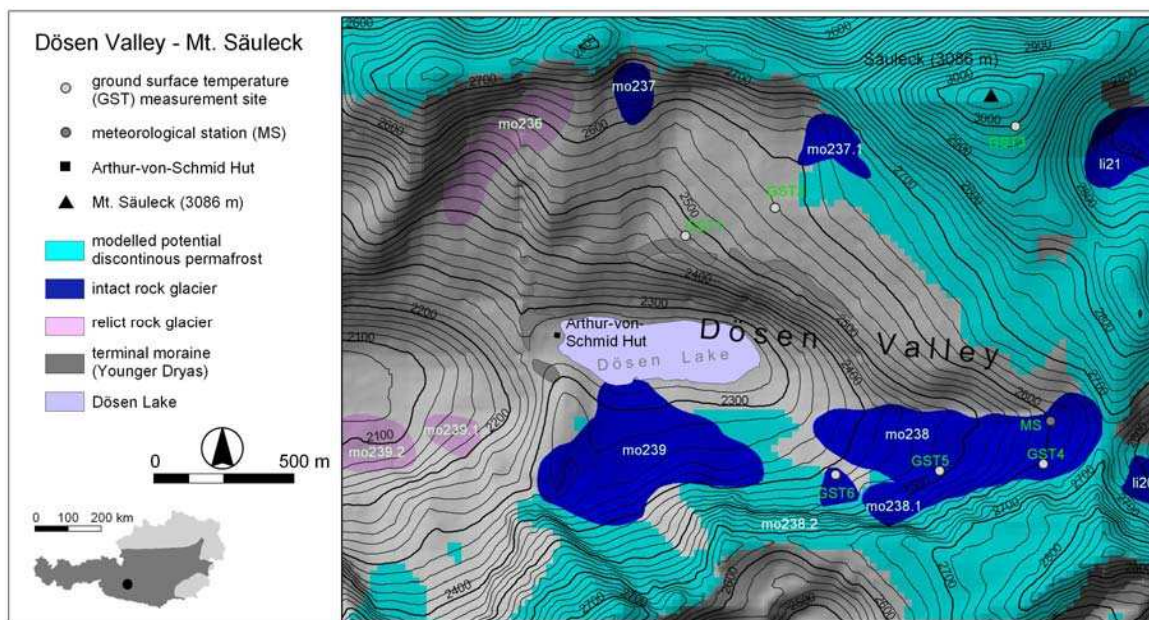


Fig. 1 – Study area Dösen Valley and its location within Austria. The distribution of rock glaciers, terminal moraines of Late Glacial age (Younger Dryas), modelled potential discontinuous permafrost, location of the meteorological station (MS) as well as the location of six miniature temperature datalogger (MTD) used for ground surface temperature (GST) measurements are indicated. Code of the rock glacier is according to the “Rock Glacier Inventory of Central and Eastern Austria” (Lieb et al. 2010, Kellerer-Pirklbauer et al. 2010).

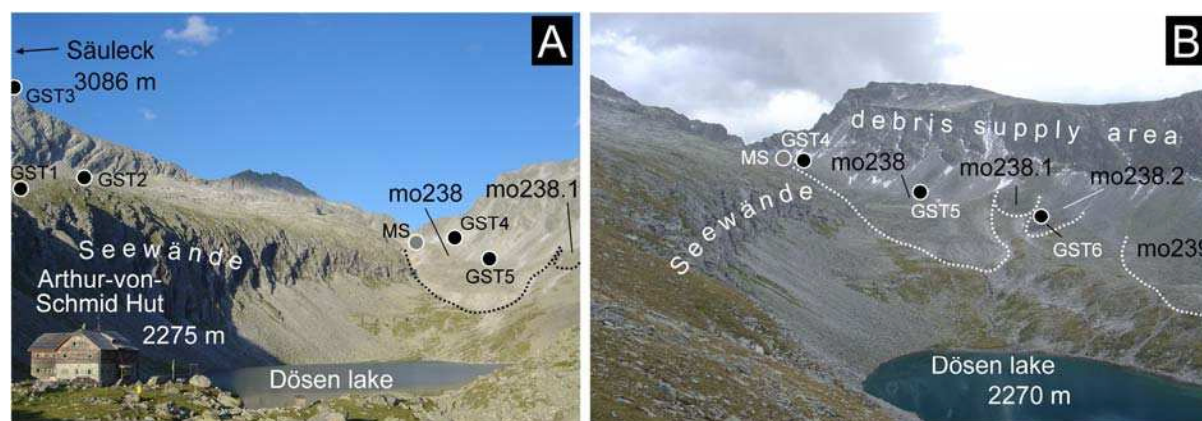


Fig. 2 – The study area Dösen Valley with four intact rock glaciers: (A) view towards E, (B) view towards SE. Note the widespread steep rock faces acting as debris supply areas, the perennial snow fields, the flowing structure of the rock glaciers and widespread vegetation (indicator for absence of alpine permafrost). Locations of the six miniature temperature dataloggers/MTD where ground surface temperature (GST) is measured and the site of the meteorological station (MS) are indicated. Code of the rock glacier is according to the “Rock Glacier Inventory of Central and Eastern Austria” (Lieb et al. 2010, Kellerer-Pirklbauer et al. 2010). Photographs by A. Kellerer-Pirklbauer.

In this paper, the present situation and the evolution of the ground surface temperature in the recent past (2006-2010) and its significance for permafrost distribution are highlighted. Furthermore, the results of the rock glacier monitoring program for the period 1954 to 2010 and its relationship to climatic conditions and climate change are discussed.

2. Permafrost indicators and recent thermal evolution

2.1 Methods

Since 1994 a suite of methods has been applied as listed above in Table 1. In this paper, results based on numerical permafrost modelling, climate monitoring by using a meteorological station as well as continuous measurements of ground surface temperature by using miniature temperature dataloggers (MTD) and photogrammetric and geodetic rock glacier displacement measurements are presented.

The spatial distribution of potential discontinuous permafrost in the study area was modelled by an adaptation of the program *PERMAKART* (Keller 1992) using GIS ArcView and ArcInfo. For this simple modelling approach, the empirical values of the lower limit of discontinuous permafrost for central Austria were used (Lieb 1998).

The meteorological station has been installed in 2006 at one large block on the surface of the rock glacier mo238 within the *ALPCHANGE* project. At this station, climate data including air temperature, air humidity, wind speed, wind direction and global radiation are continuously logged and data are available for the period 01.09.2006 to 17.08.2010.

MTDs were used at a total of 11 locations during different periods. The results from six sites with ground surface temperature (GST) measurements logged at 1 h interval are presented here (Figs. 1 & 2). The used loggers are produced by GeoPrecision, Model M-Log1 with PT1000 temperature sensors (accuracy $\pm 0.05^\circ\text{C}$, range -40 to $+100^\circ\text{C}$, calibration drift $< 0.01^\circ\text{C}/\text{yr}$). At each of the six sites, the temperature sensor is sheltered from direct solar radiation by a platy rock. Sites GST1 and GST2 are located on coarse-blocky slopes. GST2 is located between a large boulder and bedrock.

All three sites form a vertical profile on south-facing slopes. In contrast, sites GST4 to GST6 are located on the surface of the main active rock glacier in the valley (mo238) and from a vertical profile on north-facing slopes. Data of continuous measurements of ground surface temperature at the three sites GST1-GST4 and GST6 were available for the c.48-month period 01.09.2006 to 17.08.2010. At site GST5 the time series ends on 05.09.2009. To allow comparison between the six sites as well as to allow full-year data analysis, the four full-year periods 01.09.2006-31.08.2007, 01.09.2007-31.08.2008, 01.09.2008-31.08.2009 and 01.09.2009-17.08.2010 were analysed. Furthermore, the zero-degree isotherm was computed for each site using a vertical temperature gradient of $0.0065^\circ\text{C}/\text{m}$. Table 2 summarises key parameters of the six GST sites.

Temperature data (air and ground) analyses focused on frost day (FD), ice day (ID), freeze-thaw day (FTD) and frost-free day (FFD). A day got classified as FD, when the daily minimum temperature is below zero. If also the daily maximum temperature is among the freezing point, the day got classified as ice day ID. The difference between ice days and frost days, which means all days with a daily minimum temperature below 0°C and a daily maximum above this limit, got classified as FTD. Finally, a day with positive minimum temperature got classified as FFD.

Table 2 – Summary of the sites where ground surface temperature (GST) is monitored by using miniature temperature dataloggers (MTD). Location of the GST-sites is indicated in Figs. 1 and 2. The elevation of the computed zero-degree isotherm was computed by using a vertical temperature gradient of 0.0065°C/m. MAGST=mean annual ground surface temperature.

GST-site	Exposition	Elevation (m asl)	Data period	MAGST (°C)	Computed zero-degree isotherm (m asl)
GST1	South	2489	4 years: 1.09.2006 to 17.08.2010	2.0	2797
GST2	South	2586	4 years: 1.09.2006 to 17.08.2010	1.2	2771
GST3	South	3002	4 years: 1.09.2006 to 17.08.2010	-2.6	2602
GST4	North	2626	4 years: 1.09.2006 to 17.08.2010	-0.9	2488
GST5	North	2501	3 years: 1.09.2006 to 05.09.2009	-1.5	2270
GST6	North	2407	4 years: 1.09.2006 to 17.08.2010	-1.3	2207

Surface displacement measurements of the rock glacier mo238 is carried out since 1954 by using aerial photogrammetry and since 1995 by using terrestrial geodetic survey (Kaufmann & Ladstädter 2007, Kaufmann *et al.* 2007). The geodetic measurements using a total station are annually carried out in the middle of August following a proven scheme. Since 1995, the measurements were repeated apart from 2003 due to lack of funding. The annual campaigns are led by V. Kaufmann, TU Graz. In addition to the geodetic measurements satellite based radar interferometry (Kenyi & Kaufmann 2003) and photogrammetric displacement measurements based on aerial photographs (1954, 1969, 1975, 1983, 1993, 1997 and 1998) were carried out (Kaufmann *et al.* 2007, Kaufmann & Ladstädter 2007) previously.

Finally, a RDC system was set up in September 2006 in order to monitor the snow cover dynamics at the rooting zone of the rock glacier mo238. The core parts of the RDC system are a standard hand-held digital camera (Nikon Coolpix), a remote control, a water proof casing with a transparent opening, a 12V/25Ah battery and solar panels with a charge controller.

2.2 Results on current permafrost distribution

Permafrost modelling

The lower limit of potential discontinuous permafrost according to the chosen regional permafrost modelling approach indicates permafrost on slopes between 2500 m asl (north-facing) and 2900 m asl. (south-facing) and on footslope positions between 2410 m asl (north-facing) and 2690 m (south-facing). The modelling results show that only the large intact rock glacier mo238 as well as the two smaller ones slightly to the west (mo238.1 and mo238.1) as well as the south-facing rock glacier mo237.1 are predominantly in permafrost areas which is in accordance to the fresh appearance of the four rock glaciers (Fig. 2).

Air temperature regime based on the meteorological station

The meteorological station is located at 2603 m asl in the upper part of the rock glacier (Figs. 1 & 2). Results from this station show, that the number of frost days (FD), ice days (ID), freeze-thaw days (FTD) and frost-free days (FFD) was relatively stable in the 4 year period 2006 to 2010 (Fig. 3). The mean value of FD is 246 meaning that during 2/3 of the year frost occurs at 2600 m asl. in the study area. In contrast, the mean annual air temperature values indicate a substantially warmer year

2006/07, two comparable years 2007/08 and 2008/09 and a substantially cooler year 2009/10 (Fig. 3) yielding a mean value of -1.7°C . The elevation of the zero-degree isotherm is 2340 m asl. if using a vertical lapse rate of $0.0065^{\circ}\text{C}/\text{m}$.

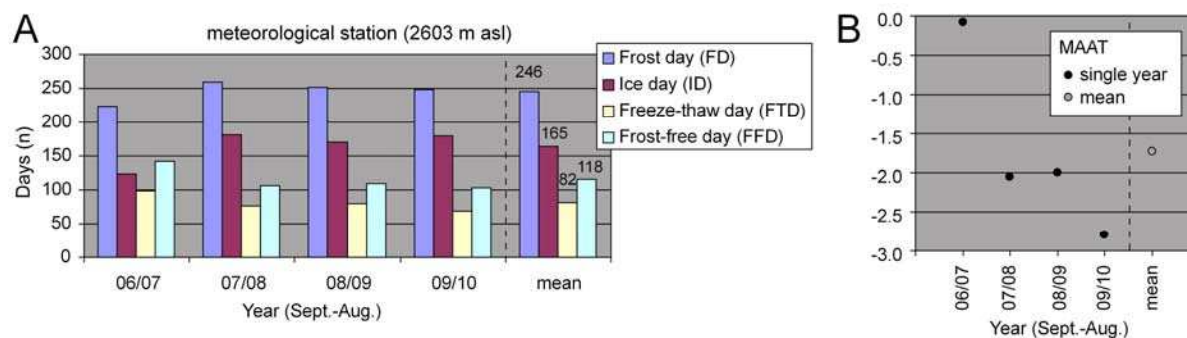


Fig. 3 – Air temperature regime at the meteorological station at the rock glacier mo238. (A) Number of frost days (including ice days), ice days, freeze-thaw days and frost-free; (B) mean annual air temperature (MAAT); both for the single years and the mean of the entire 4-years period.

Ground thermal regime based on miniature temperature datalogger

Results of the continuous measurements of ground surface temperature at the six sites GST1 to GST6 are shown in Figs. 4 and 5. Fig. 4 shows the number of frost days (including ice days), ice days, freeze-thaw days and frost-free days. In general, the lowest values in FD and ID were measured in winter 2006/07. In contrast, the highest values of FTD were measured generally in winter 2006/07 apart from the snow rich site GST5. At all six sites, the number of FFD was again highest in winter 2006/07, at site GST1 the FFD value was even higher than the FD value.

The mean value of FD is lowest at the south exposed site GST1 with only 198 days, followed by GST2 with 208 days. In contrast, at site GST3 at 3000 m asl, the mean value of FD days is almost 270. The FD value for the north exposed sites GST4 to GST6 is quite similar at all three sites with 237 to 245. Regarding interannual variation, the number of FD during the four year period varied only by 15 days between the highest and coldest site GST3. In contrast, at south exposed and warmer site GST1 the number of FD varied during the same period by 60 days (168 FD in 2006/07 vs. 228 FD in 2007/08). Considering the fact that the winter 2006/07 was exceptionally warm and the winter 2007/08 was relatively “normal”, these results suppose that permafrost sites at lower location in the study area Dösen Valley are more susceptible to climate warming.

Regarding ice days, the lowest ID values are again found at the south facing sites GST1 and GST2 with about 170 days. The coldest site with the highest number of ID is site GST5 with 234 days. This maximum in ID at this site is attributed to local topoclimatic conditions (small depression on north facing slope favouring ground cooling) and long snow cover duration (delay in ground warming in spring to mid summer). Similar ID values are found at the highest site GST3 and the two north facing sites GST4 and GST6. The interannual variation of the number of ID during the four year measurement period varied substantially by 36 (GST4) to 73 days (GST1).

The mean value of the freeze-thaw days is generally low ranging from between 11 at the snow rich site GST5 to 37 at the warm site GST2, but 50 at the highest site GST3. At site GST5, the FTD value was even only five in the winter 2007/08 related to the long-lasting snow cover at this site. In contrast, at site GST3 the number of FTD value reached 70 in the warm winter 2006/07. The differences in the number of FTD at the sites also indicate that frost weathering caused by freeze-

thaw action is important at the south-exposed sites GST1, GST2 and in particular GST3. In contrast, at the cooler and snow richer sites this weathering process is less active at present climate conditions. Finally, frost-free days is highest at the warm sites GST1 and GST2, comparable at the three north-exposed sites GST4 to GST6 and substantially lowest at site GST3.

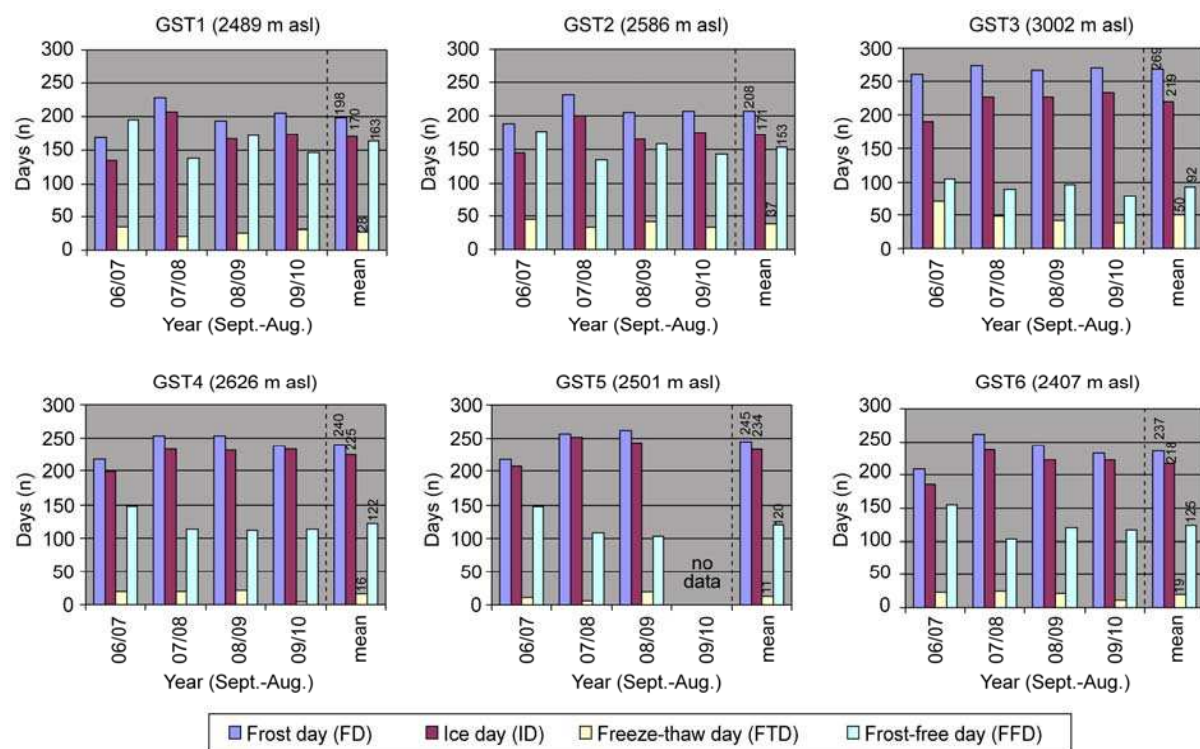


Fig. 4 – Ground thermal Regime at the six sites GST1 to GST6 between September 2006 and August 2010 with number of frost days (including ice days), ice days, freeze-thaw days and frost-free days. Results of single years and the mean for the entire period are shown.

Fig. 5 shows the mean annual ground surface temperature (MAGST) as well as the elevation of the computed-zero degree isotherm based on a lapse rate of $0.0065^{\circ}\text{C}/\text{m}$ for all six sites. Results are shown for the single measurement years between 2006 and 2010 as well as the mean of the entire period. Results show that the north-facing slopes are cooler than the south-facing slopes at comparable elevation. On the south-exposed slopes, the vertical temperature gradient for the four year period is $0.0082^{\circ}\text{C}/\text{m}$ (between GST1 and GST2) and $0.0091^{\circ}\text{C}/\text{m}$ (between GST2 and GST3). In contrast, on the north-exposed slopes the situation is more complex due to local topoclimatic conditions also influencing the characteristics of the winter snow cover (duration, thickness). A negative gradient of $-0.0048^{\circ}\text{C}/\text{m}$ was calculated between the sites GST4 and GST5, whereas a slight positive gradient of $0.0021^{\circ}\text{C}/\text{m}$ was calculated between the sites GST5 and GST6

Fig. 5 clearly depicts that the MAGST at sites GST1 and GST2 are positive with mean values of $+1.2^{\circ}\text{C}$ (GST2) to $+2.0^{\circ}\text{C}$ (GST1) indicating absence of permafrost. However, site GST1 is located on blocky material. Due to the thermal behaviour of soil material (in particular coarse-grained blocky material with open voids in between; Gruber & Hoelzle 2008), the temperature at the ground surface (i.e. MAGST) is warmer compared to the temperature at the top of permafrost (TTOP), possibly up to several degrees (“thermal offset”; Smith and Riseborough 2002). Therefore, despite the fact that positive MAGST are measured at the surface, permafrost might still exist in the ground at or around the site GST1. In contrast, the MAGST values at the other four sites GST3 to GST6 are clearly negative

(apart from 2006/07 at site GST6) with mean values of -0.9°C at site GST4 to -2.6°C at the 3000-m-site GST3 indicating at these four sites presence of permafrost.

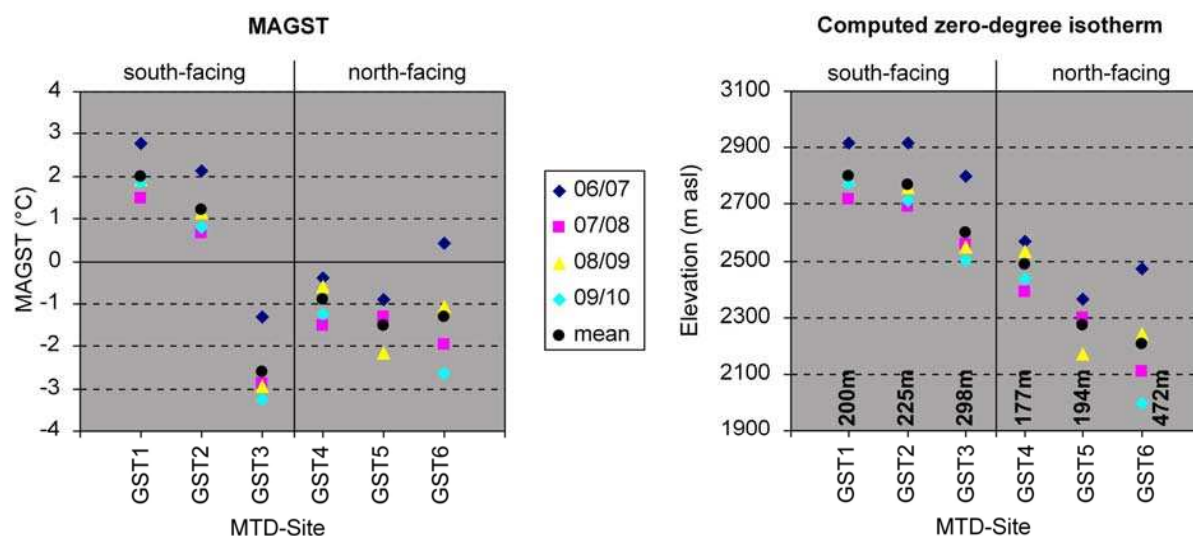


Fig. 5 – Mean annual ground surface temperature (MAGST) and computed zero-degree isotherm (using a lapse rate of $0.0065^{\circ}\text{C}/\text{m}$) at the six sites GST1 to GST6. Results of single years and the mean for the entire period are shown. The elevation range of the computed zero-degree isotherm during the four years is indicated.

The diagram showing the computed-zero degree isotherm for the six sites indicates that the lowest computed zero-degree isotherm was calculated for the north-facing and low elevated site GST6 with a mean value of 2207 m asl. In contrast, the highest computed zero-degree isotherms were calculated for the two south-facing sites GST1 (2797 m asl) and GST2 (2771 m asl). Explanation for this is the local topoclimatic condition and the buffering effect of the winter snow cover at a given site. At sites GST1, GST2, GST3 and GST6) snow cover is of minor importance (wind exposed sites with little/minor snow cover) compared to sites GST4 and GST5 (foot-slope position with more efficient snow accumulation and long lying snow cover). This also highlights the importance of snow influencing the thermal regime of the ground (“nival offset”; Smith and Riseborough 2002). Based on the calculations, the zero degree isotherm at the ground surface on north-exposed slopes is located between about 2200 and 2500 m asl, on south-facing slopes between 2600 and 2800 m asl. The computed-zero degree isotherm varied during the four years between 177 m (GST4) and 472 m (GST6) indicating substantial interannual changes. Single years such as the warm winter 2006/07 cause a substantially increase of this isotherm by 80 to 260 m.

Summarising, one might expect permafrost in the study area on north-exposed slopes covered by coarse-blocky material at elevations of 2200-2300 m asl, on south-exposed slopes at 2600-2750 m asl.

Rock glacier kinematic

Active rock glaciers are creeping phenomena of continuous or discontinuous permafrost. Their movement mode is strongly related to climatic conditions and as a consequence to ground temperatures (Kääb *et al.* 2007). Fig. 6 depicts the evolution of the mean annual horizontal surface velocity at the Dösen rock glacier mo238 between 1954 and 2010 based on geodetic and photogrammetric measurements. Note that the mean annual values in the period before 1995 are generally lower compared to the years after 1995 indicating generally lower displacement rates in the period 1954 to 1995. However, single years with displacement rates comparable to the values of

the post-1995 period are conceivable. Furthermore, note the maximum in the movement rates between 2002 and 2004, the following deceleration until 2008 followed by a remarkable new acceleration during the last two measurement years. This movement pattern over the last 1.5 decades correlates with other monitored rock glaciers in the Hohe Tauern Range (Kellerer-Pirklbauer & Lieb 2011) and in the entire Alpine Arc (Delaloye *et al.* 2008). This circumstance confirms the assumption that climatic conditions and changes in the European Alps are the dominant steering factors for rock glacier movement.

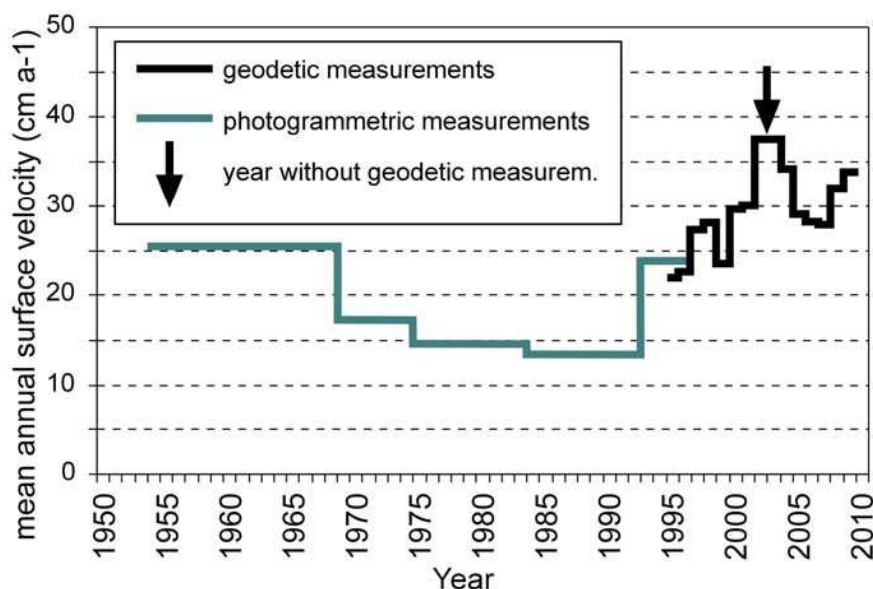


Fig. 6 – Change of mean annual horizontal surface velocity (cm a-1) at the Dösen rock glacier mo238 between 1954 and 2010 based on geodetic and photogrammetric measurements. Mean of 11 measurement points (Pt. 10-17, 21-23). Data source Kaufmann *et al.* (2007) and unpublished data.

Relationship between rock glacier kinematic and climate

The own meteorological station at the rock glacier mo238 was used to collect air temperature data for the period October 2006 to August 2010. Mean monthly air temperature data were calculated for the period January 1990 to September 2006 for the Dösen site by applying correlation analysis with the air temperature data from the meteorological observatory Sonnblick, about 24 km WNW of the Dösen Valley. Fig. 7 depicts the relationship between the geodetic measurements at mo238 and the mean annual air temperature/MAAT (running 12-month mean). This graph shows that the warm MAAT values at the end of 1994/beginning of 1995 caused an increase in surface displacement in the years 1997 to 1999. In contrast, the cooler MAAT values between end of 1996 and mid 1997 caused lower velocities in 1999-2000. The MAAT values in the period 1999 to 2004 were generally high causing a steady increase of the velocity rates peaking in 2003-2004. This was previously explained by constant warming and an increase of liquid water in the permafrost body of the rock glacier (Buck & Kaufmann 2008). According to these authors, the rock glacier velocity experienced in this period a self-reinforcing dynamic leading to a further increase in velocity. The MAAT values decreased after 2004 causing rock glacier deceleration until 2007-2008. The extreme increase of the MAAT between early 2007 to mid of 2008 caused a new acceleration in the period 2008 to 2010.

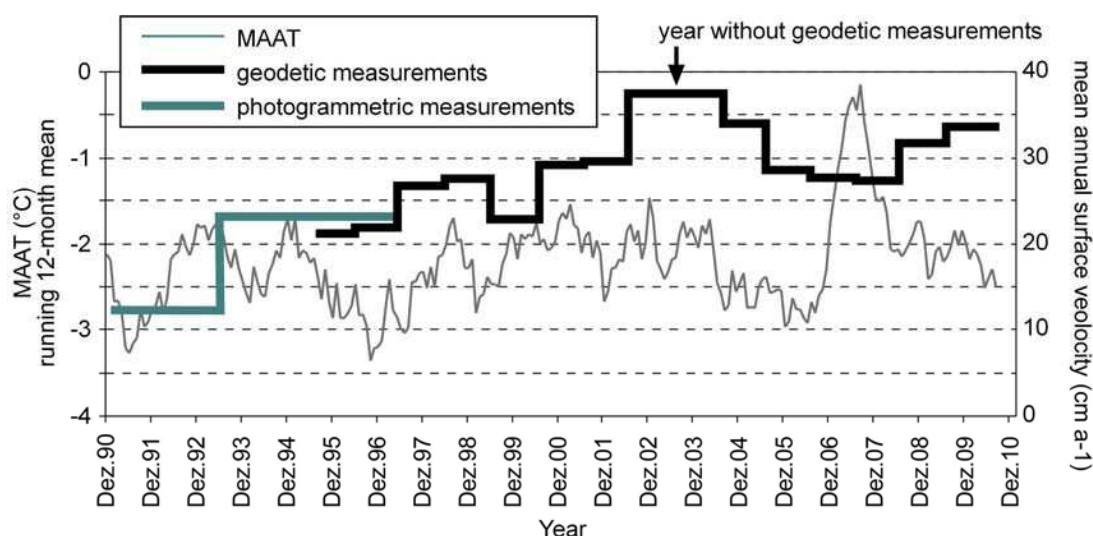


Fig. 7 – Mean annual air temperature/MAAT (running 12-month mean) and horizontal surface velocities at the Dösen rock glacier mo238 during the period 1990 to 2010. Data source of velocity values Kaufmann et al. (2007) and unpublished data. Data

2.3 Summary of current permafrost distribution and dynamics

Based on the permafrost research carried out so far, we can conclude that permafrost in the study area Dösen Valley exists at extreme sites (north-exposed slopes, well sheltered from solar radiation, and coarse-blocky material) at elevations down to 2200 m asl. In contrast, on south-exposed slopes covered by coarse-blocky material the lower limit is at around 2600 m asl. An important role plays the winter snow cover in the local permafrost distribution particularly at such coarse-blocky sites. On the one hand, snow poor sites in radiation sheltered locations (such as GST6) allow efficient ground cooling in autumn accompanied by moderate warming in spring. On the other hand, snow rich sites at footslope positions in radiation sheltered locations (such as GST5) reduce efficient ground cooling but shelter the ground from warming in spring and even summer.

On slopes not covered by coarse-blocky material, the lower limit of permafrost is substantially higher at elevations of between 2500 m asl. (north-facing) to 2900 m asl. (south-facing). At footslope positions influenced by long lasting snow, the permafrost limit seems to be at around 2400 m asl (north-facing) to 2700 m asl (south-facing). These results clearly show that local conditions influencing solar radiation, degree of ground cooling, thermal regime of the ground surface and near ground surface as well as winter snow cover conditions have a major impact on the distribution of permafrost in the study area. This impact alters the general pattern of decreasing ground surface temperature with increasing elevation substantially and makes the permafrost distribution pattern in the study area (and at comparable sites in the neighbouring area) complex at elevations between 2200 m and 2900 m asl.

The behaviour of the monitored rock glacier mo238 in the inner Dösen Valley is in accordance to other monitored rock glaciers in the Hohe Tauern Range and the entire Alpine Arc. During the last 1.5 decades, two peaks of high surface displacement rates were detected at 2003-2004 and 2008-2010 with rates exceeding 30 cm per year. The rock glacier velocity pattern indicates that the rock glacier mo238 reacts quicker after a cool period with deceleration. In contrast, the rock glacier needs more time to react to warmer periods with acceleration of the movement indicating the inertia of the rock glacier system towards ground warming and velocity changes.

3. Possible future thermal response to predicted climate change

As presented above, permafrost in the study area Dösen Valley plays an important role and covers presumably about 1/3 of the area above 2270 m asl. Besides the sole existence of permafrost in bedrock and in slope deposits, permafrost in the study area is also important for geomorphic periglacial processes such as creeping of the active rock glaciers (in particular rock glacier mo238) or rock falls caused by frost weathering observed frequently during each field campaign.

Climate change with the predicted temperature increase for the Greater Alpine Region (GAR) by using the relatively optimistic CLM A1B scenario indicates a temperature increase of around 2°C by 2050 (see Chapter 3). The air temperature at the meteorological station in the study area Dösen Valley would be slightly positive with around +0.3°C. If using a lapse rate of 0.0065°C/m and the air temperature increase of +2°C, the elevation of the zero-degree isotherm would shift by about 310 m from presently 2340 m asl to 2650 m asl causing substantial permafrost degradation in the bedrock (faster reaction) and in the intact rock glaciers (slower reaction with a longer time lag).

The estimates for frost day (FD), ice day (ID) and (FTD) for the periods 1961-1990 and 2021-2050 based on air temperature data reveal for the study area Dösen Valley the following results: The number of FD will decrease by 14 to 15 days per year. For the summit area, this would mean 246-266 FD instead of 261-280 FD. For the elevation around the active rock glacier mo238 (2350-2650, this would yield 226-246 FD instead of 241-260 FD, hence a reduction of FD by up to 5.7%. The number of ID will decrease also by some 15 to 16 days per year, hence a reduction from 201-220 to 185-205 ID in the summit areas and, respectively, from 161-180 to 145-165 at elevations at around 2350 to 2650 m asl, hence a reduction of ID by up to 10%. In contrast, the number of FTD will presumably increase slightly by 0.1 to 2 days per year. In the period 1961-1990, the number of FTD in the summit areas is about 70-80, at elevations at around 2350 to 2650 m asl about 80-90. Based on the own air temperature measurements at the meteorological station at 2603 m asl at the surface of mo238, the mean number of FD during the four year period September 2006 to August 2010 was 246. Furthermore, 165 ID and 82 FTD were measured. This suggests that the modelling results for the standard period 1961-1990 applied for the GAR are in accordance with the measurements of 2006-2010 at the Dösen Valley. However, one has to keep in mind that MAAT at the nearby meteorological observatory Sonnblick was about -1.3°C cooler during the normal period 1961-1990 compared to the period September 2006 to August 2010. This difference in the MAAT values during the two periods certainly influences the number of FD, ID and FTD. Therefore, this circumstance clearly shows that comparing local data with regional modelling results is not trivial.

Regarding rock glacier velocity and climatic conditions in the Dösen Valley, one can expect that an increase of ground temperatures in the active rock glaciers will cause permafrost warming and eventually partial thawing of the permafrost. This will lead to an increase of liquid water in the rock glacier which itself might increase the mobility and hence surface velocity of the rock glacier. Further permafrost warming and thawing will lead to increasing friction within the rock glacier due to ice loss, to complete permafrost degradation and finally to the formation of an inactive or even relict rock glacier with little to no permafrost ice.

The predicted climate change until 2050 will substantially decrease the areal extent of permafrost in the study area Dösen Valley accompanied by destabilisation of bedrock and slope deposits as well as changes in frost weathering conditions and consequently rock fall activity. South-facing slopes not covered by coarse-blocky material will be permafrost free in the entire study area and only the highest north-facing slopes will still be influenced by widespread permafrost. The role of substrate material (coarse, fine, bedrock) and snow cover dynamics will be even more important for the remaining permafrost than today. Furthermore, temperature increase will presumably cause first an increase of the creep velocities of currently moving rock glacier. In a later stage, however, this will lead to inactivation of all presently active rock glaciers in the study area Dösen Valley.

Acknowledgements. – This study was mainly carried out within the framework of the projects ALPCHANGE, financed by the Austrian Science Fund (FWF) through project no. FWF P18304-N10, and PermaNET. The PermaNET project is part of the European Territorial Cooperation and co-funded by the European Regional Development Fund (ERDF) in the scope of the Alpine Space Programme www.alpinespace.eu. Viktor Kaufmann is thanked for providing unpublished data on rock glacier velocities. The Central Institute for Meteorology and Geodynamics (ZAMG) is thanked for providing temperature data from the meteorological observatory Sonnblick.

References:

- Buck S. & Kaufmann V., 2008: The influence of air temperature on the creep behaviour of three rockglaciers in the Hohe Tauern. *Grazer Schriften der Geographie und Raumforschung*, 45, 159-169.
- Delaloye R., Perruchoud E., Avian M., Kaufmann V., Bodin X., Hausmann H., Ikeda A., Käab A., Kellerer-Pirklbauer A., Krainer K., Lambiel Ch., Mihajlovic D., Staub B., Roer I. & Thibert E. (2008): Recent interannual variations of rock glacier creep in the European Alps. *Proceedings of the Ninth International Conference on Permafrost (NICOP)*, University of Alaska, Fairbanks, June 29 – July 3, 2008, 343-348.
- Gruber S. & Hoelzle M., 2008: The Cooling effect of coarse blocks revisited: a modeling study of a purely conductive mechanism. *Proceedings of the Ninth International Conference on Permafrost (NICOP)*, University of Alaska, Fairbanks, June 29 – July 3, 2008, 557-561.
- Käab A., Frauenfelder R. & Roer I., 2007: On the response of rockglacier creep to surface temperature increase. *Global and Planetary Change*, 56, 1-2: 172-187.
- Kaufmann V. & Ladstädter R., 2007: Mapping of the 3D surface motion field of Doesen rock glacier (Ankogel group, Austria) and its spatio-temporal change (1954-1998) by means of digital photogrammetry. *Grazer Schriften der Geographie und Raumforschung*, 43, 127-144.
- Kaufmann V., Ladstädter R. & Kienast G., 2007: 10 years of monitoring of the Doesen rock glacier (Ankogel group, Austria) – A review of the research activities for the time period 1995-2005. *Proceedings, 5th Mountain Cartography Workshop*, 29 March - 1 April 2006, Bohinj, Slovenia, 129-144.
- Keller F., 1992: Automated mapping of mountain permafrost using the program PERMAKART within the Geographical Information System ARC/INFO. *Permafrost and Periglacial Processes*, 3, 133-138.
- Kellerer-Pirklbauer A., 2008: The Schmidt-hammer as a Relative Age Dating Tool for Rock Glacier Surfaces: Examples from Northern and Central Europe. *Proceedings of the Ninth International Conference on Permafrost (NICOP)*, University of Alaska, Fairbanks, June 29 – July 3, 2008, 913-918.
- Kellerer-Pirklbauer A. & Lieb G.K., 2011: Recent rock glacier velocity behaviour and related natural hazards in the Hohe Tauern Range, central Austria. PermaNET Project Report - Contribution of IGRS to Action 6.2/Group 1 – Rock glacier.
- Kellerer-Pirklbauer A., Avian M., Lieb G.K. & Rieckh M., 2008a: Temperatures in Alpine Rockwalls during the Warm Winter 2006/2007 in Austria and their Significance for Mountain Permafrost: Preliminary Results. *Extended Abstracts, Ninth International Conference on Permafrost (NICOP)*, University of Alaska, Fairbanks, June 29 – July 3, 2008, 131-132.
- Kellerer-Pirklbauer A., Avian M., Lieb G.K. & Pilz A., 2008b: Automatic Digital Photography for Monitoring Snow Cover Distribution, Redistribution and Duration in alpine Areas (Hinteres Langtal Cirque, Austria). *Geophysical Research Abstracts* 10: EGU2008-A-11359.
- Kellerer-Pirklbauer A., Lieb G.K. & Kleinfurchner H., 2010: A new rock glacier inventory at the eastern margin of the European Alps. *Geophysical Research Abstracts* 12: EGU2010-13110.
- Kenyi L.M. & Kaufmann V., 2003: Measuring rock glacier surface deformation using SAR interferometry. *Proceedings of the 8th International Conference on Permafrost*, Zurich, Switzerland, 537-541.

- Kerschner H. & Ivy-Ochs S., 2007: Palaeoclimate from glaciers: Examples from the Eastern Alps during the Alpine Lateglacial and early Holocene. *Global and Planetary Change*, 60, 58-71.
- Kienast G. & Kaufmann V., 2004: Geodetic measurements on glaciers and rock glaciers in the Hohe Tauern National Park (Austria). *Proceedings, 4th ICA Mountain Cartography Workshop*, 30 September - 2 October 2004, Vall de Núria, Catalonia, Spain, Monografies tècniques 8, Institut Cartogràfic de Catalunya, Barcelona, 101-108.
- Lieb G.K., 1991: Die horizontale und vertikale Verteilung der Blockgletscher in den Hohen Tauern (Österreich). *Zeitschrift für Geomorphologie N. F.*, 35, 345-365.
- Lieb G.K., 1996: Permafrost und Blockgletscher in den östlichen österreichischen Alpen. *Arbeiten aus dem Institut für Geographie der Karl-Franzens-Universität Graz*, 33, 9-125.
- Lieb G.K., 1998: High-mountain permafrost in the Austrian Alps (Europe). *Proceedings of the 7th International Conference on Permafrost*, Yellowknife, 663-668.
- Lieb G.K., Kellerer-Pirklbauer A. & Kleinfurter H., 2010: Blockgletscherinventar von Zentral und Ostösterreich erstellt im Rahmen des Projektes PermaNET. *Institut für Geographie und Raumforschung, Graz*
- Schmöllner R. & Fruhwirth R.K., 1996: Komplexgeophysikalische Untersuchung auf dem Dösen Blockgletscher (Hohe Tauern, Österreich). *Arbeiten aus dem Institut für Geographie der Karl-Franzens-Universität Graz*, 33, 165-190.
- Smith M.W. & Riseborough D.W., 2002: Climate and the limits of permafrost: a zonal analysis. *Permafrost and Periglacial Processes*, 13, 1-15.

3.

Case studies in the European Alps

3.4

Hoher Sonnblick, Central Austria

Citation reference

Klee A, Riedl C. (2011). Chapter 3.4: Case studies in the European Alps – Hoher Sonnblick, Central Austrian Alps. In Kellerer-Pirklbauer A. et al. (eds): *Thermal and geomorphic permafrost response to present and future climate change in the European Alps*. PermaNET project, final report of Action 5.3. On-line publication ISBN 978-2-903095-58-1, p. 59-65.

Authors

Coordination: Alexander Klee

Involved project partners and contributors:

- Central Institute for Meteorology and Geodynamics (ZAMG) – Alexander Klee, Claudia Riedl

Content

Summary

1. Introduction and study area
2. Measurements and results
3. Possible future thermal response to predicted climate change

References

Summary

Climate change in the Alps is not only related to the retreat of glaciers, but rather to the permafrost distribution. Indices for the permafrost retreat in the higher mountain area, e. g. erosion, frost shattering or instabilities of the infrastructure are observable. The relevance of permafrost long-term monitoring is widely spread. The knowledge about permafrost interaction, influences on permafrost and the temporal behaviour of permafrost is very important for several kinds of infrastructure, e. g. cable lifts, lift stations or mountain huts. Furthermore this knowledge is the basis for measuring the drinking water reservoirs of permafrost in the higher mountain areas, its quality and its usage for the future. Detailed data about the glacier-retreat is available. But the permafrost distribution - including its thickness and spatial dimension - is largely unknown. On the top of Hoher Sonnblick (3.105 m asl) in the Hohe Tauern (Austria) three boreholes have been installed to measure rock temperatures down to 20 m under the surface. This data about temperature, geophysical and geodetical measurements (available since 2007) is a first approach for the documentation of permafrost behaviour in the Alps. Furthermore the summit region of Hoher Sonnblick will be modelled with the aim to compute the behaviour of permafrost in the future with different scenarios in climate change.

1. Introduction and study area

The top of Hoher Sonnblick (3.105 m a.s.l.) is located in the range of the Eastern Alps in the region of Hohe Tauern (Austria). Neighbouring mountains of Hoher Sonnblick reach similar elevations of about 3.000 m a.s.l.. The north slope of Hoher Sonnblick is characterized by a very deep and steep north face. To the south the slope is moderate with about 30° down to the upper margin of the glacier Goldbergkees. Fig. 1 shows the summit area of Hoher Sonnblick.

In the vicinity of Hoher Sonnblick are three glaciers. The largest glacier is of the three is the glacier Goldbergkees. The two smaller ones are Kleinfleißkees and Pilatuskees both without a typical glacier tongue. Glacier ice occurrence down to about 2.500 m a.s.l.. The rock in the region consists mainly of biotit-gneiss (Exner, 1964). The thickness of the debris layer mantling the bedrock in the summit area (where the three boreholes were drilled; Fig. 1) is up to 2 m.



Fig. 1 – The summit of Hoher Sonnblick (3105 m a.s.l.) with the location of the three boreholes. To the right Zittelhaus and to the left the observatorium. The summit in the background is Mt. Hocharn (3254 m a.s.l.)

The observatory was built at the end of 19th century and a mountain hut, the Zittelhaus, is also located on top of the summit. In 2001 a study observed that fissuring of the crest demands for the necessity of a geological stabilization of the steep north face to protect the observatory. This re-development was done from 2003 to 2007. The main reason for the fissuring is the change in meteorological conditions in the 20th century. Higher temperatures and more liquid precipitation advance the physical weathering process of the rock. Higher temperature contrasts causes frost shattering, which is more active than in past times.

Climatological measurements, especially of temperature, started in 1886. Actually, each year counts 310 freezing days (daily minimum below 0° C) and 239 ice days (daily maximum below 0° C). All values refer to the period between 1971 and 2000. Up to now an unbroken temperature row exists. Next to temperature measurements and measurements of other meteorological parameters, the Sonnblick observatory is a centre of several scientific activities. E. g. measurements in atmospheric chemistry, snow chemical measurements, mass balance measurements of the surrounding glaciers, avalanche reports, of course the permafrost long-term monitoring since 2007 and many more research activities actually take place at Hoher Sonnblick.

2. Measurements and results

To measure the behaviour of permafrost and the influences of climate change for permafrost on top of Hoher Sonnblick, three 20 m deep boreholes were drilled on 14th and 15th September 2005. At the end of August 2006 the boreholes were equipped with temperature sensors in different depths (Fig. 2). Additionally, a 10 m deep borehole next to borehole 2 was drilled and equipped with extensometers. Daily actualized measurements of temperature data and extensometer data are available online at www.sonnblick.net. All boreholes are located on the southern slope (see Fig. 1). The mean slope between borehole 1 and 3 is 27° and the total elevation difference is 34 m. Borehole 1 is directly located to the Sonnblick observatory, borehole 3 is adjacent to a continuous snow field and borehole 2 is located in between.

Not only measurements in the boreholes are available. In October 2006 35 miniature temperature datalogger/MTD (20 of the type UTL-1 and UTL-2 and 15 of the type HOBO TidbiT) were installed to measure the basic temperature of the snow cover in wintertime and the ground surface temperatures during summer. The 20 logger of type UTL-1 and UTL-2 were installed on moderate slope on the southern side of the summit. In the steep north face, the 15 HOBO TidbiTs were installed. Furthermore, the air temperature change in the past since 1886 is also available. Fig. 3 shows an example of temporal variability of the temperature with increasing depth for the hydrological year in 2008. Measurements of the boreholes show that the summerly temperature amplitude is observable down to 15 m with a delay of about 6 to 7 months.

The cooling from the winter season is effective to 5 m with a delay of about 4 months. The thickness of the active layer in summer time was about in borehole 1 in 2008 1 m and 70 cm in 2009. In the boreholes 2 and 3 the active layer is less than 1 m. There, the active layer was about 60 cm in 2008. In 2009 there are no data available for borehole 2 and 3. Naturally, in the upper layers of the boreholes the differences between summer and winter seasons are larger than in deeper levels. It is also interesting to compare yearly average temperatures as it is done in Fig. 4. On the x-axis the temperature is assigned and on the y-axis the depth of the borehole. The figure shows the temperature of borehole 1 in 2008 (blue line) and in 2009 (red line). Down to about 9 m the temperature profile in 2008 is much warmer than in 2009. In 3 m there is a difference of 0.7° C. In autumn 2009 the summit region was snowless or with only a thin snow cover for a long time which caused these differences.

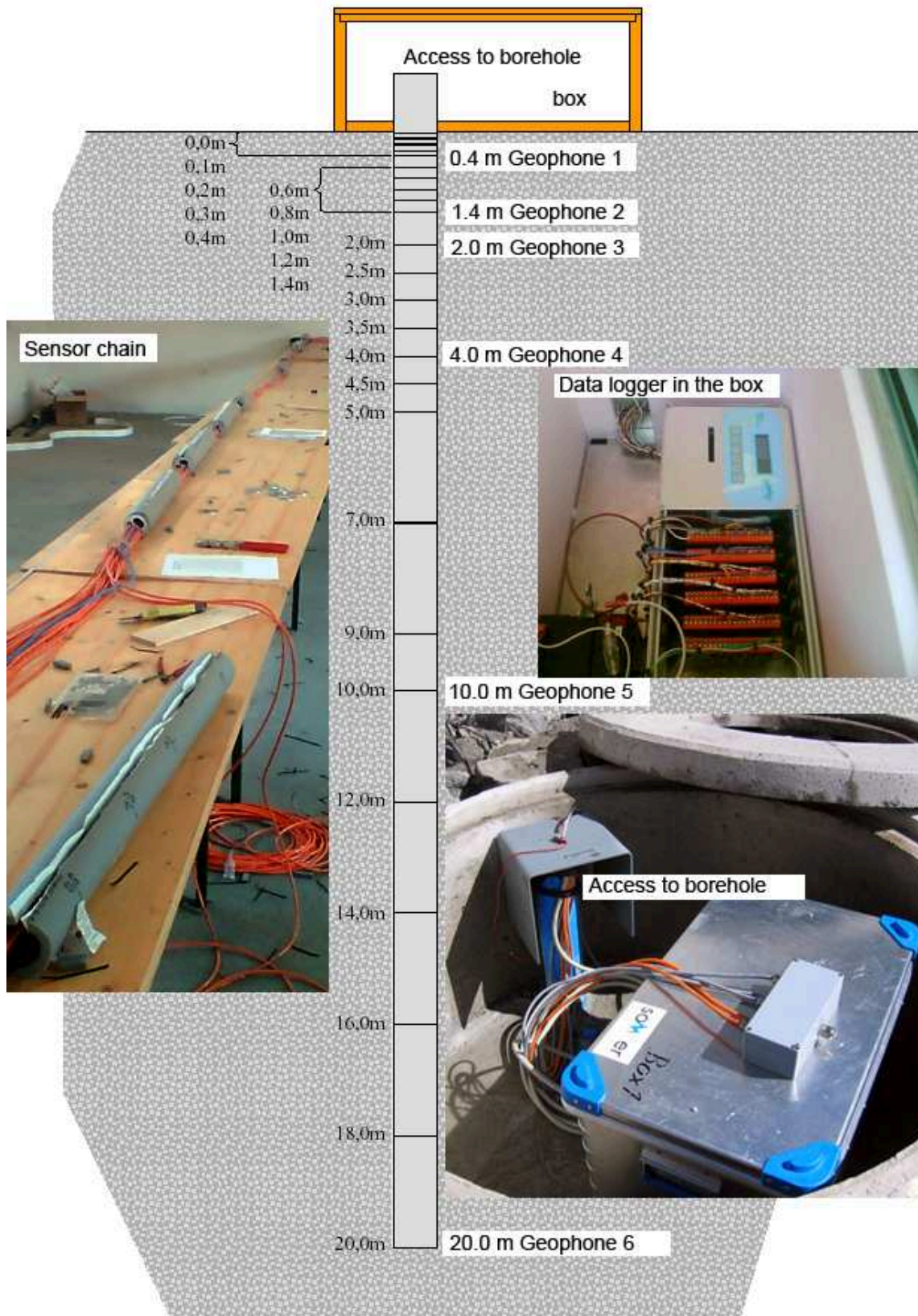


Fig. 2 - Construction of measurement chain in the boreholes with depths of the temperature sensors and geophones. Additionally, the entrance of one borehole is shown.

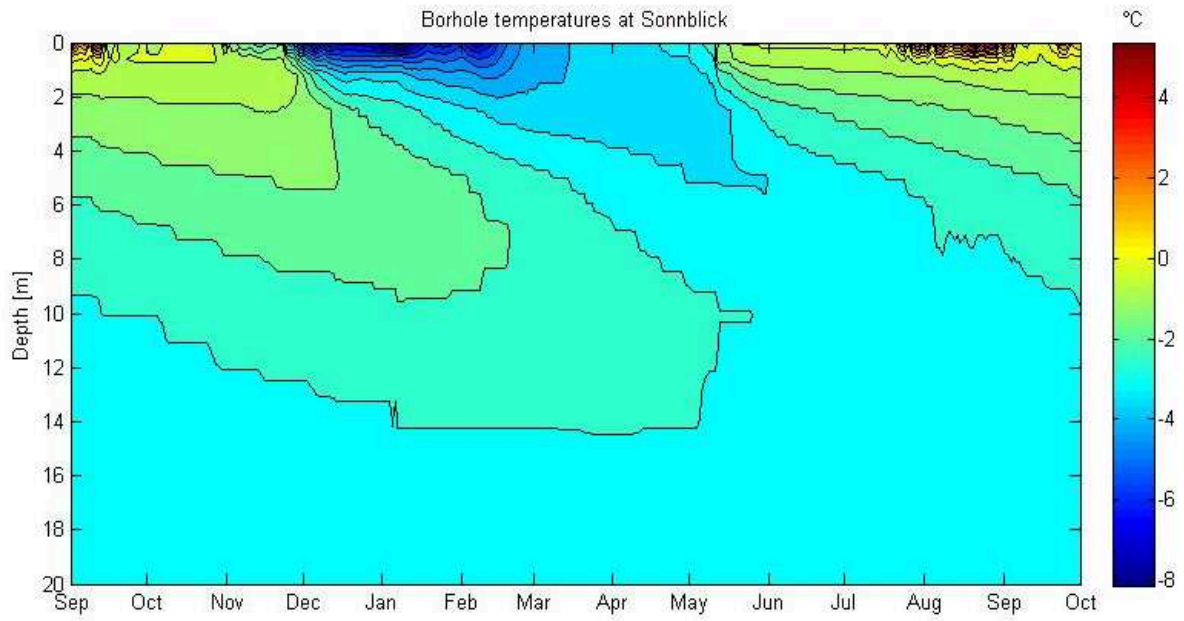


Fig 3 – Temporal temperature variability with increasing depth for borehole 1 during the hydrological year 2007/2008.

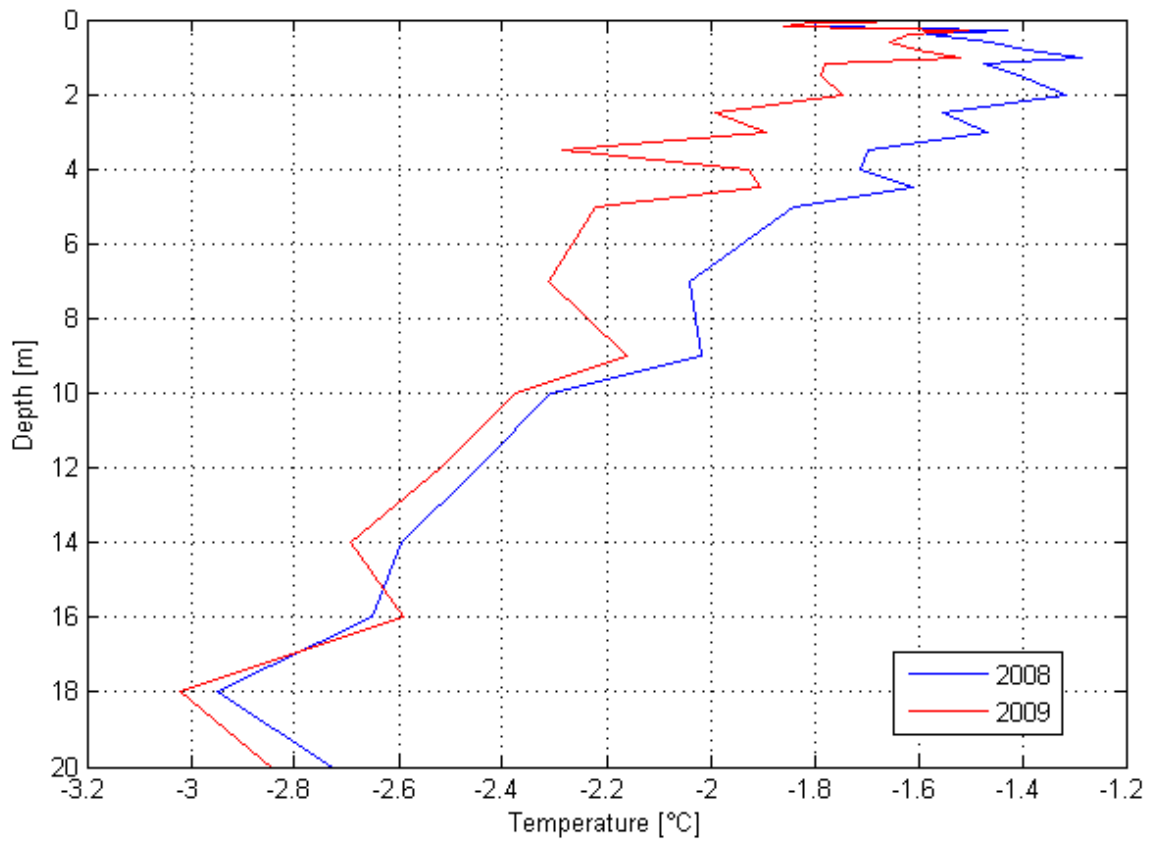


Fig. 4 – Mean temperatures of borehole 1 in 2008 (blue line) and 2009 (red line).

In winter 2008/09 an early and thick snow cover existed so the coldness could not penetrate into the ground. This fact causes the higher mean temperature in the upper layers in 2009. Another fact is illustrated in Fig. 4. Below 10 m the temperature of the years 2008 and 2009 are similar. One explanation could be that the penetration depth of seasonally temperature only reaches a depth of 15 m. This behaviour is also illustrated in Fig. 3. Below 15 m there are nearly no temporal fluctuations and between 10 and 15 m the fluctuations are very small.

As it was mentioned above, next to borehole 2 is another more shallow borehole, which was drilled down to 10 m and is equipped with extensometers. Measurements show that in autumn the extensometers measure negative values, which can be identified with compression. Not enough data are available yet for late spring and summer, but a first guess would be stretching with positive values. This hypothesis will be tested in summer 2011, when winter season is gone.

3. Possible future thermal response to predicted climate change

Because measurements exist only since 2007 it is not possible to make statements concerning permafrost retreat in the past climate warming at Sonnblick until now. But with the help of climate models which are able to compute temperature development in the future with different assumptions, it is achievable to produce possible future scenarios. As it is described in section 3.1, above 1.800 m a.s.l. ice and frost days will be reduced by about 14 days per year between 2021 and 2050 and also freeze-thaw days will increase about 3 to 5 days per year in this time-period (the reference interval is 1961 to 1990). Actually on Hoher Sonnblick 310 freezing days will be reduced to 296 and 239 ice days will be reduced to about 225 days with daily maximum below 0° C. Under these scenarios permafrost in higher mountain areas will retreat. Especially upper rock layers will react fast to the warming of the air. In deep layers, where the temperature change during one year is not observable, warming will be slower. The increase of freeze-thaw days will benefit weathering, frost shattering and fissuring. In regions with permafrost existence higher activity in rockfall will affect human infrastructure, mountain climbers and change of the landscape.

Acknowledgement. This work was partly granted by the project *Permafrost in Austria* by the Austrian Academy of Science.

References:

Exner Ch., 1964. Erläuterungen zur geologischen Karte der Sonnblickgruppe 1:50.000. Geol. B.-A. 168 S., Vienna.

3.

Case studies in the European Alps

3.5

Rock Glacier Hochebenkar, Western Austria

Citation reference

Krainer K. (2011). Chapter 3.5: Case studies in the European Alps – Rock Glacier Hochebenkar, Western Austrian Alps. In Kellerer-Pirklbauer A. et al. (eds): *Thermal and geomorphic permafrost response to present and future climate change in the European Alps*. PermaNET project, final report of Action 5.3. On-line publication ISBN 978-2-903095-58-1, p. 66-76.

Authors

Coordination: Karl Krainer

Involved project partners and contributors:

- Institute of Geology and Paleontology, University of Innsbruck (UIBK) – Karl Krainer

Content

Summary

1. Introduction and study area
2. Permafrost indicators and recent geomorphic evolution
3. Possible future thermal response to predicted climate change

References

Summary

Rock glacier Hochebenkar is a tongue-shaped active rock glacier located in a small Northwest facing cirque in the Ötztal Alps (Austria; 46°50'14''N, 11°00'46''E). Morphology and high surface flow velocities indicate that the rock glacier contains a massive ice core and thus point to a glacial origin. During winter, the temperature at the base of the snow cover (BTS) is significantly lower on the rock glacier than on permafrost-free ground adjacent to the rock glacier. Discharge of the rock glacier is characterized by strong seasonal and diurnal variations and is strongly controlled by the local weather conditions, particularly the amount of snow and rainfall events. Water temperature of the rock glacier springs remains constantly low, mostly below 1°C during the entire melt season. During the last decades changes in the velocity of the rock glacier show a close correlation with changes in the mean annual air temperature of nearby weather stations. The strong decrease in thickness in the lowermost, steep part of the rock glacier is caused by increased melting of ice and indicates the presence of a massive ice core. If increased melting will continue during the next decades flow velocity will decrease and the active rock glacier will pass into an inactive one.

1. Introduction and study area

Permafrost is widespread in the Alps which is documented by the large number of rock glaciers that have been mapped in the eastern part of the Alps, particularly in the central mountain ranges (e.g. Ötztal and Stubai Alps). As permafrost temperatures in the Alps are just slightly below 0°C and the frozen core of rock glaciers is thin, rarely exceeding 25 m, permafrost in the Alps, particularly active and inactive rock glaciers, are very sensitive to climate change. Studies on Alpine permafrost, particularly on active rock glaciers, advanced rapidly during the last two decades (see summary by Haeberli *et al.* 2006). In the Austrian Alps several rock glaciers have been studied in detail in recent years (e.g. Lieb, 1986, 1987, 1991, 1996; Lieb & Slupetzky 1993; Kaufmann, 1996a, b, Kaufmann & Ladstädter 2002, 2003, Kellerer-Pirklbauer 2007, 2008, Berger *et al.* 2004, Krainer & Mostler, 2000, 2001, 2002, 2004, 2006, Krainer *et al.* 2002, 2007, Hausmann *et al.*, 2007).

Hochebenkar rock glacier is located in Äußeres Hochebenkar, a Northwest oriented cirque in the southern Ötztal Alps, about 4.3 km SSW of Obergurgl, Ötztal (Tyrol, Austria). Although Hochebenkar rock glacier has been studied concerning flow velocities for more than 70 years (see below), only little information is available about composition, thickness, hydrology and thermal conditions.

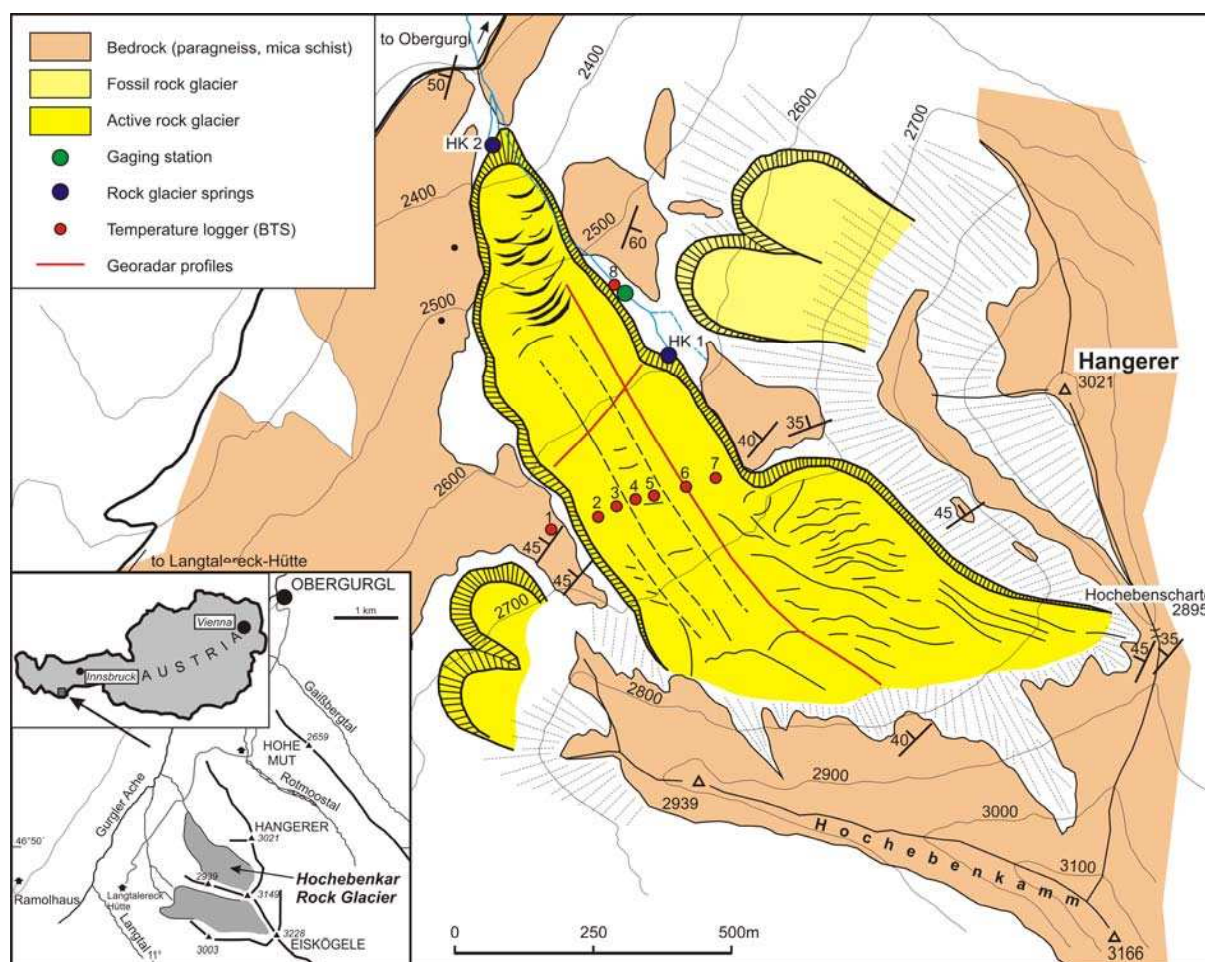


Fig. 1 – Rock glacier Hochebenkar with location of springs, gauging stations and temperature loggers (from Abermann *et al.* 2011).

Hochebenkar rock glacier is tongue shaped and extends from an altitude of 2840 m (rooting zone) to 2360 m (front). The maximum length of this active, NW-facing rock glacier is 1550 m. The width ranges from 160 m near the front to 335 m in the middle and up to 470 m in the upper part. The rock glacier covers an area of 0.4 km², the drainage area comprises 1 km².

The surface layer is coarse-grained with varying grain size and locally well developed transverse and longitudinal furrows and ridges. A depression is developed in the western part of the rooting zone. The front is steep and bare of vegetation. The highest peaks surrounding the rock glacier are Hangerer (3021 m) on the eastern side and the Hochebenkamm with its highest point at 3149 m on the southern side, separated by the Hochebenscharte (2895 m). The debris of the rock glacier is derived from the steep rock walls of the Hochebenkamm.

Bedrock in the drainage area of the rock glacier is composed of paragneiss and mica schists of the Ötztal-Stubai complex. At Hochebenkamm the bedrock is cut by numerous steep faults along which high amounts of debris are produced by frost weathering, particularly during break-up in spring and early summer.

The aim of this case study contribution is to present some preliminary data on the dynamics of Rock Glacier Hochebenkar, one of the largest and most active rock glaciers of the Austrian Alps.

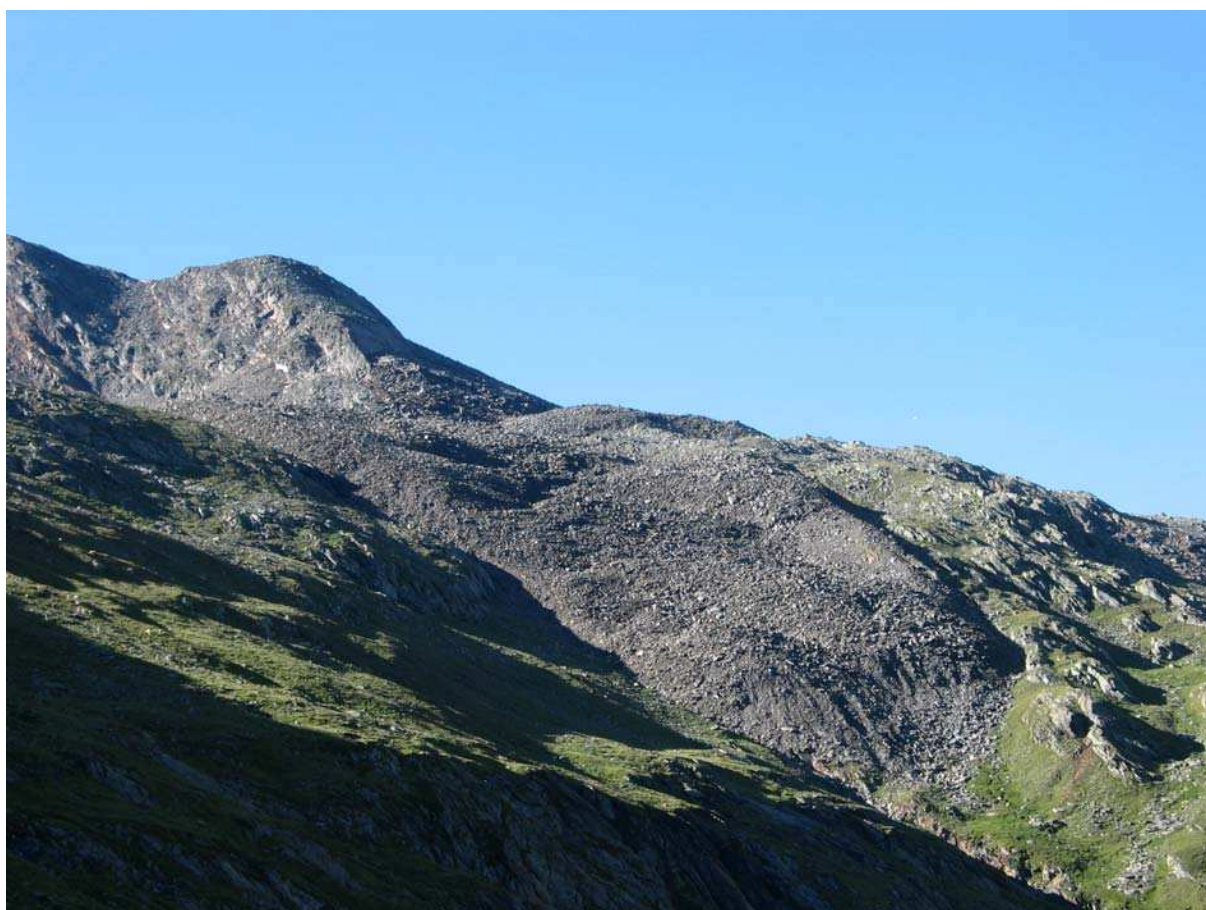


Fig. 2: View to the steep, active front of Hochebenkar rock glacier (view towards SW)

2. Permafrost indicators and recent geomorphic evolution

2.1 Previous studies

Hochebenkar rock glacier is one of the largest and most active rock glaciers in the Austrian Alps, which also shows the worldwide longest record of flow velocities. Pillewizer started to measure flow velocities on Hochebenkar rock glacier in 1938. Since that time, i.e. over a period of more than 70 years, flow velocities on this rock glacier have been measured by terrestrial photogrammetry, since 1951 by terrestrial geodetic methods (Theodolite) and since 2008 by differential GPS (Pillewizer 1938, 1957; Vietoris 1958, 1972; Haeberli & Patzelt 1982; Kaufmann 1996; Schneider & Schneider 2001; Kaufmann & Ladstädter 2002, 2003; Ladstädter & Kaufmann 2005). Haeberli & Patzelt (1982) measured the basal temperatures of the winter snow cover in February 1975, 1976 and 1977, and the water temperature of rock glacier springs during summer. They also carried out refraction-seismic measurements along 11 transects on frozen and unfrozen ground.

2.2 Rock glacier dynamics and thermal regime

During the last years intensive investigations have been carried out on Hochebenkar rock glacier to study the dynamics. These investigations include field mapping of the bedrock and sediments and geomorphologic features, grain-size analysis of the debris layer, BTS measurements, hydrology, georadar and flow velocity measurements (details in Abermann *et al.* 2011).

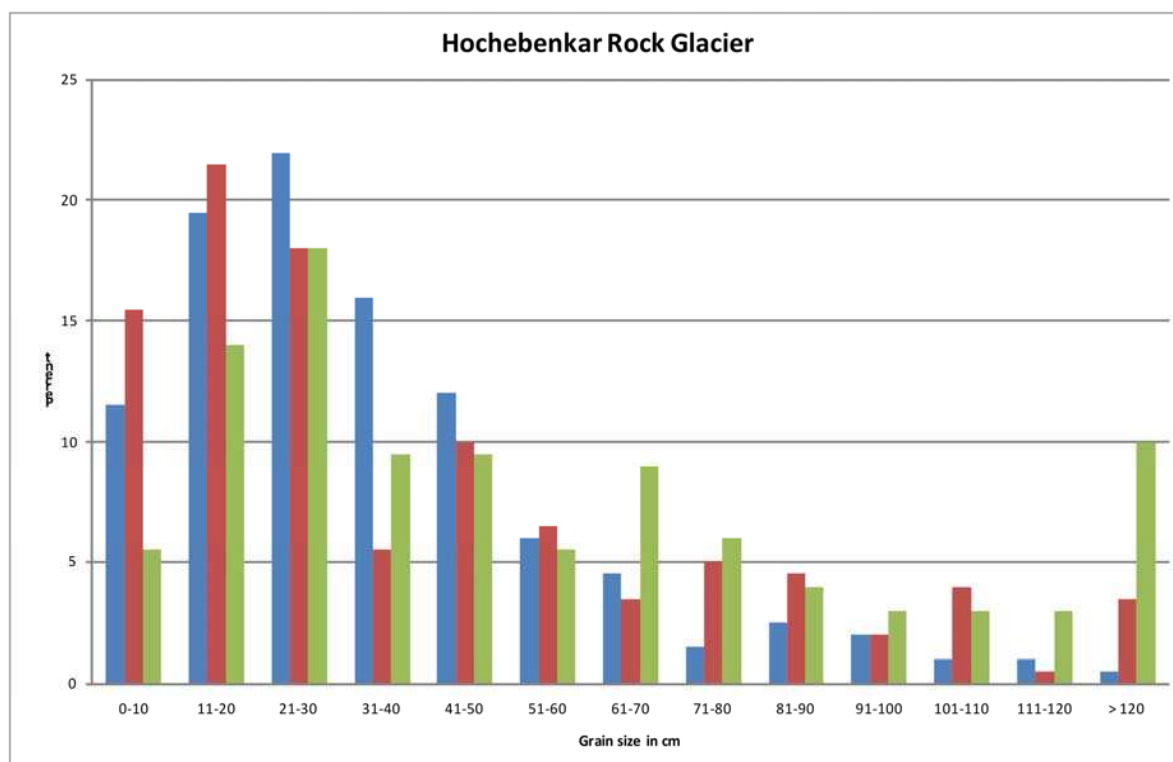


Fig. 3: Grain-size distribution of three sites on Hochebenkar rock glacier. Green bars: coarse-grained, blue bars: medium-grained, red bars: fine-grained.

Grain size of rock glacier

The surface debris layer of Hochebenkar rock glacier is coarse-grained with an average grain size (a-axis) measuring 35 cm on finer grained areas and 58 cm on coarser grained areas in the middle part (Fig. 3). Locally blocks up to a few m in diameter occur on the surface. Similar values are recorded from other rock glaciers composed of debris derived from gneisses and schists (Berger *et al.* 2004, Krainer and Mostler 2001, 2004).

The coarse-grained debris layer has a maximum thickness of 1.5 m and is underlain by debris containing higher amounts of sand and silt (Fig. 4) displaying poor to very poor sorting with values of 2.96-3.23 Phi (inclusive graphic standard deviation after Folk & Ward, 1957). Similar values have been reported from other rock glaciers (Barsch *et al.* 1979, Giardino & Vick 1987, Haeberli 1985, Krainer & Mostler 2000, 2004, Berger *et al.* 2004) and tills.

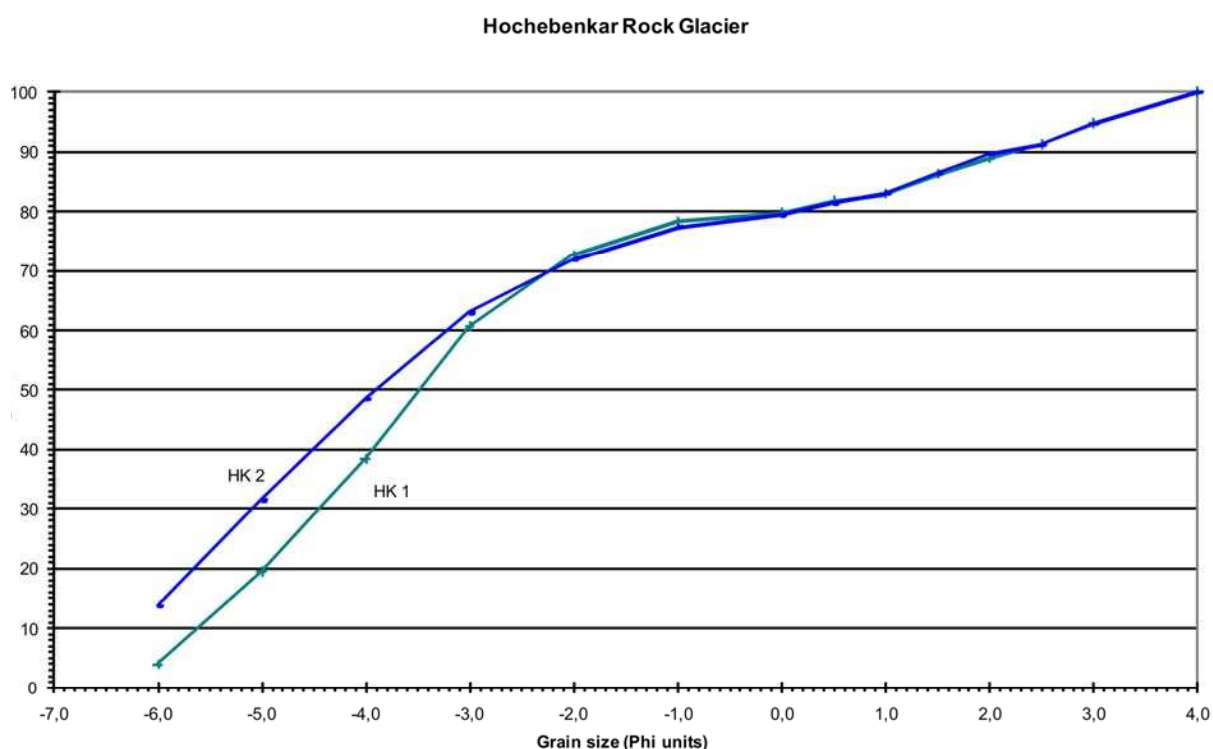


Fig. 4: Cumulative curves of two samples taken at the steep front of Hochebenkar rock glacier. Both samples show a similar trend indicating poor sorting.

Thermal regime of ground

BTS measurements performed by Haeberli & Patzelt (1982) in February 1975, 1976 and 1977 yielded mean values ranging between -4.8 and -7°C. Similar temperatures were recorded in March 2010.

During winter 2006/2007 eight temperature loggers were installed which recorded the temperature at the base of the snow cover at an interval of two hours. Results show that the temperature at the base of the snow cover on permafrost-free ground near the gauging station remained constantly between 0 and -1°C from November until May. From December until April temperatures varied between -3 and -4°C at the western margin and between -2 and -4°C at the eastern margin of the rock glacier. BTS temperatures were significantly deeper in the central part of the rock glacier ranging between -5 and -9.3°C with only minor variations. The deepest temperature (-9.9°C) was observed in early January. Snowmelt started during the first half of May.

Similar BTS temperature patterns were recorded on other active rock glaciers in the Ötztal and Stubai Alps (Ölgrube rock glacier – Berger *et al.* 2004, Reichenkar rock glacier – Krainer & Mostler 2000, Sulzkar rock glacier – Krainer & Mostler 2004) and Schober Mountains (Krainer & Mostler 2001).

Thermal regime, discharge and electrical conductivity of water springs

Water temperature of the rock glacier springs remained almost continuously $<1^{\circ}\text{C}$ during summer. Even after heavy thunderstorms in summer with rather “warm” rainfall causing peak floods in discharge of the rock glacier the water temperature did not change.

At Hochebenkar rock glacier most of the meltwater is released from springs at the front (Fig. 1). A minor amount (ca. 30%) of meltwater is released from two springs on the eastern side of the rock glacier at an altitude of 2575 m (Fig. 1). About 95 m downstream a gauging station was installed in spring 2007 at an altitude of 2555 m in order to record the water depth versus time during the melt season. Water depth of the meltwater stream is continuously recorded by a pressure transducer at intervals of 1 hour.

The discharge of the rock glacier is mainly controlled by water derived from snowmelt, summer thunderstorms and/or snowfall during summer and thus displays pronounced seasonal and diurnal variations in discharge. Runoff in 2009 started during April displaying floods with maximum flow peak during May and June caused by fair weather periods with intense melting of snow and ice (Fig. 5). A rapid decline in discharge was recorded a few hours after influx of cold air which sometimes was accompanied by snowfall. Short-term floods with peakflows $>100\text{ l/s}$ are triggered by summer thunderstorms with heavy rainfall. From July until September discharge decreased and was interrupted by single peak flows caused by rainfall events.

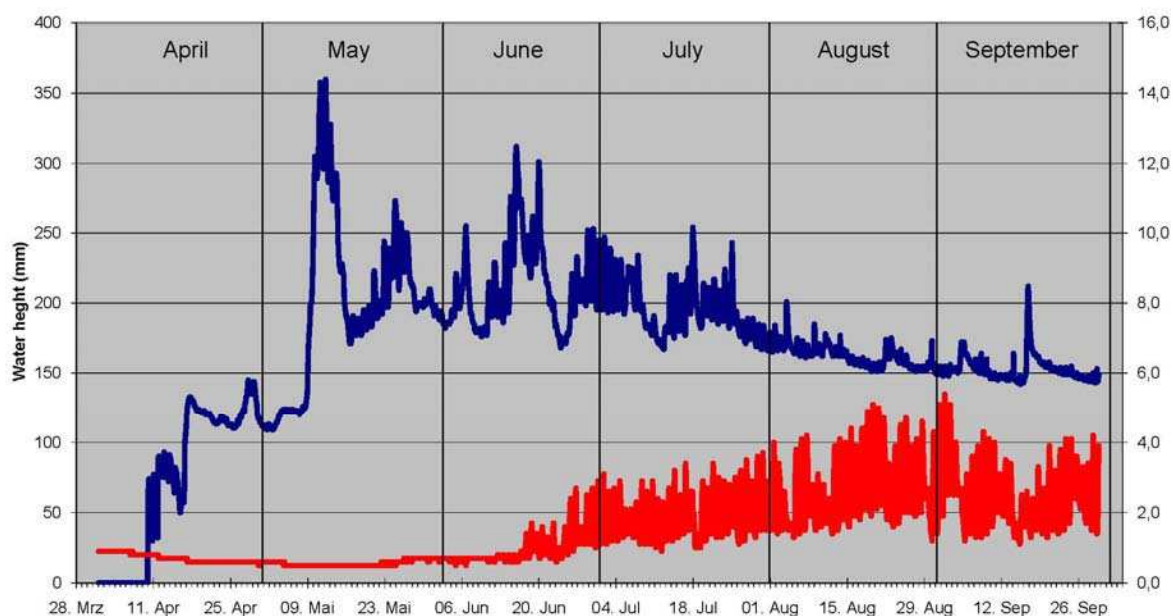


Fig. 5 – Hydrograph (water heights, blue line) of the meltwater stream released from Hochebenkar rock glacier (springs at the eastern side of the rock glacier) for the period April to September 2009. Red line indicates water temperature at the gauging station (location see Fig. 1).

The values for electrical conductivity of the water discharged from the rock glacier vary significantly over the season. At Hochebenkar rock glacier significantly higher values of electrical conductivity are recorded at the two springs on the eastern side than at the main spring at the front.

At springs which occur at the base of the steep front electrical conductivity is extremely low in May and June (20-30 $\mu\text{S}/\text{cm}$) and increases slightly reaching values of 40 $\mu\text{S}/\text{cm}$ by the end of August and 60 $\mu\text{S}/\text{cm}$ at the beginning of October. The water temperature at these springs ranges from 0.6 to 1.4°C.

At the two springs on the eastern side of the rock glacier the values of electrical conductivity are significantly higher with 100-200 $\mu\text{S}/\text{cm}$ in June, increasing to 400 $\mu\text{S}/\text{cm}$ during August and to 570 $\mu\text{S}/\text{cm}$ during September. Water temperature is very low with 0.2-0.4°C. The seasonal variation in electrical conductivity results from the different mixing ratio of low mineralized precipitation and higher mineralized groundwater (Krainer & Mostler 2001, 2002, Krainer *et al.* 2007).

Rock glacier dynamics

For the period 1938-1953 Pillewizer (1957) documented a maximum flow velocity in the upper part (profile B) of 75 cm/a, and 85 cm/a for the period 1953-1955. Profile 2 yielded flow velocities of 1.61 m for the period 1951-1952, 1.84 m for the period 1952-1953 and 1.53 m for the period 1953-1955 (Pillewizer 1957, Vietoris 1958).

Significantly higher flow velocities (average 3.9 m/a, maximum 6.6 m/a) were recorded between 1954 and 1972, whereas between 1973 and 1995 flow velocities were lower (average 1.15 m/a, maximum 2 m/a). Flow velocities again increased since 1995 reaching the highest values in 2003, and then decreased again (see Abermann *et al.* 2011).

Recent morphological changes

From 1936 to 1997 the front of the rock glacier advanced for 165 m (Schneider & Schneider 2001). According to Kaufmann (1996) the front of Hochebenkar rock glacier advanced for 148 m during 50 years, indicating a mean flow velocity of 3 m/a for that period. The lowermost profile 1 yielded the highest flow velocities of 3.57 m/a (1953-1955) which increased to 5 m/a (Vietoris 1972). Since 1995 a significant decrease in thickness was observed in the lowermost, steep part of the rock glacier.

2.3 Discussion and Conclusion

Morphology and debris properties of the active layer are very similar to other rock glaciers composed of debris derived from metamorphic rocks, particularly gneiss and schist (Berger *et al.* 2004; Krainer & Mostler 2000, 2001, 2004). Based on grain-size of the surface layer Hochebenkar rock glacier is a typical boulder rock glacier according to Ikeda and Matsuoka (2006). Temperatures at the base of the winter snow cover (BTS) are typical for active rock glaciers and similar to those recorded from other active rock glaciers in the Austrian Alps (Berger *et al.* 2004; Krainer & Mostler 2000, 2001, 2004). The pronounced seasonal and diurnal variations in discharge are strongly controlled by the weather conditions. Water released at the rock glacier springs is mainly derived from snowmelt and summer rainfall, subordinately from melting of permafrost ice and groundwater. Flood peaks are caused by intensive snowmelt on warm, sunny days during late spring and early summer and by rainfall events. The water temperature of the rock glacier springs which remains permanently below 1.5°C, mostly below 1°C, indicates that the water flows through the rock glacier in direct contact with permafrost ice (Krainer & Mostler 2002, Krainer *et al.* 2007). Extremely high values of the electrical conductivity at the spring on the eastern side of the rock glacier indicate a much longer residence time of the water compared to the water released at the springs at the steep front which is characterized by very low values indicating that the residence time is short and that the water is derived from melting of ice and snow and rainfall.

The depression in the rooting zone and the pronounced decrease in thickness in the lowermost part during the last years indicate melting of massive ice and we suggest that Hochebenkar rock glacier has a glacial origin similar to Reichenkar rock glacier (Krainer & Mostler 2000, Krainer *et al.* 2002, Hausmann *et al.* 2007). High ice-content is also indicated by annual flow velocities which are significantly higher than those of most other active rock glaciers with typical values of 0.1-1 m. Schneider & Schneider (2001) showed that the variations in flow velocity correlate with the mean annual air temperature values. Higher flow rates during warmer periods are probably caused by higher amounts of meltwater within the rock glacier and near the base, probably also to slightly higher ice temperatures.

Hochebenkar rock glacier most likely developed from a debris-covered cirque glacier due to the inefficiency of sediment transfer from glacier ice to meltwater, a model proposed by Shroder *et al.* (2000) based on studies in the Nanga Parbat Himalaya.

3. Possible future thermal response to predicted climate change

In high alpine mountain environments permafrost is warm (-2 to 0°C) and thus highly sensitive to temperature changes. Whereas warming of permafrost was observed in the northern parts of Europe of 0.5-1°C during the period 1998-2008, no clear warming trend was recorded in the Alps for this period due to high annual variations resulting particularly from varying thicknesses of the snow cover (Gärtner-Roer *et al.* 2011). However, field observations show that many rock glaciers in the Alps already reacted on the warming trend during the last decade. As most rock glaciers in the Alps are located near the lower boundary of discontinuous permafrost, which is thin and rather “warm”, these rock glaciers are expected to react more rapidly to even slight temperature changes compared to rock glaciers of colder regions.

At Hochebenkar rock glacier a significant decrease in thickness was observed during the last 15 years in the steep lower part indicating increased melting of permafrost ice. This already resulted in a decrease of flow rates. If the trend of global warming will continue, melting of permafrost ice will continue, particularly in the lower part of the rock glacier which is close to the lower limit of permafrost, resulting in a decrease in flow velocity.

But even in the upper part of the rock glacier increased melting of permafrost ice is expected. Thus Hochebenkar rock glacier will transform from a highly active rock glacier into an inactive rock glacier during the next decades. As a consequence, vegetation will start to grow on the fine-grained, steep frontal part of the rock glacier, which is still bare of vegetation.

Changes of total rock glacier discharge will depend on changes of annual precipitation. Increased melting of permafrost ice will slightly increase the amount of meltwater derived from ice, which constitutes only a small part (<10%) of the total discharge. Warming will change the discharge pattern of rock glaciers: the melting season will start earlier (in April instead of early May), and snow is expected to melt more rapidly within a shorter period during May and June causing high peak flows. These peak flows may be overprinted by single rainfall events resulting in extreme peak flows.

Height of peak flow and length of the peak flow period will depend on the snow heights which also may change. Such a discharge pattern with onset of the melt period in April and extreme peak flows due to intensive snowmelt during May and early June was already recorded in the extreme warm summer of 2003. Low discharge is expected for July until the end of the melt period, interrupted by single peak flows caused by rainfall events.

Acknowledgements: Monitoring of Hochebenkar rock glacier is funded by the Austrian Academy of Sciences (project “Impact of Climate Change on Alpine Permafrost”).

References:

- Abermann, J., Fischer, A., Krainer, K., Nickus, U., Schneider, H., & Span, N., 2011: Results of recent research on Rock Glacier Äußeres Hochebenkar. *Zeitschrift für Gletscherkunde und Glazialgeologie (submitted)*.
- Barsch D., Fierz H. & Haeberli W., 1979: Shallow core drilling and borehole measurements in permafrost of an active rock glacier near the Grubengletscher, Wallis, Swiss Alps. *Arctic and Alpine Research*, 11, 215-228.
- Berger J., Krainer K. & Mostler W., 2004: Dynamics of an active rock glacier (Ötztal Alps, Austria). *Quaternary Research*, 62, 233-242.
- Folk R.L. & Ward W.C., 1957: Brazos River Bar: A study in the significance of grain soil parameters. *Journal of Sedimentary Petrology*, 27, 3-26.
- Gärtner-Roer I., Christiansen H.H., Etzelmüller B., Farbot H., Gruber S., Isaksen K., Kellerer-Pirklbauer A., Krainer K. & Noetzi J., 2011: Permafrost. In: T. Voigt & H.M. Füssel (eds), Impacts of climate change on snow, ice, and permafrost in Europe: Observed trends, future projections, and socioeconomic relevance: 66-76.
- Giardino J.R. & Vick S.G., 1987: Geologic engineering aspects of rock glaciers. *Rock Glaciers*, Allen & Unwin, London, 265-287.
- Haeberli W., 1985: Creep of mountain permafrost: Internal structures and flow of alpine rock glaciers. *Mitteilungen der Versuchsanstalt für Wasserbau, Hydrologie und Glaziologie ETH Zürich*, 77, 1-142.
- Haeberli W. & Patzelt G., 1982: Permafrostkartierung im Gebiet der Hochebenkar-Blockgletscher, Obergurgl, Ötztaler Alpen, *Zeitschrift für Gletscherkunde und Glazialgeologie*, 18, 127-150.
- Haeberli W., Hallet B., Arenson L., Elconin R., Humlum O., Kääb A., Kaufmann V., Ladanyi B., Matsuoka N., Springman S. & Vonder Mühll D., 2006: Permafrost Creep and Rock Glacier Dynamics. *Permafrost and Periglacial Processes*, 17, 189-214.
- Hausmann H., Krainer K., Brückl E. & Mostler W., 2007: Internal Structure and Ice Content of Reichenkar Rock Glacier (Stubai Alps, Austria) Assessed by Geophysical Investigations. *Permafrost and Periglacial Processes*, 18, 351-367.
- Ikeda A. & Matsuoka N., 2006: Pebbly versus boulder rock glaciers: Morphology, structure and processes. – *Geomorphology*, 73, 279-296.
- Kaufmann V., 1996a: Der Dösener Blockgletscher – Studienkarten und Bewegungsmessungen. *Arb. Inst. Geogr. Univ. Graz*, 33, 141-162.
- Kaufmann V., 1996b: Geomorphometric monitoring of active rock glaciers in the Austrian Alps. *4th International Symposium on High Mountain Remote Sensing Cartography*. Karlstad, Kiruna, Tromsø, August 19-29, 1996, 97-113.
- Kaufmann V. & Ladstädter R., 2002: Spatio-temporal analysis of the dynamic behaviour of the Hochebenkar rock glaciers (Oetztal Alps, Austria) by means of digital photogrammetric methods. *Grazer Schriften der Geographie und Raumforschung*, 37, 119-140.
- Kaufmann V. & Ladstädter R., 2003: Quantitative analysis of rock glacier creep by means of digital photogrammetry using multi-temporal aerial photographs: two case studies in the Austrian Alps. *Proceedings of the 8th International Conference on Permafrost*, 21-25 July 2003, Zurich, Switzerland, 1, 525-530.
- Kellerer-Pirklbauer A. 2007: Lithology and the distribution of rock glaciers: Niedere Tauern Range, Styria, Austria. *Z. Gemorph. N.F.*, 51/2, 17-38.
- Kellerer-Pirklbauer A., 2008: The Schmidt-hammer as a Relative Age Dating Tool for Rock Glacier Surfaces: Examples from Northern and Central Europe. *Proceedings of the Ninth International Conference on Permafrost (NICOP)*, University of Alaska, Fairbanks, June 29 – July 3, 2008, 913-918.

- Krainer K. & Mostler W., 2000: Reichenkar Rock Glacier: a Glacier Derived Debris-Ice System in the Western Stubai Alps, Austria. *Permafrost and Periglacial Processes*, 11, 267-275.
- Krainer K. & Mostler W., 2001: Der aktive Blockgletscher im Hinteren Langtal Kar, Gößnitztal (Schobergruppe, Nationalpark Hohe Tauern, Österreich). *Wiss. Mitt. Nationalpark Hohe Tauern*, 6, 139-168.
- Krainer K. & Mostler W., 2002: Hydrology of Active Rock Glaciers: Examples from the Austrian Alps. *Arctic, Antarctic, and Alpine Research*, 34, 142-149.
- Krainer K. & Mostler W., 2004: Aufbau und Entstehung des aktiven Blockgletschers im Sulzkar, westliche Stubaier Alpen. *Geo.Alp*, 1, 37-55.
- Krainer K. & Mostler W., 2006: Flow Velocities of Active Rock Glaciers in the Austrian Alps. *Geografiska Annaler*, 88A, 267-280.
- Krainer K., Mostler W. & Span N., 2002: A glacier-derived, ice-cored rock glacier in the Western Stubai Alps (Austria): Evidence from ice exposures and ground penetrating radar investigation. *Zeitschrift für Gletscherkunde und Glazialgeologie*, 38, 21-34.
- Krainer K., Mostler W. & Spötl C., 2007: Discharge from active rock glaciers, Austrian Alps: a stable isotope approach. *Austrian Journal of Earth Sciences*, 100, 102-112.
- Ladstädter R. & Kaufmann V., 2005: Studying the movement of the Outer Hohebenkar rock glacier: Aerial vs. ground-based photogrammetric methods. *Second European Conference on Permafrost*, Potsdam, Germany, Terra Nostra 2005(2), 97.
- Lieb G.K., 1986: Die Blockgletscher der östlichen Schobergruppe (Hohe Tauern, Kärnten). *Arb. Inst. Geogr. Univ. Graz*, 27, 123-132.
- Lieb G.K., 1987: Zur spätglazialen Gletscher- und Blockgletschergeschichte im Vergleich zwischen den Hohen und Niederen Tauern. *Mitt. Österr. Geogr. Ges.*, 129, 5-27.
- Lieb G.K., 1991: Die horizontale und vertikale Verteilung der Blockgletscher in den Hohen Tauern (Österreich). *Z. Geomorph. N.F.*, 35, 345-365.
- Lieb G.K., 1996: Permafrost und Blockgletscher in den östlichen österreichischen Alpen. *Arb. Inst. Geogr. Univ. Graz*, 33, 9-125.
- Lieb G.K. & Slupetzky H., 1993: Der Tauernfelck-Blockgletscher im Hollersbachtal (Venedigergruppe, Salzburg, Österreich). *Wiss. Mitt. Nationalpark Hohe Tauern*, 1, 138-146.
- Pillewizer W., 1938: Photogrammetrische Gletscheruntersuchungen im Sommer 1938. *Zeitschrift der Gesellschaft für Erdkunde*, 1938(9/19), 367-372.
- Pillewizer W., 1957: Untersuchungen an Blockströmen der Ötztaler Alpen. *Geomorphologische Abhandlungen des Geographischen Institutes der FU Berlin (Otto-Maull-Festschrift)*, 5, 37-50.
- Schneider B. & Schneider H., 2001: Zur 60jährigen Messreihe der kurzfristigen Geschwindigkeitsschwankungen am Blockgletscher im Äusseren Hohebenkar, Ötztaler Alpen, Tirol. *Zeitschrift für Gletscherkunde und Glazialgeologie*, 37(1), 1-33.
- Shroder J.F., Bishop M.P., Copland L. & Sloan V.F., 2000. Debris-covered glaciers and rock glaciers in the Nanga Parbat Himalaya, Pakistan. *Geografiska Annaler*, 82: 17-31.
- Vietoris L., 1958: Der Blockgletscher des äußeren Hohebenkars. *Gurgler Berichte*, 1, 41-45.
- Vietoris L., 1972: Über die Blockgletscher des Äußeren Hohebenkars. *Zeitschrift für Gletscherkunde und Glazialgeologie*, 8, 169-188.

3.

Case studies in the European Alps

3.6

Rock Glacier Laurichard, Northern French Alps

Citation reference

Schoeneich P., Bodin X., Krysiecki J.-M. (2011). Chapter 3.6: Case studies in the European Alps – Rock Glacier Laurichard, Northern French Alps. In Kellerer-Pirklbauer A. et al. (eds): *Thermal and geomorphic permafrost response to present and future climate change in the European Alps*. PermaNET project, final report of Action 5.3. On-line publication ISBN 978-2-903095-58-1, p. 77-86.

Authors

Coordination: Philippe Schoeneich

Involved project partners and contributors:

- Institut de Géographie Alpine, Université de Grenoble, France (IGA-PACTE) – Philippe Schoeneich, Xavier Bodin, Jean-Michel Krysiecki

Content

Summary

1. Introduction and study area
2. Permafrost indicators and recent geomorphic and thermal evolution
3. Possible future thermal and dynamic response to predicted climate change

References

Summary

The Laurichard rock glacier in the French Alps is monitored for surface displacements and repeated geoelectrical soundings and tomographies since the 1980's. The 25 years velocity record, together with the repeated geoelectrical surveys and ground surface temperature record, allows to draw some essential conclusions on the influence of climate on the behaviour and evolution of rock glaciers. Rock glaciers react to climate and show interannual velocity variations. Their reaction time is thus much shorter than previously assumed. Velocity variations are linked to temperature variations – an increase in temperature induces an increase in velocity. The air temperature only partly explains the observed ground surface temperature and velocity variations. The ground surface temperature shows the best link with velocity variations, with a time lag of around one year. The snow cover explains most of the difference between air temperature and ground surface temperature, and thus appears as the main driving factor both for ground surface temperatures and for velocity variations. Thus, the evolution of the permafrost will not only depend on the air temperature, but will be strongly influenced by the evolution of the snow cover, especially its early or late onset in autumn. A late onset of the snow cover can at least partially compensate a rise in air temperature.

1. Introduction and study area

The Laurichard rock glacier RGL1 is situated in the granitic Combeynot massif on a North facing slope. It is a well developed bouldery rock glacier with distinct compression ridges and a steep frontal and lateral slope (Fig. 1). The RGL1 extends from the rooting zone (2650 m a.s.l.) at the contact with the rock face to 2450 m a.s.l. at its front and is advancing onto Holocene glacial and periglacial deposits. It is 490 m long, between 80 and 200 m wide, and has an apparent thickness (based on the vertical height of the sides and front) of 20-30 m. The rock glacier has a three stepped longitudinal profile, with moderate slopes in the upper part, a steep median part, and again a moderate slope in the frontal part. It displays morphological features typical of an active landform: longitudinal ridges in the central steep part and a succession of transverse ridges and furrows in the compressive part of the tongue (Table 1).



Fig. 1 – The Laurichard rock glacier. Photograph by X. Bodin.

Table 1 – Characteristics of the Laurichard rock glacier

Method	initiated /carried out
Latitude	N 45.0181°
Longitude	E 06.3997°
Elevation [m a.s.l.]	2440-2650 m
Slope	Variable: moderate on top and toe, steep (50%) in middle part
Aspect	North
Type of rock glacier	talus; lobate to tongue shaped; active
Evidence of permafrost	Observation of ground ice, ground surface temperature, geoelectric
Evidence of movement	Aerial photograph, geodetic, Lidar
Typology of movement	Velocity changes
Mean velocity range	From 0.3 to 1.6 m/yr
Change in velocity	20% increase 2000-2004, decrease 2004-2006
Year of first data	(1979) 1985

2. Permafrost indicators and recent geomorphic and thermal evolution

2.1 Methods

Movements have been measured since 1979 and regularly repeated since 1985. Thus it represents one of the longest displacement measurement record on a rock glacier in the Alps. Classical geodetic measurements are made under supervision of the Parc National des Ecrins on a transverse and on a longitudinal line of points, with a classical total station. The survey was carried out every two to three years from 1979 to 1999 and subsequently every year. Four marked blocks were added at the upper end part of the longitudinal profile in 1999. Annual velocity (downslope, vertical and horizontal), actual vertical change after removing total displacement of the block downslope and variation in inter-block distance can be calculated from these data (Bodin *et al.* 2009). Measured velocities range from 0.2 to 1.6 m/a. The highest velocities are measured in the steep median part (Fig. 2). Compared to other surveyed rock glaciers, it can be considered as a rather fast moving rock glacier.

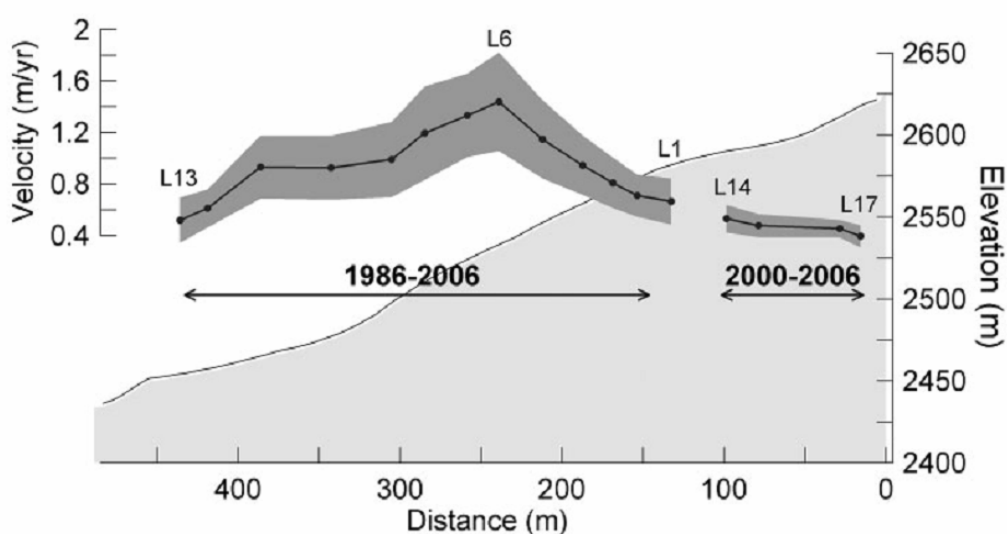


Fig. 2 – Downslope mean annual surface velocities of the Laurichard rock glacier along longitudinal profile line L (1986-2006 or 2000-06). Grey band represents one standard deviation for each measurement location (from Bodin *et al.* 2009).

Geophysical investigations have been repeated regularly since 1986. In total 12 vertical electrical soundings (VES) and six electrical resistivity tomography (ERT) profiles have been undertaken on the rockglacier to investigate its internal structure: two VES in 1986 (Francou & Reynaud, 1992), five VES in 1998 (V. Jomelli & D. Fabre, unpublished work), four VES and two ERT in 2004, and one VES in 2006. All of the VES were carried out using the Schlumberger configuration and the results were interpreted with two or three-layered resistivity models, whereas a pole-dipole configuration proved to be the best for ERT. The two ERT profiles were measured again in 2007 and 2009. These repeated measurements allow some interpretations on the evolution of the ice content.

Ground surface temperature (GST) measurements have been performed on the Laurichard rock glacier since 2003, with seven UTL mini dataloggers buried just below the blocky surface to protect them from direct solar radiation. One logger is placed outside the rock glacier in a non-permafrost area, whereas the six others are distributed over the surface of the landform. An automated weather station has been installed in 2004 beside the rock glacier. Meteorological data from nearby stations can be used in addition

2.2 Rock glacier velocity variation

One of the typical characteristics of the Laurichard rock glacier RGL1 are significant velocity variations all over the 25 years observation period. The rock glacier showed an increasing trend in flow velocities from 1985 to 1999, oscillations around a high velocity rate from 2000 to 2004, a decrease from 2004 to 2006, and again a moderate increase since 2007. Previous to 2000, the velocity changes are more difficult to interpret, due to the non-annual measurements. Mean velocities on periods of 2 to 3 years do not show significant changes, but the measurement interval induces a smoothing of the values that possibly hides more significant interannual variations.

The velocity changes can be compared to the mean annual air temperature (MAAT) using the nearby station of Monêtier-les-Bains (Meteo-France), using a 12 month running mean (Fig. 3). The overall picture shows a correspondence between the increasing temperature trend and the increasing velocity trend from 1985 to 1999, the high level of both temperature and velocity between 2000 and 2004, and the decrease in both temperature and velocity since 2004. This shows at least that a general dependence of velocity on temperature seems to exist. When looking on details, however, the correspondence appears to be less evident. Before 2000 strong temperature variations are not expressed in the velocity changes, but as mentioned above, this could be partly due to a smoothing of the velocity curve by the measurement interval. Between 2000 and 2004, some velocity variations appear to be inverted compared to temperature variations. This could indicate either a time lag or the influence of other parameters.

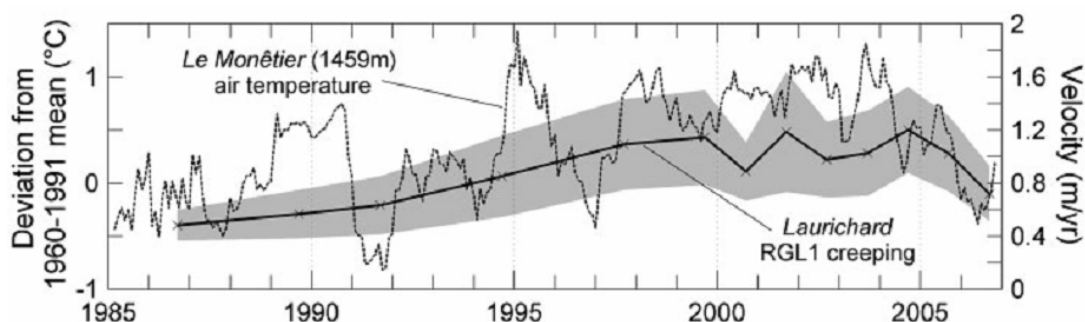


Fig. 3 – Mean surface velocity of the Laurichard rock glacier (RGL1) and 1σ range (grey band) from 1986-2006 (based on points L1-L3, L5-L8, L10-L12), and 12-months running mean air temperature anomaly (relative to the 1960-91 average) at the Monêtier station (Meteo France data) (from Bodin et al. 2009).

Since 2000 velocity variations can be compared on an annual basis with ground surface temperature records (using a data set from Valais for the period before 2004). The velocity changes show a good correspondence with the MAGST (mean annual ground surface temperature), averaged over the previous 12 months. This shows that creep rates are strongly dependent on ground surface temperatures, which appear as the main controlling factor with a time lag in the order of 1 year (Fig. 4).

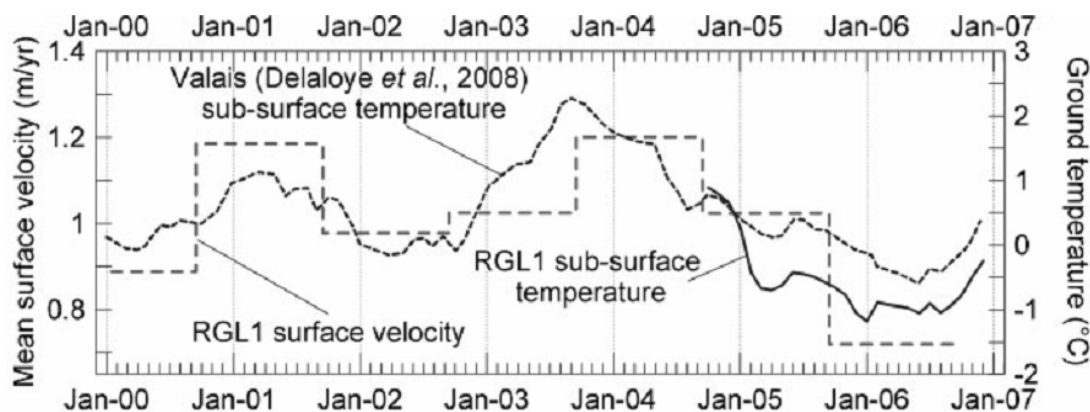


Fig. 4 – Ground surface temperatures and rock glacier movement, 2000-06: mean surface velocity (profile L) of the Laurichard rock glacier (RGL1), and ground surface temperatures on RGL1 (2003-06, 12-months running mean, average of four dataloggers) and in the Valais region (2000-06, 12-months running mean; western Swiss Alps; about 2500m a.s.l., data from Delaloye et al., 2008)(from Bodin et al. 2009).

2.3 Evolution of ground surface temperature

Ground surface temperatures (GST) show some deviations from the air temperature. The main controlling factor for ground surface temperature appears to be the snow cover thickness, especially in autumn and early winter. This is well demonstrated by the GST measurement series performed at Laurichard since 2003 (fig. 5, Schoeneich et al. 2010).

An early and sufficiently thick snow cover protects the ground surface from cooling during the cold and short days of November-December, whereas a late or shallow snow cover allows a strong cooling of the ground. When the subsequent snow cover is thick enough, its insulation effect preserves the “thermal memory” during the whole winter, as is shown by the winter equilibrium temperatures (WeqT) measured in March.

Thus the ground surface can experience an average cooling even in warm years, if the snow cover onset is late, and/or if the snow cover remains thin. On the other hand, the cumulative effect of an early snow rich winter preceded or followed by a hot summer is most efficient for inducing a warming of the ground surface.

2.4 Evolution of ice content and state

Repeated vertical electric soundings (VES) and electrical resistivity tomography (ERT) profiles show an evolution of apparent resistivities measured on the rock glacier body. All data show the typical profile expected on rock glaciers, with a moderately resistant surface layer corresponding to the blocky active layer, a high resistive main layer corresponding to the permafrost body, and a basal less resistive layer. The discussion will thus focus on differences with time.

Four successive VES were performed on the tongue (1986, 1998, 2004, 2006) and three at the root (1986, 1998, 2004). The accuracy of relocation of the 1986 sites is judged to be about 5m for the lower one and 10m for the upper one. There was a general decrease in the maximum apparent resistivity (ramax) at the VES sounding sites located at the root and on the tongue from 1986 to 2004-06 (Fig. 6). At the root (for an inter-electrode spacing $AB/2=50\text{m}$), ramax decreased by 35-50 % from $8.10^5\Omega\cdot\text{m}$ in 1986 to $3-4.10^5\Omega\cdot\text{m}$ 18 years later. At the tongue, ramax decreased by 20-50 % cent from $5.10^4\Omega\cdot\text{m}$ in 1986 ($AB/2=30\text{m}$) to $1.5-4.10^4\Omega\cdot\text{m}$ in 2004 ($AB/2=20\text{m}$).

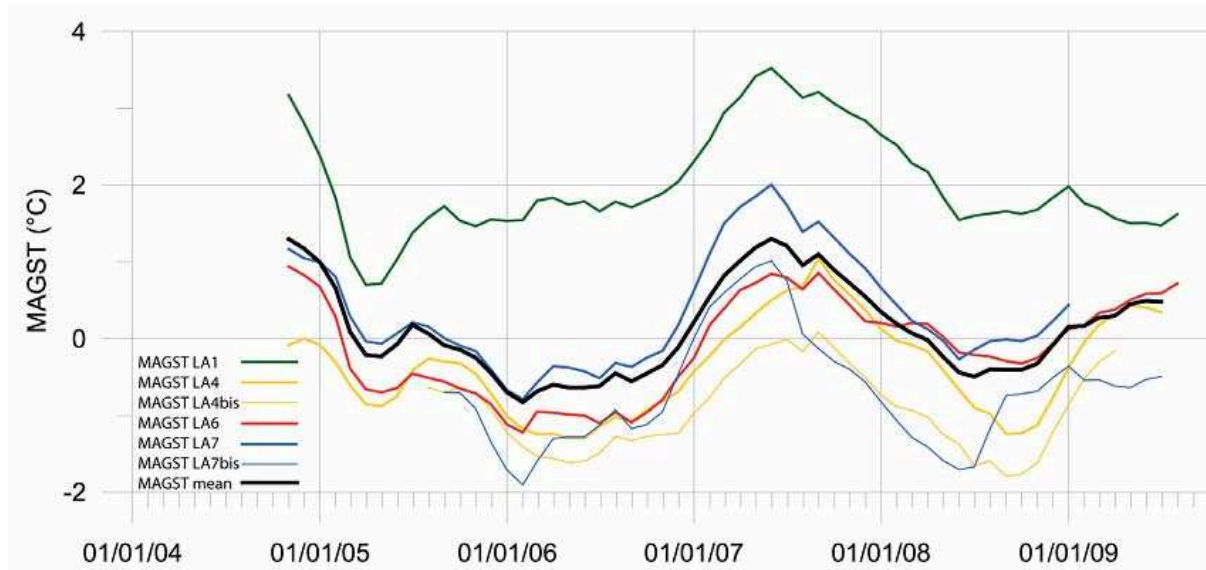


Figure 5 – Ground surface temperatures measured on 5 locations on the Laurichard rock glacier (2003-2009, running mean of the 12 previous months). LA 1 is outside of the rock glacier, the others are on it. The effect of the snow poor winters 2004/05 and 2005/06 is clearly visible, as well as the cumulative effect of the hot summer 2006 and the snow rich winter 2006/07.

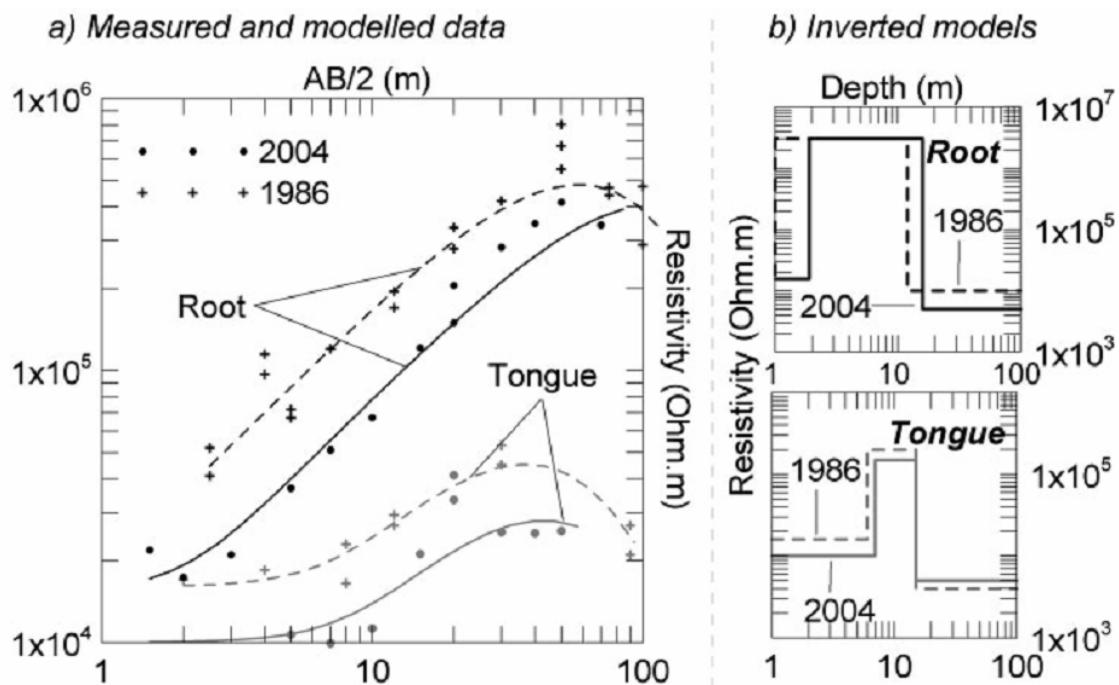


Fig. 6 – (a) Measured and modelled resistivity at the root (black curves and dots) and tongue (grey curves and dots) of the Laurichard rock glacier in 1986 and 2004; (b) inverted models for the root (top) and tongue (bottom) in 1986 and 2004 (from Bodin et al. 2009).

The relatively large variations in resistivity over the period 1998-2006 suggest that it may be difficult to distinguish resistivity changes due to long-term modification of the permafrost (e.g. a thickening of the active layer, an increase in ground temperature, a decrease in ice content) from those relating to seasonal changes in ground properties (e.g. differing water contents during the sounding campaigns in the active layer and/or within the icy layer), and/or localised changes in the internal structure related to permafrost deformation. Despite these limitations, the diachronic VES measurements can be interpreted using inversion models to depict hypothetical vertical changes in structures composed of homogeneous horizontal layers (Figure 6b). Taking into account the infinity of solutions and the well-established electrical properties of similar ground materials (Fabre & Evin 1990, Hauck 2001, Delaloye 2004), changes at the root can be interpreted as being due to thickening of the active layer from 1-2m to 2-3m with no noticeable modification of the icy layer. In contrast, those at the tongue could represent a thickening of the active layer and a lower ice content, and/or a thinning of the icy layer. These results are less reliable, however, due to strong lateral variations of the internal structure which are not ideal for layered modelling.

2.5 Lessons from the Laurichard case

The 25 years velocity record, together with the repeated geoelectrical surveys and ground surface temperature record allows to draw some essential conclusions on the influence of climate on the behaviour and evolution of rock glaciers.

- Rock glaciers react to climate and show interannual velocity variations. Their reaction time is thus much shorter than previously assumed.
- Velocity variations are linked to temperature variations – an increase in temperature induces an increase in velocity.
- The air temperature only partly explains the observed ground surface temperature and velocity variations.
- The ground surface temperature shows the best link with velocity variations, with a time lag of around 1 year.
- The snow cover explains most of the difference between air temperature and ground surface temperature, and thus appears as the main driving factor both for ground surface temperature and for velocity variations.

Thus, the evolution of the permafrost will not only depend on the air temperature, but will be strongly influenced by the evolution of the snow cover, especially its early or late onset in autumn. A late onset of the snow cover can at least partially compensate a rise in air temperature.

Several open questions remain, however. The main question may be how to explain the very rapid response of velocity to ground surface temperature. The rock glacier movement takes place in the permafrost body and mainly at its base. The thermal conductivity of the permafrost is low and the surface temperature variations need time to diffuse through the profile and are strongly attenuated with depth. It seems unlikely that the temperature variations alone are sufficient to induce strong velocity variations. Another factor could be the presence of liquid water percolating through the permafrost body or at its base. This would mean that the velocity variations are controlled by the amount of available liquid water. This would imply a permafrost temperature close to the melting point.

A similar question arises concerning the resistivity measurements on the rock glacier tongue. The low resistivity measured in the VES are considered as typical for ice poor permafrost, and ERT profiles suggest a discontinuous and ice poor permafrost body. Such interpretations however are

inconsistent with the high velocity rates measured on the tongue, which imply an ice supersaturated permafrost body. The explanation could be the presence of liquid water in “temperate” permafrost.

This means that the evolution of rock glacier permafrost with rising temperature could be characterized by an increase of the permafrost temperature to values close to the melting point, and an increase of interstitial liquid water during the melting season.

3. Possible future thermal and dynamic response to predicted climate change

The results from the Laurichard rock glacier and from other similar cases show that (i) the dynamic response of rock glaciers will strongly depend on the thermal evolution of the permafrost and (ii) that the thermal response will depend on the temperature evolution as well as on the evolution of winter precipitation and snow cover onset and duration.

For ground surface temperature, the direct influence of the snow cover onset date and thickness is well documented at Laurichard, and shows a strong interannual variability. No temperature profile is available at Laurichard, but other existing long time series show an overall warming trend at ca 10 m depth (Permos reports). So the most probable scenario of thermal response could be the following:

- Warming temperatures will induce a general warming trend of the permafrost.
- A strong interannual variability will continue to exist, and cooling periods of one to several years will continue to happen.
- The interannual variability depends mainly on the snow cover. Increased winter precipitations could induce a stronger warming of ground surface temperature, especially if increased precipitation means earlier onset of the snow cover.
- An earlier snow melt due to warmer spring temperatures would induce a warming of ground surface temperatures.
- The thermal effect of increased amounts of melting water due to increased winter precipitation is unknown.

The dynamic response of the rock glacier depends on the ice content, temperature and state. The following responses can be deduced from the observations:

- The decrease observed in electrical resistivity will possibly continue, reflecting the presence of increasing amounts of water within the ice-rock mixture. The amount of ice in the rock glacier body is still high, however, and should remain so for a long time.
- Interannual velocity variations will continue to occur, in relation to ground surface temperature variations. Velocity increases are expected especially after very warm summers associated with snow rich winters.
- The geomorphological settings of the Laurichard rock glacier are not favourable to a strong acceleration, and a destabilization of the rock glacier is not expected. Due to its already relatively high mean velocity, this point however needs to be monitored.

Acknowledgements. – The study of the Laurichard rock glacier was supported by the Fondation MAIF. The annual displacement measurements are performed by the Parc National des Ecrins. We thank Denis Fabre and Adriano Ribolini for allowing the use of geophysical data.

References:

- Bodin X., 2007: *Géodynamique du pergélisol de montagne: fonctionnement, distribution et évolution récente. L'exemple du massif du Combeynot (Hautes Alpes)*. PhD thesis, University of Paris-Diderot Paris 7. 272 pp.
- Bodin X., Thibert E., Fabre D., Ribolini A., Schoeneich P., Francou B., Reynaud I. & Fort M., 2009: Two decades of responses (1986–2006) to climate by the Laurichard rock glacier, French Alps. *Permafrost and Periglacial Processes*, 20, 331-344.
- Delaloye R., 2004: *Contribution à l'étude du pergélisol de montagne en zone marginale*. PhD thesis, Université de Fribourg. 260 pp.
- Delaloye, R., Perruchoud, E., Avian, M., Kaufmann, V., Bodin, X., Ikeda, A., Hausmann, H., Käab, A., Kellerer-Pirklbauer, A., Krainer, K., Lambiel, C., Mihajlovic, D., Staub, B., Roer, I. and Thibert, E., 2008: Recent Interannual Variations of Rockglaciers Creep in the European Alps. In: Kane, D.L. and Hinkel, K.M. (eds), *Proceedings, Ninth International Conference on Permafrost (NICOP)*, University of Alaska, Fairbanks, 343-348.
- Fabre D. & Evin M., 1990: Prospection électrique des milieux à très forte résistivité: le cas du pergélisol alpin. *6ème Congrès International de AIGI*, Rotterdam.
- Francou B. & Reynaud L., 1992: Ten years of surficial velocities on a rock glacier (Laurichard, French Alps). *Permafrost and Periglacial Processes* 3: 209–213.
- Hauck C., 2001: *Geophysical methods for detecting permafrost in high mountains*. PhD thesis, VAW, Zürich. 204 pp.
- Schoeneich P., Bodin X., Krysiecki J.-M., Deline P. & Ravelin L., 2010: *Permafrost in France. Report N°1*. PermaFrance network, Grenoble, Institut de Géographie Alpine.

3.

Case studies in the European Alps

3.6

Rock Glacier Bellecombes, Northern French Alps

Citation reference

Schoeneich P., Krysiecki J.-M., Le Roux O., Lorier L., Vallon M. (2011). Chapter 3.7: Case studies in the European Alps – Rock Glacier Bellecombes, Northern French Alps. In Kellerer-Pirklbauer A. et al. (eds): *Thermal and geomorphic permafrost response to present and future climate change in the European Alps*. PermaNET project, final report of Action 5.3. On-line publication ISBN 978-2-903095-58-1, p. 87-96.

Authors

Coordination: Philippe Schoeneich

Involved project partners and contributors:

- Institut de Géographie Alpine, Université de Grenoble, France (IGA-PACTE) – Philippe Schoeneich, Jean-Michel Krysiecki
- Association pour le développement de la recherche sur les glissements de terrain, France (ADRGT) – Lionel Lorier, Olivier Le Roux
- Laboratoire de Glaciologie et de Géophysique de l'Environnement, Université de Grenoble, France (LGGE) – Michel Vallon

Content

Summary

1. Introduction and study area
2. Permafrost indicators and recent geomorphic and thermal evolution
3. Possible future thermal and dynamic response to predicted climate change

References

Summary

The rock glacier Bellecombes is a shallow slow moving rock glacier. However, surface movements associated with settlement due to ice melting are sufficient to induce strong disturbance to a chairlift station built on its surface. Two boreholes were drilled through the rock glacier, revealing a total thickness of ca 9.50 m, but with a very ice-rich layer, 6-7 m thick, lying directly on bedrock. The temperature profiles show a very stable and constant temperature of the ice-rich layer around -0.2°C , with almost no seasonal variation. The ground surface temperature shows cold winter equilibrium temperatures (down to -4°C) and strong seasonal variations limited to the ice-poor blocky surface layer. The temperature profile arises the question of the status of the ice: the ice temperature, very close to 0°C , could indicate that the ice is at the melting point temperature. On the other hand, very high electrical resistivity values indicate low liquid water content, and velocities show that no basal sliding is occurring so far. The question of the melting point temperature of an ice-rock mixture could be crucial for the future dynamic behavior of rock glaciers like Bellecombes. More knowledge is needed on the physics of ice-rock mixtures. One dimensional modelling was run with different scenarios. Results show that the very ice-rich permafrost body seems to be very stable under present day conditions, and a strong warming would be necessary to induce significant changes in ice-content and temperature.

1. Introduction and study area

The Bellecombres rock glacier is situated on the ski resort Les Deux Alpes, in the Ecrins massif, French Alps (Table 1). It is a shallow, topographically smooth rock glacier. It develops on a North oriented slope from ca 2800 to 2600 m a.s.l. The two last pylons and the upper station of a chair lift are built on the rock glacier. During construction work, an ice layer of 2-4 m thickness was removed under the future chair lift station. Despite this, the chairlift station is subjected to settling movements, indicating that there is still ice below it.

The site has therefore been monitored since 2007 for ground surface temperature and surface displacements. It has become a reference test site for various geophysical methods (geoelectrical sounding and tomography, refraction and reflexion seismics, surface waves, seismic ground noise, georadar). Two boreholes were drilled in autumn 2009 through the rock glacier down to the bedrock and equipped with sensor chains for temperature profile monitoring.



Fig. 1 – The Bellecombres rock glacier. Photograph by Philippe Schoeneich.

Table 1 – Characteristics of the Bellecombres rock glacier

Method	initiated /carried out
Latitude	N 44.99 °
Longitude	E 06.16 °
Elevation [m a.s.l.]	2710 m
Slope	moderate
Aspect	North
Type of rock glacier	talus; lobate to tongue shaped; active
Evidence of permafrost	Observation of ground ice, ground surface temperature, borehole profile
Evidence of movement	Aerial photograph, DGPS
Typology of movement	Very slow movement
Mean velocity range	From 0.03 to 0.10 m/yr
Change in velocity	No significant change
Year of first data	2007

2. Permafrost indicators and recent geomorphic and thermal evolution

2.1 Ground surface temperatures

Ground surface temperatures are monitored since 2007 with 4 UTL-1 mini data loggers (3 on the rock glacier surface, 1 outside of the rock glacier in non-permafrost terrain). In addition, several BTS-mapping campaigns were performed in late winter, in order to map the ground surface temperature distribution during winter equilibrium conditions.

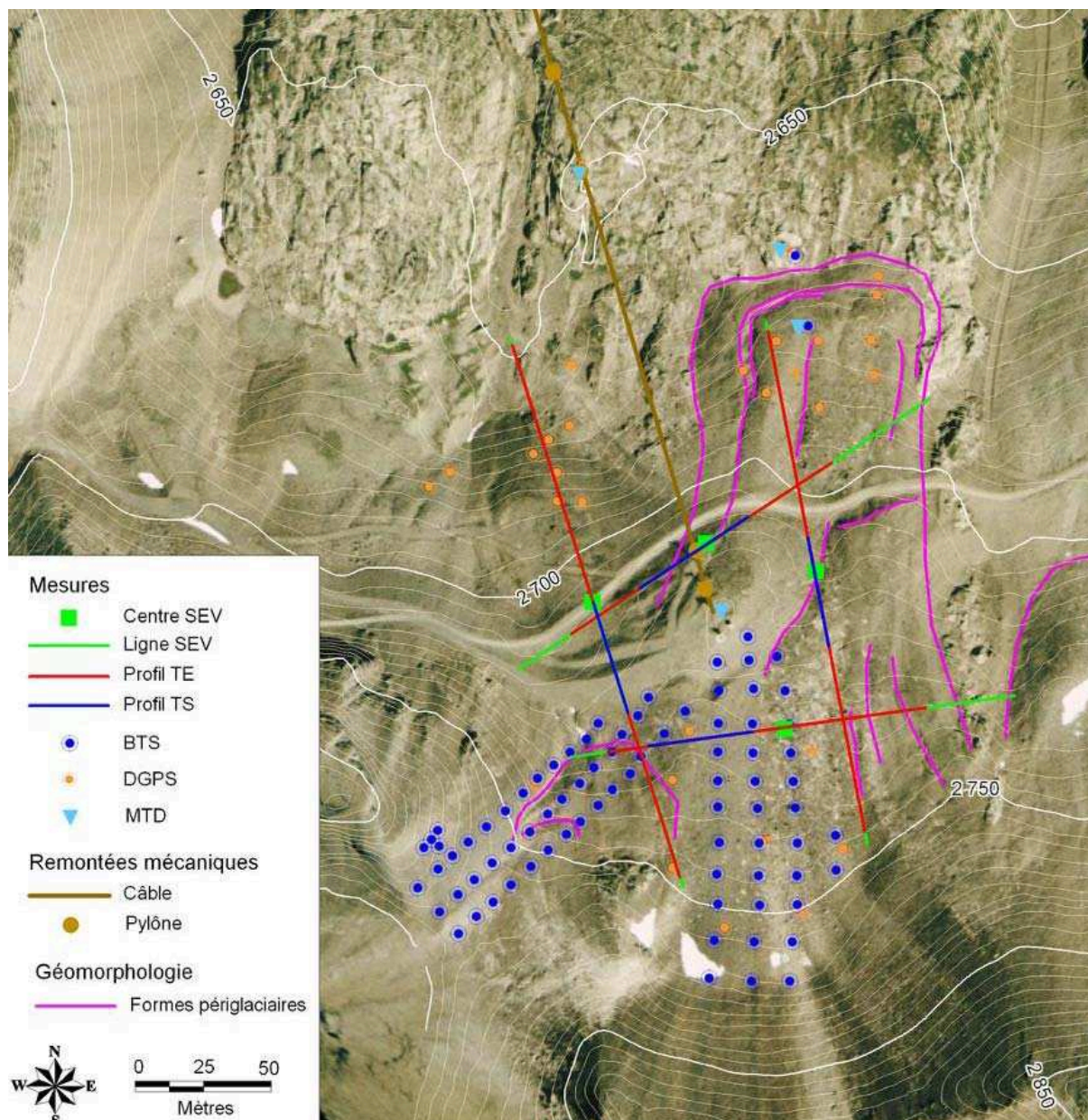


Fig. 2 – Orthophoto of the Bellcombes rock glacier, and position of monitoring devices.

The results show :

- A generally low winter equilibrium temperature on the rock glacier surface, with values as low as -4 to -5°C.
- A strong temperature contrast with the non-permafrost area surrounding the rock glacier, where only slightly negative temperatures are recorded. This contrast appears on the loggers as well as on the BTS-maps.
- The BTS-mapping shows an almost perfect match between low ground surface temperature and geomorphological extent of the rock glacier (fig. 3).

These results clearly indicate the presence of permafrost on the entire area of the rock glacier.

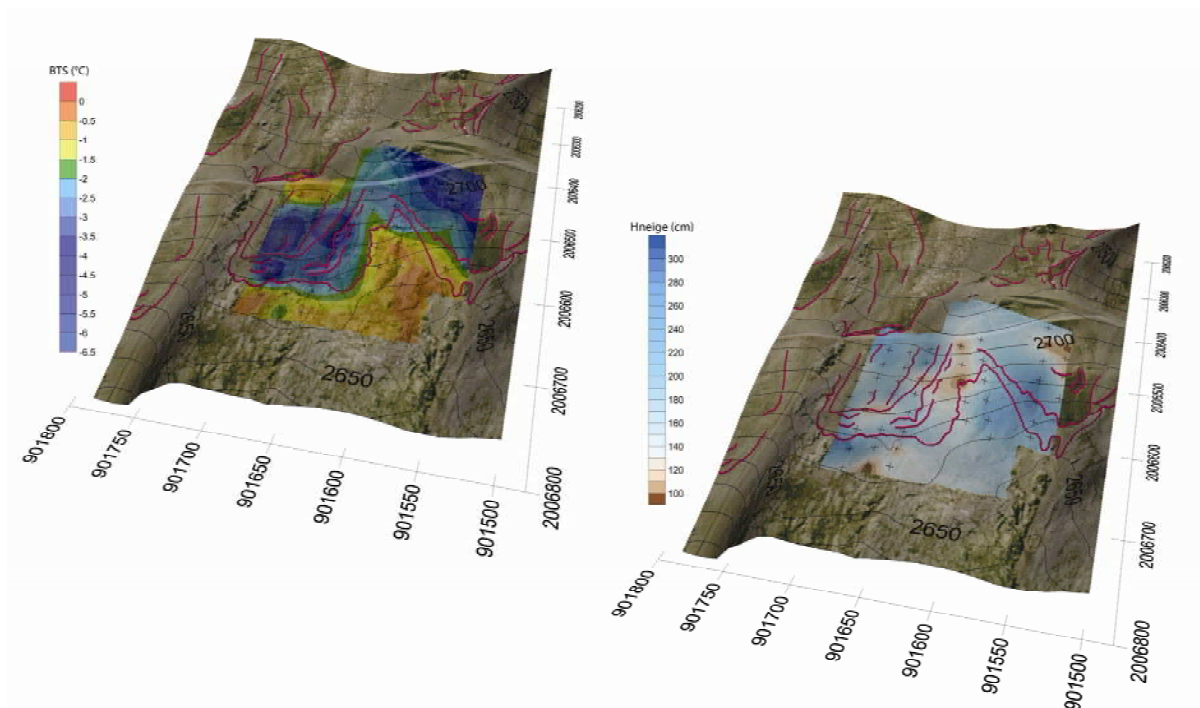


Fig. 3 – Ground surface temperature distribution at winter equilibrium, from BTS-mapping in March 2009 (left) and snow cover thickness (right). The left map shows distinct limits of the permafrost zone, consistent with the geomorphological limits of the rock glacier.

2.2 Rock glacier velocity

The surface displacements are measured with DGPS on 32 points distributed over the surface of the rock glacier. The annual displacement values are very low on most of the points, in the order of a few cm/a, at the accuracy limit of the measurement method. In addition to horizontal displacements, vertical settlements are observed at the chairlift station and on the pylons. These movements, in the order of several millimeters, are sufficient to need periodic cable alignments.

2.3 Ice content and stratigraphy

Vertical resistivity soundings (VES) and electrical resistivity tomography (ERT) were performed in 2007 and 2009 on four profiles across the rock glacier. No significant changes have been observed between 2007 and 2009. All ERT profiles show very high resistivity values, typical of high ice content. This high ice content was subsequently confirmed by two boreholes.

Both destructive boreholes show a similar stratigraphy (fig. 4):

- On top, 2.1 m of dry debris, corresponding to the blocky active layer.
- 7.5 m of very ice-rich material. From the interpretation of the penetration logs and of the cuttings, this layer can be subdivided on borehole SD1 into an upper ice-rock mixture and a lower almost pure ice layer, whereas in borehole SD2 the whole layer is made of an ice-rock mixture.
- Bedrock was reached in both boreholes at ca 9.5 m depth. The ice-rich layer lies in both boreholes directly on the bedrock.

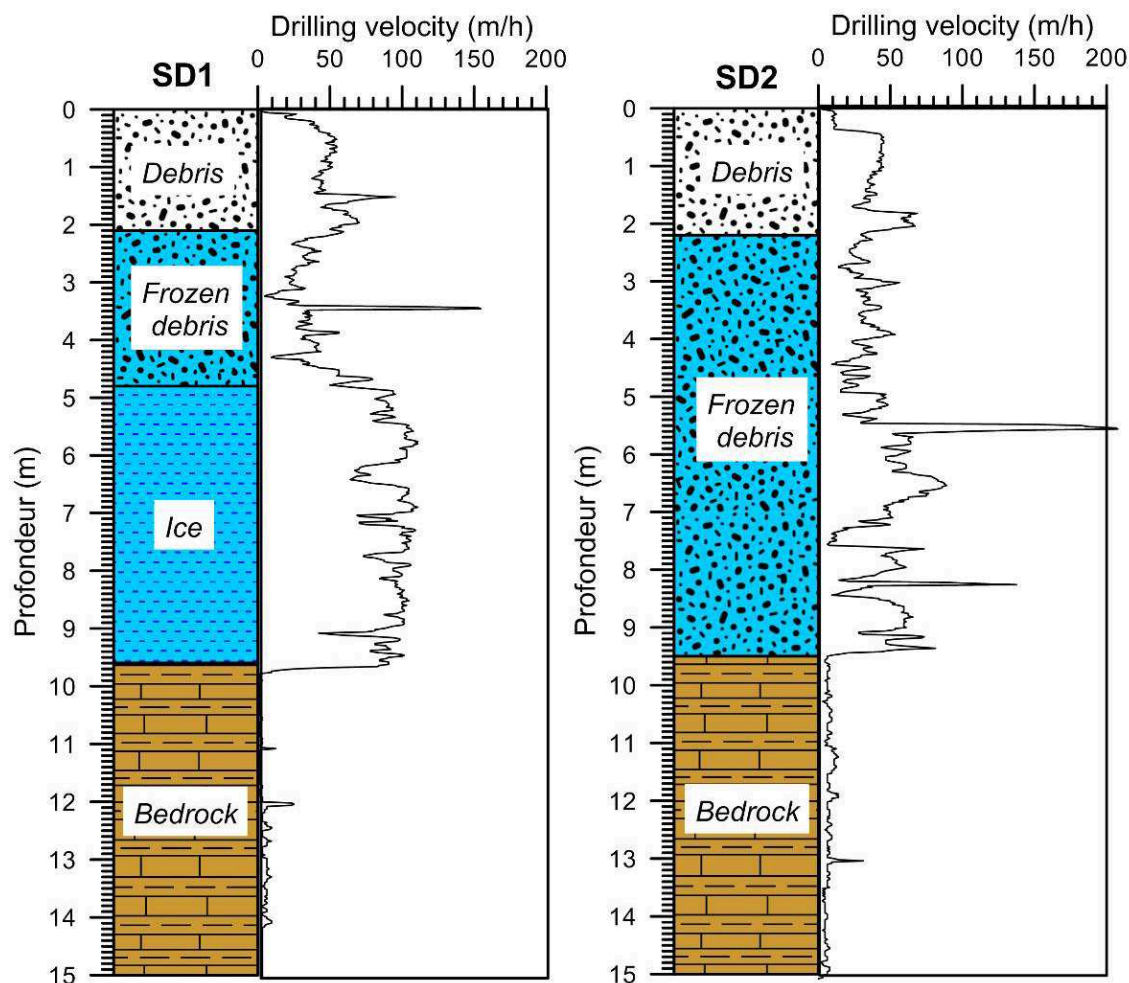


Fig. 4 – Borehole stratigraphy of the two boreholes at Bellecombès rock glacier.

The boreholes confirmed the presence of very high ice content, as deduced from the ERT profiles. However, the thickness interpreted from the ERT proved to be largely overestimated, due to the very high resistivity values. This known drawback of the ERT method limits its use for the determination of the thickness of permafrost bodies. Combined tests of several geophysical methods on the same profiles show that only the georadar can possibly help to determine the real thickness of the permafrost body.

2.4 Temperature profiles

The two boreholes were equipped with thermistor chains (PT 100 sensors) connected to a logger for temperature profile monitoring. The results of borehole SD1 are shown in fig. 5. The influence of the ice content on the temperature variations appears very obviously:

- Strong seasonal temperature variations occur within the 2 m thick active layer with almost no ice content.
- The seasonal temperature variations are drastically attenuated at ca. 2 m depth, at the boundary with the ice-rich layer.
- The zero annual amplitude can be set at the transition from frozen debris to massive ice.

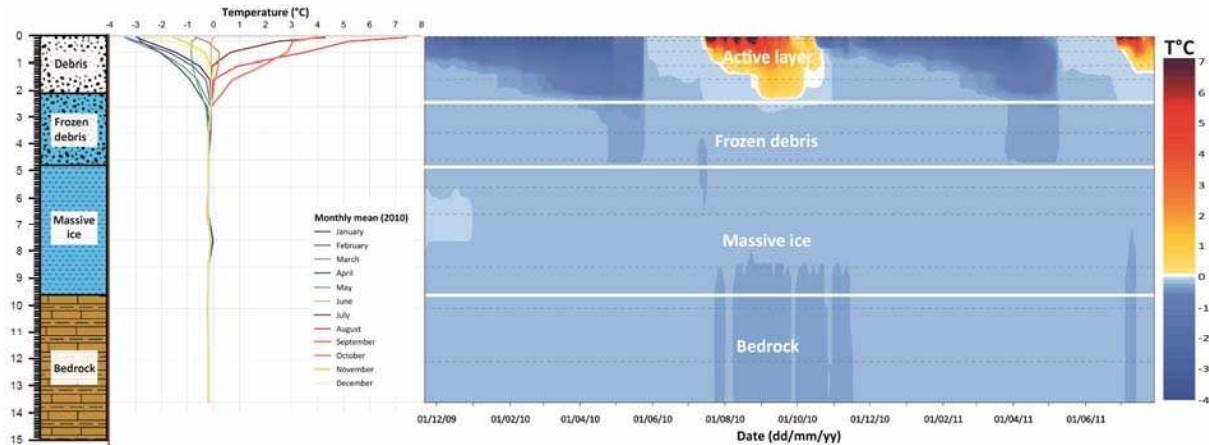


Fig. 5 – Temperature profile of borehole SD1 and evolution from November 2009 to July 2011.

- In the ice-rich layer, as well as in the bedrock below, temperature variations are almost absent or limited to a range of $\pm 0.1^{\circ}\text{C}$.

The temperature of the ice-rich layer is very constant and stable:

- The absolute value is around -0.2°C , very close to the melting point.
- It shows no trend towards depth, but the profile is very short (ca 13 m total depth).
- Variations are limited to a very narrow range.

2.5 Lessons from the Bellecombès case

The investigations on the Bellecombès rock glacier show the limits of geophysical methods for the determination of ice body thickness and geometry. The most favourable geophysical method used in permafrost, geoelectrical tomography (ERT), proves to strongly overestimate the thickness of the permafrost body in case of a very high ice content inducing very high resistivity values. This point is very critical, as the knowledge of the thickness is crucial for a correct management of geotechnical problems like the one of the chairlift station. So far, boreholes remain the best method to assess the stratigraphy of permafrost bodies.

The most interesting aspect of the Bellecombès study case is the temperature profile of the boreholes. The very “warm” temperatures registered in the permafrost body contrast with the low winter equilibrium temperatures registered on the surface. Moreover, the values very close to 0°C and their constancy with depth and stability in time raise the question of the status of the ice:

- The constancy of temperature in time and depth suggests that the ice could be at the melting point temperature, similar to “temperate” glaciers.
- However the values are still negative, and the consistency of the values on both sensor chains seem to indicate that they are reliable and not due to a lack of accuracy.

Actually the physics of ice-rock mixtures is poorly known, and the value of the melting point temperature in such a material is unknown. It could be slightly below zero, in the range measured in the Bellecombès boreholes. On the other hand, the very high resistivity values indicate the absence of liquid water in the ice body, and the very low displacement rates indicate that no basal sliding occurs, like it would be expected in case of “temperate” basal ice. The question remains open and needs further investigations.

3. Possible future thermal and dynamic response to predicted climate change

The knowledge of the stratigraphy and of the geophysical properties of the rock glacier body allowed the calibration of a thermal diffusion model. The model was run for various temperature evolution scenarios. The model used is a one dimensional model that calculates temperature and ice content at a spacing of 0.2 m, and for time slices of 0.01 days. It uses as input the mean monthly air temperature and a geothermal flux of 0.05 watt.m^{-2} .

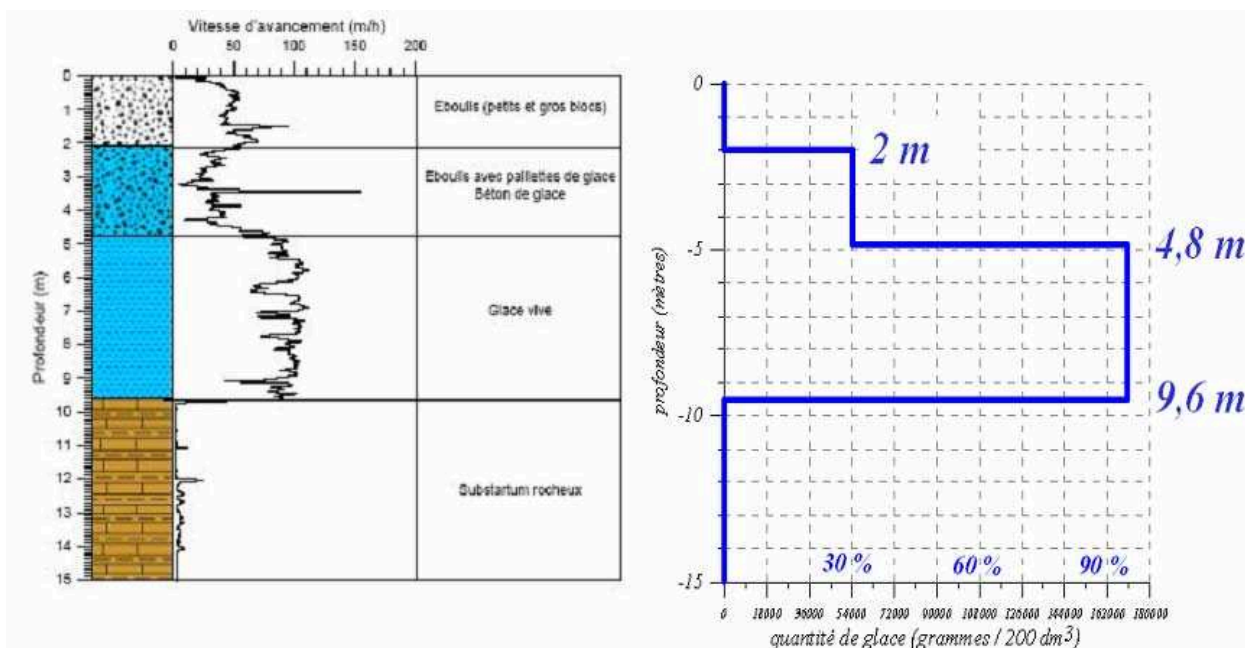


Fig. 6 – Log of borehole SD1 and model settings for structure and ice content.

The ice content was estimated from the cuttings and the drilling progression graph, according to figure 6. The model characteristics were set with the values of table 2.

Table 2 – Intrinsic values used for model calculations

	Thermal conductivity $K \text{ w.m}^{-1}.\text{°C}^{-1}$	Specific mass $\rho \text{ kg.m}^{-3}$	Massic heat $C_p \text{ J.kg}^{-1}.\text{°C}^{-1}$
Snow	0.20	300	2009
Ice	2.10	900	2009
Debris	0.50	1800	900
Bedrock	2.50	2600	900

The model needs to set a mean air temperature as well as precipitation, and uses a climatic scenario to drive the model. To avoid uncertainties related to altitudinal gradient extrapolations, initial values were taken from the meteorological station of Saint-Sorlin, situated ca 20 km North of the site, at almost exactly the same altitude and a similar situation in the Alpine range: the mean annual air temperature during the years 2006-2009 is -0.35°C , and the mean precipitation during the last 35 years is between 1 and 2 m per year. For the variability, the history of deviations against mean temperature and precipitation values measured at the station Chamonix from October 1959 to September 1994 was transferred.

The model was run for various scenarios. The main results are the following ones:

- All scenarios with a mean annual air temperature $< -3^{\circ}\text{C}$ and precipitation > 1 m per year lead to the persistence of the snow cover and to the formation of a glacier. In these conditions, the ground ice volume doesn't change and its temperature rises to the melting point. The permafrost under the permanent snow becomes temperate.
- With a mean air temperature of -0.5°C and a precipitation of 1 m per year, nothing happens within the first ten years. The snow cover, with a mean thickness of 1 m in high winter prevents the soil from cooling, and the high ice content absorbs the heat flux. Under present conditions, the permafrost and ice body seems to be stable.
- To test the effect of a strong and brutal warming, a warming of 5°C was set from the second model year, leading to a mean annual air temperature of 4.5°C . After three years, the ice volume has not yet changed, but has totally disappeared after 20 years. This corresponds to the melting of 150 to 200 $\text{kg}/\text{m}^2/\text{year}$. The thermal equilibrium however is still not reached after 30 years, and the temperature at 20-30 m depth is still close to 0°C (figure 7). In this simulation, the winter snow cover is often very thin (0 to 1.5 m depending on the year).

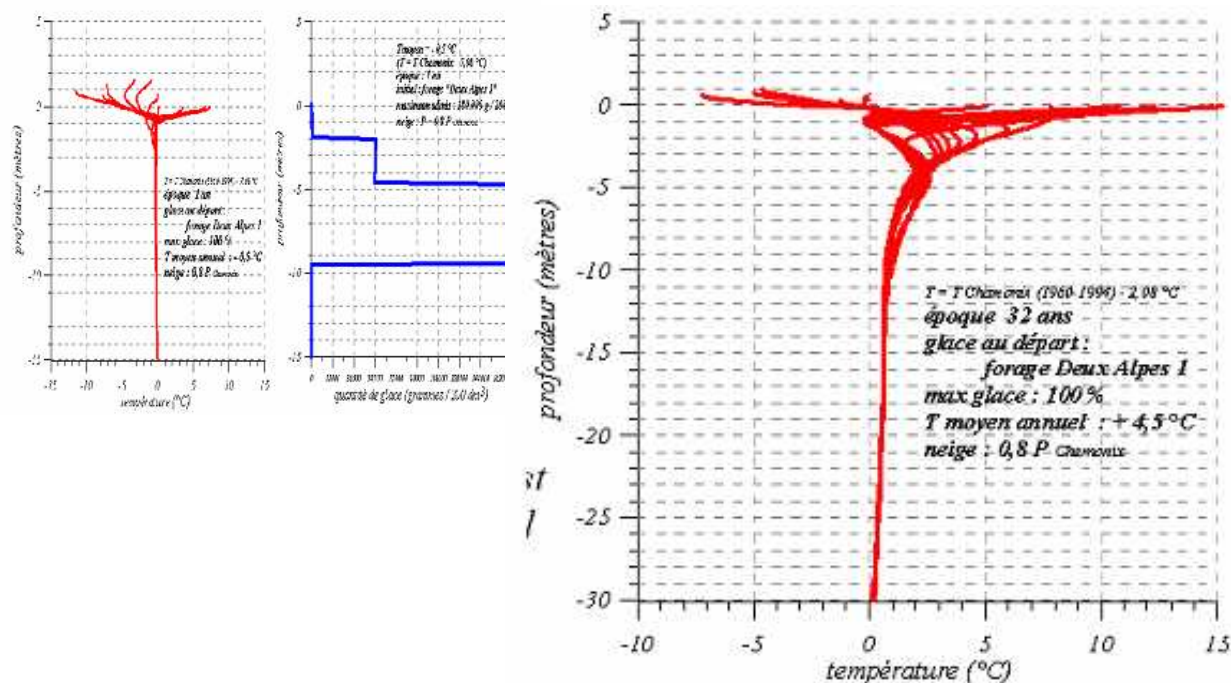


Fig 7 – Borehole SD1. Left: initial state, year 1 (MAAT -0.5°C). Right: monthly geotherms of year 32, 10 years after total disappearance of ground ice, 31 years after sudden warming of 5°C .

The results show that:

- The high ice content totally explains the damping of seasonal variations at the active-layer/ice-rich body transition. The latent heat transfer due to ice melting/freezing absorbs almost the total heat flux.
- The site is stable under present day conditions.
- In case of a progressive temperature rise, the heat flux increase would be almost totally absorbed by latent heat during the first decade, and neither ice temperature would rise nor significant ice volume loss would occur.

- Significant changes would occur only after several decades or in case of a very strong warming.

Thus, very ice-rich permafrost could show a high resistance to climate change. However, the model run considered a melting point at 0°C and does not take into account the effect of possible melt water flows.

Acknowledgements. – The study of the Bellecombes Rockglacier was supported by the Fondation MAIF. The boreholes were co-financed by the Region Rhône-Alpes through the CIBLE 2008 program. The ski resort Deux-Alpes facilitated the work and provided help for logistics.

References:

Lorier L. et al., 2010: *Analyse des risques induits par la dégradation du permafrost alpin*. Rapport final, projet Fondation MAIF. ADRGT, Gières.

Schoeneich P., Bodin X., Krysiecki J.-M., Deline P. & Ravanel L., 2010: *Permafrost in France. Report N°1*. PermaFrance network, Grenoble, Institut de Géographie Alpine.

3.

Case studies in the European Alps

3.8

Aiguille du Midi, Mont Blanc Massif, French Alps

Citation reference

Deline P., Cremonese E., Drenkelfluss A., Gruber S., Kemna A., Krautblatter M., Magnin F., Malet E., Morra di Cella U., Noetzli J., Pogliotti P., Ravel L. (2011). Chapter 3.8: Case studies in the European Alps – Aiguille du Midi, Mont Blanc massif, French Alps. In Kellerer-Pirklbauer A. et al. (eds): *Thermal and geomorphic permafrost response to present and future climate change in the European Alps*. PermaNET project, final report of Action 5.3. On-line publication ISBN 978-2-903095-58-1, p. 97-108.

Authors

Coordination: Philip Deline

Involved project partners and contributors:

- EDYTEM, Université de Savoie, France (EDYTEM) – Philip Deline, Velio Coviello, Florence Magnin, Emmanuel Malet, Ludovic Ravel
- Regional Agency for the Environmental Protection of the Aosta Valley, Italy (ARPA VdA) – Edoardo Cremonese, Umberto Morra di Cella, Paolo Pogliotti
- University of Bonn – Anja Drenkelfluss, Andreas Kemna, Michael Krautblatter
- University of Zurich – Stephan Gruber, Jeanette Noetzli

Content

Summary

1. Introduction and study area
2. Permafrost indicators and recent thermal evolution
3. Possible future thermal response to predicted climate change

References

Summary

We develop investigations at the Aiguille du Midi (3842 m a.s.l), where rockwalls are of diverse aspects and slope angles, and galleries are accessible year-round. In the framework of the project *PermaNET*, we monitor the rock thermal regime (i) with 9 sensors with one to three thermistors installed up to a depth of 55 cm; (ii) with three 10 m deep boreholes equipped with thermistor chains; and (iii) by using Electrical Resistivity Tomography (ERT), based on the temperature-resistivity relationship of the local granite. These measurements were completed by two mobile automatic weather stations. Combined with a 3D-high-resolution DEM made using long- and short-range Terrestrial Laser Scanning (for rockwalls and galleries, respectively), these data will be used for physically-based model validation or construction of statistical models of rock temperature distribution and evolution in the rockwalls. The site started to be instrumented in 2005, and some methods are still experimental. Here we focus on the thermal monitoring device installed on the site and present some first results.

1. Introduction and study area

Starting off in the framework of the EU co-funded French-Italian *PERMAdataROC* project and presently under development within the project *PermaNET*, our investigations at the Aiguille du Midi (N 45°52', E 6°53') began in November 2005. We choose this site (Fig. 1) because of (i) its elevation (3842 m a.s.l.), (ii) its steep rockwalls characterized by different aspects, slope angles, rock structures, and snow covers, and (iii) its accessibility throughout the year from Chamonix by a cable car from 1955 – half a million tourists visit the site each year; rockwalls of the Piton central are accessible by abseiling from the upper terrace, and galleries allow to penetrate into the rock mass – which is rare in high mountain areas, and led e.g. to observe a significant circulation of water during the hot Summer of 2003, for the first time since the opening of the site. Aiguille du Midi has become a major site for the study of rockwall permafrost in the Alps.

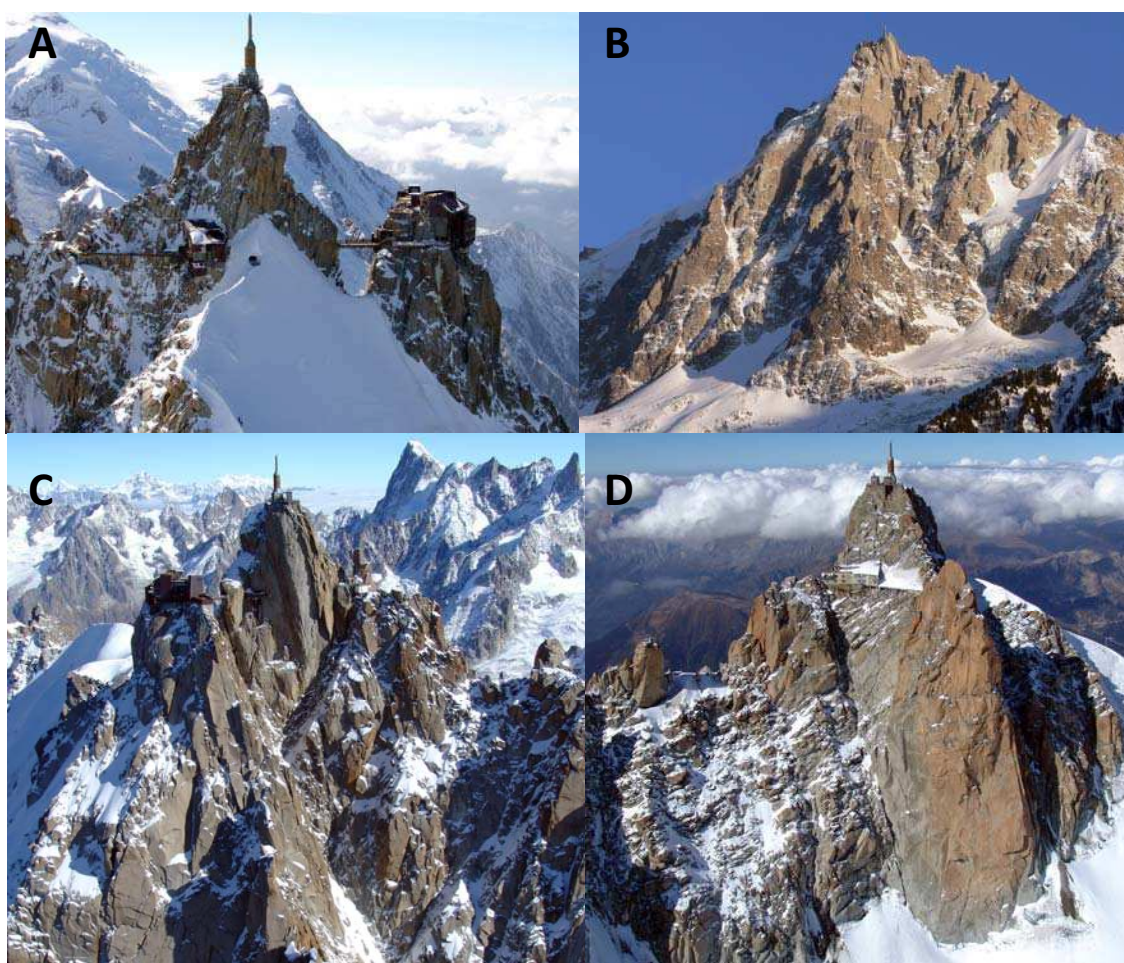


Fig. 1 – The Aiguille du Midi (3842 m a.s.l.): (A) view from the east. At the center: Piton central; on the right: Piton nord, with the cable car station. (B) west side (1000-m-high). At its bottom: Glacier des Bossons et Glacier Rond; on the left, in the shadow: north side of the group of the Aiguille du Midi, mainly glaciated. (C) under the pylon: subvertical northwest side of the Piton central (100-m-high). (D) Southeast side (200-m-high). On the left: beginning of the Arête des Cosmiques; on the right: Pilastre sud-est. Photographs by P. Deline and S. Gruber (A, C, D: 11.10.2005; B: 30.09.2007)

The group of the Aiguille du Midi, at the western end of the Aiguilles de Chamonix, develops asymmetrically over 2 km between the Col du Midi and the Col du Plan (Fig. 2). It forms a rocky scarp whose west face and north face (which is glaciated on its upper half) are towering the Glacier des Bossons (by 1000 m) and the Glacier des Pélerins (by 1350 m) respectively (Fig. 1B). However, the back of this scarp is occupied by the western basin of Glacier du Géant, separated from west and north faces by the rocky Arête des Cosmiques and the summit of the Aiguille du Midi.

The bulk of the rock is granite of Mont Blanc, a massive rock with a grained facies that contributes to the steepness of the Aiguille du Midi faces – 50° for the north face, 57-58° for the southeast (only 200 m high) and west sides. Many rockwalls within these faces are subvertical, as the north face of the Piton central (Fig. 1C) or the Pilastre sud-est (Fig. 1D), because of the subvertical dip of the two main families of faults whose dense network cuts across the Mont Blanc massif. Because of a dense secondary fracturing unevenly distributed very massive rockwalls alternate with very densely fractured ones (Fig. 1D). Our study focuses on the summit of the Aiguille du Midi, between 3740 and 3842 m a.s.l., here termed “Aiguille du Midi”.

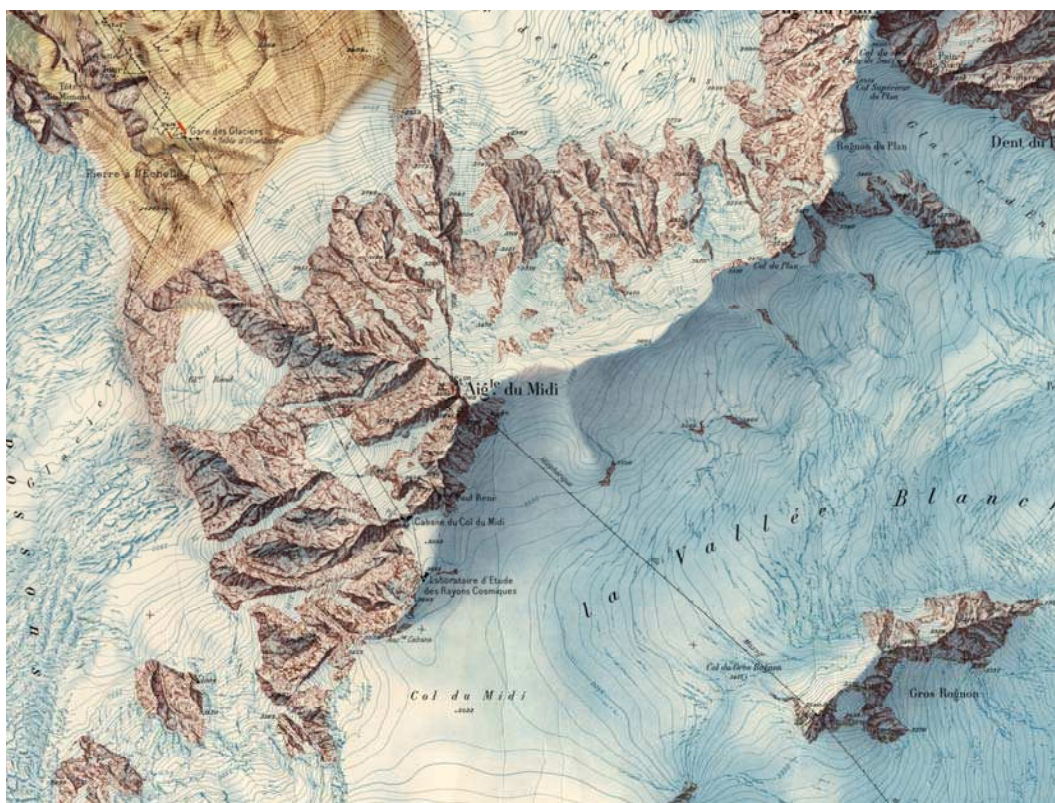


Fig. 2 – Group of the Aiguille du Midi. The instrumented site is the peak labelled Aig^{le} du Midi. Detail of the map Mont Blanc n°1 Nord-Aiguille du Midi (IGN, 1952) at 1:10 000 (contour interval: 10 m). This extract is 4 km large.

2. Permafrost indicators and recent thermal evolution

2.1 Methods

Rock temperature monitoring

The rock surface temperature is measured every hour over all faces of the Piton central since 2005 by several mini-dataloggers with thermistors placed at depths of 3, 10, 30 and 55 cm below the surface. Three 10 m deep boreholes have also been drilled in September 2009 (Fig. 3), normal to the rock

surface of: (i) the northwest face (borehole at 3738 m a.s.l.), a vertical rockwall in a very massive granite; snow can only accumulate on a small 2 m wide terrace; (ii) the southeast face (borehole at 3745 m a.s.l.), a 55° slope angle in a highly fractured area snow covered during a part of the year; and (iii) the northeast face (borehole at 3753 m a.s.l.), with a 65° slope angle in a very fractured couloir, where snow occurs over a large part of the year due to the concave topography. These boreholes are located well below the cable car infrastructure level in order to minimize its thermal influence on rock temperature. They are equipped with 10 m long chains of 15 thermistors that measure rock temperature every 3 hours since December 2009 on the northwest and southeast faces, since April 2010 on the northeast face.



Fig. 3 – Drilling of a 10 m deep borehole in the southeast face of Piton central in September 2009. Photograph by P. Deline 17.09.2009

Electrical resistivity tomography

Electrical Resistivity Tomography (ERT) is increasingly being used as a non-invasive imaging tool in alpine permafrost studies (Krautblatter & Hauck, 2007; Krautblatter *et al.*, 2010). Key objectives of this method are (i) the mapping of temperature distributions inside the rock to infer the presence of permafrost, and (ii) the delineation of fracture zones given their influencing role on permafrost dynamics and stability. For the first purpose a preliminary relationship between temperature and resistivity of the rock has been established in laboratory. The imaging of fractures, however, is a notoriously difficult task using conventional ERT approaches which rely on smoothness-constraint regularization. At the Aiguille du Midi, we investigate regularization schemes for improved fracture delineation by means of numerical simulations and application to field data.

Since 2008, four ERT surveys were conducted at the site. Each one comprised the acquisition of more than 10,000 normal and reciprocal dipole-dipole data over three different arrays of altogether 144 electrodes. The electrodes of two arrays could be placed to almost surround the Piton central and the Piton nord in a horizontal plane, offering a favourable tomographic coverage. A vertical north-south transect across the Piton central was installed by abseiling on the near vertical north and south faces. The ERT data were inverted using isotropic smoothing, anisotropic smoothing, and a focussing regularization scheme based on the so-called minimum-gradient support (MGS), and employing a finite-element grid which captures the irregular geometry of the rock as well as the electrode layout.

Air temperature monitoring

Air temperature and relative humidity are measured on south and north faces by the mean of mini-dataloggers placed inside radiation shields. On the south face, meteorological parameters (incoming and outgoing solar radiation in both shortwave and longwave bands, wind speed and direction) were measured during nearly 4 years (December 2006 to October 2010) by an automatic weather station adapted and installed directly on the rockwall.

Terrestrial Laser Scanning

A DEM is necessary (i) to accurately represent the rock volume, (ii) as a basis for a geological structure analysis, (iii) to refine the modeling of rock temperature distribution, and (iv) to study the water flow into the rock mass. A high-resolution DEM was made using long- and short-range Terrestrial Laser Scanning – for rockwalls and galleries, respectively (Fig. 4).

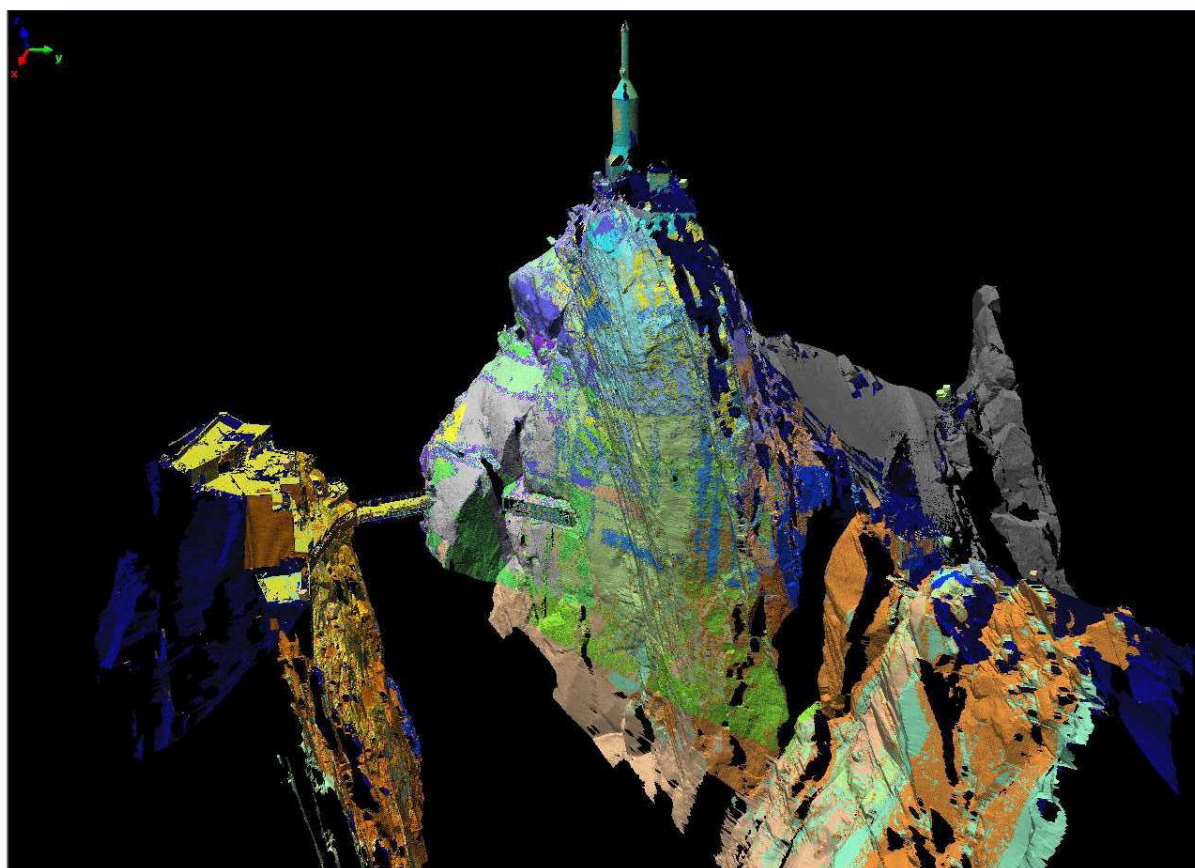


Fig. 4 – Triangulated Irregular Network (TIN) model of the rockwalls of the Pitons nord (left) and central, obtained by long-range terrestrial laser scanning.

2.2 Preliminary results about rock temperature

All the sub-surface data are collected mainly for initialization, calibration and validation of rock temperature and permafrost distribution models. However their statistical analysis allows quantifying the great spatial variability of sub-surface temperatures in such complex morphologies. Preliminary results (Table 1; Fig. 5) show that: (i) the mean annual ground surface temperature can vary of more than 6°C within few meters of distance, depending on the aspect; (ii) freeze-thaw cycles on southern aspect are nearly twice as frequent than in the north but markedly shallower; (iii) a significant thermal-offset probably exists despite the compact rock mass and the absence of ground covers (e.g. debris, snow) on south faces.



Fig. 5 – Mean daily rock temperature on the south and north faces of the Piton Central for the hydrological year 2008-09 at three different depths below the surface.

Table 1 – Rock temperature 55 cm below the surface on south and north faces of the Piton Central of the Aiguille du Midi for 2007-08, 2008-09, and 2009-10 hydrological years. MAGT: mean annual ground temperature; MAX/MINabs: absolutely warmest and coldest temperature; DateMAX/MINabs: occurrence date of MAX/MINabs; $\Delta T_{avg}/max/min$: mean, maximal and minimal amplitude of daily temperatures; ZCD: Zero Crossing Days, i.e. number of days per year where the 0°C-isotherm is crossed; MAX/MINday: warmest and coldest mean daily temperature; DateMAX/MINday: occurrence date of MAX/MINday; DBZ: Days Below Zero, i.e. number of days with maximum temperature below 0°C.

ADM South Face – Rock Temperature 55 [cm]														
H.Y.	MAGT (°C)	MAXabs (°C)	MINabs (°C)	DateMAXabs (dd/mm/yy)	DateMINabs (dd/mm/yy)	ΔT_{avg} (°C)	ΔT_{max} (°C)	ΔT_{min} (°C)	ZCD days	MAXday (°C)	MINday (°C)	DateMAXday (dd/mm/yy)	DateMINday (dd/mm/yy)	DBZ days
'07/08	-	-	-	-	-	-	-	-	-	-	-	-	-	-
'08/09	0.36	14.15	-15.78	30/09/09	13/02/09	2.45	6.74	0.19	37	12.85	-14.45	29/09/08	13/02/08	165
'09/10	0.26	14.14	-15.48	02/07/10	08/03/10	2.28	5.68	0.44	26	13.04	-13.67	20/07/08	08/01/08	167

ADM North Face – Rock Temperature 55 [cm]														
H.Y.	MAGT (°C)	MAXabs (°C)	MINabs (°C)	DateMAXabs (dd/mm/yy)	DateMINabs (dd/mm/yy)	ΔT_{avg} (°C)	ΔT_{max} (°C)	ΔT_{min} (°C)	ZCD days	MAXday (°C)	MINday (°C)	DateMAXday (dd/mm/yy)	DateMINday (dd/mm/yy)	DBZ days
'07/08	-6.34	2.9	-17.36	01/07/08	25/03/08	0.74	2.71	0.14	25	2.5	-17.12	01/07/08	25/03/08	290
'08/09	-6.6	2.72	-19.47	08/08/09	14/02/09	0.71	3.75	0.08	12	2.46	-19.28	07/08/08	14/02/08	306
'09/10	-	-	-	-	-	-	-	-	-	-	-	-	-	-

Deeper borehole thermistor chains show a very sharp contrast between the three surveyed faces (Fig. 6). A time lag of approximately half a year between minimal and maximal air temperature periods (January-February, and July, respectively) and minimal and maximal rock temperature periods at a depth of 10 m (June-July, and December-January, respectively; Fig. 7). In 2010, the active layer thickness varied from 1.80 m in the northwest face to 5.20 m in the southeast face.

While anisotropic smoothing can be adjusted such as to allow a correct interpretation of the ERT image, inversion with MGS-based regularization provides most convincing results in terms of resolving sharp structural features associated with lithological changes such as fractures, but at the same time preserving smooth changes typical of temperature variations in the rock. Low-resistivity zones could be delineated at the Piton nord, which seem to coincide with water-containing fractures caused by artificial heat supply; continuation of these fractures outside the heated gallery indicates permafrost conditions. At the Piton central, resistivity values were below $200\,000\ \Omega\text{m}$ in October 2010, which is quite reasonable with respect to the temperature range (Fig. 8).

Meteorological data on the rockwall show that: (i) the peak of SW radiation occurs during the winter ($>1300\ \text{W/m}^2$) giving strong daily temperature amplitudes at rock surface (up to 30°C); (ii) there is a clear prevalence of upslope winds with speeds ranging from 4 to 9 m/s; (iii) the mean annual air temperature is around -7°C on average (Table 2), with 5 to 6°C of daily amplitude and an absolute temperature range between -25 to $+12^\circ\text{C}$.

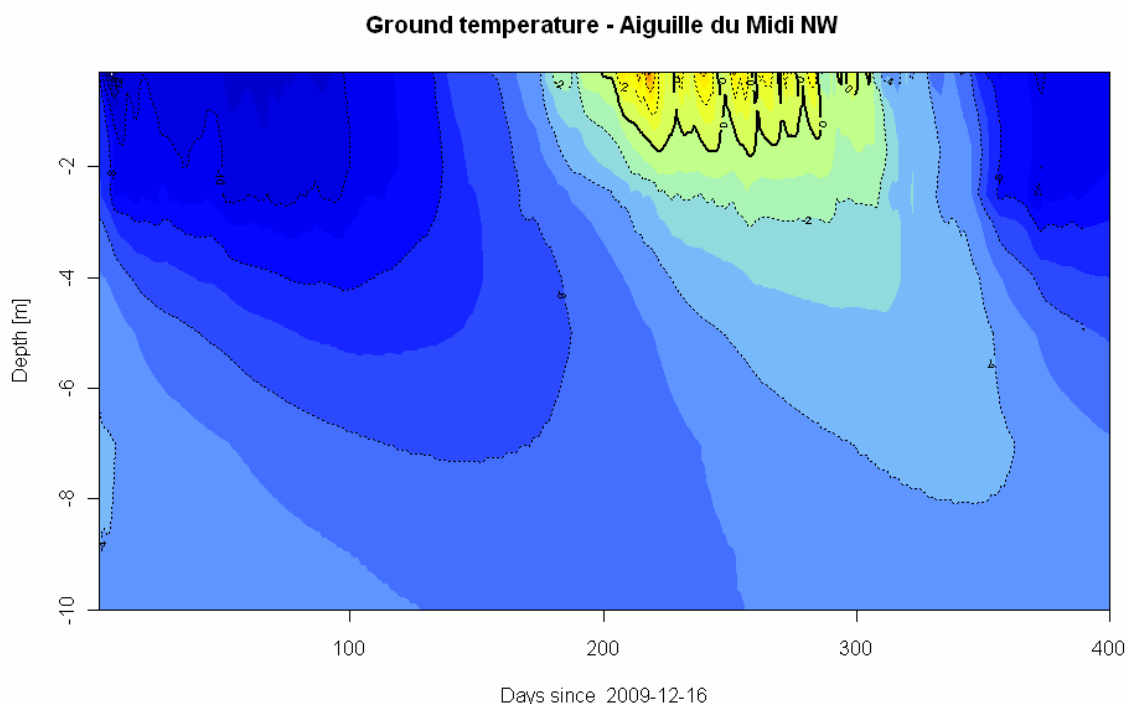
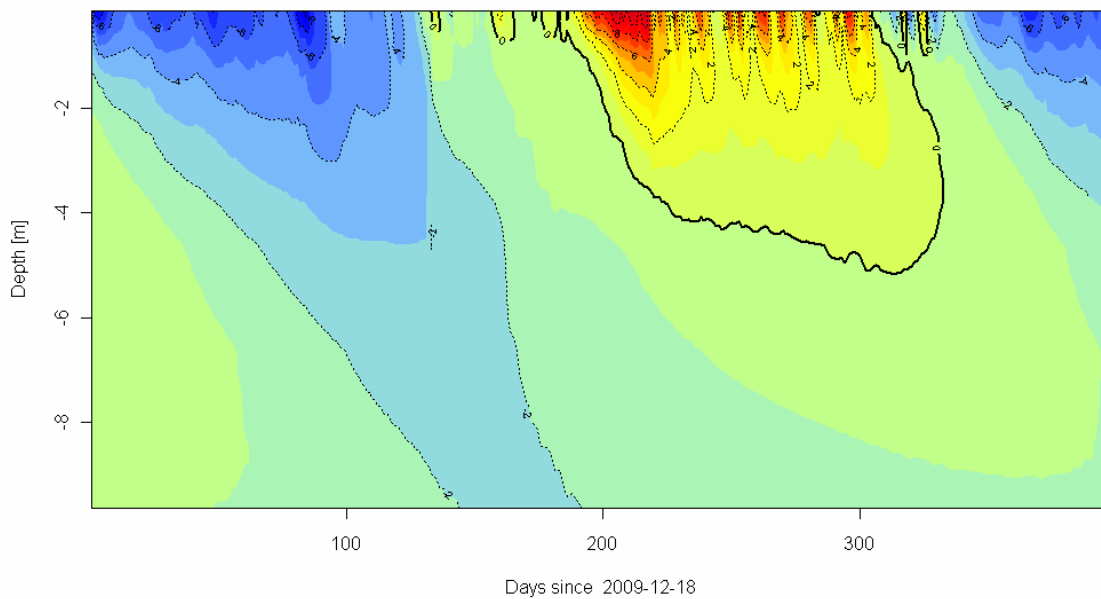


Fig. 6 – Plots of rock temperature from the surface to 10 m depth for the period 18.12.2009 to 21.01.2011 at the northwest and southeast faces, and 13/04/2009 to 21/01/2011 at the northeast face of the Aiguille du Midi (continued next page)

Ground temperature - Aiguille du Midi SUD



Ground temperature - Aiguille du Midi NE

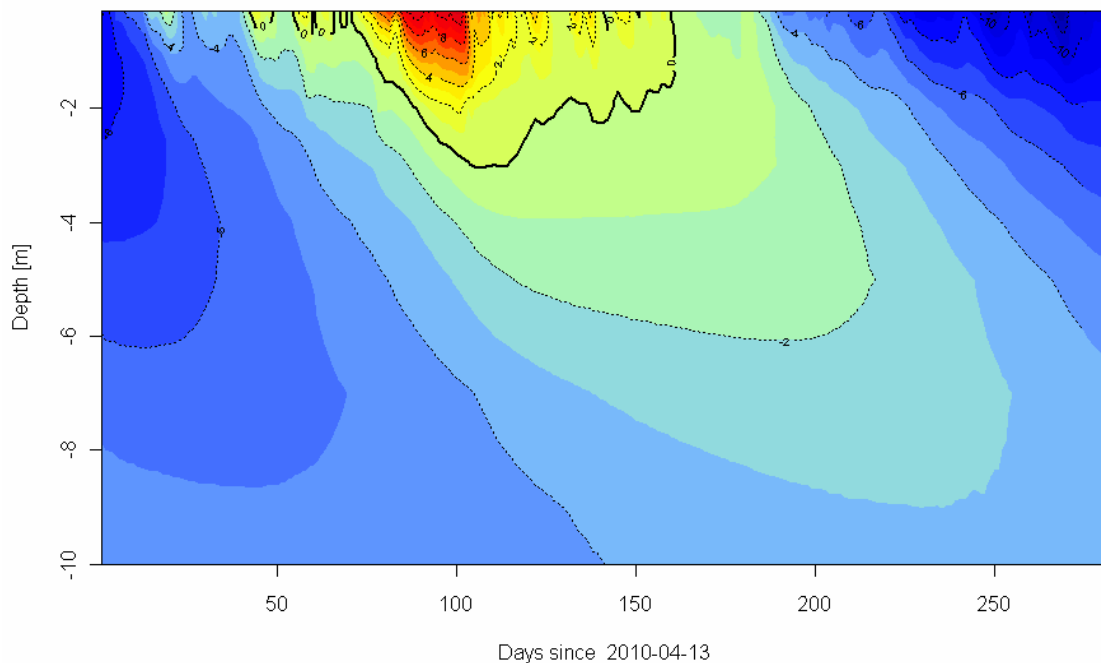


Fig. 6 – continued

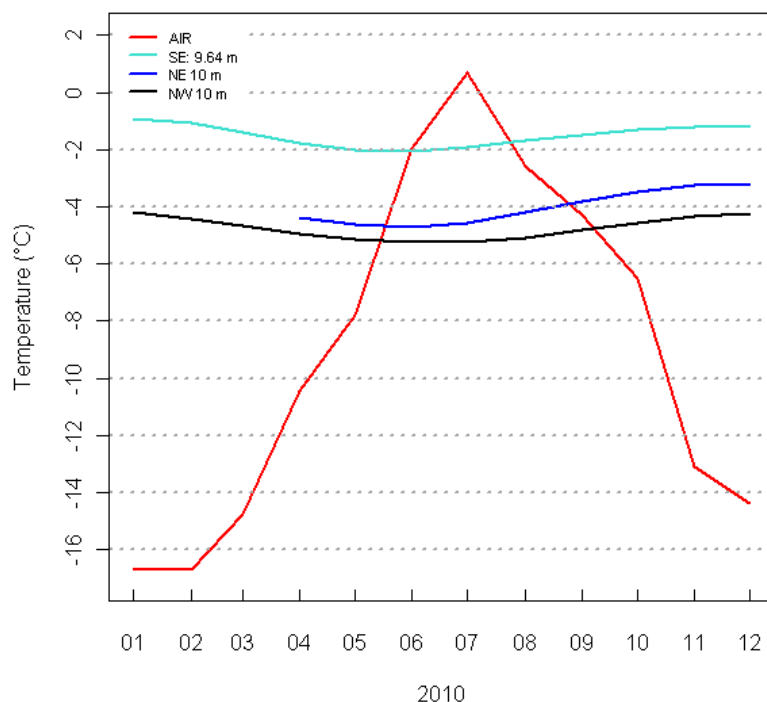


Fig. 7 – Time lag between air temperature and 10 m deep rock at the southeast, northeast and northwest faces of the Piton central of the Aiguille du Midi.

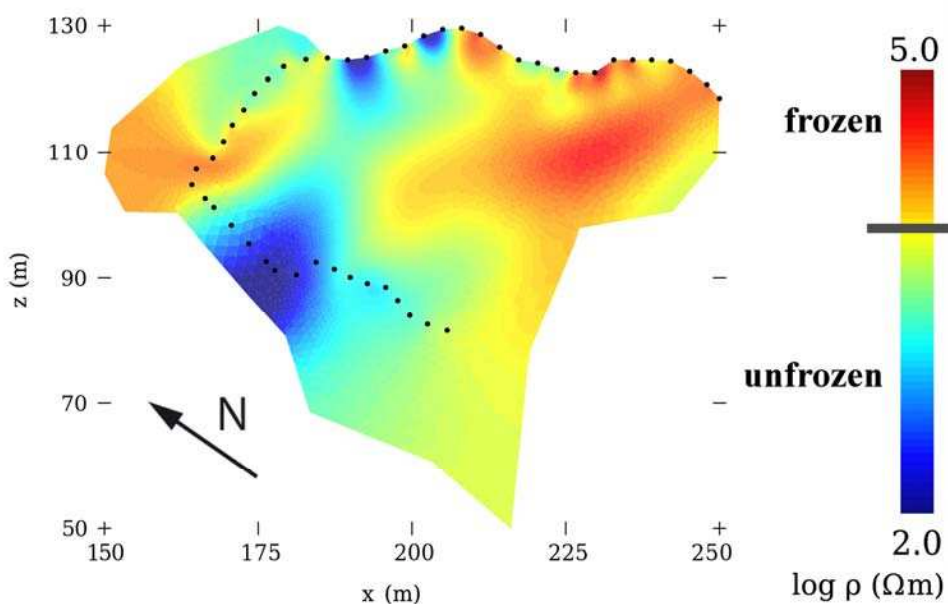


Fig. 8 – Electrical resistivity tomography in a horizontal plane at the Piton central of the Aiguille du Midi on 22.10.2010. Black dots are electrode locations; blue/green: unfrozen; yellow: transition from unfrozen to frozen; red: frozen; resistivity is in the range 102. -105.0 Ω m. Reliable results are only inside the arc that is enclosed by the 48 electrodes.

Table 2 – Air Temperature on the south face (A) and north face (B) of the Piton Central of the Aiguille du Midi for 2007-08, 2008-09 and 2009-10 hydrological years. Mean annual air temperature (MAAT), frost days (FD), ice days (ID) and freeze-thaw days (FTD) calculated as suggested in chapter 2. On the north face, hydrological year 2007-08 is the only one without missing data.

(A)	South face	2007-08	2008-09	2009-10	Mean	(B)	North face 2007-08
	MAAT (°C)	-6.77	-6.85	-7.33	-6.98		-7.53
	FD (d)	352	336	335	341		353
	ID (d)	246	241	249	245		275
	FTD (d)	106	95	86	96		77

2.3 Outlook

Aiguille du Midi is the most elevated Alpine site to study permafrost in rockwalls. During the next years numerical modelling of the transient 3D subsurface temperature fields, combining a distributed energy balance model with a 3D heat conduction scheme, will be accomplished (Noetzli *et al.*, 2007; Deline *et al.*, 2009). Several statistical models of distribution of surface temperatures of the rockwalls began to be developed for the Mont Blanc massif, but comparing temperature data at the Aiguille du Midi with one of these models shows some discrepancies: whereas the Piton central north face modeled temperature is in the range of -7° to -13°C (Fig. 9), its monitored average temperature is ca. -6°C (Table 1).

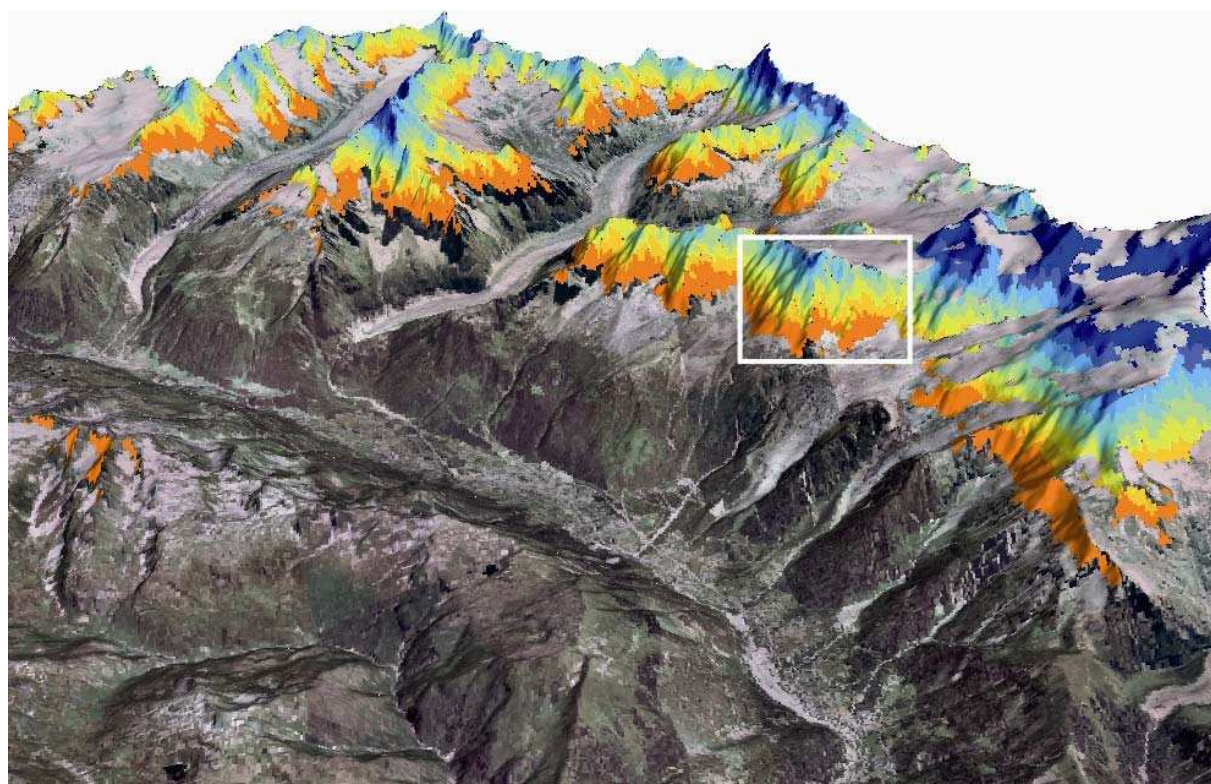


Fig. 9 – Modeled distribution of rock surface mean annual temperature in the Mont Blanc massif (French side) with the model TEBAL (view from the west; image draping: E. Ployon). The temperature is in the range -1°C (dark orange) to -13°C (dark blue); group of the Aiguille du Midi (north and west sides) is delimited.

The combination of process understanding, statistical analyses and/or modelling (e.g. numerical modelling of water flow in rock fractures) will help to improve our understanding of the characteristics of the mountain permafrost degradation. Secondly, we are interested in how a reduction in the uncertainty of data, process understanding and models may contribute to our predictive skill of corresponding effects. This long-term monitoring and modelling approach at Aiguille du Midi will be a strong support to take into account future thermal response of rockwall permafrost to predicted climate change in the next 50 years and its geomorphic consequences.

3. Possible future thermal response to predicted climate change

As suggested in chapter 2, frost days, ice days and freeze-thaw days have been computed using the available air temperature dataset of the south face of Aiguille du Midi (Table 2A). Referring to maps and predictions in chapter 2, the air temperature measurements conducted on both south and north faces of the Aiguille du Midi from 2007 to 2010 are in accordance with the means of the period 1961-1990 for the Great Alpine Region (GAR). That is a number of ID in the range 241-260 and a number of FD greater than 320. Only the number of FTD is above the mean in the measurements (96 vs. 70/80 of the mean 1961-1990), probably because the sensor is placed on a south near vertical rockwall where daily temperature variations are very strong, especially during winter.

The predictions for the period 2021-2050 in the study area are a decrease of ID ranging from -13/-16 days per year that means 232-229 ID instead of 245, and a decrease of FD ranging from -14/-15 days per year that means 326 FD instead of 341. Applying these scenarios to the data of the north face (Table 2B) the number of ID could fall to about 260 days per year that means conditions more similar to those observed today on the south faces. These changes could lead to a doubling of the active layer thickness of the north exposed rockwalls of the Alps in the future, with a consequently increase of instabilities and rockfall events.

Acknowledgements. – Compagnie du Mont Blanc, especially E. Desvaux, are acknowledged for their assistance to our study at Aiguille du Midi. Participation of Chamonix Alpine guides M. Arizzi, L. Collignon, and S. Frendo, and EDYTEM colleagues P. Paccard and M. Le Roy, to the September 2009 drilling was crucial for its success. Many thanks are due to R. Bölhert, S. Jaillet, A. Rabatel, B. Sadier, S. Verleysdonk for their help and contributions.

References:

- Deline P., Bölhert R., Coviello V., Cremonese E., Gruber S., Krautblatter M., Jaillet S., Malet E., Morra di Cella U., Noetzli J., Pogliotti P., Rabatel A., Ravel L., Sadier B., Verleysdonk S., 2009: L'Aiguille du Midi (massif du Mont Blanc): un site remarquable pour l'étude du permafrost des parois d'altitude. *Collection EDYTEM, 8 – Cahier de Géographie*, 135-146.
- Krautblatter M., Hauck, C., 2007: Electrical resistivity tomography monitoring of permafrost in solid rock walls. *Journal of Geophysical Research*, 112, F02S20, doi:10.1029/2006JF000546.
- Krautblatter M., Verleysdonk S., Flores-Orozco A., Kemna A., 2010: Temperature-calibrated imaging of seasonal changes in permafrost rock walls by quantitative electrical resistivity tomography (Zugspitze, German/Austrian Alps). *Journal of Geophysical Research*, 115, F02003.
- Noetzli J., Gruber S., 2009: Transient thermal effects in Alpine permafrost. *The Cryosphere*, 3, 85-99.
- Noetzli J., Gruber S., Kohl T., Salzmann N., Haeberli W., 2007: Three-dimensional distribution and evolution of permafrost temperatures in idealized high-mountain topography. *Journal of Geophysical Research*, 112, F02S13. doi:10.1029/2006JF000545:

3.

Case studies in the European Alps

3.9

Rockfalls in the Mont Blanc massif, French-Italian Alps

Citation reference

Deline P., Ravanel L. (2011). Chapter 3.9: Case studies in the European Alps – Rockfalls in the Mont Blanc massif, French-Italian Alps. In Kellerer-Pirklbauer A. et al. (eds): *Thermal and geomorphic permafrost response to present and future climate change in the European Alps*. PermaNET project, final report of Action 5.3. On-line publication ISBN 978-2-903095-58-1, p. 109-118.

Authors

Coordination: Philip Deline

Involved project partners and contributors:

- EDYTEM, Université de Savoie, France (EDYTEM) – Philip Deline, Ludovic Ravanel

Content

Summary

1. Introduction and study area
2. Permafrost indicators and recent thermal evolution
3. Possible future thermal response to predicted climate change

References

Summary

The frequency and volumes of rockfalls as well as their triggering factors remain poorly understood due to a lack of systematic observations. In the framework of the project *PermaNET*, this study case analyses inventories of rockfalls acquired in the whole Mont Blanc massif by innovative methods in order to characterize the link between climate and rockfalls, and to emphasize the role of permafrost. In two sectors of the massif, the comparison of photographs taken since the end of the Little Ice Age allowed the identification of 50 rockfalls. In most cases these rockfalls occurred during the hottest periods. On another time scale, a network of local observers allowed the documentation of the 139 rockfalls that occurred in 2007, 2008 and 2009 in the central area of the Mont Blanc massif. Furthermore, the analyses of a satellite image allowed the identification of 182 rockfalls in the whole massif at the end of the 2003 summer heat wave. For most of those rockfalls, the permafrost degradation seems to be the main triggering factor.

1. Introduction and study area

A rockfall corresponds to the sudden collapse of a rock mass from a steep rockwall, with a volume exceeding 100 m^3 . In the last two decades, many rockfalls and rock avalanches (volume $> 0.1 \cdot 10^6 \text{ m}^3$) occurred from permafrost affected rockwalls throughout the world (Noetzli *et al.* 2003). Rockfalls generally occur in hard rocks along pre-existing fractures. In high mountains, three major factors – possibly combined – can trigger rockfalls: (i) glacial debuttressing due to glacial retreat, (ii) seismic activity, and (iii) permafrost degradation, generating physical changes of the potential interstitial ice (Gruber & Haeberli 2007).

The characterization of rockfall events and the understanding of their evolution are prerequisites to any response of management. However, data on rockfalls at high elevation are rare and it is difficult to interpret non-representative data (few isolated examples).

Started in the framework of the EU co-funded French-Italian *PERMAdataROC* project, our investigations are presently carried out within the project *PermaNET*. In this context, we systematically collect and process historical and current data on rockfalls (Ravel 2010) in order to better characterize this process (triggering conditions, frequency, and volumes).

The first aim of this study case is to show the correlation existing between rockfalls in the Mont Blanc massif and global warming. The second one is to highlight the probably crucial role of the permafrost degradation on the rockfall trigger.

2. Permafrost indicators and recent thermal evolution

2.1 Methods

Photo-comparison approach

Written and oral evidences of rockfalls are not sufficient to accurately reconstruct the recent rockwall morphodynamics. The photo-interpretation of a series of photographs is therefore the most appropriate method. We focus on two areas of the Mont Blanc massif with a rich existing documentation: the West face of the Petit Dru (3730 m a.s.l.) and the north side of the Aiguilles de Chamonix (3842 m a.s.l. for the Aiguille du Midi). The proximity of these peaks with Chamonix, their morphology and their symbolism allow a rich iconography since the end of the Little Ice Age (LIA).

The first step consists in setting up documentary corpus, which is very time consuming. Nearly 400 photographs of the two studied areas have been gathered but only a few dozen could finally be used. Photographs are compared and interpreted in different steps: (i) delineation of the rockfall scars (Fig. 1), (ii) determination of the periods characterized by morphological and colour changes caused by rockfalls – it was often necessary to diversify and cross-check information sources in order to precise dates of collapse –, and (iii) estimation of the involved volumes. 50 rockfalls occurred in the two areas during the period from the end of the LIA to 2009, involving rock volumes ranging from 500 to $265\,000 \text{ m}^3$ (Fig. 2; Ravel & Deline 2008, 2011).

Network of observers, SPOT-5 image and GIS analysis

Besides the inventories of post-LIA rockfalls, it is important to characterize current rockfalls. Only a structured network of observation coupled with fieldwork can allow a near completeness of the inventory of the current rockfalls.

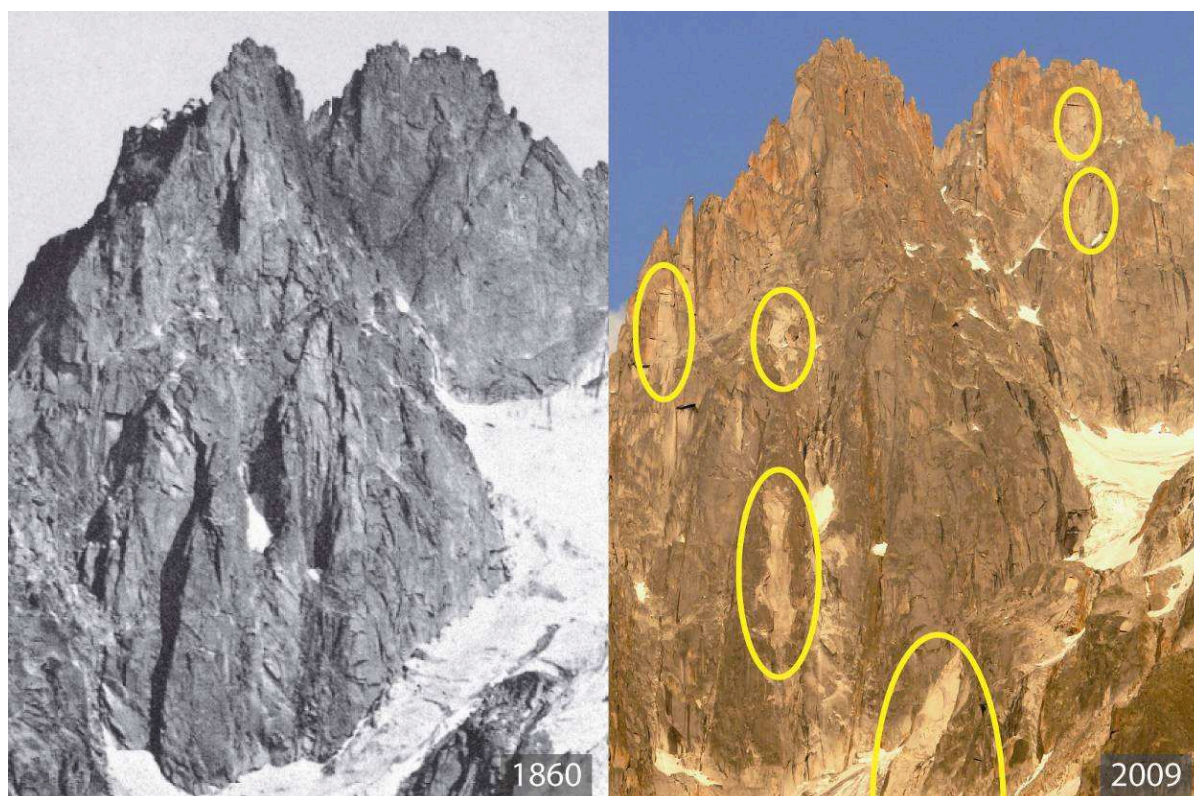


Fig. 1 – Comparison between photographs of 1862 and 2009 of the west face of the Grands Charmoz and the Aiguille du Grépon, and of the north face of the Rognon des Grands Charmoz. Yellow ellipses indicate areas affected by rockfalls between the two dates (Ravel & Deline 2011, slightly modified).

The network consists of dozens of guides, hut keepers and mountaineers. Initiated in 2005, this observer network became fully operational in 2007. Focused on the central part of the Mont Blanc massif, the inventory is carried out with reporting forms, indicating the main characteristics of the rockfalls and the conditions of the affected rockwall. An important fieldwork is conducted every fall in order to check and to complete the reported observations.

Meanwhile, in order to compare the data obtained by the network with the exceptional morphodynamics of the three month 2003 summer heat wave, the 2003 rockfalls were surveyed on the base of supraglacial deposits through the analysis of a SPOT-5 image of the entire massif taken at the end of the heat wave (23.08.200, 10:50 GMT).

Characteristics of each collapse are determined using several methods. Altitude of scars, slope angle and orientation of the affected rockwalls, and the deposit areas are calculated in a GIS. Because direct measurements of the scar volumes were not possible, the area of the deposits was multiplied with an estimate of their thicknesses in order to assess the collapsed volumes. Geological parameters are derived from geological maps, and the possible presence of permafrost was determined from a model of mean annual ground surface temperature.

The network of observers allowed the documentation of 45 rockfalls in 2007, 22 in 2008 and 72 in 2009 (Fig. 3), involving rock volumes ranging from 100 to 33 000 m³ (Deline *et al.* 2008, Ravel *et al.* 2010, Ravel & Deline in press). Furthermore, the analysis of the SPOT-5 image allowed the identification of 182 rockfalls in the whole massif at the end of the 2003 summer heat wave (Fig. 4; Ravel *et al.* 2011).

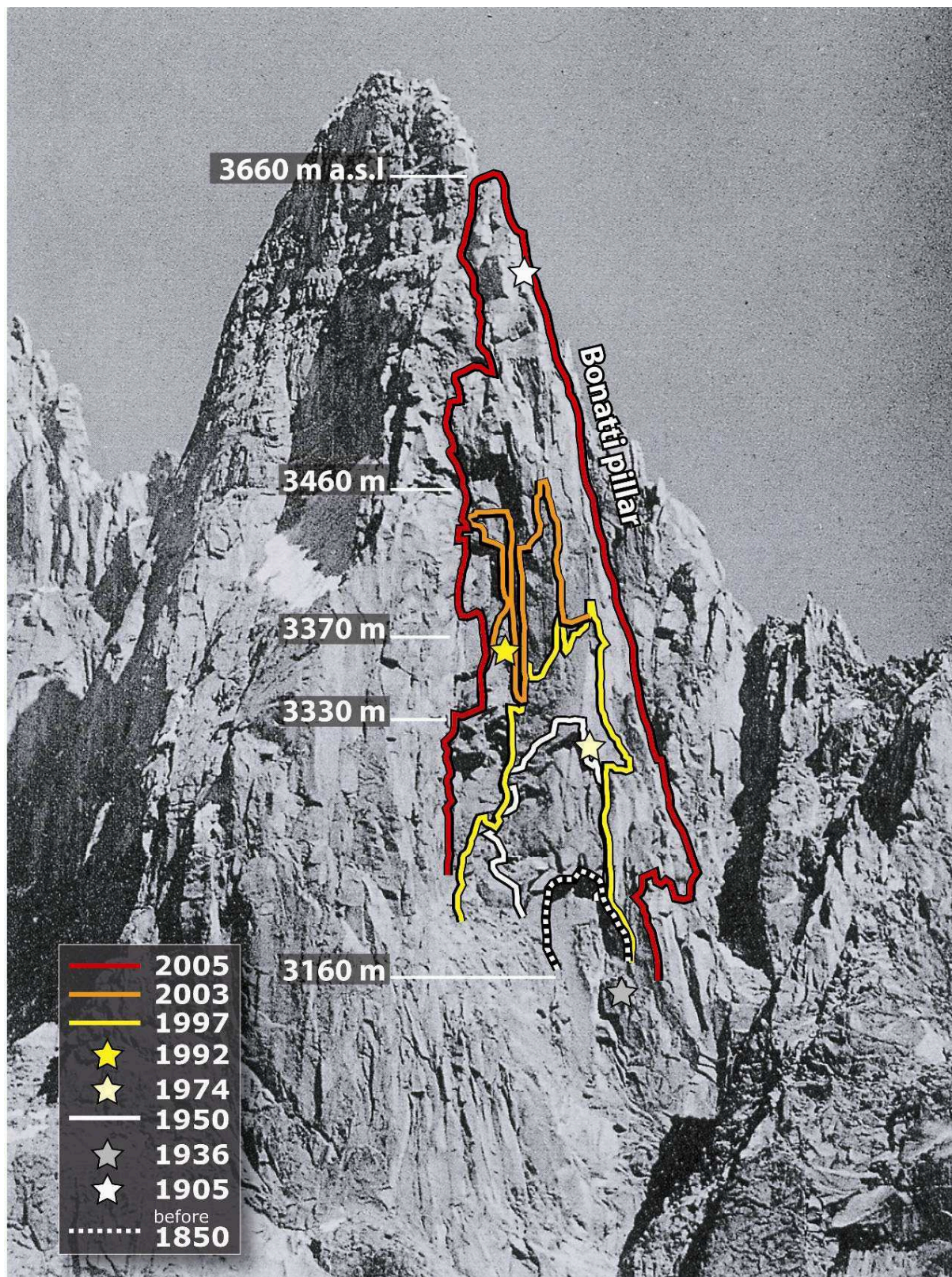


Fig. 2 – Location of the 8 scars of the main (outlines) and secondary (stars) rockfalls at the west face of the Drus.

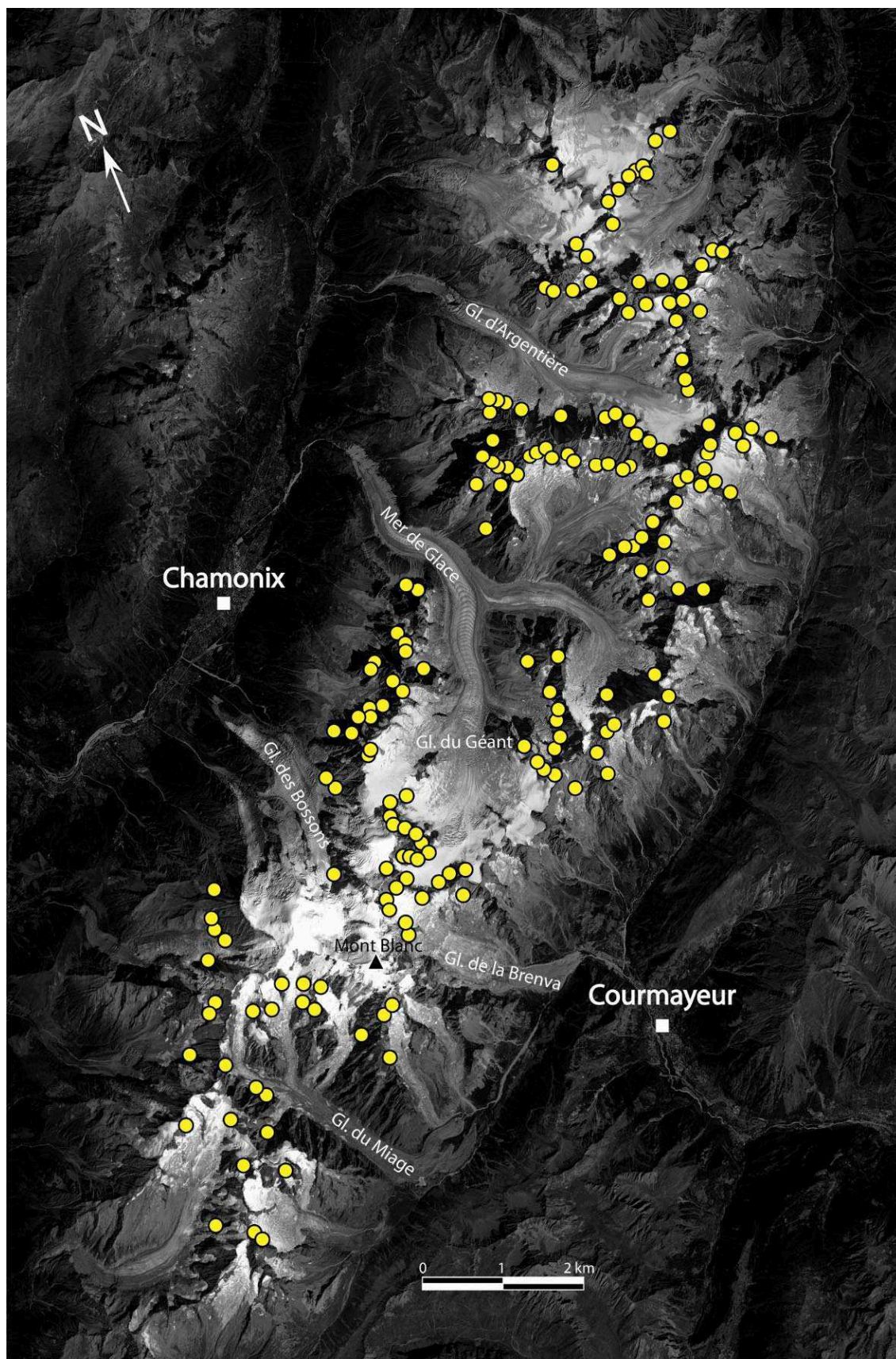


Fig. 4 – Location of the 182 rockfalls that occurred during the hot summer 2003 on the panchromatic SPOT-5 satellite image 051/257 of the 23.08.2003 (Ravanel et al. 2011, slightly modified).

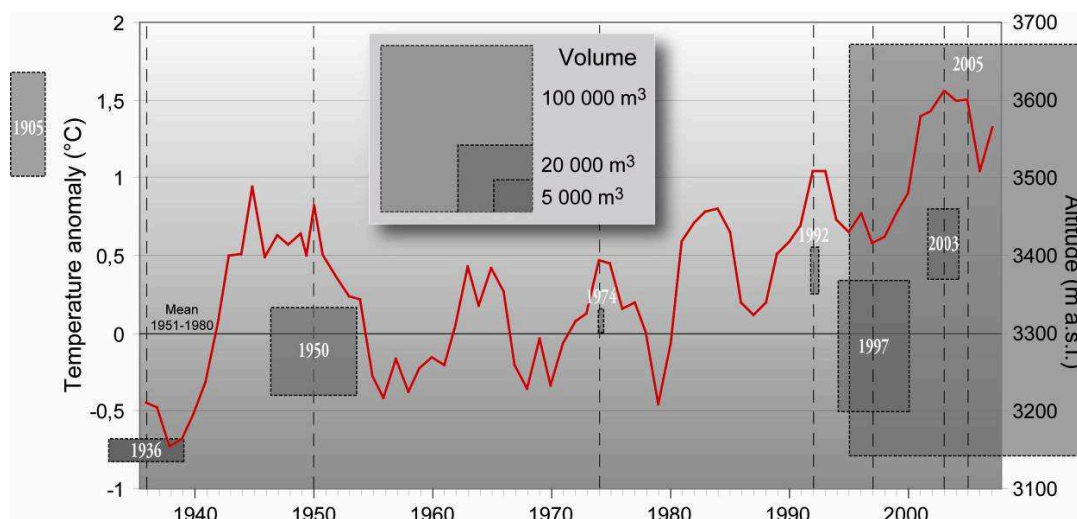


Fig. 5 – Changes in Chamonix mean summer temperature, volume and elevation of documented rockfalls in the west face of the Drus (a five-year filter has been applied to remove interannual noise). Dotted quadrilaterals represent the different rockfalls.

There is also correspondence between the 2003, 2007, 2008 and 2009 rockfalls and climatic conditions of those years – in particular with temperatures (Fig. 6). 139 rockfalls have been documented between 2007 and 2009 in the central area of the Mont Blanc massif, 53 of them being precisely dated (38 %). Among them, 51 rockfalls (96 %) occurred between June and September, i.e. during the hottest months of the year. The 2003 summer heat wave, with a positive Mean Daily Air Temperature (MDAT) located at very high elevation, has generated extremely active morphodynamics. In the area covered by the network of observers, with 152 rockfalls reported in 2003 out of the 182 observed, 2003 has been quite exceptional in terms of rockfall occurrence. Some intense storms during summer 2003 may have caused high fluid pressure in fractures that triggered rockfalls, but this factor remains difficult to assess. Finally, it is worthy to note that 38 (72 %) of the 53 precisely dated rockfalls of 2007, 2008 and 2009 occurred after a period of MDAT warming of at least two days (Ravanel 2010).

2.3 The probable role of permafrost

The role of climate – especially the one of the thermal factor – has been demonstrated by the analysis of the rockfalls documented in the Mont Blanc massif. This relation can only be fully explained by temperature-dependent factors: permafrost degradation, glacial debuttressing and evolution of ice/snow cover on rockwalls (cryospheric factors). The two last factors may only explain a little part of the rockfalls. Furthermore, it is sometimes difficult to distinguish between rockfalls linked to glacial debuttressing or to ice/snow cover retreat, and rockfalls due to permafrost degradation, as both factors are often closely related and favoured by summer temperatures.

Secondly, topographic factors are highlighting the importance of permafrost in rockfall triggering. The average rockwalls elevation in the Mont Blanc massif is around 3000 m a.s.l., whereas the average elevation of rockfall scars of 2003 and 2007-2009 is 3335 m a.s.l. Although rockwalls are very common below 3000 m a.s.l., they are affected by very few collapses. The most affected altitudinal belt is 3200-3600 m a.s.l., which corresponds to areas of “warm” permafrost (close to 0°C, with fast degradation). Moreover, observations are consistent with permafrost distribution and its evolution: (i) the hotter the summer, the higher the scar elevations; (ii) a sharp contrast in the scar elevations between north and south faces. Rockfalls occur more frequently in context of pillars, spurs and ridges, particularly affected by permafrost degradation.

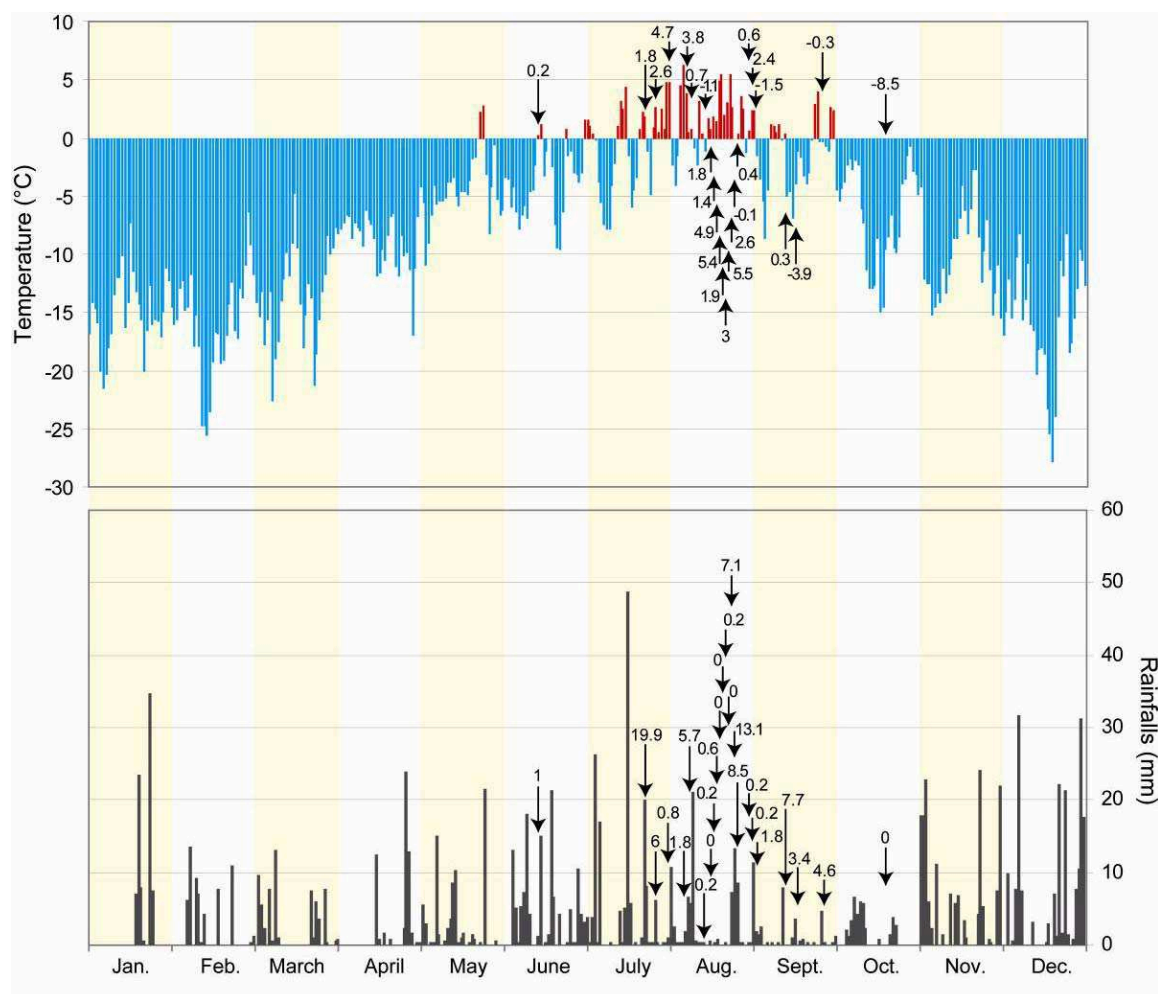


Fig. 6 – Mean daily air temperature at the Aiguille du Midi (3842 m a.s.l.) and daily total rainfall at Chamonix for the year 2009. Arrows indicate the days when one or several collapses occurred, with the value of temperature and rainfall for these days.

Finally, the permafrost degradation appears to be the most likely triggering factor for several other reasons (Ravello 2010):

- Almost all of the recorded rockfalls (98 %) occurred in possible or probable modelled permafrost;
- Rockfalls occur primarily during summer time, which is prone to permafrost degradation;
- Massive ice was observed in at least 22 scars of the 2007-2009 rockfalls;
- Summer 2003 rockfalls were unusually numerous and could mainly be explained only by permafrost degradation (Gruber *et al.* 2004);
- For the largest identified rockfalls (*e.g.* June 2005 at the Drus), the formation of a deep thaw corridor in the permafrost may have predisposed rockwalls to collapse.

When rockfalls in high-Alpine steep rockwalls are considered individually, the role of permafrost in their triggering is difficult to establish. On the other hand, this role in the Mont Blanc massif is strongly supported by the analysis of: (i) the 50 surveyed rockfalls (ranging in volume from 500 to 265 000 m³) at the west face of the Drus and on the north side of the Aiguilles of Chamonix since 1862; (ii) the 182 surveyed rockfalls (ranging in volume from 100 to 65 000 m³) in the whole Mont Blanc massif at the end of the 2003 summer heat wave; and (iii) the 139 surveyed rockfalls between 2007 and 2009 in the central part of the massif (ranging in volume from 100 to 33 000 m³).

3. Possible future thermal response to predicted climate change

Within the global warming prediction for the 21th century, rockfalls from high-Alpine steep rockwalls are expected to occur more frequently, with volumes that are likely to increase. The frequency that is currently increasing should maintain the same trend in the next decades, due to the deepening of the active layer as the temperature rise above 1800 m a.s.l. in the Alps for the 21th century will be higher by nearly 1°C than the global one, as reported in chapter 2. Moreover, heat advection by triggering of water circulation at depth along thaw corridors would increase the collapsed volumes.

Acknowledgements. – Alpine guides and hut keepers from Chamonix and Courmayeur who are involved in the rockfall inventory of the Mont Blanc massif since 2005 are kindly acknowledged.

References:

- Deline P., Kirkbride M., Ravanel L., Ravello M., 2008: The Tré-la-Tête rockfall onto the glacier de la Lex Blanche (Mont-Blanc massif, Italy) in September 2008. *Geografia Fisica e Dinamica Quaternaria*, 31, 251-254.
- Gruber S., Hoelzle M., Haeberli W., 2004: Permafrost thaw and destabilization of Alpine rock walls in the hot summer of 2003. *Geophysical Research Letter*, 31. L13504. doi:10.1029/2004GL020051.
- Gruber S., Haeberli W., 2007: Permafrost in steep bedrock slopes and its temperature-related destabilization following climate change. *Journal of Geophysical Research*, 112. F02S18. doi:10.1029/2006JF000547.
- Noetzli J., Hoelzle M., Haeberli W., 2003: Mountain permafrost and recent Alpine rock-fall events: a GIS-based approach to determine critical factors. *Proceedings of the 8th International Conference on Permafrost*, Zurich, Switzerland, 827-832.
- Ravanel L., 2010: Caractérisation, facteurs et dynamiques des écroulements rocheux dans les parois à permafrost du massif du Mont Blanc. *Thèse de Doctorat*, Université de Savoie, Le Bourget du Lac, France, 322 pp.
- Ravanel L., Deline P., 2008: La face ouest des Drus (massif du Mont-Blanc): évolution de l'instabilité d'une paroi rocheuse dans la haute montagne alpine depuis la fin du Petit Age Glaciaire. *Géomorphologie*, 4, 261-272.
- Ravanel L., Deline P., 2011: Climate influence on rockfalls in high-Alpine steep rockwalls: the north side of the Aiguilles de Chamonix (Mont Blanc massif) since the end of the Little Ice Age. *The Holocene*, 21, 357-365.
- Ravanel L., Deline P., in press: On the trigger of rockfalls in high alpine mountain. A study of the rockfalls occurred in 2009 in the Mont Blanc massif. *Proceedings of the Rock Slope Stability Conference*, Paris, France.
- Ravanel L., Allignol F., Deline P., Gruber S., Ravello M., 2010: Rockfalls in the Mont Blanc Massif in 2007 and 2008. *Landslides*, 7, 493-501.
- Ravanel L., Allignol F., Deline P., 2011: Les écroulements rocheux dans le massif du Mont Blanc pendant l'été caniculaire de 2003. *Actes du Colloque 2009 de la SSGm*, Olivone, Suisse, 245-261.

3.

Case studies in the European Alps

3.10

Cime Bianche Pass, Italian Alps

Citation reference

Pogliotti P, Cremonese E., Morra di Cella U. (2011). Chapter 3.10: Case studies in the European Alps – Cime Bianche Pass, Italian Alps. In Kellerer-Pirklbauer A. et al. (eds): *Thermal and geomorphic permafrost response to present and future climate change in the European Alps*. PermaNET project, final report of Action 5.3. On-line publication ISBN 978-2-903095-58-1, p. 119-128.

Authors

Coordination: Paolo Pogliotti

Involved project partners and contributors:

- Regional Agency for the Environmental Protection of the Aosta Valley, Italy (ARPA VdA) – Paolo Pogliotti, Edoardo Cremonese, Umberto Morra di Cella

Content

Summary

1. Introduction and study area
2. Permafrost indicators and recent thermal evolution
3. Possible future thermal response to predicted climate change

Reference

Summary

Cime Bianche Pass (45°55'N 7°41'E) is located at the head of the Valtournenche Valley in the northeastern corner of the Aosta Valley Region (Italy) at an elevation of 3100 m a.s.l. Two boreholes of different depth (6 and 41 m) drilled 30 m apart in different morphological conditions have been realized in 2005 and instrumented in 2006. The active layer thickness reflects the different snow-cover conditions of the two boreholes: in the deep borehole it is almost twice the value observed in the shallow one. The temperature profiles of the deep borehole allow to identify the depth of zero annual amplitude (ZAA) at ca. 17 m. The mean permafrost temperature is about -1.36°C in this depth. In the next future a probable decrease in the number of ID/year will strongly affect the ground thermal regime leading to a thickening of the active layer, increasing water pressure and permafrost degradation in the study area. All these changes will probably affect the spatial distribution of the hydro-geological risk in such a region.

1. Introduction and study area

Cime Bianche Pass (45°55'N 7°41'E) is located at the head of the Valtournenche Valley in the northeast corner of the Aosta Valley Region at an elevation of 3100 m a.s.l. (Fig. 1). The site is characterized by bare fractured bedrock locally mantled by shallow coarse-debris deposits. The lithology is mainly consisting of garnetiferous micaschists and calcschists belonging to the upper part of the Zermatt-Saas ophiolite complex (Dal Piaz *et al.* 1992). Several gelifluction lobes, terracettes and sorted polygons occur on the deposits.

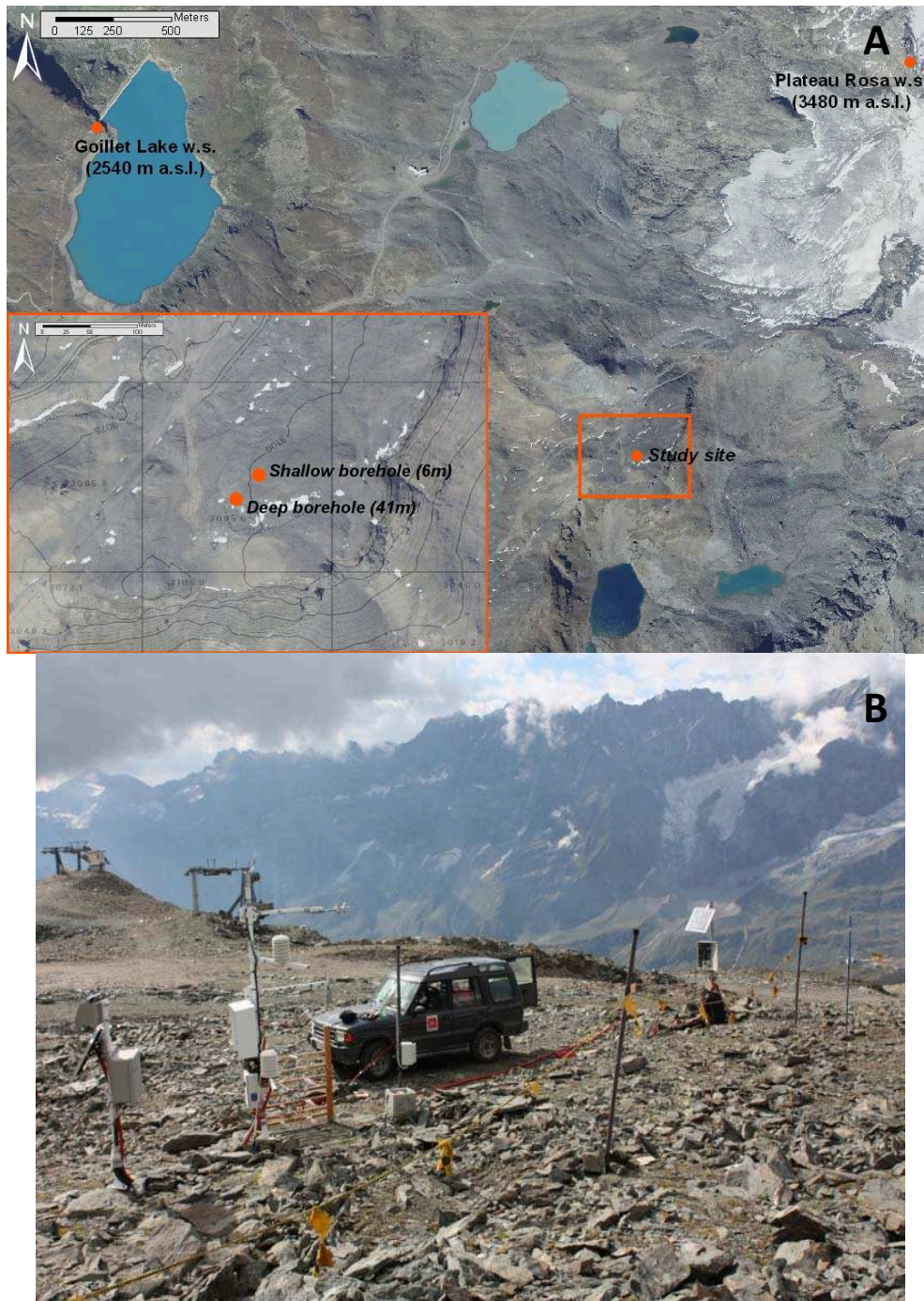


Fig. 1 – Study area: (A) localization of the study area. (B) Site overview and instruments; in the foreground a GST-grid area (fenced by the yellow flags) and in the background from right to left: boreholes dataloggers, GST-grid datalogger, automatic weather station and related dataloggers. Ski-lifts of the Breuil-Cervinia Valtournenche Zermatt resort are visible in the background.

The local climate can be defined as slightly continental with mean precipitation around 1000 mm/a (mean of the period 1931-1996 at the Lake Goillet weather station, 2540 m a.s.l., 1.5 km far, Fig. 1A-left). The mean air temperature (derived from Plateau Rosà weather station (3480 m a.s.l., 2 km far, Fig. 1A-right) is about -3.2°C for the period 1951-2000 (Mercalli *et al.* 2003). The mean monthly air temperatures over the same period give positive values only from June to September. February is the coldest month and July is the hottest one. The site is very windy and mainly influenced by northeast-northwest air masses. The combined effect of irregular morphology and strong wind action lead to a high variability of snow cover thickness within few meters.

The permafrost monitoring is performed by:

- Two boreholes of different depth (6 and 41 m) drilled 30 m apart in different morphological conditions (Fig. 1A). The shallow borehole (SH) is drilled on a convex coarse-debris land-form highly subject to wind erosion which usually avoids the formation of thick snow covers. On the other hand the deep borehole (DP) is located in a depression where the snow tends to accumulate, assuring a snow thickness always greater and more durable than those observed in SH. Temperature measurements in the borehole started in January 2005 for the SH and in August 2008 for DP.
- A small GST-grid area equipped with the purpose to quantify the spatial variability of surface temperature in a small area. The grid has an extension of 40x10 m and is active since January 2005. The GST is measured at 5 nodes: 4 at the grid corners and 1 in the centre of the area. In each node the ground temperature is measured 2 and 30 cm below the surface with hourly frequency. The surface is characterized by coarse blocky material slightly pending and irregular which gives great variability of snow cover among the nodes (Fig. 1B).

The site is equipped with an automatic weather station for the measurement of snow-depth, air temperature and relative humidity, wind speed and direction as well as radiation. The site is accessible all over the year, by cable car and ski in winter and by off-road vehicle during summer.

2. Permafrost indicators and recent thermal evolution

2.1 Meteorological records

Air temperature and snow depth are the parameters that mainly affect the ground thermal regime in permafrost environments (Zhang 2005). On the study site both parameters are measured in correspondence of the SH borehole.

The Fig. 2A shows monthly air temperature anomalies calculated comparing the monthly means measured at Cime Bianche Pass with long-term monthly means (1951-1998) derived from the Plateau Rosà meteorological station. An extrapolation method based on monthly lapse rates was used to shift-down the long-term dataset from the elevation of Plateau Rosà to Cime Bianche Pass. The Fig. 2B shows the mean snow depth of the period November 15th-June 15th over the borehole SH for 3 available hydrological years.

2.2 Active Layer Thickness

The active layer thickness reflects the different snow-cover conditions of the two boreholes. The combined effect of morphology and wind leads to thick snow cover above the DP borehole and a thin snow cover above the SH. These morphological differences strongly affect the ground thermal regime: it follows that the thickness of the active layer (ALT), defined as the maximum depth of the 0°C -isotherm, in the deep borehole is almost twice the one observed in the shallow one. Table 1 summarizes the values of ALT of some years obtained by linear interpolation among the measured temperatures at different depths.

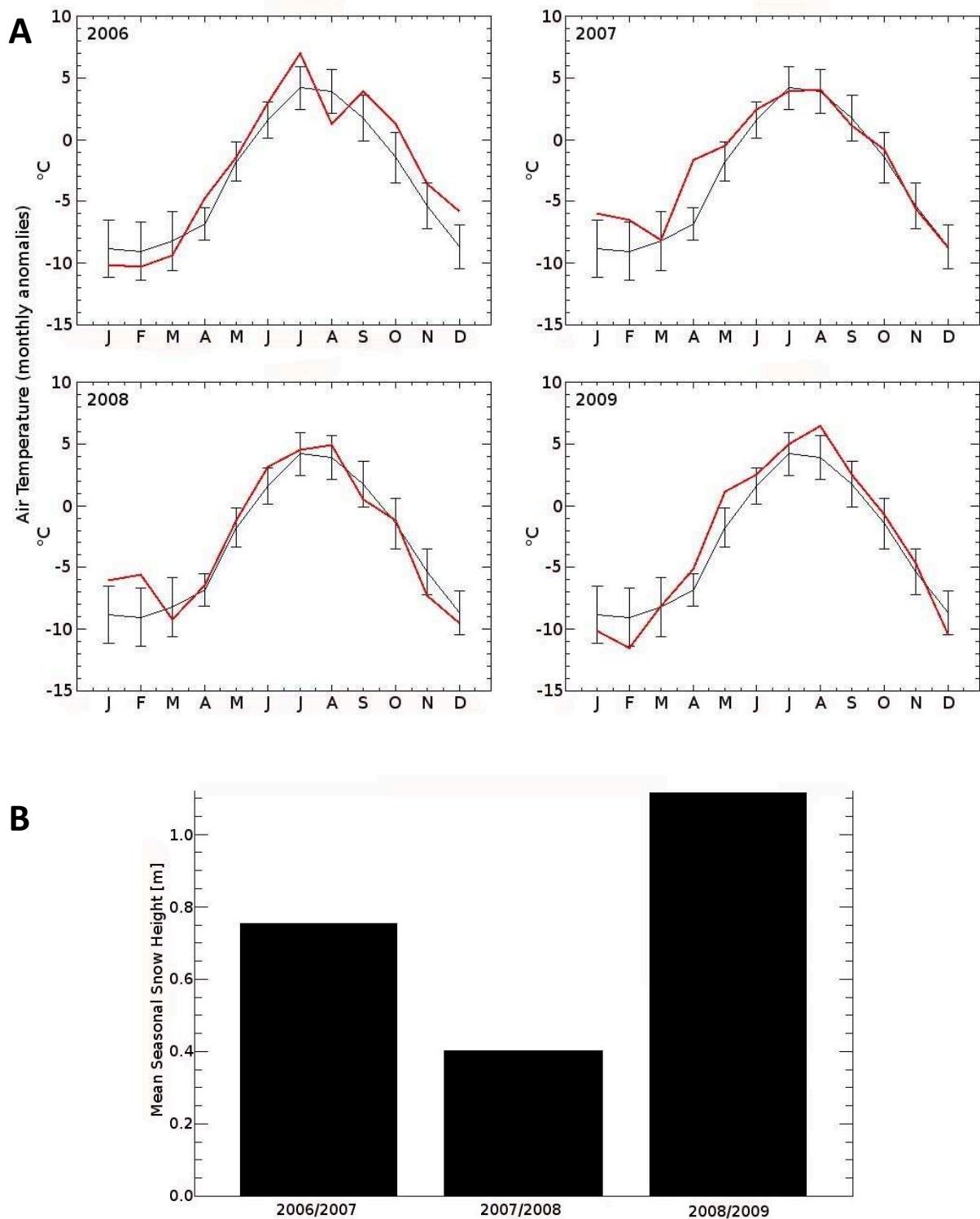


Fig. 2 – (A): monthly air temperatures from 2006 to 2009 compared with a long term mean (1951-1998) derived from Plateau Rosa observations. The vertical lines give the standard deviation of the long term monthly means. Red lines are the monthly means measured at Cime Bianche Pass. (B) mean seasonal snow depth above the borehole SH calculated over the period November 15th-June 15th.

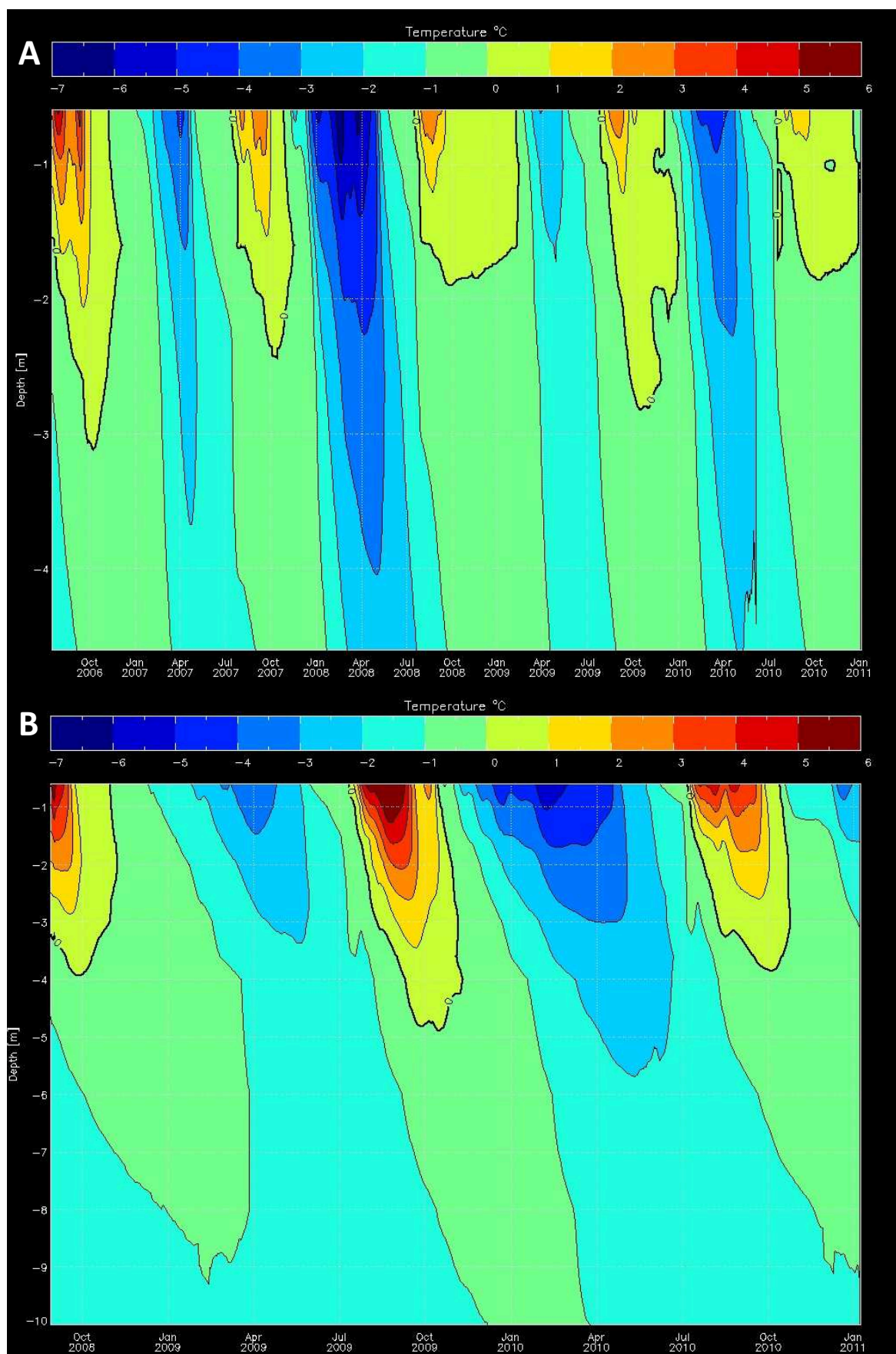


Fig. 3 – Maximum daily ground temperature vs. time in the SH (A) and DP (B) boreholes. The black line is the 0°C-isotherm. Note that y-axes have different ranges.

Table 1 – Values of the maximum active layer thickness (ALT) in the two boreholes at Cime Bianche Pass and day of the year in which the value has been reached.

Hydrological Year	Active Layer Thickness (ALT)(m)		Occurrence day of maximum ALT	
	Shallow Borehole	Deep Borehole	Shallow Borehole	Deep Borehole
2005/2006	3.12	-	October 7 th	-
2006/2007	2.36	-	October 11 th	-
2007/2008	1.9	3.9	September 30 th	September 27 th
2008/2009	2.8	4.85	October 22 th	October 17 th

Comparing the contour plots of both boreholes (Fig. 3) with the snow-depth measures of Fig. 2B, a good correlation between the mean seasonal snow depth and the active layer thickness can be seen. The difference in the active layer thickness from 2008 to 2009 in both boreholes shows the same behaviour: 2009 maximum depth has an increase of about 1 m compared to 2008, due to the exceptional snow falls of the winter season 2008/09 which lead to important snow cover throughout the winter on both boreholes.

2.3 Permafrost Temperature

The temperature profiles of the deep borehole allow to identify the depth of zero annual amplitude (ZAA) at around 17 m. The mean permafrost temperature at this depth is about -1.36°C (Fig. 4A). The thermal-offset, defined in accordance to Romanovsky & Osterkamp (1995) as the difference between TTOP (mean annual permafrost surface temperature) and MAGST (mean annual ground surface temperature), seems quite variable from year to year. The available values for both boreholes are reported in Table 2.

Table 2 – Values of thermal-offset in the boreholes. MAGST is calculated using the node at -2cm from the ground surface. TTOP is calculated at the depth of ALT (Table 1) by linear interpolation among the mean annual temperatures of the first node above and first node below the ALT value.

Hydro. Year	Shallow Borehole			Deep Borehole		
	MAGST ($^{\circ}\text{C}$)	TTOP ($^{\circ}\text{C}$)	Th-Offset ($^{\circ}\text{C}$)	MAGST ($^{\circ}\text{C}$)	TTOP ($^{\circ}\text{C}$)	Th-Offset ($^{\circ}\text{C}$)
'08-'09	-0.05	-0.73	-0.67	-0.01	-0.81	-0.8
'09-'10	-1.1	-1.24	-0.14	-1.17	-1.23	-0.05

Fig. 4 shows the borehole temperature profiles at specific days of the year. Mean daily temperature profile of 1st April are representative of ground temperatures at the end of the winter season while those of 1st October are representative of ground temperatures at the end of the hydrological year near the occurrence of the maximum ALT.

The effect of different snow amount during the winter season is clearly reflected in the 1st April profiles of borehole SH. The profiles differ very much from each other with the colder ones corresponding to the less snowy years. The great differences at the end of the winter are systematically levelled during the spring/summer period, indeed the 1st October profiles differ less from each other. From the beginning of the measures the hydrological year 2007/08 shows the coldest ground temperature profiles and shallower ALT (Table 1). This results from a combination of

scarce snow accumulation and summer air temperature around the mean (Fig. 2). In contrast the seasons which show warmer ground temperature profiles and deeper ALT are those with abundant snow during the winter and air temperature above the mean during the winter-summer period. This is mainly true for the hydrological year 2008/09 while in 2005/06 the quite cold ground temperature profile of April is completely overhung by the extremely warm spring/summer 2006. All these considerations suggest that even if winter conditions are strongly favourable to ground cooling they are often not enough to restrain the effect of very hot spring-summer conditions on ground temperatures.

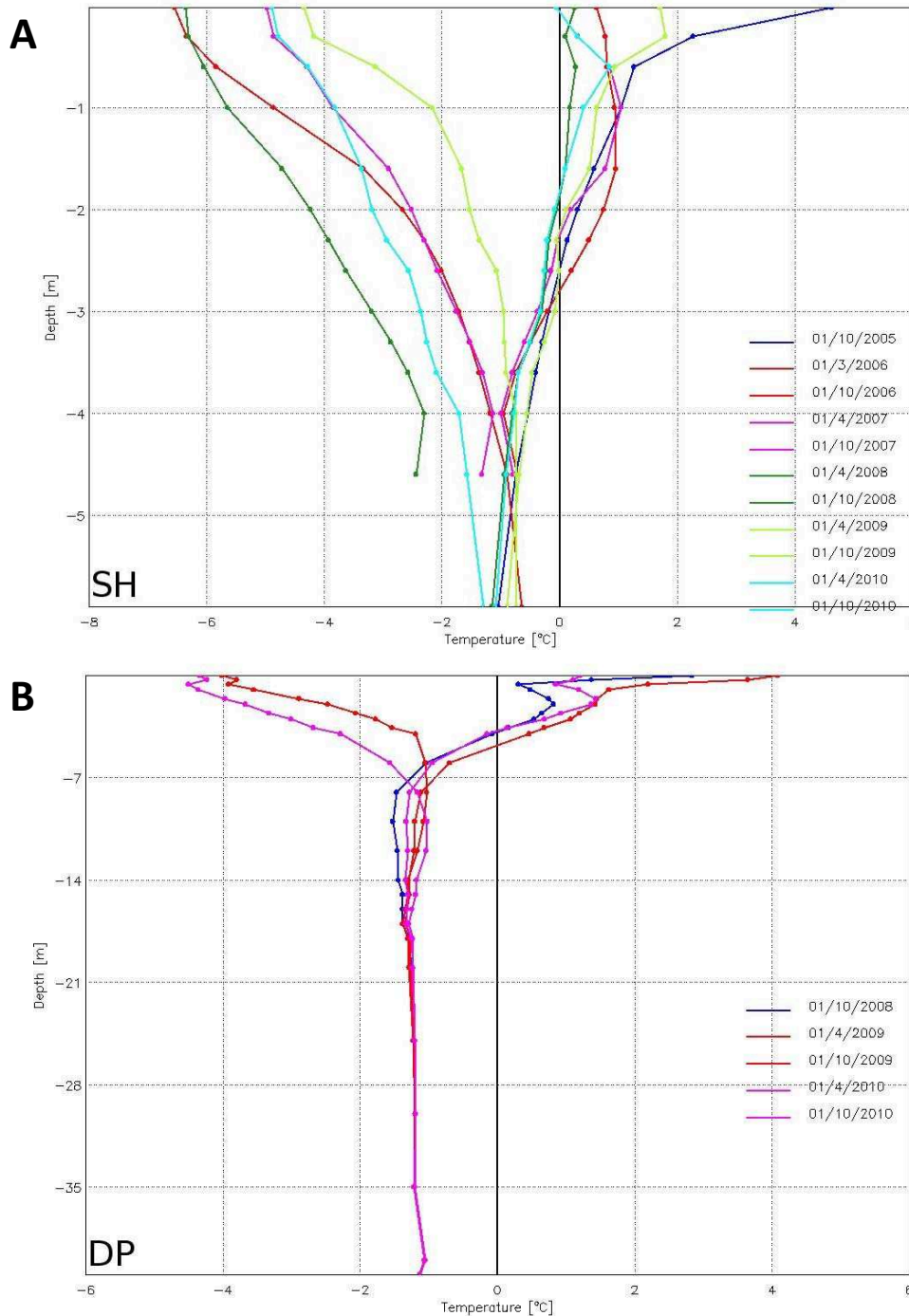


Fig. 4 – Ground temperature profiles over the SH (A) and DP (B) boreholes at specific days at the end of winter and summer seasons.

3. Possible future thermal response to predicted climate change

As suggested in chapter 2, frost days (FD), ice days (ID) and freeze-thaw days (FTD) have been computed using the air temperature dataset of the Cime Bianche Pass over the available years of observation (Table 3).

Table 3 – Frost days (FD), Ice Days (ID) and Freeze-Thaw Days (FTD) occurrence at the Cime Bianche site during the available hydrological years (October 1st-November 30th). The last column reports the mean value of the period.

	2006/07	2007/08	2008/09	2009/10	Mean
MAAT (°C)	-1.73	-3.01	-3.4	-3.75	-2.97
FD	275	284	275	282	279
ID	149	202	198	201	187.5
FTD	126	82	77	81	91.5

Referring to the maps and predictions of chapter 2, the air temperature measurements conducted at Cime Bianche Pass from 2006 to 2010 are in accordance with the means of the period 1961-1990 computed for the Great Alpine Region (GAR). That is a number of ID in the range of 261-280, a number of FD in the range of 181-200 and a number of FTD in the range of 80-90. The prediction for the period 2021-2050 in the study area are a decrease of ID ranging from -15/-16 days/year that means 172 ID instead of 187 and a decrease of FD ranging from -15/-16 days/year that means 264 FD instead of 279.

Comparing the data of Table 3 and plots of Figure 3 year by year, it is evident that the air temperature is not the only factor controlling the ground temperatures. In fact, as already highlighted, the snow cover plays a key role. Despite this, looking at the hydrological year 2006/07 a clear correlation between warmer air temperature and deeper ALT exists. Looking at table 3 it is interesting to note that the number of ID is the most affected value by this anomalous winter. Probably a future decrease in the number of ID/year will strongly affect the ground thermal regime leading to a thickening of the ALT, increasing water pressure and permafrost degradation. All these changes will probably affect the spatial distribution of the hydrogeological risk in such a region.

References:

- Dal Piaz G. *et al.*, 1992: Le Alpi dal Monte Bianco al Lago Maggiore. *Guide Geologiche Regionali a cura della Società Geologica Italiana*, 3/II, 211pp.
- Mercalli L., Castellano C., Cat Berro D., Di Napoli G., Montuschi S., Mortara G., Ratti M. & Guindani N., 2003: *Atlante Climatico della Valle d'Aosta*. Editions SMS, 405 pp.
- Zhang T., 2005: Influence of the seasonal snow cover on the ground thermal regime: an overview. *Review of Geophysics*, 43: RG4002.

Romanovsky V. E. & Osterkamp T. E., 1995: Interannual variations of the thermal regime of the active layer and near-surface permafrost in northern Alaska. *Permafrost and Periglacial Processes*, 6, 313-335.

3.

Case studies in the European Alps

3.11

Maroccaro rock glacier, Val di Genova, Italian Alps

Citation reference

Seppi R., Baroni C. Carton A., Dall'Amico M., Rigon R., Zampedri G., Zumiani M. (2011). Chapter 3.11: Case studies in the European Alps – Maroccaro rock glacier, Val di Genova, Italian Alps. In Kellerer-Pirklbauer A. et al. (eds): *Thermal and geomorphic permafrost response to present and future climate change in the European Alps*. PermaNET project, final report of Action 5.3. On-line publication ISBN 978-2-903095-58-1, p. 129-139.

Authors

Coordination: Roberto Seppi

Involved project partners and contributors:

- University of Pavia – Roberto Seppi
- University of Pisa – Carlo Baroni
- Mountain-eering srl – Matteo Dall'Amico
- University of Trento – Riccardo Rigon
- Geological Survey, Autonomous Province of Trento – Giorgio Zampedri
- Geologist – Matteo Zumiani

Content

Summary

1. Introduction and study area
2. Permafrost indicators and recent thermal and geomorphic evolution
3. Possible future thermal and geomorphic response to predicted climate change

References

Summary

In 2001 we started a topographic study on an active rock glacier (named Maroccaro rock glacier, acronym MaRG, coordinates: 46° 13' 06" N, 10° 34' 34" E) located in the Adamello-Presanella massif (Central Italian Alps). Since 2004, also the near-surface ground temperature was measured using a miniature data logger. Our data show that in eight years (2001-2009) MaRG has moved downslope with average velocities ranging from 0.02 to 0.21 m/year. The velocity reaches a maximum in the middle and the lower part of the rock glacier, and decreases towards the upper sector, where the surveyed boulders are almost stationary. A considerable different velocity from year to year has been observed, but no clear trends seem to emerge from the mean annual displacement rate. On the rock glacier the evolution of the ground temperature since 2004 is directly associated with the air temperature and the snow conditions, in terms of thickness and duration of the snowpack. The ground has warmed significantly both in 2007, after a very mild and little snowy winter, and in 2009, after a cold but exceptionally snowy winter. The displacement rate of MaRG seems to rapidly react to the ground temperature variations, apparently without any time delay. The exceptionally snowy winter 2008/09 seems to have played a significant role on the displacement rate, causing a ground temperature increase and, probably, an increase in velocity, which reached its maximum in that year.

1. Introduction and study area

In the Adamello-Presanella Group (Central Italian Alps), an active rock glacier (MaRG) located in Val Genova has been selected for carrying out multitemporal topographic surveys (Fig. 1). The measurements aim at studying its surface displacement rate and its dynamic behaviour. The displacement rates of the rock glacier are compared with the near-surface thermal regime of the ground and with the major climatic parameters, in order to investigate the potential relationships between its dynamic behaviour and the local climatic conditions. This rock glacier is included in an inventory published by Baroni *et al.* (2004), in which it has the number 41 and is also briefly described.

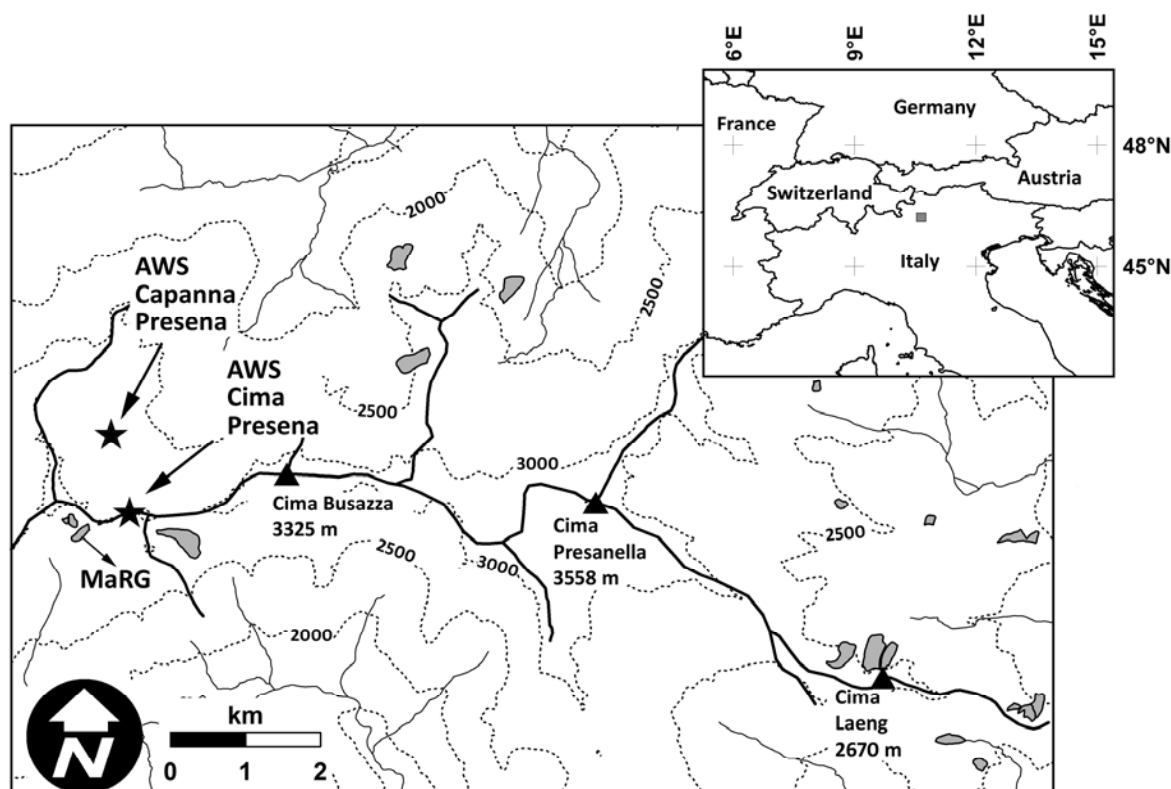


Fig. 1 – Geographical setting of the study area with rock glacier MaRG and automatic weather stations (AWS)

The topographic measurements started in 2001 and have been repeated in late summer of the following years (2002, 2004, 2006, 2007, 2008 and 2009). On the rock glacier surface, a monitoring network of 25 large boulders marked with steel bolts has been established and a laser theodolite has been used for performing the surveys. For monitoring the near-surface temperature of the ground, a miniature temperature data logger (UTL1, accuracy: $\pm 0,25^{\circ}\text{C}$; Hoelzle *et al.* 1999) has been placed in 2004 few centimetres below the surface, in a place where fine-grained material outcrops. Detailed meteorological data (i.e. air temperature and snow thickness) covering the full monitoring period are available from two high-altitude automatic weather stations (AWS) located near the studied rock glacier (Cima Presena, 3015 m a.s.l., and Capanna Presena, 2730 m a.s.l.).

MaRG is a tongue-shape rock glacier, about 280 m long and 100 m wide. It faces southwest and its lower part (top edge of the frontal slope) reaches an altitude of 2760 m a.s.l. (Fig. 2). The surface of MaRG doesn't display the typical morphological features of active rock glaciers, such as longitudinal and transversal ridges, furrows and hollows. MaRG is composed of talus material coming from the shattered rockwalls situated above, and no field evidences of Little Ice Age glaciation are present in

its rooting area. It is almost completely covered by large and very angular boulders (from few decimetres to some meters in diameter), and fine-grained rock material outcrops only on the steep frontal and lateral slopes. According to the definition given by Barsch (1996), MaRG can be defined as a talus rock glacier.



Fig. 2 – General view of MaRG. The elevation at the front is about 2760 m a.s.l., the highest peaks in the background reach elevations of about 3000 m a.s.l. Photography by R. Seppi (21.08.2009)

On this rock glacier, BTS measurements carried out in late March 2003 recorded very cold temperatures, consistent with the presence of a frozen core into the debris deposit. The BTS values ranged between -2.1°C and -6.1°C (average value of 23 measurement points: -4.2°C) and the average thickness of the snowpack was 230 cm. The temperature of a spring emerging from the bottom of the frontal slope is also under measurements since 2004. The water temperature measured during the late summer season is constantly below 1°C , indicating furthermore the presence of permafrost in the rock glacier.

2. Permafrost indicators and recent thermal and geomorphic evolution

Fig. 3 shows the total horizontal displacement of MaRG in the full period of measurements (2001-2009). On this rock glacier, the total displacement ranges between 0.12 m (boulder 19) and 1.67 m (boulder 2), corresponding to a velocity of 0.02 and 0.21 m/year, respectively (Table 1). The surveyed boulders moved along the maximum gradient of the slope in a rather homogeneous pattern. The velocity reaches a maximum in the middle and the lower part of the landform, and decreases towards the upper sector, where the slowest boulders (18, 19 and 20) are located. After the second survey (2002) the boulder 3 fell down from the frontal slope.

The mean displacement of MaRG in all the measurement intervals is shown in Fig. 7 (top graph), where all the surveyed boulders of the rock glacier have been taken into account. The average velocity is significantly variable from year to year, ranging from a minimum of 0.08 m/year (2007-2008) to a maximum of 0.17 m/year (2008-2009). No clear trends seems to emerge from the evolution of the mean annual displacement. The interannual variability of the velocity and an accelerating trend have been recently reported for several rock glaciers in the European Alps (Roer *et al.* 2005, Delaloye *et al.* 2008, PERMOS 2009, Bodin *et al.* 2009).

Table 1 – Horizontal displacements of MaRG. The first six columns show the displacement for each period of measurements, the column seven the total displacement, and the column eight the annual displacement rate. (*) Measurement period of two years; (**) The boulder number 3 fell from the frontal slope after 2002.

Boulder ID	Horizontal displacement (m)						2001-09 total horizontal displacement (m)	2001-09 horizontal displacement rate (m/yr)
	2001-02	2002-04(*)	2004-06(*)	2006-07	2007-08	2008-09		
01	0.16	43.2	27.6	0.21	0.08	0.22	1.38	0.17
02	0.21	51.9	34.1	0.24	0.11	0.25	1.67	0.21
03(**)	0.20
04	0.18	47.4	29.7	0.20	0.11	0.24	1.50	0.19
05	0.17	43.6	26.2	0.17	0.12	0.23	1.38	0.17
06	0.17	46.6	26.5	0.20	0.09	0.25	1.44	0.18
07	0.16	44.2	25.3	0.18	0.08	0.23	1.34	0.17
08	0.15	35.9	22.0	0.12	0.10	0.18	1.13	0.14
09	0.11	25.9	14.6	0.06	0.06	0.12	0.77	0.10
10	0.17	46.7	24.9	0.18	0.10	0.24	1.41	0.18
11	0.16	45.0	22.9	0.17	0.08	0.21	1.31	0.16
12	0.15	37.1	20.8	0.14	0.08	0.19	1.13	0.14
13	0.16	40.9	23.9	0.16	0.08	0.21	1.26	0.16
14	0.13	27.2	16.3	0.07	0.08	0.15	0.87	0.11
15	0.15	34.0	19.2	0.11	0.08	0.19	1.05	0.13
16	0.13	30.6	16.4	0.11	0.06	0.17	0.94	0.12
17	0.08	12.6	5.4	0.07	0.0	0.07	0.39	0.05
18	0.08	5.6	4.4	0.0	0.04	0.04	0.22	0.03
19	0.07	2.0	1.8	0.01	0.0	0.03	0.12	0.02
20	0.08	-0.5	2.1	0.02	0.0	0.04	0.14	0.02
21	0.05	10.8	8.3	0.06	0.0	0.07	0.35	0.04
22	0.09	19.9	10.6	0.11	0.02	0.09	0.61	0.08
23	0.12	29.7	14.3	0.12	0.06	0.15	0.88	0.11
24	0.15	38.0	20.6	0.16	0.08	0.19	1.17	0.15
25	0.10	21.2	9.0	0.10	0.01	0.10	0.61	0.08

The near-surface temperature of the ground recorded on MaRG from August 2004 to August 2009 is shown in Fig. 4 (bottom graph). In this figure the ground temperature (daily mean) is associated to the air temperature (central graph) and to the thickness of the snow cover (top graph), recorded at two meteorological stations located about 1 km from the rock glacier (Cima Presena AWS and Capanna Presena AWS).

Focusing on the ground thermal regime during winter, the coldest temperatures were recorded in the 2004-2005 and 2005-2006 winter seasons. During the first winter, the ground reached a minimum temperature of about -10°C in late February, and a strong warming followed in March due

to an early starting of the snow melt. In the winter of 2005-2006, the ground cooled very quickly towards the minimum values of about -8°C . The strong cooling of the ground in these two winters may be due to the combined effect of cold air temperature and relatively thin snowpack in autumn and early winter. In the two following winters, the ground temperature was warmer and reached a phase of winter equilibrium temperature (WEqT) of about -5°C . The winter 2006-2007 was very mild and the snowpack was relatively thin until mid winter, while the following winter was colder and snowier.

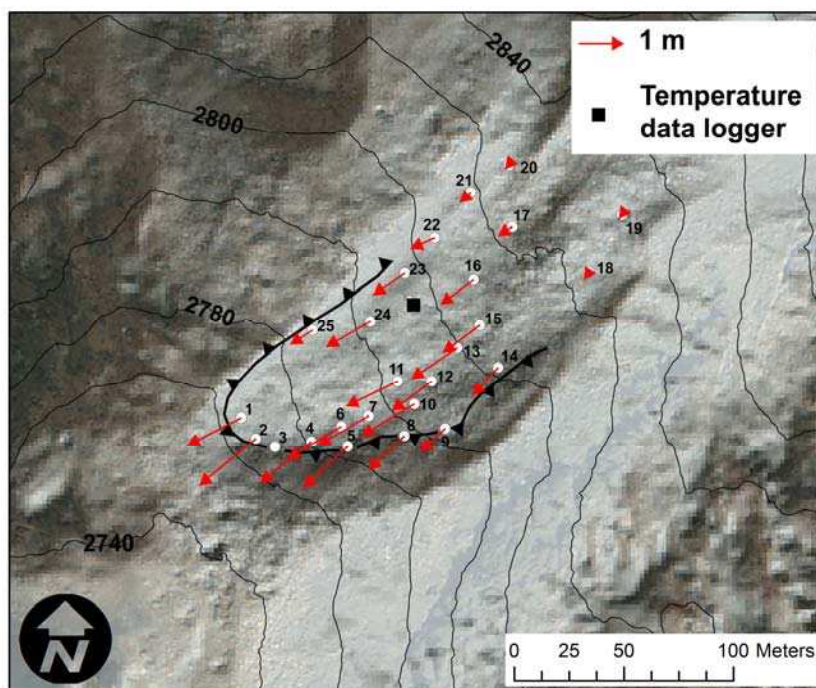


Fig. 3 – Total horizontal displacement (2001-2009) of MaRG.

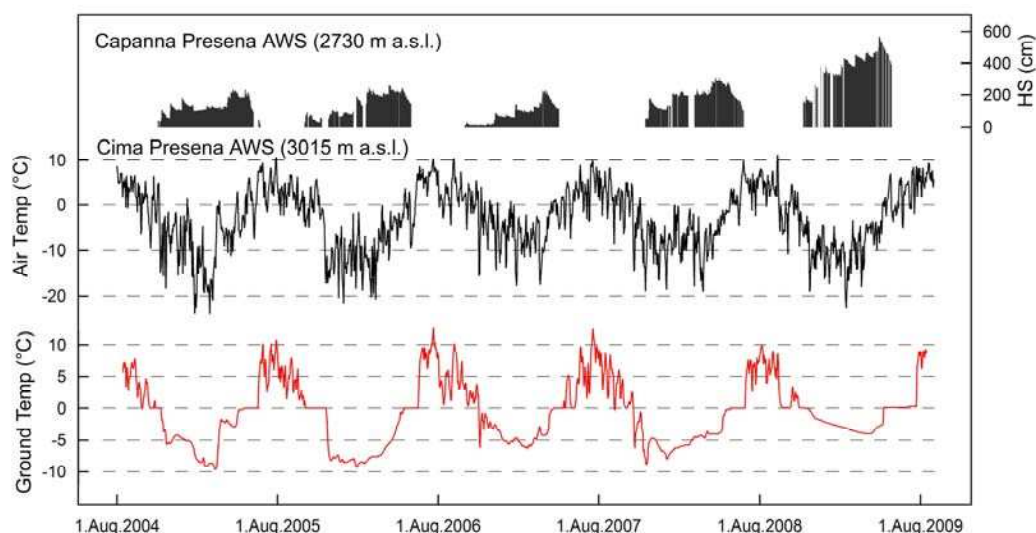


Fig. 4 – Top and middle graphs: snow thickness and air temperature at Capanna Presena automatic weather station; bottom graph: ground near-surface temperature from August 2004 to August 2009 for MaRG. For location of temperature data logger refer to Fig. 3.

With respect to the previous years, the ground temperature was comparatively warmer during the 2008-2009 winter season, and reached a relatively short WEqT of about -4°C . Although in this winter the air temperature was not particularly mild compared to the preceding ones, the snowpack already reached a significant thickness in autumn and early winter, preventing the cooling of the ground. Moreover, the snowpack further thickened in the following winter months. This underlines the strong control of the snow cover on the winter temperature of the ground and, consequently, on the mean annual ground temperature.

The Ground Freezing Index (GFI), computed as the cumulative value of the negative daily mean ground temperatures between 1st October and 30th June, is shown in Fig. 5. The lowest values were recorded in the winter 2005-2006 and 2007-2008 ($-1197^{\circ}\text{C}\cdot\text{day}$ and $-1052^{\circ}\text{C}\cdot\text{day}$, respectively). Despite a thin and late-appeared snow cover in winter 2006-2007, the GFI was less negative than the previous and the following winter, probably because of the relatively high air temperature (see Cima Presena AWS in Fig. 4). The highest GFI ($-471^{\circ}\text{C}\cdot\text{Day}$) since the beginning of the measurements was recorded in winter 2008-2009, when a very thick snowpack was present on the rock glacier since the middle of autumn.

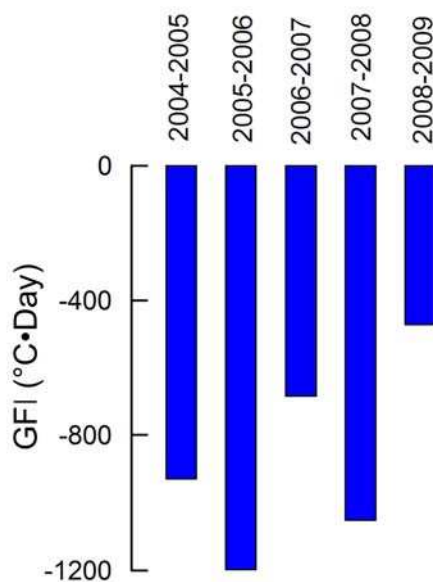


Fig. 5 – Annual ground freezing index (GFI) at MaRG from 2004 to 2009.

The effect of the snow cover on the ground temperature can be observed in Fig. 6. In the graph, the evolution of the mean annual air temperature (MAAT) at Cima Presena AWS and the evolution of the mean annual ground temperature at MaRG are compared on the same period of time. The temperatures are displayed as 12-months running means, and the date on the x-axis corresponds to the end of the period used for the calculation. The mean ground temperature on MaRG ranged between 0°C and -2°C in the period of measurements (mid 2005 to mid 2009), reaching the highest values in 2007 and in 2009. The first warming phase (2007) occurred after a winter season that was very mild and with little snow, while the second (2009) followed an exceptionally snowy winter with relatively cold air temperature. On this rock glacier, the evolution of the ground temperature seems to be well correlated with the MAAT, at least until 2008. In fact, the strong warming of the ground observed in 2009 is more due to an effect of the thick snow cover of the previous winter than to a corresponding warming in the air temperature.

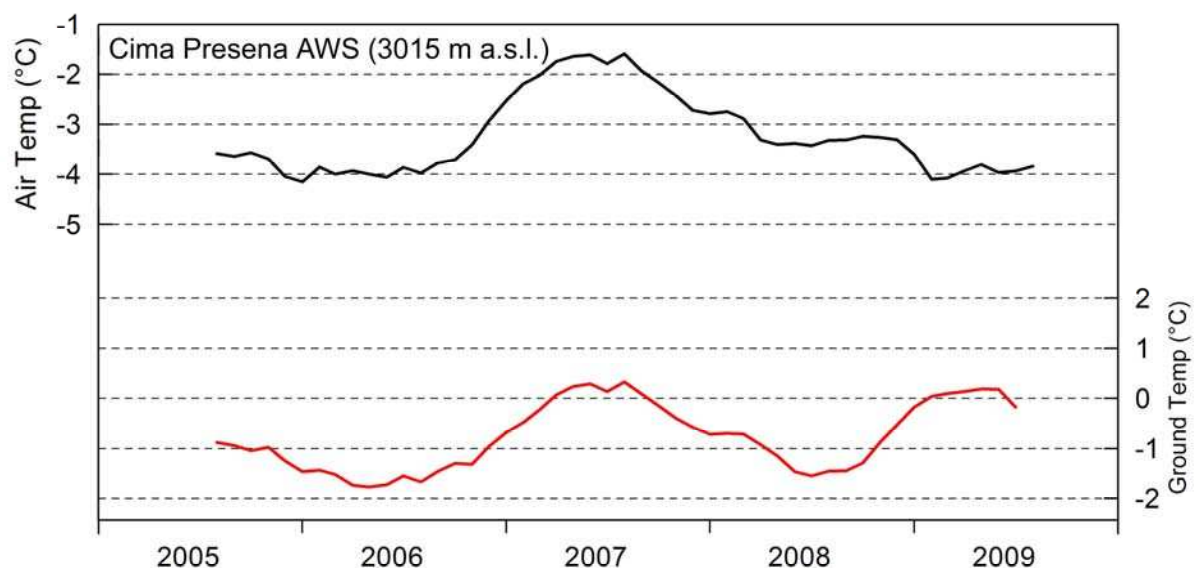


Fig. 6 – Evolution of the mean annual air temperature at Cima Presena automatic weather station (top graph) and of the near-surface ground temperature at MaRG (bottom graph). All the temperatures are displayed as 12-months running means, and the date on the x-axis corresponds to the end of the period used for the calculation.

In Fig. 7 all the observations carried out on MaRG are summarized. The top graph shows the mean annual displacement since 2001 and has been described above. The intermediate graph shows the mean annual near-surface temperature of the ground, and the bottom graph reports the mean annual air temperature at Cima Presena AWS. In order to emphasize the contribution of the winter seasons, the values of the mean annual temperature (both for the ground and for the air) have been calculated taking into account an annual basis extending from the 15th August of the previous year to the 14th August of the following year. For this reason, an extremely warm summer like 2003 is not as well visible in the data record as a mild winter like 2006-2007.

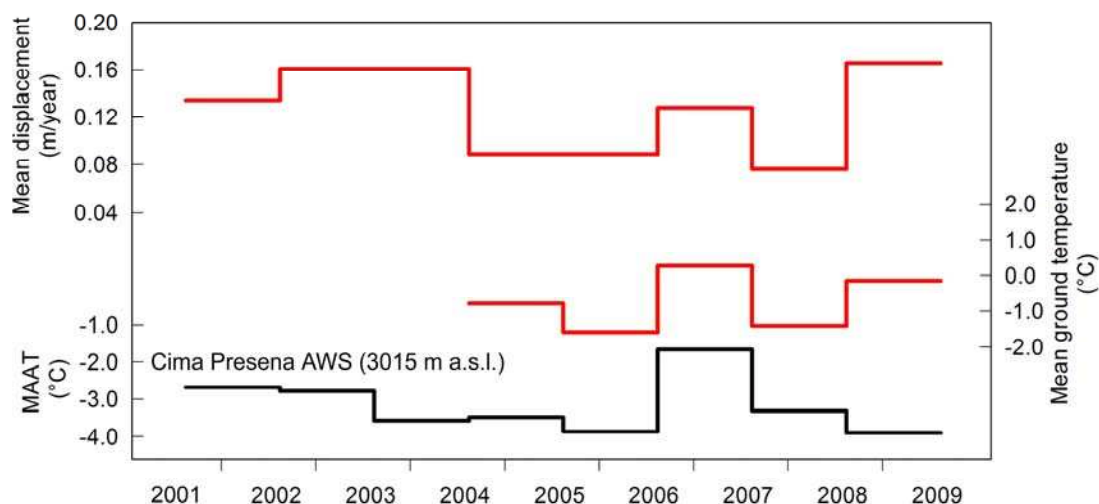


Fig. 7 – Mean displacement of MaRG (top graph) compared with the mean annual ground temperature (middle graph) and the mean annual air temperature at Cima Presena automatic weather station (bottom graph).

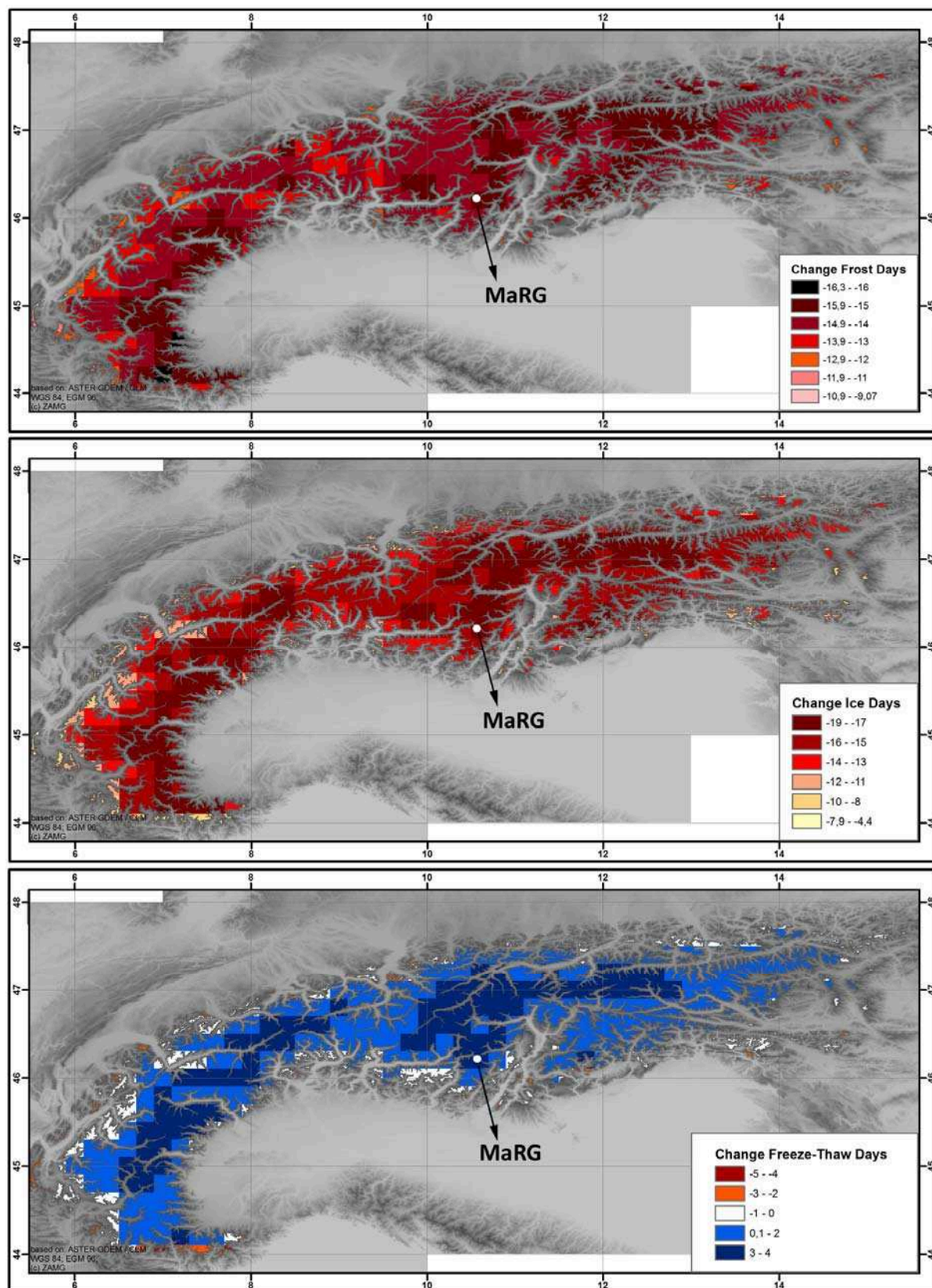


Fig. 8 – Potential change of frost, ice and freeze-thaw days for 2020-2050, as proposed in chapter 2. The location of MaRG is shown.

The displacement of the MaRG seems to react rapidly to the ground temperature variations, apparently without any time delay. In the last three years, indeed, higher ground temperatures correspond rather well with higher displacement velocities, as clarified e.g. in the year 2006-2007. In this year, the rock glacier has moved faster than in the previous and in the following years, in close relation with the higher mean temperature of the ground that was slightly above 0°C. In the last year of measurements (2008-2009) MaRG reached the highest velocity since the beginning of the observations. This acceleration corresponds with a mean ground temperature that approached again 0°C, but the effect seems to be amplified by the snow cover. In fact, the exceptionally snowy winter of 2008-2009 could have played a role in determining the displacement rate, probably because of the long melting phase of the snow cover associated to the long zero curtain phase of the ground that characterized MaRG (from early May to late July; see Fig. 4, bottom graph). The long melting phase could have induced a prolonged infiltration of meltwater into the active layer and, possibly, into the frozen core of the rock glacier, causing the observed acceleration. A similar effect has recently been observed and described by Ikeda *et al.* (2008) on a rock glacier of the Swiss Alps.

3. Possible future thermal and geomorphic response to predicted climate change

According to the analyses in chapter 2, some speculations on the future evolution of MaRG can be done. In the area where MaRG is located, the modelled average number of frost days in the period 1961-1990 ranges between 280 and 300 per year, and the predicted change for 2021-2050 shows a decrease of 15/16 days/year. In the same area and the same period, the average number of ice days is between 201 and 220 per year, with a predicted decrease of 17/19 days/year for 2021-2050. Regarding the average number of freeze-thaw days, it has been modelled as ranging between 70 and 80 per year in the 30-year reference period, and an increase of 3/4 days/year is predicted for 2021-2050. In Fig. 8 the location of MaRG (white dot) on the maps of the predicted change in frost, ice and freeze-thaw days is displayed. Some changes in the dynamic response of MaRG to climate change can be expected, because of the close relationship between its behaviour and the climatic variables. However, an assessment of its future evolution should carefully take into account the future evolution of the precipitation (amount and distribution) and not only the predicted rise in air temperature.

Acknowledgements. – Mauro Degasperi and Franco Crippa (Geological Survey, Autonomous Province of Trento) conducted the topographic surveys and processed the rough topographic data. Field collaboration was provided by Luca Carturan, Stefano Fontana and Davide Tagliavini. This work was partly funded by the PRIN 2008 project “Climate Change effects on glaciers, on glacier-derived water resource and on permafrost: Quantification of the ongoing variations in the Italian Alps”.

References:

- Baroni C., Carton A. & Seppi R., 2004: Distribution and behaviour of rock glaciers in the Adamello-Presanella Massif (Italian Alps). *Permafrost and Periglacial Processes*, 15, 243-259.
- Barsch D., 1996: *Rockglaciers: Indicators for the Present and Former geocology in High Mountain Environments*. Springer, Berlin, 331 pp.

- Bodin X., Thibert E., Fabre D., Ribolini A., Schoeneich P., Francou B., Louis Reynaud L. & Fort M., 2009: Two Decades of Responses (1986–2006) to Climate by the Laurichard Rock Glacier, French Alps. *Permafrost and Periglacial Processes*, 20, 331-344.
- Delaloye R., Perruchoud E., Avian M., Kaufmann V., Bodin X., Ikeda A., Hausmann H., Käab A., Kellerer-Pirklbauer A., Krainer K., Lambiel C., Mihajlovic D., Staub B., Roer I. & Thibert E., 2008: Recent interannual variations of rock glaciers creep in the European Alps. *Proceedings of the 9th International Conference on Permafrost (NICOP)*, University of Alaska, Fairbanks, June 29-July 3, 2008, 343-348.
- Haeberli W., Hallet B., Arenson L., Elconin R., Humlum O., Kaab A., Kaufmann V., Ladanyi B., Matsuoka N., Springman S. & Vonder Muehll D., 2006: Permafrost creep and rock glacier dynamics. *Permafrost and Periglacial Processes*, 17, 189-214.
- Hoelzle M., Wegmann M. & Krummenacher B., 1999: Miniature temperature dataloggers for mapping and monitoring of permafrost in high mountain areas: first experience from the Swiss Alps. *Permafrost and Periglacial Processes*, 10, 113-124.
- Käab A., Frauenfelder R. & Roer I., 2007: On the response of rockglacier creep to surface temperature increase. *Global and Planetary Change*, 56, 172-187.
- Ikeda A., Matsuoka N. & Käab A., 2008: Fast deformation of perennially frozen debris in a warm rock glacier in the Swiss Alps: An effect of liquid water. *Journal of Geophysical Research* 113, F01021.
- PERMOS, 2009: Permafrost in Switzerland 2004/2005 and 2005/2006. Noetzli, J., Naegeli, B., and Vonder Muehll, D. (eds.), *Glaciological Report Permafrost No. 6/7 of the Cryospheric Commission of the Swiss Academy of Sciences*, 100 pp.
- Roer I., Käab A. & Dikau R., 2005: Rockglacier acceleration in the Turtmann valley (Swiss Alps) – probable controls. *Norwegian Journal of Geography*, 59, 157-163.

3.

Case studies in the European Alps

3.12

Amola rock glacier, Val d’Amola, Italian Alps

Citation reference

Seppi R., Baroni C. Carton A., Dall’Amico M., Rigon R., Zampedri G., Zumiani M. (2011). Chapter 3.12: Case studies in the European Alps – Amola rock glacier, Val d’Amola, Italian Alps. In Kellerer-Pirklbauer A. et al. (eds): *Thermal and geomorphic permafrost response to present and future climate change in the European Alps*. PermaNET project, final report of Action 5.3. ISBN 978-2-903095-58-1, p. 140-150.

Authors

Coordination: Roberto Seppi

Involved project partners and contributors:

- University of Pavia – Roberto Seppi
- University of Pisa – Carlo Baroni
- Mountain-eering srl – Matteo Dall’Amico
- University of Trento – Riccardo Rigon
- Geological Survey, Autonomous Province of Trento – Giorgio Zampedri
- Geologist – Matteo Zumiani

Content

Summary

1. Introduction and study area
2. Permafrost indicators and recent thermal and geomorphic evolution
3. Possible future thermal and geomorphic response to predicted climate change

References

Summary

Topographic measurements are in progress since 2001 on a glacier-derived, active rock glacier (named Amola rock glacier, acronym AmRG, coordinates: 46° 12' 09" N, 10° 42' 46" E) located in the Adamello-Presanella group, Central Italian Alps. In addition, data on the ground temperature measured few centimetres below the surface are available since 2004. The displacement data show that some areas of the rock glacier currently (2001-2009) move with velocities ranging from 10 to 20 cm/year, while other sectors can be defined as "dynamically inactive". The average velocity is significantly variable from year to year, ranging from a minimum of 0.06 m/year (2007-2008) to a maximum of 0.13 m/year (2006-2007), and a slowing trend has been recorded in the last two years. In 2006-2007 a higher rate of displacement seems to be related to a rise in the mean air temperature that probably caused a corresponding rise in the ground temperature. However, in the last year of measurements (2008-2009), an increase in the ground temperature caused by the large amount of snow of the preceding winter, did not result in a corresponding increase of the displacement rate. The dynamic behaviour of this rock glacier reacts very fast to the external forcing, and its response seems to be modulated by the amount and evolution of the snow during winter, due to its effect on the ground temperature. Thus, not only the temperature but also the projected changes in the amount and distribution of precipitation, especially as snow, should be taken into account in assessing the response of this landform to future climate change.

1. Introduction and study area

Active rock glaciers originate from the creep of perennially frozen debris (i.e. permafrost) and move downslope with typical velocities ranging from few cm to more than 1 m per year. The surface displacement of active rock glaciers is markedly variable from year to year, and in the European Alps a recent speeding-up trend has been underlined on some landforms (Roer *et al.* 2005, Haeberli *et al.* 2006, Delaloye *et al.* 2008, PERMOS 2009). The interannual variability of the surface velocity seems to be related to the climatic factors influencing ground surface temperature of the deposits, such as the air temperature, the thickness and duration of the winter snow cover and the processes of water infiltration (Kääb *et al.* 2007, Ikeda *et al.* 2008; Bodin *et al.* 2009)

In 2001 we choose an active rock glacier located in Val d'Amola for performing topographic measurements, in order to study its surface displacement rate and the potential velocity variations (Fig. 1). This rock glacier is one of the active landforms included in the rock glacier inventory of the Adamello-Presanella massif (Baroni *et al.* 2004), where it has the number 51 and is also briefly described. The measurements have been carried out using a laser theodolite and after the first survey have been repeated in the late summer/early autumn of the following years (2002, 2004, 2006, 2007, 2008, 2009). The surveys were conducted every year between early September and mid October. On the surface of the rock glacier, a monitoring network of 25 large boulders marked with steel bolts has been established.

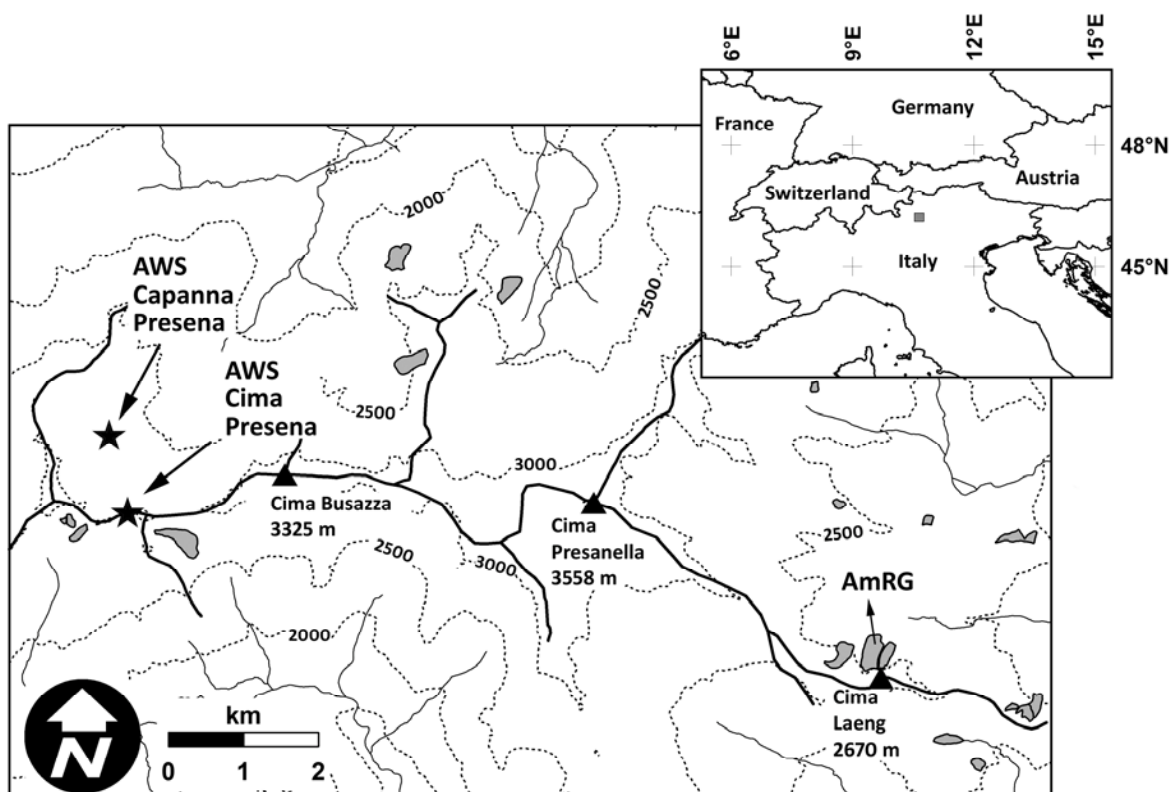


Fig. 1 – Geographical setting of the study area with rock glacier AmRG and automatic weather stations (AWS)

In 2004 we also started to measure the temperature of the ground few centimetres below the surface, using a miniature temperature data logger (UTL1, accuracy: $\pm 0,25^{\circ}\text{C}$; Hoelzle *et al.* 1999) placed in fine-grained debris on the lower part of the rock glacier. The data logger had a malfunction in 2006 and stopped to collect data between March and August 2006. In order to compare the ground temperature with the air temperature and the evolution of the winter snow cover, we used

the meteorological data of two high-altitude automatic weather stations/AWS (Cima Presena AWS, 3015 m a.s.l., and Capanna Presena AWS, 2730 m a.s.l.) located about 10 km from the rock glacier.

AmRG is a tongue-shape rock glacier located in a north facing glacial cirque, between an upper altitude of 2480 m a.s.l. and a lower altitude of 2360 m a.s.l. (top edge of the frontal slope) (Fig. 2). It is about 530 m long and 250 m wide and shows a distinctive set of longitudinal and transversal ridges on its surface. In its intermediate and upper sector, a wide hollow located between two elongated longitudinal ridges is present, while the compressive ridges can be mainly observed in its lower area. The rock glacier surface is mostly composed of matrix-free, large and very angular granite boulders (up to some meters in diameter), while the fine-grained material frequently outcrops not only on the lateral and frontal slopes, but also on the top of the longitudinal and transverse ridges. In the rooting area of the rock glacier, snow patches are present over the whole summer only in the most favourable years (i.e. with a large amounts of snow during the preceding winter).



Fig. 2 – General view of AmRG. The elevation at the front is about 2300 m a.s.l., the highest peaks in the background reach elevations of about 2700 m a.s.l. Photography by R. Seppi (26.09.2009).

Field evidences, confirmed by historical maps, show that a cirque glacier was present in the rooting area of the rock glacier during and after the Little Ice Age. This little glacier is still reported in a 1:75.000 map of 1903, while in more recent maps (e.g 1:25.000 map of 1973) the cirque is indicated without a glacier. The material composing this rock glacier is probably of different origin, but glacial till seems prevailing. Therefore, this landform is developing from glacial deposits and thus can be defined, according to the definition of Barsch (1996), as a debris rock glacier.

Several springs emerge at the base of the frontal slope of MaRG. Beside the other investigations, in 2004 we started to measure the temperature of the water, in order to get additional information on the presence of a frozen core within the rock glacier. The water temperature was measured several times during summer using a hand-held thermometer and continuously from early August to late September 2004 using data loggers (Hobo H8 Temp, accuracy: $\pm 0,4$ °C).

2. Permafrost indicators and recent thermal and geomorphic evolution

The water temperature that was monitored continuously in late summer 2004 showed very cold values (below 1°C). Therefore, this data support the presence of permafrost in the rock glacier (Fig. 3).

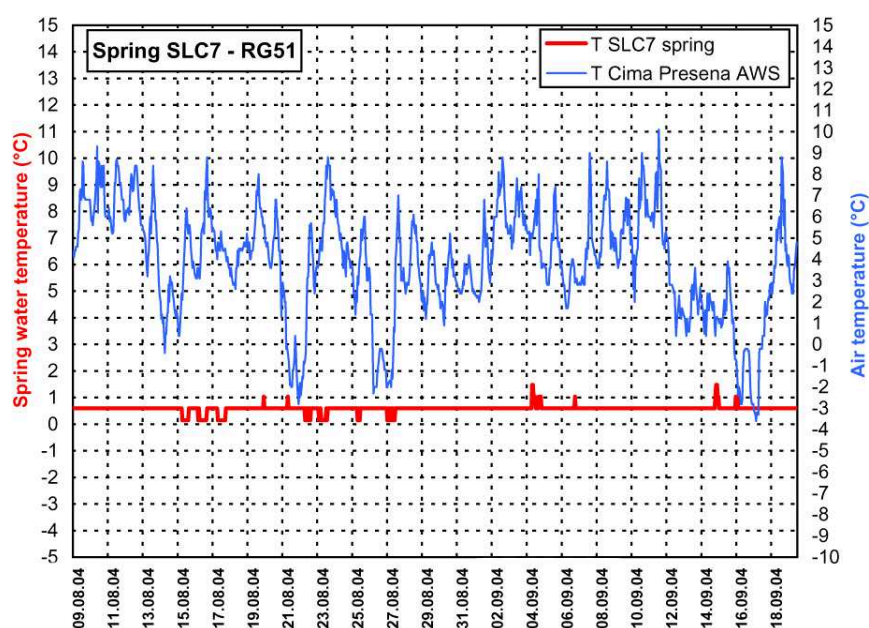


Fig. 3 – Water temperature of a spring (SLC7) emerging from AmRG continuously measured between August and September 2004. The location of the spring is indicated in Fig. 4.

The total displacement (2001-2009) of AmRG ranges between 0.05 m (boulder 9) and 1.60 m (boulder 15), corresponding to a velocity of 0.01 and 0.20 m/year, respectively (Fig. 4 and Tab. 1). The frontal area of this rock glacier shows a very different behaviour, with an active sector (boulders 1 to 6) close to a sector that can be regarded as dynamically inactive (boulders 7 to 11). Similarly, the right side of the rock glacier (boulders 12 to 20) is more active than the middle and the left sectors (boulders 21 to 25). The surveyed boulders located on the longitudinal ridge move toward the centre of the landform, where a wide hollow is present.

The mean displacement of AmRG in all interval of measurements is shown in Figure 8 (top graph), where all the surveyed points have been taken into account. The average velocity is significantly variable from year to year, ranging from a minimum of 0,06 m/year (2007-2008) to a maximum of 0,13 m/year (2006-2007). A slowing trend seems to emerge in the last two years of measurements.

The near-surface temperature of the ground recorded on AmRG from August 2004 to August 2009 is shown in Fig. 5 (bottom graph). In this graph, the ground temperature (daily mean) is associated to the air temperature (central graph) and to the thickness of the snow cover (top graph).

Table 1 – Horizontal displacement of AmRG. The first six columns show the displacement for each period of measurements, the column seven the total displacement, and the column eight the displacement rate. (*) Measurement period of two years.

Boulder ID	Horizontal displacement (m)						2001-09 total horizontal displacement (m)	2001-09 horizontal displacement rate (m/yr)
	2001-02	2002-04(*)	2004-06(*)	2006-07	2007-08	2008-09		
01	0.13	40.42	17.83	0.17	0.09	0.10	1.08	0.13
02	0.13	39.59	9.61	0.12	0.08	0.10	0.93	0.12
03	0.15	39.05	13.58	0.14	0.06	0.09	0.97	0.12
04	0.12	34.71	12.50	0.12	0.08	0.06	0.85	0.11
05	0.06	19.33	6.74	0.08	0.06	0.11	0.57	0.07
06	0.05	9.10	3.70	0.07	0.02	0.01	0.28	0.03
07	0.02	10.55	0.00	0.09	0.01	0.00	0.16	0.02
08	0.04	6.08	0.00	0.06	0.00	0.01	0.13	0.02
09	0.04	3.23	0.00	0.07	0.00	0.01	0.05	0.01
10	0.04	14.80	0.87	0.06	0.00	0.06	0.32	0.04
11	0.02	0.00	5.90	0.08	0.00	0.00	0.08	0.01
12	0.07	25.56	10.75	0.13	0.04	0.10	0.71	0.09
13	0.13	36.30	25.13	0.21	0.11	0.17	1.23	0.15
14	0.11	36.44	23.37	0.22	0.13	0.25	1.30	0.16
15	0.16	39.15	39.09	0.36	0.19	0.10	1.60	0.20
16	0.04	15.26	6.88	0.13	0.02	0.00	0.39	0.05
17	0.07	24.13	17.22	0.21	0.05	0.02	0.76	0.10
18	0.04	18.79	5.97	0.16	0.02	0.04	0.51	0.06
19	0.15	32.93	31.83	0.34	0.18	0.00	1.31	0.16
20	0.07	24.89	10.23	0.07	0.05	0.14	0.69	0.09
21	0.08	19.96	8.94	0.13	0.05	0.03	0.58	0.07
22	0.04	12.59	4.91	0.05	0.02	0.07	0.36	0.04
23	0.06	23.01	5.15	0.06	0.05	0.07	0.53	0.07
24	0.04	15.25	0.03	0.10	0.04	0.00	0.29	0.04
25	0.04	13.15	0.00	0.09	0.03	0.00	0.28	0.03

Focusing on the winters the coldest temperatures were recorded in the 2004-2005 and 2005-2006 seasons. During both winters, the ground reached temperatures below -10°C . The strong cooling of the ground may be due to the combined effect of cold air temperature and relatively thin snowpack in autumn and early winter. In the two following winters (2006-2007 and 2007-2008), the ground temperature was warmer, with a marked phase of WEqT (Winter Equilibrium Temperature) of about -5°C . The winter 2006-2007 was very mild and the snowpack was relatively thin until mid winter, while the following winter (2007-2008) was colder and snowier.

The highest winter temperatures were recorded during the 2008-2009 season and reached a WEqT phase of about -3°C . This was mainly due to the presence of a very thick snow cover, which appeared early in autumn and further increased in the following winter months. The snow, with its thermal insulating effect, prevented the cooling of the ground already in the first part of the winter, while the air temperature was not particularly mild compared to the preceding winters. This underlines the strong control of the snow cover on the winter temperature of the ground and, consequently, on the mean annual ground temperature.

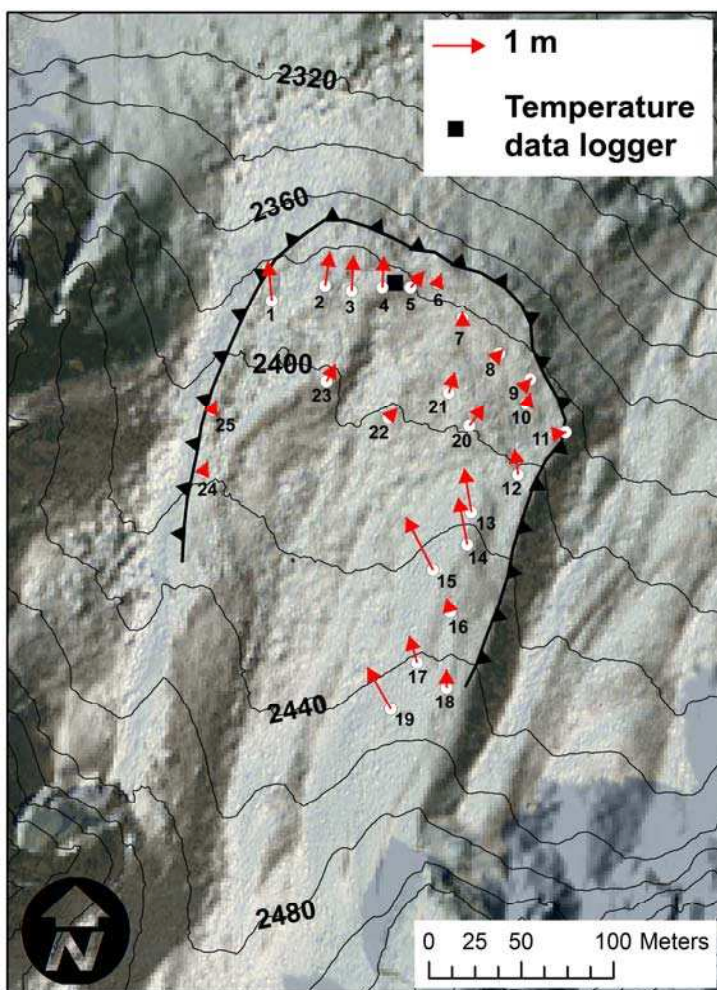


Fig. 4 – Total horizontal displacement (2001-2009) of AmRG. The location of the spring mentioned in Fig. 3 is indicated.

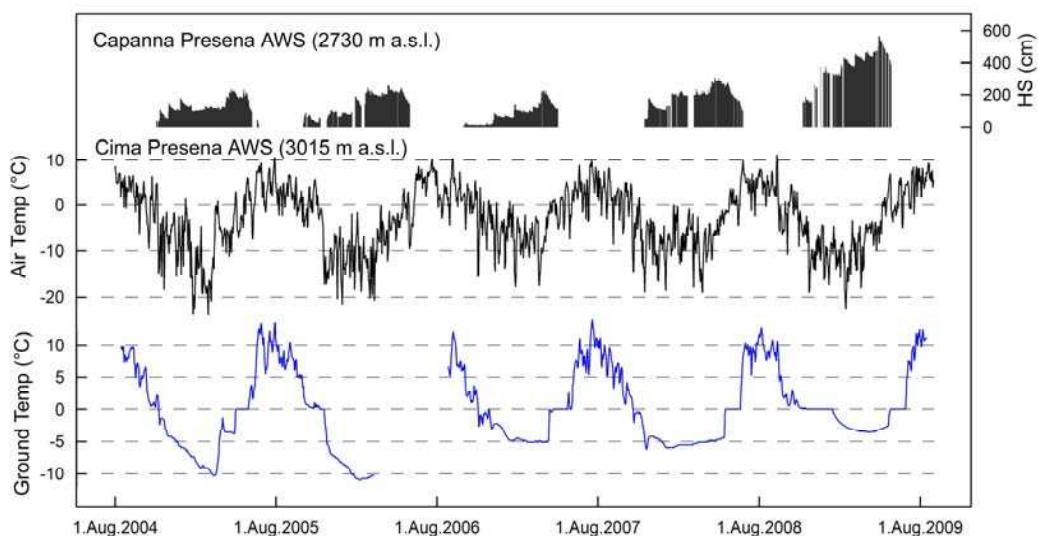


Fig. 5 – Top and middle graphs: snow thickness and air temperature at Capanna Presena automatic weather station; bottom graph: ground near-surface temperature from August 2004 to August 2009 for AmRG. The lack of data in the first half of 2006 was due to a data logger failure. For location of temperature data logger see Fig. 4.

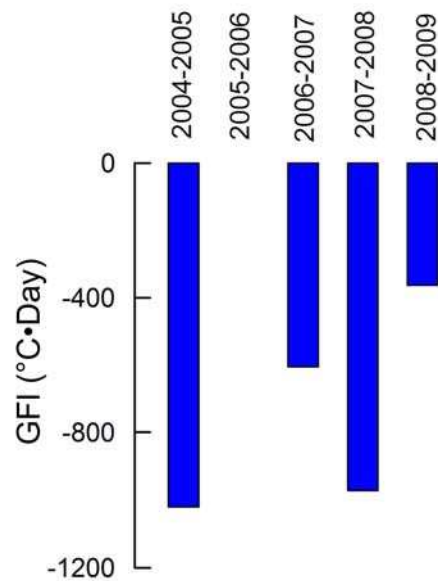


Fig. 6 – Annual ground freezing index (GFI) at AmRG from 2004 to 2009. No data were available for the 2005-2006 period.

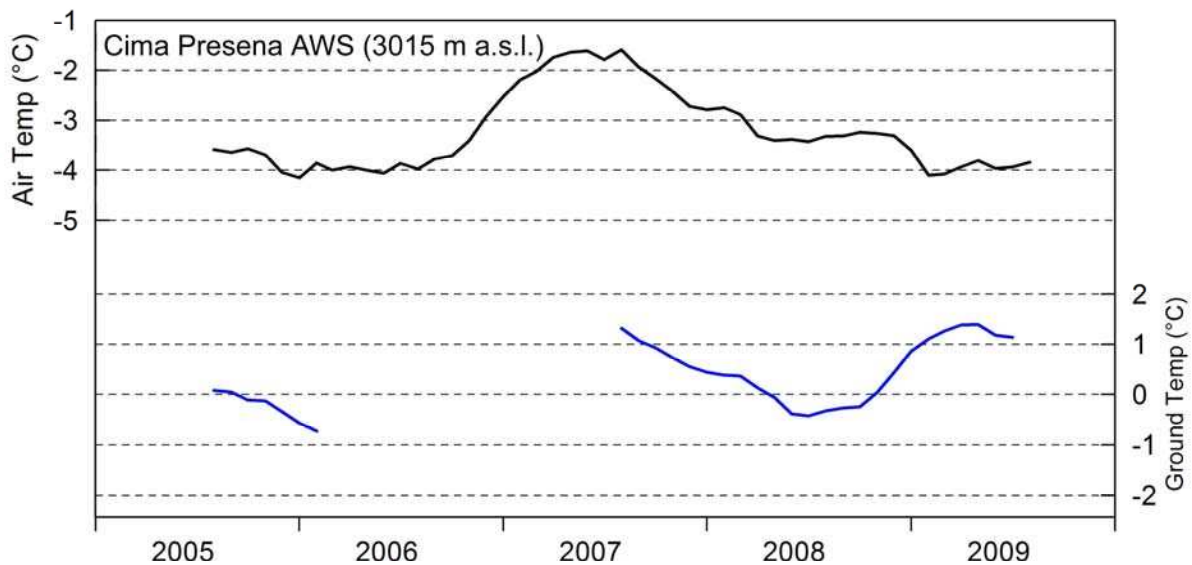


Fig. 7 – Evolution of the mean annual air temperature at Cima Presena automatic weather station (top graph) and of the near-surface ground temperature at AmRG (bottom graph). All the temperatures are displayed as 12-months running means, and the date on the x-axis corresponds to the end of the period used for the calculation.

The cooling of the ground during the winter season is also highlighted by the Ground Freezing Index (GFI), calculated as the cumulative value of the negative daily mean ground temperatures between 1st October and 30th June (Fig. 6). The coldest winter (-1020°C-day) was recorded in 2004-2005 due to a combination of very cold air temperature and relatively thin snow cover. The index was also very

low in the winter 2007-2008 ($-972^{\circ}\text{C}\cdot\text{day}$), as a result of the strong cooling of the ground at the beginning of the winter due to cold air temperature during autumn and early winter. A very high GFI value ($-360^{\circ}\text{C}\cdot\text{day}$) was recorded in 2008-2009, mainly due to the very thick snow cover of that winter.

The role of the winter snow cover on the ground temperature can also be observed in Fig. 7, where the evolution of the mean annual air temperature (MAAT) at Cima Presena AWS and the evolution of the MAGST are compared on the same period of time. The temperatures are displayed as 12-months running means, and the date on the x-axis corresponds to the end of the period used for the calculation. Ground temperature data are missing in 2006 and 2007 because of the failure of the data logger. For example, a strong warming of the ground in 2009 (temperatures above 1°C) and a clear separation between the temperature trends of soil and air can be observed. This is due more to the effect of the thick snow cover of the previous winter than to a corresponding warming of the air temperature.

Finally, in Fig. 8 the mean annual displacement rate is compared with the mean annual temperature of the ground and the air. In order to emphasize the role of the winter seasons, the values of the mean annual temperature (both for the ground and for the air) have been calculated taking into account an annual basis extending from the 15th August of the previous year to the 14th August of the following year. For this reason, an extremely warm summer like 2003 is not as well perceptible in the data record as a mild winter like 2006-2007. The ground temperature data are missing for 2005-2006 and 2006-2007.

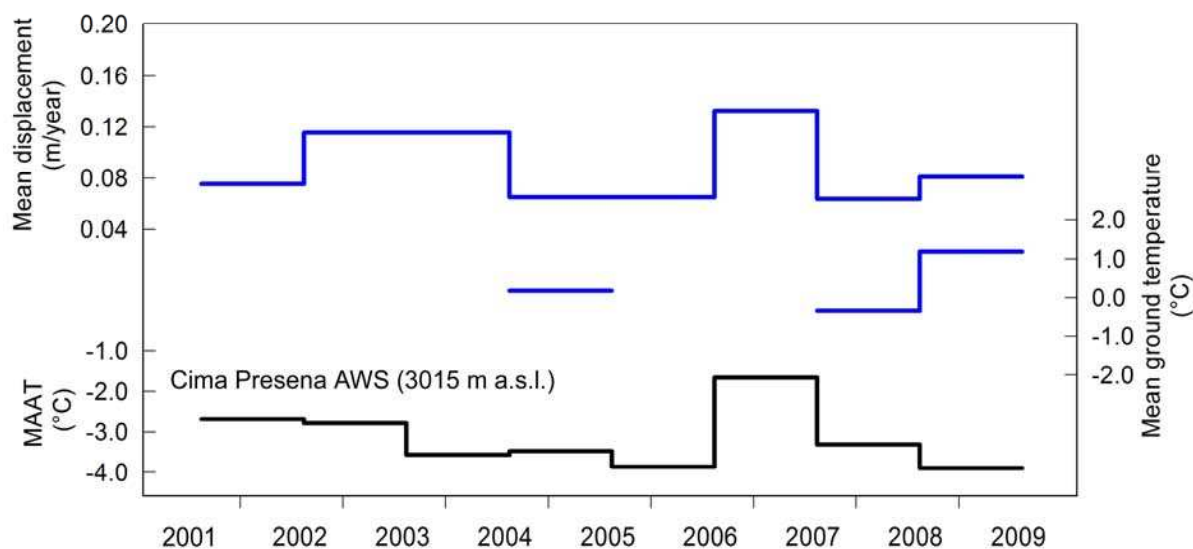


Fig. 8 – Mean displacement of AmRG (top graph) compared with the mean annual ground temperature (middle graph) and the mean annual air temperature at Cima Presena automatic weather station (bottom graph).

In 2006-2007, an increase in the displacement rate corresponds quite well with a higher air temperature compared to the preceding year. In the following year, the displacement rate decreased considerably, in good agreement with a lower air temperature. In the last year of measurements (2008-2009), the displacement rate was only slightly higher and the mean air temperature somewhat lower than in the preceding year. In the same year, a significant increase in the ground temperature due to the large amount of snow (see above) was recorded, but this does not seem to have resulted in an increase of the displacement rate.

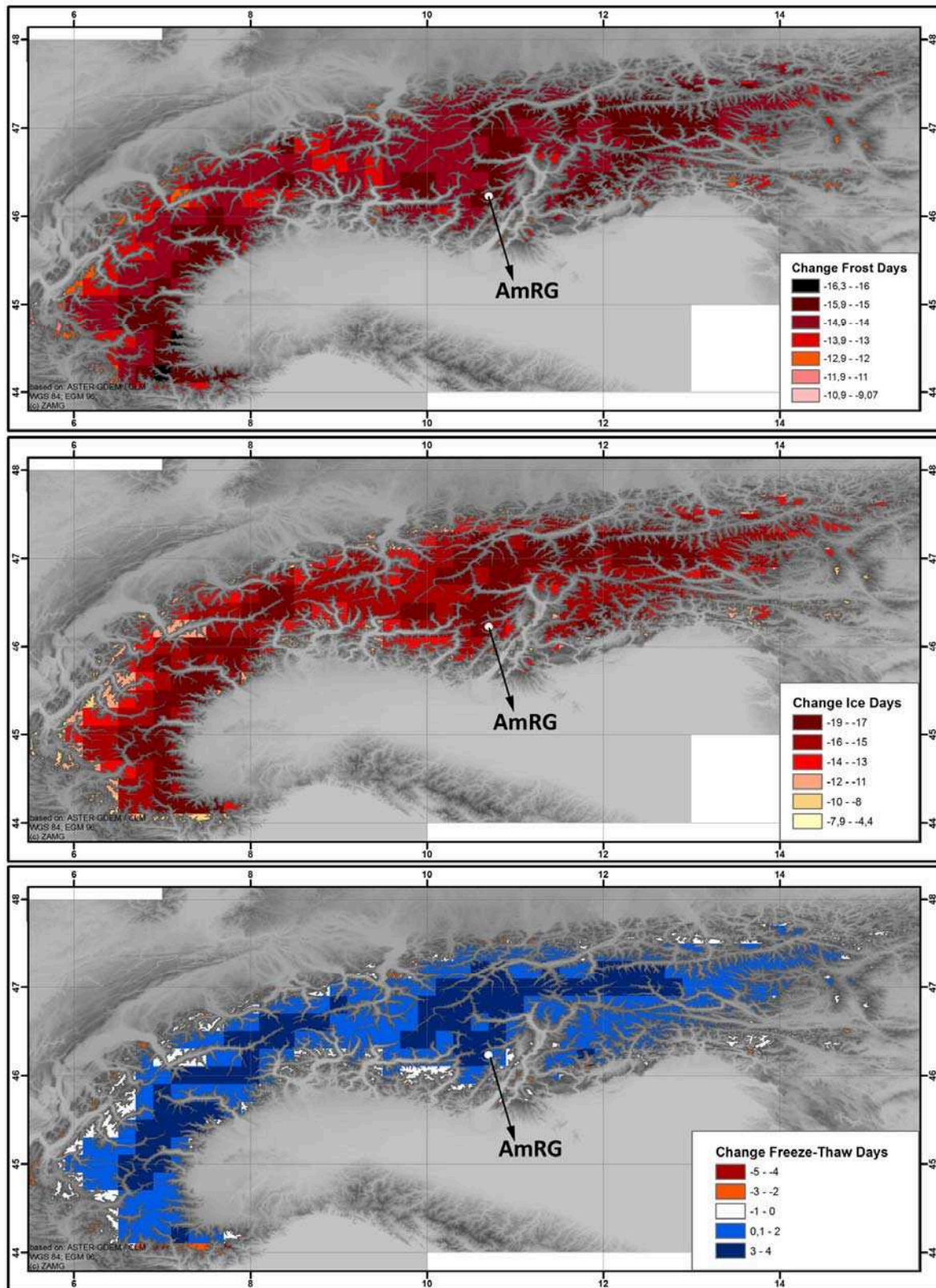


Fig. 9 – Potential change of frost, ice and freeze-thaw days for 2020-2050, as proposed in chapter 2. The location of AmRG is shown.

3. Possible future thermal and geomorphic response to predicted climate change

Future evolution and geomorphic response of AmRG to climate change are difficult to hypothesize. As reported in chapter 2, not only changes in the temperature for the end of the 21st century (a warming of 4.2°C in the alpine areas above 1800 m a.s.l.), but also significant changes in the number of frost, ice and freeze-thaw days for the period 2021-2050 can be expected. According to this, in the area where AmRG is located, we expect a decrease in the frost days of 15/16 days/year, a decrease in the ice days of 15/19 days/year and a slight increase in the freeze-thaw days of 0/4 days/year (Fig. 9). As highlighted above, the dynamic response of AmRG seems to be related to the changes in the amount and evolution of the snow during winter, due to its effect on the ground temperature. Thus also the future changes in the amount and distribution of precipitations, especially as snow, should be taken into account in assessing the response of this landform to future climate change.

Acknowledgements. – Mauro Degasperi and Franco Crippa (Geological Survey, Autonomous Province of Trento) conducted the topographic surveys and processed the rough topographic data. Field collaboration was provided by Luca Carturan, Stefano Fontana and Andrea Paoli. This work was partly funded by the PRIN 2008 project “Climate Change effects on glaciers, on glacier-derived water resource and on permafrost. Quantification of the ongoing variations in the Italian Alps”.

References:

- Baroni C., Carton A. & Seppi R., 2004: Distribution and behaviour of rock glaciers in the Adamello-Presanella Massif (Italian Alps). *Permafrost and Periglacial Processes*, 15, 243-259.
- Barsch D., 1996: *Rockglaciers: Indicators for the Present and Former geocology in High Mountain Environments*. Springer, Berlin, 331 pp.
- Bodin X., Thibert E., Fabre D. Ribolini A., Schoeneich P, Francou B., Louis Reynaud L. & Fort M., 2009: Two Decades of Responses (1986–2006) to Climate by the Laurichard Rock Glacier, French Alps. *Permafrost and Periglacial Processes*, 20, 331-344.
- Delaloye R., Perruchoud E., Avian M., Kaufmann V., Bodin X., Ikeda A., Hausmann H., Käab A., Kellerer-Pirklbauer A., Krainer K., Lambiel C., Mihajlovic D., Staub B., Roer I. & Thibert E., 2008: Recent interannual variations of rock glaciers creep in the European Alps. *Proceedings of the 9th International Conference on Permafrost (NICOP)*, University of Alaska, Fairbanks, June 29 – July 3, 2008, 343-348.
- Haeberli W., Hallet B., Arenson L., Elconin R., Humlum O., Kaab A., Kaufmann V., Ladanyi B., Matsuoka N., Springman S. & Vonder Mühll D., 2006: Permafrost creep and rock glacier dynamics. *Permafrost and Periglacial Processes*, 17, 189-214.
- Hoelzle M., Wegmann M. & Krummenacher B., 1999: Miniature temperature dataloggers for mapping and monitoring of permafrost in high mountain areas: first experience from the Swiss Alps. *Permafrost and Periglacial Processes*, 10, 113-124.
- Käab A., Frauenfelder R. & Roer I., 2007: On the response of rockglacier creep to surface temperature increase. *Global and Planetary Change*, 56, 172-187.
- Ikeda A., Matsuoka N. & Käab A., 2008: Fast deformation of perennially frozen debris in a warm rock glacier in the Swiss Alps: An effect of liquid water. *Journal of Geophysical Research* 113, F01021.
- PERMOS, 2009: Permafrost in Switzerland 2004/2005 and 2005/2006. Noetzli, J., Naegeli, B., and Vonder Muehll, D. (eds.), *Glaciological Report Permafrost No. 6/7 of the Cryospheric Commission of the Swiss Academy of Sciences*, 100 pp.
- Roer I., Käab A. & Dikau R., 2005: Rockglacier acceleration in the Turtmann valley (Swiss Alps) – probable controls. *Norwegian Journal of Geography*, 59, 157-163.

3.

Case studies in the European Alps

3.13

Piz Boè rock glacier, Dolomites, Eastern Italian Alps

Citation reference

A. Crepaz A., Cagnati A., Galuppo A., Carollo F., Marinoni F., Magnabosco L., Defendi V. (2011). Chapter 3.13: Case studies in the European Alps – Piz Boè rock glacier, Dolomites, Eastern Italian Alps. In Kellerer-Pirklbauer A. et al. (eds): *Thermal and geomorphic permafrost response to present and future climate change in the European Alps*. PermaNET project, final report of Action 5.3. On-line publication ISBN 978-2-903095-58-1, p. 151-158.

Authors

Coordination: Andrea Crepaz

Involved project partners and contributors:

- Regional Agency for the Environmental Protection of Veneto, Italy (ARPAV) – Andrea Crepaz, Anselmo Cagnati
- Regione Veneto, Direzione Geologia e Georisorse, Servizio Geologico (GeoVE) – Anna Galuppo, Laura Magnabosco, Valentina Defendi
- E.P.C. European Project Consulting S.r.l. – Federico Carollo
- Freelancer – Francesco Marinoni

Content

Summary

1. Introduction and study area
2. Permafrost indicators and recent thermal evolution
3. Possible future thermal response to predicted climate change

References

Summary

Recently, ARPAV in collaboration with GeoVE started to monitor the periglacial environment of Piz Boè (46.51° N, 11.83° E), in Veneto region, at an altitude of 2900 m a.s.l. In the past, some preliminary geoelectrical and geoseismic surveys were carried out on the rock glacier, but only in the framework of the PermaNET project the characteristics of the permafrost are extensively studied. Continuous GST (Ground surface temperature) measurements were carried out in the winter 2009/2010; a 30 m deep borehole was drilled in Dolomite bedrock and an automatic weather station was installed in summer 2010. Later we planned to carry out a second electrical resistivity tomography (ERT) campaign (first one in 2005) on the rock glacier. In this report we present the first results on the comparison of ERT measurements carried out in 2005 and 2010. The data comparison does not show significant changes in the structure of the ice covered with debris during the last five years. In particular, it seems that the covered ice did neither modify its consistence nor its extent. Due to the short monitoring time and the lack of other experimental data on the Piz Boè site, it is very difficult to explain its future behaviour. ARPAV manages also a broad weather station network on Veneto mountain region, so the highest station data (Ra Vales) was used to make some analysis of the last years. For the next century climate models estimate a dramatic increase of air temperature. This condition will directly influence the thickness, the extension and the displacement of the rock glacier at Piz Boè.

1. Introduction and study area

The Piz Boè site is located in the North-East of Italy (46.51°N, 11.83°E; Fig. 1), on the border of Veneto region, at 2900 m a.s.l. on the Sella Group, near Piz Boè peak (Fig 2). The Sella Group represents one of the most important massifs of the Dolomites. Its base is constituted by the “Dolomia dello Sciliar” Formation (Ladinian-Lower Carnian). The thickness of this non-stratified coral reef varies from 300 to 600 m. The top of the massif is made up by “Dolomia Principale” (Norian). The geological boundary between the two above mentioned formations is very clear and marked by layers of marls and clays of the “Raibl Formation” (Carnian). The white/clear grey Dolomia Principale Formation is well stratified and its thickness reaches its maximum (300-350 m) at Piz Boè, where it is covered by the most recent “Calcarei di Dachstein” (Lias), nodular limestones of the “Rosso Ammonitico” Formation (Jurassic) and “Marne del Puez” Formation (Lower Cretaceous).

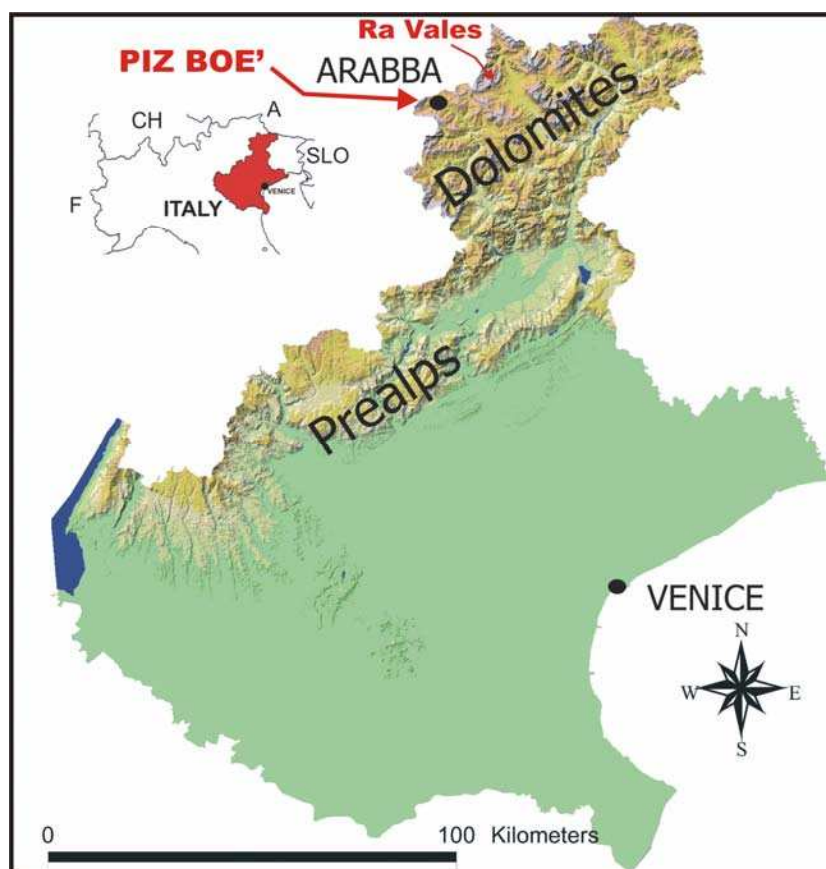


Fig. 1 – Geographical setting of Veneto region and Piz Boè in the Dolomites, Eastern Italian Alps

At North-East of the peak Piz Boè there was a glacier, listed in 1980's campaign survey with about a surface of 0.04 km². Nowadays the glaciated area is very limited (about 0.014 km²), but a debris covered glacier (in some maps it is considered a rock glacier) has been formed below the glacier. At the bottom of the debris there is a small shallow lake (Lech Dlacé, Fig. 3), which is completely covered by snow and ice in the most part of the year over (November to June).



Fig. 2 – Sella Group and Piz Boè (3151 m a.s.l.) from East (Livinallongo). Location of the study site is indicated with an arrow. Photograph by Bruno Renon (ARPAV) (30.07.2008).

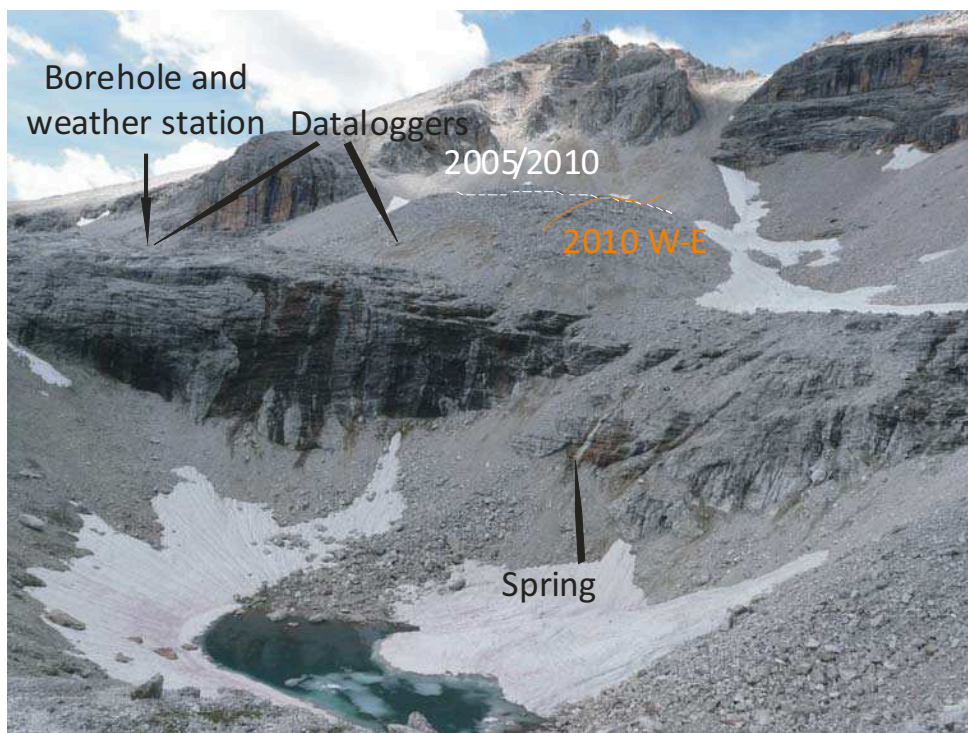


Fig. 3 – View towards South-West of the lake Lech Dlacé and the rock glacier of Piz Boè with the location of the borehole and the weather station, dataloggers, ERT profiles and the spring. Elevation of the lake is 2833 m a.s.l., elevation of the peak in the background (Piz Boè) is 3151 m a.s.l. Note the widespread appearance of late-lying snow patches. Photograph by Bruno Renon (ARPAV) (30.07.2008).

2. Permafrost indicators and recent thermal evolution

2.1 Methods

In July 2010 a borehole was drilled into the bedrock down to a depth of 30 m and a thermistor chain of 16 sensors (at 0.02, 0.3, 0.6, 1.0, 1.5, 2.0, 3.0, 3.5, 4.5, 5.5, 10.0, 15.0, 20.0, 25.0, 30.0 m from the surface) was placed to measure the ground temperatures. In September 2010 a weather station was installed at the location indicated in fig. 3; it measures air temperature, relative humidity, snowpack height, wind direction and velocity, incoming and outgoing (shortwave and longwave) radiation.

During Summer 2010 water samples were collected from the spring coming out from the rock glacier and from the Lech Dlacé with a temporal resolution of about 15 days, in order to evaluate chemical composition and its relative seasonal changes; water temperatures were measured as well.

Since October 2009 two dataloggers (Hobo Pro V2 U23-001, Onset Computer Corp.), logging every 30 minutes, have been placed near Piz Boè rock glacier in order to measure the ground surface temperature. The first one was put on the rock glacier front and the second one outside of the rock glacier, below the front, where the weather station was planned to be installed in September 2010 (see Fig. 3 for location). They were recovered in the melting season in July 2010. At the end of October, one datalogger was replaced in the same previous site, a few centimeters below the surface of the rock glacier, while the other one, outside of the rock glacier, was moved about 30 m towards South-East.

During the summer 2005 a detailed topographic survey was carried out and in the summer 2010 a Laser Scanner survey was performed by IRPI CNR.

The study area was furthermore investigated on 01.09.2010 by performing an electrical resistivity profile (ERT) of 124 m, using the device electrode Wenner-Schlumberger with a distance between the electrodes equal to 4 m and maximum depth of exploration of 25 m. The inversion of geoelectrical tomographic data was performed using the method proposed by LaBreque *et al.* (1996), using a finite element algorithm based on the concept of reverse OCAM'S (Oldenburg, 1994) and implemented in software PROFILER (Binely, 2003). The configuration was comparable to the one of the ERT campaign on 04.08.2005, the length of which was 141 m.

2.2 Results on current permafrost existence

Fig. 4 shows the measured temperatures during the period 09.10.2009 and 02.07.2010 also depicting some significant events. On 22nd October the first snowfall occurred (about 5-10 cm of fresh snow), melting the following days. The next significant snowfall occurred at the beginning of November with about 50-60 cm of fresh snow; this part of snow pack remained all the winter, even though at the end of November the air temperature increased with freezing level at about 3200-3500 m. During all the winter, ground surface temperatures remained at about -4 to -2°C. In February, March and part of April GST was about -4°C in both sites (winter equilibrium temperature – WeqT). At the end of April on the rock glacier zero curtain was reached, while on the monitoring site temperatures remained below 0°C, except on 29th April when temperatures increased up to 0°C. On 17th May 2010 a snow pit was dug on the monitoring site and a bottom temperature of snow cover (BTS) of -1.5°C was measured (datalogger values were around -1.7°C). Zero curtain on the bedrock started on 11th June, while on the rock glacier snow was already completely melted; at the beginning of July the datalogger on the bedrock was buried in a melting ice layer.

These temperature results indicate the possible presence of permafrost on the bedrock and on the debris, where in 2005 ERT measurements were performed, as well. In summer 2010, the ERT measurements were repeated along the same section and the investigation was extended to a new orthogonal W-E oriented transect, along the maximum slope gradient. In this work we compare the profiles carried out in 2005 and 2010 along the same section.

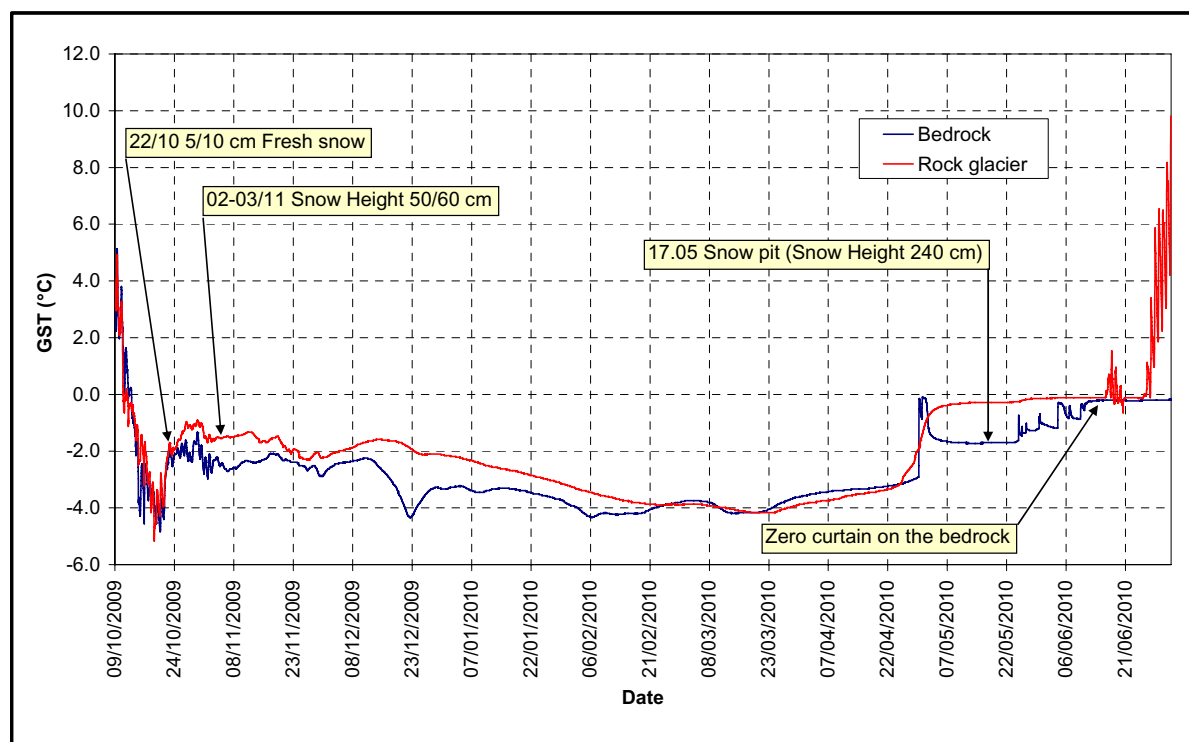


Fig. 4 – Evolution of the ground surface temperature between 09.10.2009 and 02.07.2010. In red GST from the rock glacier, in blue from the site of the planned borehole.

The two-dimensional model obtained by inversion of apparent resistivity data (Fig. 5) returns the actual distribution of values of resistivity in the subsurface; it is highlighted both by isolines and by colour scale. The first contour has been traced to a value of $5 \cdot 10^4 \Omega \cdot \text{m}$. The second isoline is $1 \cdot 10^5 \Omega \cdot \text{m}$, while the subsequent ones are placed at intervals of $2 \cdot 10^5 \Omega \cdot \text{m}$ up to the value of $1 \cdot 10^6 \Omega \cdot \text{m}$; for higher resistivity the spacing between the iso-resistive lines is higher.

Highest resistivity values (above $1.5 \cdot 10^6 \Omega \cdot \text{m}$) might be related to massive ice; values between $1 \cdot 10^5 \Omega \cdot \text{m}$ and $1.5 \cdot 10^6 \Omega \cdot \text{m}$ should correspond to ice mixed with boulders, while lower values ($5 \cdot 10^4 \Omega \cdot \text{m} < \rho < 1 \cdot 10^5 \Omega \cdot \text{m}$) might detect the active layer.

Comparing the two profiles we can make the following observations. The geometry of the body at very high resistivity is similar in the two sections. At 2940 m altitude a.s.l., the width of the anomaly resistive ($\rho > 1.5 \times 10^6 \Omega \cdot \text{m}$) is approximately equal to 99 m. The surface material layer (about 2 m of boulders mixed to fine grained debris) shows more or less the same thickness in both profiles ($\rho < 5 \cdot 10^4$).

The thickness of the rock glacier is more or less the same, greater than 23 m in both cases. In both profiles the maximum depth of investigation was not sufficient to achieve resistance values attributable to the bedrock. The analysis of the two sections also shows the limited differences in the pattern of deeper sections; in the section of the 2005 iso-resistive lines remain open on values ranging from 1.5 to $5 \cdot 10^6 \Omega \cdot \text{m}$, while in the section of 2010 they reach values close to $2 \cdot 10^6 \Omega \cdot \text{m}$. These differences are not significant because the slight discrepancy in the positioning of two profiles on the ground and high difference of resistivity on surface layer, which may affect, in part, the results of the reverse processes.

The section of 2005 showed a difference in the resistive body, with two anomalies at very high resistivity ($\rho > 4 \times 10^6 \Omega \cdot \text{m}$), separated by a strip with slightly lower resistivity ($\rho = 1.5 \times 10^6 \Omega \cdot \text{m}$). The

section of 2010 shows these two anomalies, too, but their separation is more weakened. Also this difference can be explained in part with the considerations listed above.

We can conclude that these two profiles are very similar and that the slight differences are mainly attributable to the method uncertainty.

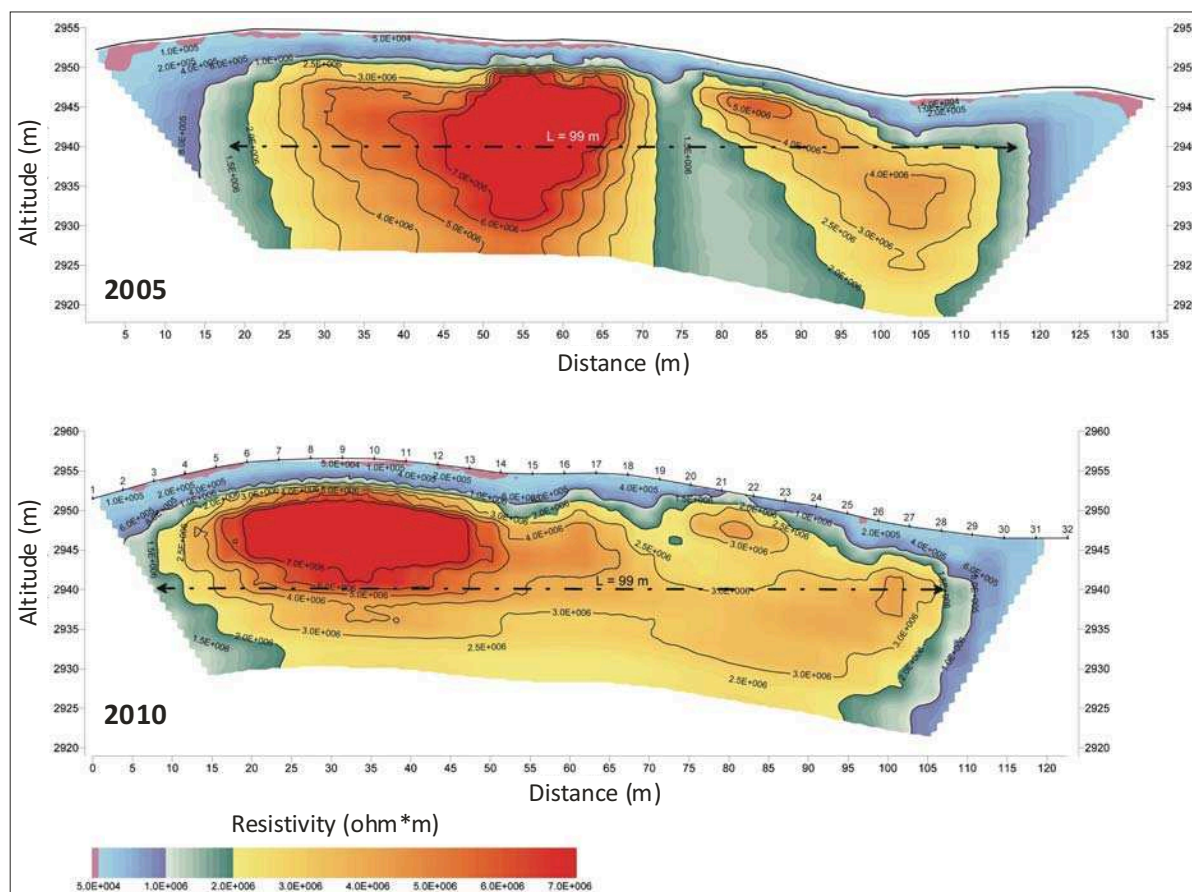


Fig. 5 – Results of the electrical tomography (ERT) campaigns on 04.08.2005 and 01.09.2010.

3. Possible future thermal response to predicted climate change

The Piz Boè rock glacier is monitored since 2005. From 2005 to 2010 no air temperatures data are available because the weather station was not installed before September 2010. However, time series of both air temperature (until 2009) and snow height is available for Ra Vales station, at 2615 m a.s.l., about 19 km to the East-North-East of Piz Boè.

Taking into account the last ten years (Table 1); the first period (2000-2005) seems to be colder than the last one (2005-2010). MAAT was significant lower all the years, while it increased in the last five years, when values were above 0°C in 2006, 2007 and 2008. The number of frost and ice days decreased in the last years. Snow cover duration is similar during these two periods. A little difference can be observed in June; in the last three years snow cover duration was longer in the early summer, while in 2000-2005 some years were characterized by a total absence of snow cover. Winter snow height was not so high in 2005-2008, while in the last two years snow amount was higher.

Table 1 – Different temperature derived parameters from the meteorological station Ra Vales (2615 m a.s.l.) 19 km to the East-North-East of Biz Poè (DSC=days with snow cover; MAAT=mean annual air temperature; JJA=June-July-August).

Ra Vales	2000	2001	2002	2003	2004	2005	2006	2007	2008	2009	2010
Frost days	221	239	238	225	233	229	218	202	215	211	247
Ice days	141	140	131	137	134	133	110	104	120	138	157
Freeze/Thaw days	80	99	107	88	99	96	108	98	95	73	90
Days of Snow cover	173	255	265	240	166	248	207	231	247	235	266
June DSC	0	30	17	0	30	1	12	6	22	20	23
MAAT	-0.38	-0.89	-0.30	-0.14	-0.97	-1.46	0.10	0.94	0.51	-0.06	-2.13
JJA Mean Air Temp	6.10	6.28	6.55	9.08	5.95	5.66	5.99	6.94	7.26	7.23	6.36

Summer mean temperature (JJA) seems to increase during the last ten years with a peak in 2003; this very hot summer certainly influenced the melting of the seasonal snowpack and of the ice as well. The last year (2010) was the coldest one of the last eleven, with a very long snow cover duration; this might have significantly influenced ERT profile of the 2010. This meteorological behaviour allowed a quasi-steady situation for the debris covered glacier of Piz Boè in the last five years.

Climate models show a dramatic air temperatures increase for the next century (see chapter 2), especially at high altitudes, and this will certainly influence covered ice. In the next decades, according to SRES A1B, frost and ice days will decrease by about 14-15 days. Covered ice will likely melt quickly during the next decades and the displacement of ice will increase. The more important factors that will determine the velocity of melting and displacement, will be the summer temperatures and snow cover duration in the early summer. During the next years ARPAV is going to investigate the future evolution of permafrost at Piz Boè.

Acknowledgements. – The authors thank Abu Zeid Nasser for his work during field campaign.

References:

- Binely A., 2003: *2D inversion of apparent resistivity data using "Profiler"*. Institute of Environmental and Natural Sciences, Lancaster University, LANCASTER, UK. 6 pp.
- LaBreque D.J., Miletto M., Daily W., Ramirez A., Owen E., 1996: The effects of noise on Occam's inversion of resistivity tomography data. *Geophysics*, 61, 538-548.
- Oldenburg D., L. Y., 1994: Inversion of induced polarization data. *Geophysics*, 59, 9: 1327.

3.

Case studies in the European Alps

3.14

Upper Sulden Valley, Ortler Mountains, Italian Alps

Citation reference

Zischg A., Mair V. (2011). Chapter 3.14: Case studies in the European Alps – Upper Sulden Valley, Ortler Mountains, Italian Alps. In Kellerer-Pirklbauer A. et al. (eds): *Thermal and geomorphic permafrost response to present and future climate change in the European Alps*. PermaNET project, final report of Action 5.3. On-line publication ISBN 978-2-903095-58-1, p. 159-169.

Authors

Coordination: Andreas Zischg

Involved project partners and contributors:

- Abenis Alpinexpert GmbH/srl – Andreas Zischg
- Autonomous Province of Bolzano - South Tyrol, Office for Geology and Building Materials Testing (GeoLAB) – Volkmar Mair

Content

Summary

1. Introduction and study area
2. Permafrost indicators and recent thermal and geomorphic evolution
3. Possible future thermal response to predicted climate change

References

Summary

The case study from the Upper Sulden Valley (46°29'37.87"N, 10°36'57.31"E), Ortler Mountains, Italian Alps, showed the geomorphic response of flat or gently inclined areas covered by debris in a high-mountain ski resort outside of rock glaciers. The subsidence of the surface due to the melting of the ground ice lies in a dimension of 4 m in 11 years (1996-2006). The measured surface subsidence is accompanied with geomorphic signs such as thermokarst phenomena or with increasing surface temperatures. In steeper areas, geomorphic signs of slope movements are found in areas with probable presence of permafrost. The subsidence of surface is relevant for ski infrastructures and must be handled with some technical effort. In the vicinity of the pillar no. 12 of the ski lift *Madritschjoch*, most probably the ground ice has melted totally. Therefore, the subsidence process of the surface near the pillar is finished. However, this can be concluded only for this specific location in the study area. In other areas where ground ice is still present, the degradation process will continue with the expected increase of temperatures.

1. Introduction and study area

The study area is situated in the ski resort "Sulden-Madritsch" in the Upper Sulden Valley, community of Stilfs/Stelvio, Autonomous Province of Bozen/Bolzano (46°29'37.87"N, 10°36'57.31"E, Figs. 1, 2 and 3). The study area is situated in the Ortler mountain range near the Stilfserjoch pass. The extent of the study area is about 5 km². The area is mostly free of vegetation and is partially covered by debris. One small rock glacier is situated in the study area. During the period between 1805 and 1850, parts of the area were covered by a small glacier.

In the early 1990s, a team of the University of Munich began its first permafrost investigations in this area (Stötter 1994). In 1992 first measurements of the temperatures at the bottom of the snow cover (BTS), topographic surveys and geophysical measurements (seismics) for mapping the permafrost distribution had been made. Since 2004, the BTS measurements have been repeated in the years 2004, 2006, 2007, 2008 and 2009. BTS measurements were carried out at more than 1100 points in the study area. Since 2006, devices for measuring the ground surface temperatures (UTL dataloggers) were installed on 10 locations in the study area.

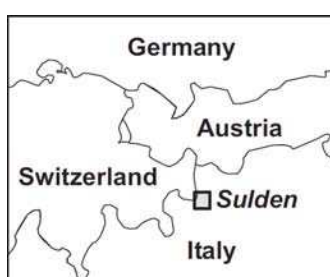


Fig. 1 – Location of the study area Upper Sulden Valley.



Fig. 2 – Overview of the study area Upper Sulden Valley. Photograph taken from the upper station of the "Madritschjoch" ski lift located at 3150 m a.s.l. Photograph by A. Zischg (09.03.2007). The study area is the ski resort in the foreground of the picture.

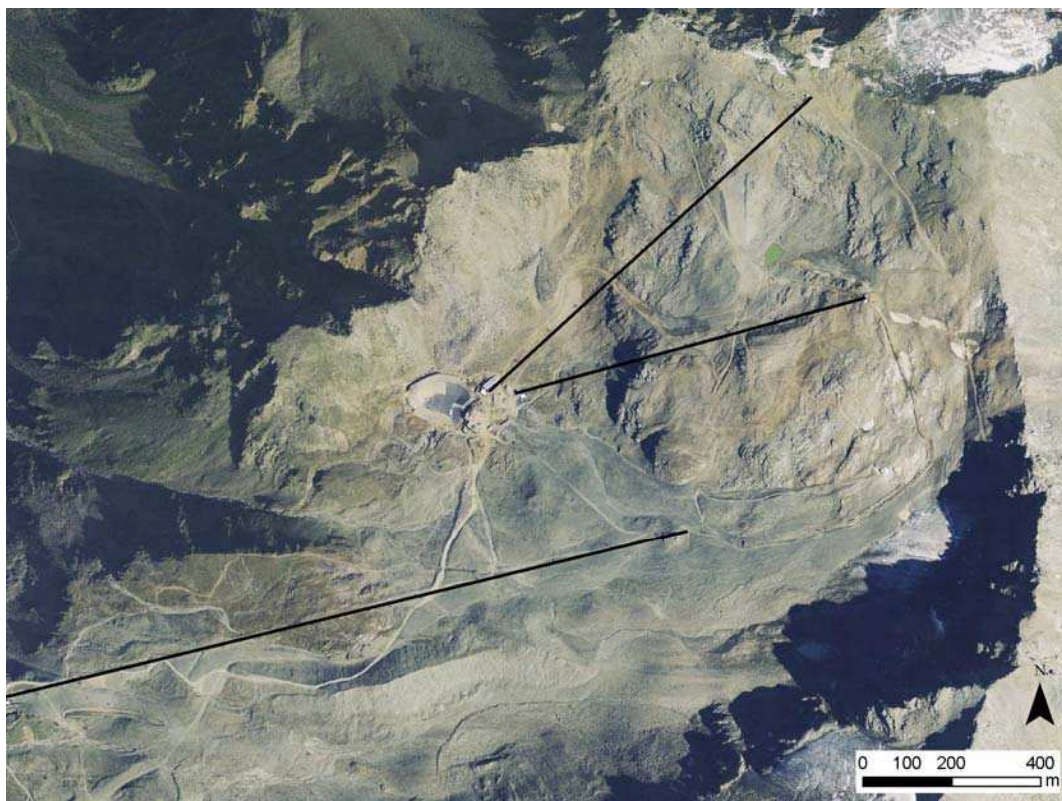


Fig. 3 – Overview of the study area Upper Sulden Valley. The black lines indicate the location of the chairs lifts of the Madritsch ski resort. Orthoimage 2008.

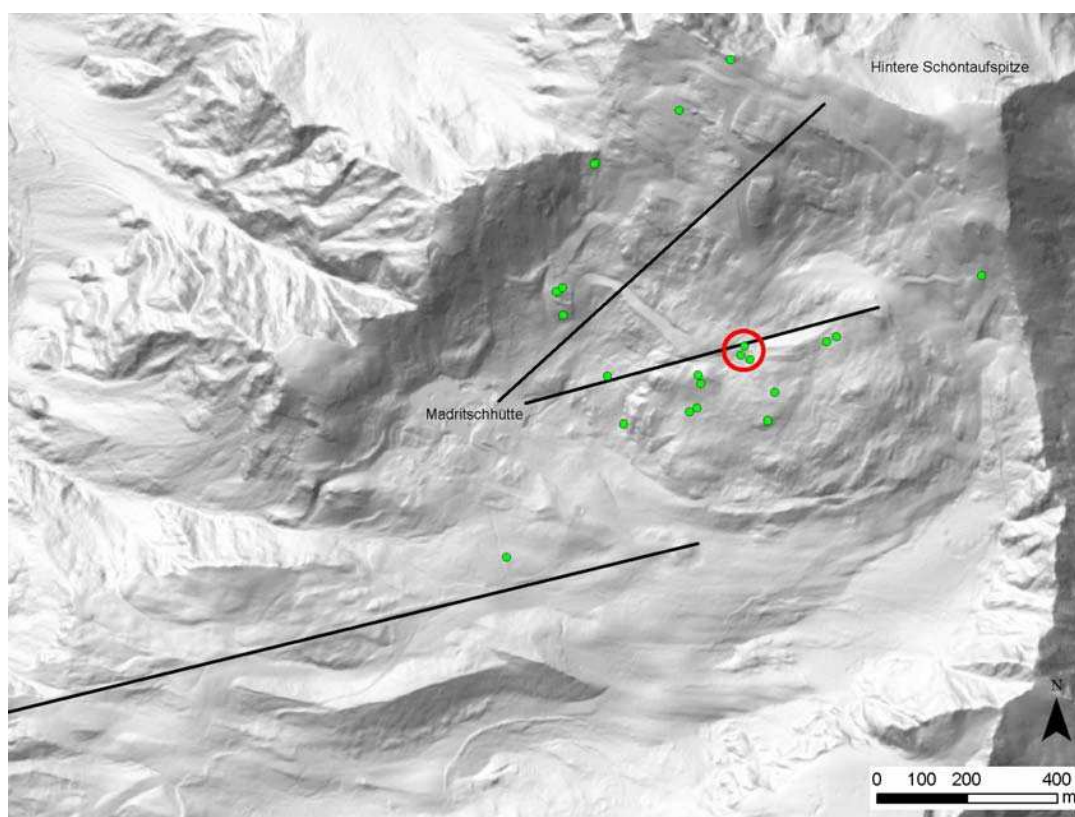


Fig. 4. – Overview of the study area Upper Sulden Valley. Hillshade of the air-borne Lidar-DEM 2006. The red circle shows the location of the pillar no. 12 of the ski lift "Madritschjoch" mentioned in the text. The green dots show the location of the GST measurement devices (UTL dataloggers).

2. Permafrost indicators and recent thermal and geomorphic evolution

The measurements of the temperatures at the bottom of the snow cover in 1992 and 1996 showed the main areas with probable presence of permafrost. Geophysical measurements (seismic refraction) and the construction of the ski lifts proved the existence of compact ice lenses in the area around the pillar no. 12 of the ski lift “Madritschjoch”. In August 1992, massive ice was found during the foundation of this pillar (Fig. 5).

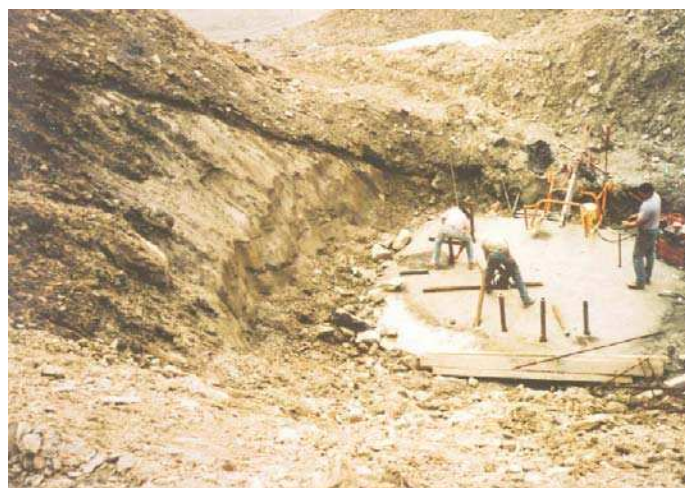


Fig. 5 – Excavation works for the foundation of the pillar no. 12 of the ski lift “Madritschjoch” in August 1992. Photograph by M. Maukisch. Source: Stötter et al. (2003). Ground ice was observed in the construction site and under the moraine at the left of the construction site.

The first measurements of the temperatures at the bottom of the snow cover (BTS) in the area were carried out in 1992 and 1996 by means of mobile devices in the months February and March. Since 2004, the measurements have been repeated. During the winter half years between 2004 and 2008 the measurements have been repeated only in the parts where a snow depth of at minimum 60 cm was existent (Figs. 6 and 7, Table 1).

Table 1 – Summary of the five BTS-measurement campaigns in the study area Upper Sulden Valley.

Year	Measurement date/period	Number of BTS-measurements	Probable permafrost (n)	Possible permafrost (n)	No permafrost (n)
1992	March 1992	371	227	58	34
1996	March 1996	184	157	19	8
2004	24.02., 03.03., 16.03., 07.04.	70	27	9	34
2006	25.04.	51	4	6	38
2007	09.03., 27.03., 29.03.	249	133	51	65
2008	06.03., 07.03.	236	73	37	89
<i>All years</i>		<i>1161</i>	<i>621</i>	<i>180</i>	<i>268</i>

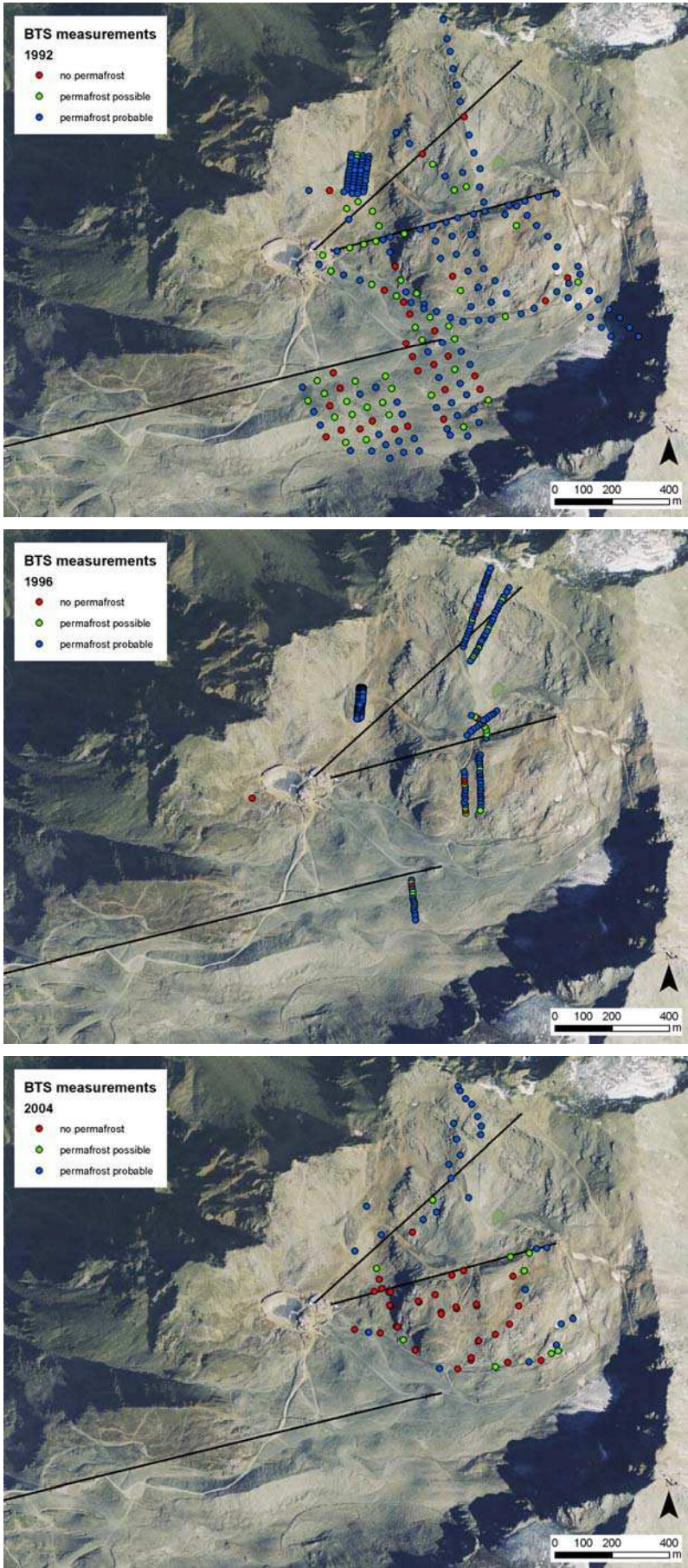


Fig. 6 – Results of the assessment of permafrost existence using BTS measurements in 1992, 1996 and 2004.

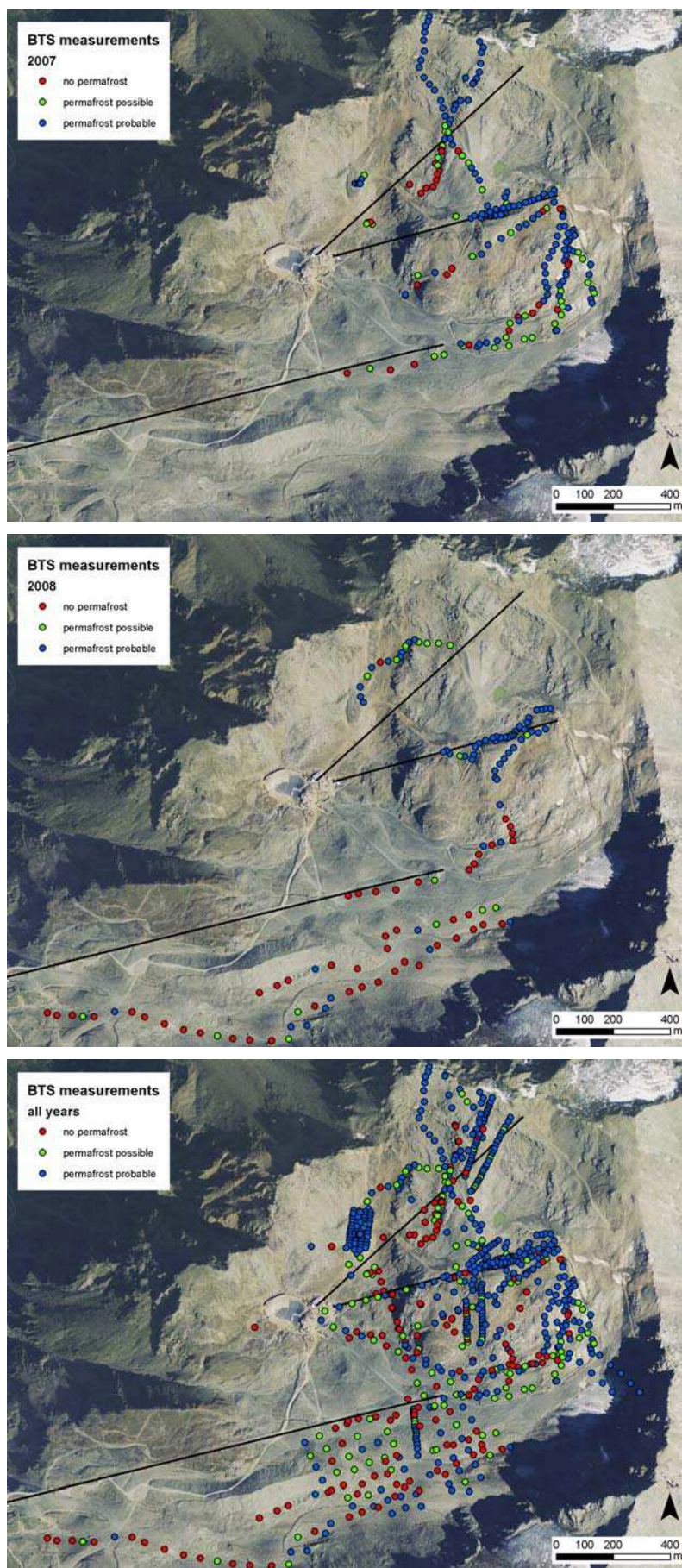


Fig. 6 – Results of the assessment of permafrost existence using BTS measurements in 2007, 2008 and all years.

Since 2006, the ground surface temperatures (GST) have been monitored continuously by 10 miniature temperature dataloggers situated in different parts of the study area (UTL datalogger, logging interval 1 hour, for locations see Fig. 4).

The comparison of the BTS measurements of the different years showed an increase of temperatures at the bottom of the snow cover in the area near the mentioned pillar no. 12 of the ski lift “Madritschjoch”.

The GST measurements in this area showed a high interannual variability. Despite this fact the following patterns could be found: The upper part of the slope of the Hintere Schöntaufer peak shows constantly negative temperatures (ca. -6°C) over all observed periods. The lowest parts of the hill between the bottom and the upper station of the ski lift “Madritschjoch” showed an increase of the temperatures over the years.

In the years before the construction of the ski lift, topographic surveys had been made. These measurements have been repeated regularly since the construction of the ski lift. In this time period between 1992 and 2004, the surface of the areas in the alignment of the ski lift “Madritschjoch” that are covered by debris were supposed to subsidence processes. In the vicinity of pillar no. 12, the surface sagged for 4 m (topographic surveys by the ski resort operator). This subsidence of surface was due to the melting of ground ice. In the vicinity of pillar no. 12 geomorphologic evidences for surface subsidence have been observed (Fig. 7).



Fig. 7 – Photograph of subsidence processes in the vicinity of pillar no. 12 of the ski lift "Madritschjoch" in July 2006. Photograph by A. Zischg.

The foundation of the pillar moved sideward and disarranged the position of the pillar no. 12. Therefore, the pillar had to be adjusted several times since 1992 until the foundation of the pillar was re-constructed by means of a deeper foundation reaching the bedrock under the debris cover (Fig. 8).



Fig. 8 – Photograph of the re-adjustment of the position of the pillar no. 12 of the ski lift "Madritschjoch". Photograph by A. Zischg.

During the construction of the ski lift, the ridge of debris material alongside the skilift (Fig. 9) had been grabbed slightly with an excavator. In 1996, the ridge showed an outcrop of massive ice on its lateral part exposed towards the ski lift. The slope was nearly vertical. In the meantime the ridge slumped down. The slope exposed towards the alignment of the ski lift is recontoured and flattened. The outcrop of ice disappeared.



Fig. 9 – Photograph of the debris ridge along the ski lift "Madritschjoch" in July 2006. Photograph by A. Zischg. The red arrow shows the location with of the observed slope deformation.

In the steeper parts of the areas covered with debris, some evidences for slope movements could be observed (Fig. 10). The evidences for moving downwards of the slope were more frequently in the areas that are showing warmer ground temperatures of the measurements during the last years. The geomorphic signs for slope movements in this area were observed for the first time in 2006.



Fig. 10 – Photograph of evidences for slope movements in the active layer of the south-western slope of the peak Hintere Schöntaufspitze in the ski resort Sölden-Madritsch in July 2007. Photograph by A. Zischg.

3. Possible future thermal response to predicted climate change

The observations of the surface subsidence are relevant for the infrastructure of the ski resort. With some technical efforts, the problem for the stability of the foundation of a pillar of the ski lift due to this geomorphic phenomenon of subsidence could be handled. The phenomenon has accelerated in the years from 2000 to 2007. In the vicinity of the pillar no. 12 most probably the ground ice has been melted totally. Therefore, the further subsidence of the surface nearby of the pillar is finished. However, this can be concluded only for this specific location in the study area. In other areas where ground ice is still present, the degradation process will continue with the increase of temperatures.

After the analyses provided in Chapter 2, the number of frost days in the Madritsch ski resort is likely to decrease for 15 days and the number of ice days will decrease for 17-19 days. The freeze-thaw days will increase about 3-4 days. This will have consequences for a further continuation of the permafrost degradation process. The monitoring of the permafrost degradation in this area will be continued. In case of a beginning subsidence process in other parts of the study area, the course of this event will be observed.

References:

- Stötter J., 1994: *Veränderungen der Kryosphäre in Vergangenheit und Zukunft sowie Folgeerscheinungen – Untersuchungen in ausgewählten Hochgebirgsräumen im Vinschgau (Südtirol)*. Habilitationsschrift, München.
- Stötter J., Fuchs S., Keiler M., Zischg A., 2003: Oberes Suldental. Eine Hochgebirgsregion im Zeichen des Klimawandels. In: E. Steinicke (ed.): *Geographischer Exkursionsführer Europaregion Tirol, Südtirol, Trentino. Spezialexcursionen in Südtirol. Innsbrucker Geographische Studien Band 33/3*, 239-281, Innsbruck

4.

Synthesis

Citation reference

Lieb G.K., Kellerer-Pirklbauer A. (2011). Chapter 4: Synthesis of case studies. In Kellerer-Pirklbauer A. et al. (eds): *Thermal and geomorphic permafrost response to present and future climate change in the European Alps*. PermaNET project, final report of Action 5.3. On-line publication ISBN 978-2-903095-58-1, p. 170-177.

Authors

Coordination: Gerhard Karl Lieb

Involved project partners and contributors:

- Institute of Geography and Regional Science, University of Graz, Austria (IGRS) –Gerhard Karl Lieb, Andreas Kellerer-Pirklbauer
- Institut de Géographie Alpine, Université de Grenoble, France (IGA-PACTE) – Philippe Schoeneich
- EDYTEM, Université de Savoie, France (EDYTEM) – Philip Deline
- Regional Agency for the Environmental Protection of the Aosta Valley, Italy (ARPA VdA) – Paolo Pogliotti

Content

Summary

1. Case studies: Methods and overall results
2. Thermal permafrost reaction in the past and future
3. Geomorphic permafrost reaction in the past and future

References

Summary

In the framework of Action 5.3 of the PermNET projects investigations on the thermal and permafrost response to climate change were carried out in 13 test sites distributed nearly all over the Alps. This research work was based on a great variety of methods ranging from geomorphological mapping over monitoring of ground surface temperature to borholes thus making the results well reliable. Nearly all hypothesis established in the initial phase of the work could be verified and quantified in at least one of the case studies. From this the following conclusions can be drawn:

Thermal permafrost reactions

An increase in ground temperatures and hence permafrost warming as a response to climate warming can already be observed and will continue in the future. However, there is also a strong control of snow cover to the thermal regime of the ground thus complicating the relationship between climate warming and permafrost warming or degradation. Air, ground and permafrost temperatures as well as snow cover should be monitored at as much locations as possible.

There is already a lot of evidence of thawing of permafrost in the Alps which leads and will increasingly lead to a reduced spatial extent of permafrost and to active layer thickening. However, little is yet not known about the assumed increasing ground water circulation and pressure which should be one focus of future research.

In specific altitudinal belts the number of freeze/thaw cycles as well as the duration and intensity of freezing and thawing periods will change significantly. Thus the subsequent processes like rock falls will shift to higher altitudes affecting areas which are not yet prone to these processes. From this it is advisable to monitor the thermal regime of the ground at many sites.

Geomorphic permafrost reactions

Rock glaciers react with a surprisingly short time lag on air and ground temperature variations. It can be assumed that most rock glaciers will creep faster in the next years to decades and then will become climatically inactive due to permafrost degradation. The surface velocity of rock glaciers should be monitored at least at the sites in which infrastructure is placed on rock glaciers.

The displacement mode of rock glaciers already changes and will continue to change significantly in the next decades. Especially surface lowering can be observed at several sites due to melting of the permafrost ice. In the future collapse of ice rich rock glaciers will occur more frequently thus endangering infrastructure. Damage can only be avoided if the internal structure of the permafrost using geophysical techniques is well known.

Volume and extent of destabilized materials increase as a response to active layer thickening and decreasing permafrost extent. Thus the disposition to gravitative processes increases making the reevaluation of existing hazard protecting measures necessary.

Increasing frequency and magnitude of mass movement events are clearly evident. A further increase is possible, a shift of rockfall scars to higher elevations even very probable. Monitoring and modelling of these processes will help to reduce the hazard.

The melting of ice in thaw-sensitive permafrost makes surfaces instable thus leading to subsidence in flat areas or on gentle slopes and to different erosional processes on steep slopes. The consequence is damage of infrastructure if the internal structure of the permafrost is not known.

1. Case studies: Methods and overall results

In the 13 case studies of Action 5.3 high mountain permafrost has been investigated by a great methodological variety (Tab. 1) comprising nearly all techniques which are available. Thus the results are well reliable, particularly since all the case studies also provide similar evidences from other study sites situated within and without the Alps (see the respective references). According to the thematic aspect of Action 5.3 ground surface temperatures (GST) play a crucial role and thus have been used in all of the case studies. GST is the key parameter in giving information on how the warming of the atmosphere is coupled with the thermal regime of the ground. GST can be easily measured by cheap and tough equipment (miniature data logger MDL). Therefore this simple but in terms of its relevance for understanding thermal (and subsequently geomorphic) changes in permafrost areas very efficient method can be recommended for even more widespread usage in the future.

*Table 1 – Overview of permafrost related methods used in more than one of the case studies of Action 5.3 (Abbreviations: BTS = Basic temperature of winter snow cover, ERT = electrical resistivity tomography, GPR = ground penetrating radar, GST = ground surface temperature, MDL = miniature data logger, TLS = terrestrial laser scanning). Annotations: * Modelling of permafrost distribution was the task of Action 5.1 in the PermaNET project. ** At the study sites which were not equipped with automatic weather stations meteorological data from stations in the vicinity have been used. *** In some study sites measurements take place in shallow boreholes (down to depths of +/- 1 m) which are included in this category. **** Only these BTS sites are listed where special BTS campaigns were carried out (and BTS values were not just taken from GST measurements).*

Method	Case study (chapter)	Gained information
Geomorphological mapping	3.2., 3.3., 3.5., 3.7.	Geomorphology of study areas
Continuous photographic documentation	3.2., 3.3., 3.8.	Snow cover, rock fall events
Numerical permafrost modelling*	3.2., 3.3.	Spatial distribution of permafrost
Automatic weather station	3.2., 3.3., 3.6., 3.8., 3.9., 3.10., 3.13.	Atmospheric conditions**
GST logging (using MTD)	all case studies	GST and near GST*** (evidence of permafrost)
BTS measurement****	3.2., 3.3., 3.5., 3.7., 3.11., 3.14.	BTS (evidence of permafrost)
Spring (water) temperature measurement	3.3., 3.5., 3.11., 3.12., 3.13.	Water temperature (evidence of permafrost)
Discharge measurement and chemical analysis of water	3.5., 3.13.	Runoff and chemical properties of water
Geodetic measurement	3.3., 3.5., 3.6., 3.7., 3.11., 3.12.	Displacement of surface
Photogrammetry and TLS	3.3., 3.5., 3.8., 3.13.	Displacement of surface
Geophysical soundings (in most cases geoelectrics/ERT or GPR)	3.2., 3.3., 3.5., 3.6., 3.7., 3.8., 3.13., 3.14.	Internal structure and temperature of permafrost
Borehole	3.4, 3.7, 3.8., 3.10., 3.13.	Internal structure and temperature of permafrost

Summarizing the results presented in the case studies it has to be mentioned that with respect to the aim of identifying and quantifying the response of high mountain permafrost to climate change one problem remains unsolved –it is the lack of long term data concerning permafrost. Most of the sites were not established before around 2005 and there is e.g. no GST record longer than 10 years in any study site (with the exception of Sonnblick where the meteorological observatory provides also GST

data which have not been considered in Chapter 3.4.). Thus we are far away from having sufficient information on long term thermal reaction of permafrost – a statement which can only lead to the conclusion that is absolutely necessary to establish a long term monitoring network as it was the main objective of the *PermaNET* project.

The only aspect showing a record of a few decades for at least some sites (the longest one at Hochebenkar since 1938, *cf.* Chapter 3.5.) is the surface velocity of rock glaciers. Natural scientists became aware of creeping rock masses a long time before they were recognised as being the most striking features of high mountain permafrost. The results of the existing geodetic and photogrammetric measurements which are presented and discussed especially at the examples of Doesen rock glacier (Chapter 3.3.) and Laurichard rock glacier (Chapter 3.6.) clearly reveal significant geomorphodynamic changes over the last decades which can only be explained with changes in the thermal regime of the permafrost.

In order to provide a closer look to the “overall results” it is helpful to distinguish between different types of permafrost environments which have been investigated in the study sites (Tab. 2). Most of the work has been done on active rock glaciers which have become the most important object of permafrost research in high mountains. Thus the processes taking place in rock glacier systems are understood increasingly well although, of course, a lot questions still remains open. However, there are still fewer permafrost investigations outside of rock glaciers leading to a relative lack of information on the other environment types which is regrettable due to the fact that most of the infrastructure – mainly for touristic purposes – is built in these environment and not on rock glaciers whose unfavourable conditions for construction work is in the meantime well known to technicians leading them to avoid rock glacier surfaces wherever possible.

Table 2 – Overview of permafrost environments investigated by the case studies of Action 5.3 (Annotations: Some of the case studies refer to different types of permafrost environments, in the table only the most significant ones are indicated).

Type of permafrost environment	Case study (chapter)	Annotations
Active rock glacier	3.3., 3.5., 3.6., 3.7., 3.11., 3.12., 3.13.	Debris or talus derived rock glaciers which are at least partly active, bouldery surface
Slope	3.2., 3.3., 3.10., 3.14.	Slopes outside of active rock glaciers, mostly covered by glacial or periglacial sediments
Rock wall	3.8., 3.9.	Steep rock faces with little or no coverage by sediments, snow or ice
Summit and ridge	3.2., 3.4., 3.8., 3.9.	Summit areas mostly consisting of heavily weathered bedrock, partly with mountain top detritus

The general thermal reaction of permafrost to climate change can be described in the way that permafrost temperatures increase, active layers thicken and permafrost thus becomes more prone to degradation. Based on this the main statements on the four environmental types derived from the results of the case studies can be summarized as follows:

- *Active rock glaciers* react surprisingly fast on annual or seasonal temperature variations in the way that warmer conditions result in higher surface velocities. This is due to the fact that deformation rates increase with temperature as well as to the presence of more liquid water in the rock glacier system.

- On *slopes* the active layer thickening and degradation of permafrost leads to destabilization of sediments which then are prone to erosional processes of different kind (especially debris flows) when the inclination is high. In flatter terrain frost settling and subsequent subsidence of the surface is the most important process as far as permafrost is thaw-sensitive.
- *Rock walls* free of sediments or cryospheric cover are directly coupled to atmospheric changes which therefore have direct consequences on the thermal regime and thus geomorphic processes in rock faces. Depending on the rock type and its properties (strata, fracturing, clefts) rock falls of increasing frequency and magnitude are likely to occur.
- On *summits and ridges* the conditions are similar to that in rock walls. Regardless of the existence of mountain top detritus the tendency of summits and ridges to collapse is given.

2. Thermal permafrost reaction in the past and future

2.1 Increasing ground temperature and permafrost warming

The entire evidence available so far – not only from the case studies of Action 5.3 but also from the literature (Harris *et al.* 2003) – clearly shows that the rising air temperatures causes an increase of GSTs and via heat flux to the ground an increase of permafrost temperatures. As recorded in the case studies all measured permafrost temperatures are quite close to 0°C (e.g. -1.02°C as mean value for the period 2008-10 at the permafrost table in the deep borehole at Cime Bianche Pass, calculated from Table 2 in Chapter 3.10.). This means that only a slight further increase in temperature would be sufficient to induce permafrost degradation in vast areas currently underlain by permafrost. A model approach on this aspect is discussed in Chapter 3.7.

On the other hand many of the case studies have shown that there is obviously no linear correlation between rising air temperatures and rising permafrost temperatures. Instead of this the characteristics of the substrate as well as the snow cover play a crucial role for the temperature regime in the ground. Especially the latter aspect has been elaborated intensively in all the case studies where high resolution GST measurements using MDL have been carried out. So the conclusion that *“the evolution of the permafrost will not only depend on the air temperature, but will be strongly influenced by the evolution of the snow cover, especially its early or late onset in autumn. A late onset of the snow cover can at least partially compensate a rise in air temperature”* (Chapter 3.6.) can be applied to all the case studies and finally can be considered as a rule valid for the entire Alps. Yet this has to be qualified by the fact that there are hardly any (and within Action 5.3 none at all) long term data series of permafrost temperature available so far.

2.2 Thawing of permafrost with different effects

Thawing of permafrost in the Alps which has already been proven by a lot of evidence is assumed to create the following effects. (i) *The spatial extent of permafrost is reduced*: This fact can e.g. be seen at the Sulden Valley study site (Chapter 3.14.) where the pillar of a ski lift was originally placed on a buried body of massive ice which in the meantime has disappeared so that the pillar could be reconstructed on the underlying bedrock. Unfortunately, due to the lack of knowledge on previous permafrost distribution, the complete degradation of permafrost in recent years can undoubtedly be proven only in a limited number of cases. However, the now available information on the existence of permafrost not only at specific sites – as documented e.g. within Action 5.3 – but also for the entire Alps will provide the possibility to observe the (probably accelerated) future degradation process in detail. (ii) *Active layer thickening* has been detected in some of the study sites, e. g. well documented by repeated geoelectrical soundings on Laurichard rock glacier (Chapter 3.6.). However, also this statement contains some uncertainties because of the lack of long term data availability. It has to be kept in mind that the interannual variability of the active layer depth is very high depending

especially on the beginning, duration and thickness of the winter snowcover. This can e.g. be seen in the respective graphs from Cime Bianche Pass (Chapter 3.10.) in which the active layer thickness shows a great temporal variation but not yet a trend to increase. (iii) *Increasing ground water circulation and pressure* has been worked out as a possible contribution to increasing rates of permafrost creep on rock glaciers at several study sites (e.g. Doesen Valley, Chapter 3.3., and Hochebenkar, Chapter 3.5.). However, there is not yet any unambiguous proof for this assumption because at least in the case studies investigated in Action 5.3 there was no specific research on the hydrological system within permafrost bodies.

Summarizing from the considerations on ground temperatures, permafrost warming and permafrost thawing given in this and the previous subchapter the conclusion can be drawn that the thermal regime of permafrost should be monitored more intensively in the future. This means that measurements of GST and temperatures in different depths (in boreholes) have to be carried out at more sites than today and – above all – over longer periods than it has happened until now. A further focus of future research should be the investigation of the existence, dynamics and significance of liquid water in permafrost areas.

2.3 Changes in the number of freeze/thaw cycles and magnitude of freezing and thawing periods

The basic information on this topic is given in Chapter 2 providing data on the numbers of freeze days, ice days and freeze-thaw days for the entire Alpine Arc. The analysis is based on the period 1961-90 and the difference in the number of these days to the period 2021-2050 is given. E.g. considering the number of frost days a decrease of 9-18 days per year between the periods 1961-90 and 2021-2050 is expected. The change of freeze/thaw days which are of specific relevance for geomorphic processes (e.g. frost weathering, rock fall activity) is estimated between -4 and +5 days per year. This does not seem to be a high value, yet one must keep in mind the altitudinal shift of temperature belts upwards. As it has been pointed out e.g. in the study area Mont Blanc (Chapter 3.9.) the subsequent processes like rock falls will affect higher altitudes which are not yet prone to these processes. In any case also from this point of view it is advisable to monitor the thermal regime of the ground at as many sites as possible.

3. Geomorphic permafrost reaction in the past and future

3.1 Changes in the rate of rock glacier displacement

All the 7 case studies on rock glaciers (Tab. 2) have revealed the fact that the dynamics of rock glacier creep strongly depends on temperature variations. The measured surface velocities on rock glaciers react on air temperature and especially on GST variations within a surprisingly short time lag. According to the Action 5.3 studies this time ranges between less than one and a few years. As reported e. g. from Doesen rock glacier (Chapter 3.3.) interannual temperature variations of 1-2°C can result in velocity changes of approx. +/- 20%. The conclusion for the evidence available on surface velocity changes on rock glaciers can be taken from Chapter 3.6.: *“Rock glaciers react to climate and show interannual velocity variations. Their reaction time is thus much shorter than previously assumed. Velocity variations are linked to temperature variations: an increase in temperature induces an increase in velocity. The air temperature only partly explains the observed ground surface temperature and velocity variations. The ground surface temperature shows the best link with velocity variations, with a time lag of around 1 year. The snow cover explains most of the difference between air temperature and ground surface temperature, and thus appears as the main driving factor both for ground surface temperature and for velocity variations”*.

For the near future (next years to decades) it can be assumed that most rock glacier will show a trend to faster surface velocities although there will be subordinate periods of reduced dynamics as a

consequences of colder years. After this phase of increased dynamics permafrost degradation with melting of the ice will reduce the ice content of rock glaciers until the substrate is not supersaturated in ice any more. Given this situation the rock glacier will fall into the status of a climatically inactive one, i.e. the movement will stop and the remaining ice will slowly melt away. Depending on the size and elevation of the rock glacier this will probably last several decades to centuries.

Vertical displacement on rock glacier surfaces may be due to the dynamic behaviour of rock glaciers (areas with extending or compressing “flow”). However, if there is a net lowering of the entire rock glacier surface there can be no doubt that there is an ice loss. Such a situation is e. g. described for Hochebenkar rock glacier in Chapter 3.5., but it also applies e. g. to Doesen rock glacier (Kaufmann & Ladstädter 2007; Kaufmann *et al.* 2007). It has to be expected that a surface lowering due to melting of the ice will occur on most of the alpine rock glaciers in the first phase of acceleration due to permafrost warming as well as in the second phase of ice disappearance.

The measurement of surface displacements on rock glaciers should be continued where it is already carried out in order to achieve long term data series. Furthermore such monitoring should be established at the few sites where infrastructure is placed on the surface of rock glaciers.

3.2 Changes in displacement mode of rock glaciers

The displacement mode of rock glaciers already changes as it has been described considering the vertical surface changes in the previous subchapter. These already ongoing processes will continue in the next decades accompanying the acceleration and subsequently the deactivation of rock glaciers. With regard to the acceleration basal sliding of rock glaciers can be taken into account (Hausmann *et al.* 2007) as a consequence of a changing hydrological system. However, as already mentioned above no empirical findings on this aspect are available in Action 5.3.

Thus statements only on surface lowering are possible which can be observed at several sites due to melting of the permafrost ice. In the future collapse processes on ice rich rock glaciers will occur more frequently creating thermokarst structures which can already be observed on several alpine rock glaciers (e.g. Murfreit Rock Glacier, Italy; Krainer & Mussner 2010), but not on the ones investigated in Action 5.3. Collapse of course can cause damage to infrastructure which can only be avoided if the internal structure of the permafrost using geophysical techniques is well known.

3.3 Changes in solifluction rates and cryogenic weathering

No empirical evidence has been provided on these two topics by the case studies of Action 5.3.

3.4 Changes in volume and extent of unstable/unconsolidated materials

As it has been shown e.g. in the Sulden Valley study site (Chapter 3.14.) volume and extent of destabilized materials increase as a response to active layer thickening and decreasing permafrost extent. Because more loose material is present meteorological events like heavy rainfalls can mobilize these sediments. Thus the disposition to gravitative and erosional processes has already increased at many locations and will further increase in the future affecting more and larger areas. In many cases these changes will certainly make the re-evaluation of existing hazard protecting measures necessary.

3.5 Changes in frequency and magnitude of mass movement events

This aspect has been highlighted in much detail by the Mont Blanc study in Chapter 3.9. even at different time scales. The results undoubtedly reveal that the increasing frequency and magnitude of mass movement events can only be caused by permafrost degradation. Thus the conclusions can be taken from this chapter: “... *rockfalls from high-Alpine steep rockwalls are expected to occur more frequently, with volumes that are likely to increase. The frequency that is currently increasing should maintain the same trend in the next decades, due to the deepening of the active layer as the temperature rise ... in the Alps for the 21st century will be higher by nearly 1°C than the global one Moreover, heat advection by triggering of water circulation at depth along thaw corridors would increase the collapsed volumes*”. Furthermore for purposes one must be aware of the fact that rockfall scars will shift to higher elevations. Therefore more initiatives of monitoring and modelling of these processes should be carried out in order to provide knowledge for reducing rock fall hazards.

3.6 Surface instabilities caused by thermokarst processes/melting of permafrost ice

Surface instabilities are of special significance in permafrost areas where infrastructure – in the Alps in most cases constructions and edifices for touristic needs – is present. Thus the most striking examples of Action 5.3 are the Madritsch skiing area in Sulden Valley (Chapter 3.13) as well as the observatory and tourist hut on the summit of Hoher Sonnblick (though Chapter 3.4. does not provide much information on this aspect). Melting of ice in thaw-sensitive permafrost (in the Alpine context permafrost supersaturated with ice) makes surfaces unstable thus leading to subsidence (ground settling) in flat areas or on gentle slopes. Additionally different erosional processes may occur on steep slopes due to the same process. The consequence is damage to infrastructure if the internal structure of the permafrost is not sufficiently known and thus measures to avoid such problems cannot be taken in time.

Acknowledgements. The *PermaNET* project is part of the European Territorial Cooperation and co-funded by the European Regional Development Fund (ERDF) in the scope of the Alpine Space Programme www.alpinespace.eu

References:

- Harris C., Vonder Muhll D., Isaksen K., Haeberli W., Sollid J.L., King L., Holmlund P., Dramis F., Guglielmin M. & Palacios D., 2003: Warming permafrost in European mountains. *Global and Planetary Change*, 39, 215-225. doi:10.1016/j.gloplacha.2003.04.001.
- Hausmann H., Krainer K., Brückl E. & Mostler W. 2007: Internal Structure and Ice Content of Reichenkar Rock Glacier (Stubai Alps, Austria) Assessed by Geophysical Investigations. *Permafrost and Periglac. Process.* 18: 351-367.
- Kaufmann V. & Ladstädter R., 2007: Mapping of the 3D surface motion field of Doesen rock glacier (Ankogel group, Austria) and its spatio-temporal change (1954-1998) by means of digital photogrammetry. *Grazer Schriften der Geographie und Raumforschung* 43: 127-144.
- Kaufmann V., Ladstädter R. & Kienast G., 2007: 10 years of monitoring of the Doesen rock glacier (Ankogel group, Austria) – A review of the research activities for the time period 1995-2005. *Proceedings, 5th Mountain Cartography Workshop, 29 March - 1 April 2006, Bohinj, Slovenia*, 129-144.
- Krainer K. & Mussner L., 2010: Blockgletscher und Naturgefahren: Der aktive Blockgletscher 'Murfreit' in der nördlichen Sellagruppe, Dolomiten. *Geo.Alp*, 7: p. 99.